Universität für Bodenkultur Wien

DI Veronika Perz

Polyesterases from aerobic and anaerobic environments for hydrolysis of synthetic polyesters

DISSERTATION

zur Erlangung des Doktorgrades an der Universität für Bodenkultur Wien

Univ. Prof. DI Dr. Georg Gübitz
Institut für Umweltbiotechnologie
Universität für Bodenkultur Wien

2016

Statutory declaration

I declare that I have authored this thesis independently, that I have not used other than the declared sources/resources, and that I have explicitly marked all material which has been quoted either literally or by content from the used source.

…… ……..

date signature

Acknowledgements

I would like to thank

…**Georg Gübitz** for giving me the possibility to work in this interesting project, present results at several international conferences, the fruitful discussions, countless interesting ideas, your confidence in me and my work and for your tireless effort to finance us Ph.D. students until the end of our studies. I can imagine that this is not always easy in times of economic crisis. Thank you also for persuading me to taste Clam chowder in San Francisco – I would never have guessed that I like this kind of food! :-D

…**Doris Ribitsch** for endless hours of discussions, scientific and personal support and staying positive no matter what.

…my master student **Klaus Bleymaier** and my trainee **Astrid Perz** – it was a pleasure to work with you guys!

… all people from the Tullner cooking group. (**Barbara**, **Benjamin**, **Cornelia**, **Clemens**, **Doris**, **Günther**, **Martin**, **Kati**, **Lydia**, **Lina**, **Ramiro**) Delicious food and nice company at lunchtime definitely motivates a lot! :-D

…the colleagues from Graz and Tulln for the great working atmosphere. Thank you **Alex**, **Andi**, **Angelika**, **Anto**, **Armin**, **Barbara**, **Caro**, **Clemens**, **Dani**, **Gibson**, **Karolina**, **Katrin**, **Lu**, **Marion**, **Michi**, **Orti**, **Oskar**, **Quique**, **Robert**, **Rosario**, **Sarah**, and all the others that were part of the Gübitz group in the last years!

…the collegues from our company partner: **Carsten Sinkel**, **Ulf Küper** and **Katharina Schlegel**.

…**my parents** – for everything and believing in me so much more than I do. Thank you for taking care of Benjamin with lots of patience and love while I was writing this thesis. You are just great!

…**Helga** for being there for me all the time and your support with English language.

…**Claudia** – because of you I smiled during my weekly business trips to Tulln. ;-)

…all my friends and family

Thank you to **Alex**, my partner in live, for everything and being there for me in good and bad times. I am sooooo happy that you walked into my lab, um, well,…. life almost six years ago! ☺ …and our sunshine **Benjamin** – you changed my live in such a positive way, make it worth living and conjure a smile on my face every day. I love you both. ☺

Contents

Preamble

This thesis is divided into 5 main chapters. Chapter 1 gives a general introduction to the topic, including information about synthetic polymers in general, biodegradable polymers, the investigated polymers poly(butylene adipate-co-butylene terephthalate) (PBAT) and the aliphatic polyester poly(1,4-butylene adipate) (PBA), polyester active enzymes and a summary about potential industrial application of polyesterases. Chapters 2 describes the overall aim of this work.

Chapters 3 lists five publications that were published throughout this thesis. The first manuscript describes the hydrolysis and substrate specificities of the aliphatic-aromatic polyesters PBAT by two well-known cutinases (Thc_Cut1 and HiC) from aerobic compost inhabitants. The synthesis of the tested oligomeric and polymeric model substrates is described in the second paper. Publications three and four present novel esterases from anaerobic *Clostridium* strains that were found to hydrolyze PBAT and were characterized in detail. The crystal structures and models of these esterases were evaluated regarding their activities towards the polyester. Moreover, anaerobic batch tests were performed to investigate the biodegradation of PBAT under anaerobic conditions. In paper number five the effect of a polymer binding domain fused to the Cutinase 1 from *Thermobifida cellulosilytica* on the hydrolysis of the aliphatic PBA was investigated.

This thesis is closed with a general conclusion in Chapter 4. Finally, the appendix (Chapter 5) gives an overview about all publications, oral presentations and most relevant posters that were presented throughout the time frame of this thesis.

Abstract

In the beginning of the last century, one of the main goals of synthetic polymer development was the design of highly stable and durable materials. Nowadays, these features lead to serious environmental problems. Researchers are working to develop efficient polyester recycling strategies as well as to improve polyesters that are biodegradable and show required material properties.

Aliphatic-aromatic copolyesters like PBAT (poly(butylene adipate-co-butylene terephthalate)) are frequently used in organic waste bags or in food packaging. Organic waste is increasingly converted to energy in biogas plants and therefore polyesters could accumulate in biogas plants. Several studies have clearly demonstrated the biodegradability of PBAT under aerobic conditions. However, only little information exists on PBAT degradation in anaerobic environments and the enzymes involved in this process.

In a first step, two cutinases from typical soil and compost inhabitants were tested for their ability to hydrolyze PBAT. The fungal cutinase from *Humicola insolens* (HiC) and the bacterial cutinase from *Thermobifida cellulosilytica* (Thc_Cut1) hydrolyzed PBAT as well as oligomeric and polymeric PBAT model substrates. Higher concentrations of aromatic building blocks lowered the enzymatic hydrolysis rates. Moreover, the influence of the melting temperature (T_m) on the enzymatic degradability was confirmed.

Subsequently, several potentially interesting enzymes from different *Clostridium* species were identified in an *in-silico* approach. Two new esterases from the anaerobic strain *Clostridium botulinum* (Cbotu_EstA and Cbotu_EstB) and one from *Clostridium hathewayi* (Chath_Est1) were heterologously expressed in *E. coli* BL21-Gold(DE3). The three esterases showed their maximum activity at around pH 7.0. Cbotu_EstA and Cbotu_EstB exhibit a sequence identity of approximately 40 %. Comparison of the Cbotu_EstA crystal structure and Cbotu_EstB model revealed several structural differences that might explain the lower activity of Cbotu_EstB on PBAT. Analysis of the Chath_Est1 and Cbotu_EstA crystal structures showed that theses esterases belong to the α/β-hydrolases. Additionally, the ability of anaerobic biogas sludge to hydrolyze PBAT was evaluated. Accumulation of the hydrolysis product terephthalic acid (Ta) was observed using RP-HPLC analysis. After 14 days a decrease in Ta concentration was measured, which could be an indication for microbial metabolism.

Finally, Thc_Cut1 was fused to the hydrophobic binding module of a polyhydroxyalkanoate depolymerase from *Alcaligenes faecalis* (Thc_Cut1_PBM) in order to improve the sorption process to the hydrophobic polymer. Indeed, the hydrolysis rate of the

aliphatic polyester poly(1,4-butylene adipate) was two times higher for Thc_Cut1_PBM when compared to the native enzyme.

The findings, presented in this thesis, will improve the understanding of synthetic polyester hydrolysis in both natural and man-made, aerobic and anaerobic environments. Moreover, the new esterases could have a potential for industrial applications like polyester hydrolysis, recycling of building blocks or functionalization of polymer surfaces.

Kurzfassung

Eines der wichtigsten Ziele der Polymerentwickung zu Beginn des 20. Jahrhunderts war es, Stoffe von hoher Stabilität und Langlebigkeit zu entwickeln. Heutzutage bringen diese Eigenschaften jedoch schwerwiegende Umweltprobleme mit sich. Daher wird in der Forschung sowohl an der Entwicklung effizienter Recyclingstrategien von synthetischen Polymeren wie Polyester gearbeitet, als auch an der Verbesserung biologisch abbaubarer Polyester, welche die erforderlichen Materialeigenschaften aufweisen.

Aliphatisch-aromatische Polyester wie PBAT (poly(butylene adipate-co-butylene terephthalate) werden häufig in Biomüllsäcken und Lebensmittelverpackungen eingesetzt. Erst in jüngerer Vergangenheit wird aus Biomüll auch in Biogasanlagen Energie erzeugt, was jedoch dazu führt, dass sich Polyester in Biogasanlagen ansammeln kann. Mehrere Studien zeigten bereits die biologische Abbaubarkeit von PBAT unter aeroben Bedingungen. Weniger erforscht ist hingegen der Abbau von PBAT unter anaeroben Bedingungen sowie auch die am Abbau beteiligten Enzyme.

Für diese Arbeit wurden zunächst zwei Cutinasen aus typischen Boden und Kompostbewohnern auf ihre Fähigkeit getestet, PBAT zu hydrolysieren. Die pilzliche Cutinase aus *Humicola insolens* (HiC) und die bakterielle Cutinase aus *Thermobifida cellulosilytica* (Thc_Cut1) hydrolysierten PBAT wie auch oligomere und polymere Modellsubstrate. Höhere Konzentrationen aromatischer Bausteine senkten die enzymatischen Hydrolyseraten signifikant. Darüber hinaus wurde der Einfluss der Schmelztemperatur (T_m) auf die enzymatische Abbaubarkeit bestätigt.

In weiterer Folge wurden einige potentiell interessante Enzyme der Gattung *Clostridium* in einem *in-silico* Verfahren identifiziert. Zwei neue Esterasen vom anaeroben Stamm *Clostridium botulinum* (Cbotu_EstA und Cbotu_EstB) sowie eine weitere aus *Clostridium hathewayi* (Chath_Est1) konnten erfolgreich in *E. coli* BL21-Gold(DE3) heterolog exprimiert werden. Die drei Esterasen zeigten ihre maximale Aktivität jeweils bei einem pH Wert von rund 7.0. Cbotu_EstA und Cbotu_EstB wiesen eine Sequenzidentität von etwa 40% auf. Ein Vergleich, zwischen der Kristallstruktur von Cbotu_EstA und dem Cbotu_EstB Modell, ergab einige strukturelle Unterschiede, welche die niedrigere Aktivität von Cbotu_EstB auf PBAT erklären könnten. Des Weiteren zeigte die Analyse der Chath_Est1 und Cbotu_EstA Kristallstrukturen, dass diese Esterasen zur Gruppe der α/β-Hydrolasen gezählt werden können. Zusätzlich wurde anaerober Biogasschlamm auf die Fähigkeit untersucht PBAT zu hydrolysieren. Mittels RP-HPLC-Analyse konnte eine Akkumulation des Hydrolyseprodukts Terephtalsäure (Ta) nachgewiesen werden. Nach 14 Tagen wurde ein

Rückgang der Ta-Konzentration gemessen, was auf mikrobielle Verstoffwechselung hinweisen könnte.

Schließlich wurde Thc_Cut1 mit dem hydrophoben Bindemodul einer Polyhydroxyalkanoatdepolymerase aus *Alcaligenes faecalis* fusioniert (Thc_Cut1_PBM) um die Sorptionseigenschaften an das hydrophobe Polymer zu verbessern. Die Hydrolyserate des aliphatischen Polyesters poly(1,4-butylene adipate) war beim Fusionsprotein Thc_Cut1_PBM doppelt so hoch wie bei Referenzversuchen mit der nativen Cutinase.

Die Ergebnisse dieser Arbeit tragen maßgeblich zum Verständnis der Hydrolyse synthetischer Polyester in natürlichen wie auch künstlich geschaffenen, aeroben und anaeroben Umgebungen bei. Darüber hinaus könnten die neuen Esterasen Potential für industrielle Anwendungen wie die Polyesterhydrolyse, Recycling von Bausteinen oder Funktionalisierung von Polymeroberflächen haben.

1

1 Introduction

The work performed throughout this Ph.D. thesis was performed within a project between the Austrian Centre of industrial biotechnology (ACIB GmbH) and an industrial partner.

1.1 Polymers – applications, advantages and environmental impact

The mass production of synthetic polymers started during the 1940s and 1950s and very quickly these materials affected all areas of our life [1]. These novel polymers quickly began to replace different other materials like glass, wood, metal, china or paper. Compared to e.g. paper based products, the advantages of plastics are obvious: higher strength, lighter weight, and resistance to water and microorganisms [2].

A polymer is defined as a large molecule that is built up from one or more repeating units of small molecules (=monomers). These monomers are the building blocks of the polymer. A polymer's size is either specified by the number of repeating units, also called degree of polymerization, or by its mass. Molecules with a relative molar mass of at least 1000 $g*mol^{-1}$ or a degree of polymerization of 100 or more are generally considered to be polymers. [3]

"Plastics", as polymers are often called, are based on (synthetic) polymers, typically produced through polymerization of monomers that are most often derived from fossil fuels. Plastics can be easily processed and shaped – the name refers to these properties. It must be stated that polymers and plastics are no synonyms since polymers are the raw materials for plastics. [4]

Within the last few decades, the availability of cheap synthetic polymeric materials for everyday products has changed our daily life drastically. Modern society is completely unimaginable without polymers, since they are the principally used materials or at least an important component of most modern products including clothes, footwear, cars, airplanes,

furniture, products for building and construction, packaging, products for public health, and many others... [5].

The benefits for public health derived through the usage of polymers become evident when thinking of medical devices like drips, aseptic packaging material, blister packs, surgical equipment or the easy supply of clean drinking water [5]. In this respect also the protective function of polymers in food packaging, necessary for e.g. inert atmosphere or vacuum packaging, needs to be mentioned leading to prolonged shelf lives and a reduction of food waste [6]. Another benefit of polymers used e.g. in cars or airplanes is their light weight that leads to substantial energy savings when they replace heavy materials like metals [7].

Some of the advantages of polymeric materials that explain their incredibly wide fields of application are: interesting thermal and insulation properties, low production costs, durability and stability, corrosion and light resistance, low density (lightweight), they do not break, their high strength to weight ratio, stiffness and toughness [1, 5]. In fact polymers can be designed and prepared in almost every desired quality. These versatile material properties have opened the way for significant technological advances in basically all industrial fields. For all those reasons it is not surprising that the worldwide production of polymers is steadily increasing. The global plastics production reached 299 million tons in 2013, meaning an increase of 3.9% compared to the global production in 2012. For the next years a further growth is expected [8].

However, beside these benefits that polymeric materials have in daily life, in recent years the severe environmental consequences and potential health risks came more and more into the focus of the society and policymakers. Polymeric materials and micro plastics enter in large scale our environment including all existing ecosystems [9]. Beside the more visible pollutions of forests, soils or densely populated areas, aquatic ecosystems like rivers [10], lakes and oceans [11-13] are nowadays highly contaminated with polymeric materials. Beside the aesthetic problem of polymer litter accumulating in nature, shorelines, towns and countryside, polymer debris can also lead to severe consequences for animals that e.g. inhale or swallow polymers or get caught in larger polymeric structures [9]. Moreover, there exist reasonable concerns that potentially toxic chemicals that are added to the polymers during the manufacturing process in order to improve their performance are entering the food chain and cause adverse health effects [14, 15].

Table 1: Polymer waste generated by end-use [3].

End-use	Approximate life time [years]	% Discard
Packaging	1	100
Transport	5	20
Furniture & housewares	10	10
Electrical appliances	10	10
Building and construction	50	2

Another interesting factor is the very broad range of lifetimes of polymers that are strongly depending on the end use of a polymer. Table 1 gives an overview of the disposal rates and lifetimes of polymers used for different end-use application. The European plastics demand of the different application sectors of the year 2013 is summarized in Figure 1. Packaging applications exhibit clearly the largest demand for plastics in Europe with a proportion of 39.6% of total used plastics. Additionally, polymers used for packaging are discarded after just 1 year and their discard rates reach almost 100%. Taking into account the huge amounts of plastics used for packaging, it gets obvious that packaging generates substantial quantities of waste that lead to environmental problems, while other applications with longer lifetimes of the polymers are more justifiable [3].

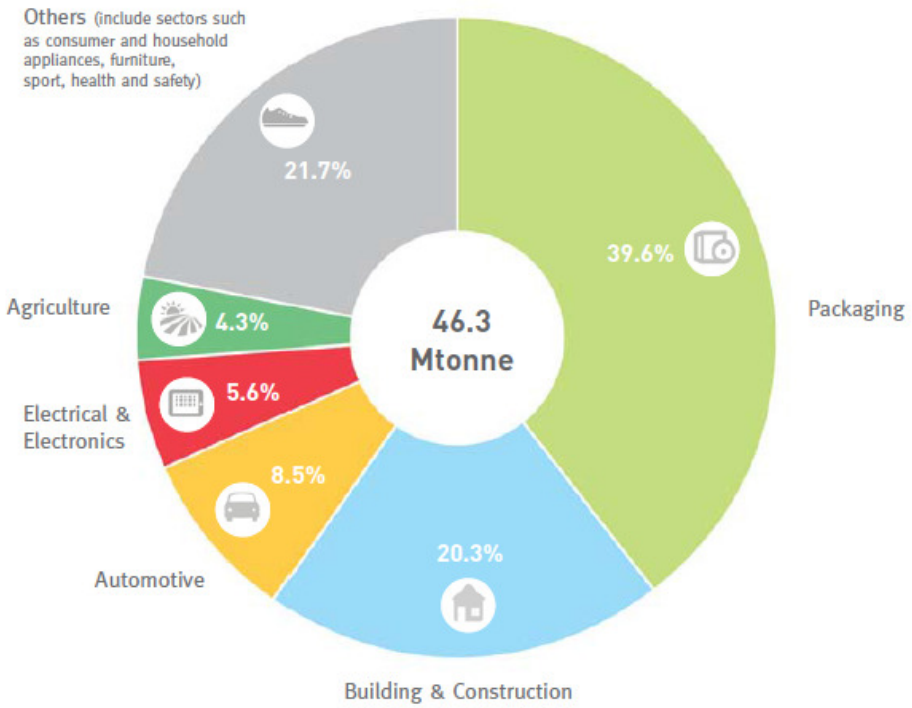

Figure 1: Plastics demand in the EU27 plus Norway and Switzerland by segments in 2013 [8].

In Figure 2, the European plastics demand is illustrated by segments [16]. The most commonly used polymers are polyethylene, polypropylene, polyvinyl chloride, polystyrene, polyurethane and polyethylene terephthalate (beside many other polymers that are on the markets).

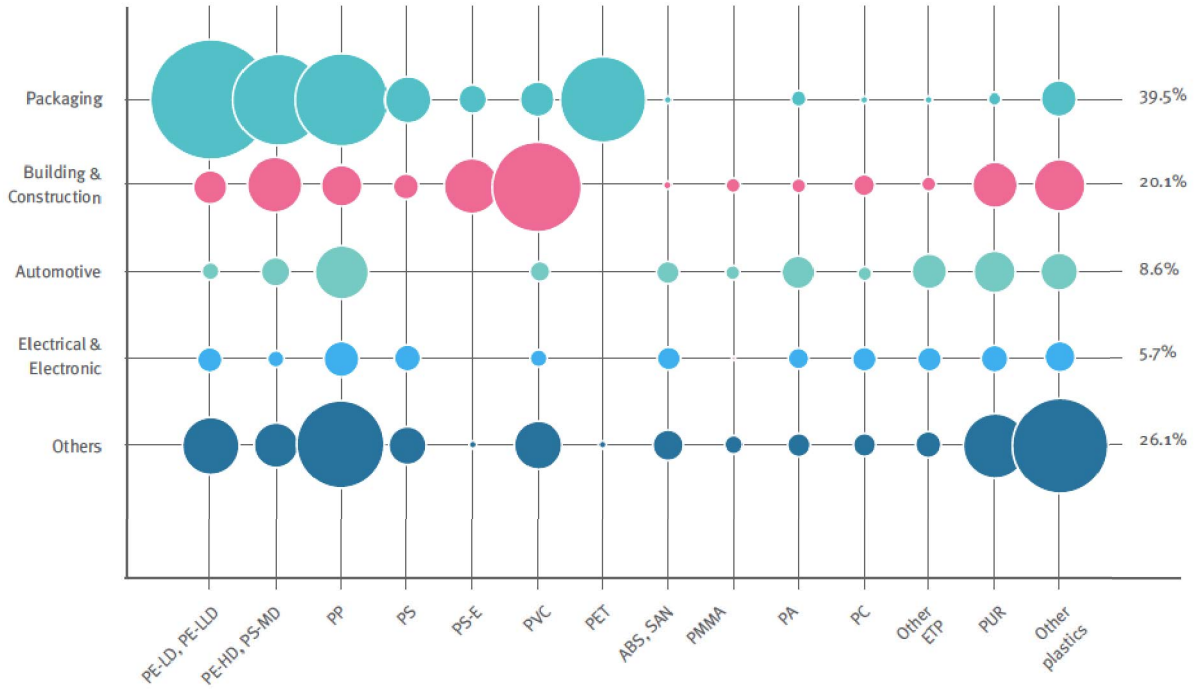

Figure 2: European plastics demand by segments and polymer type in the year 2014 [16]. (PE-LD: low density polyethylene, PE-LLD: linear low density polyethylene, PE-HD: high density polyethylene, PS: polystyrene, PP: polypropylene, PS-E: polystyrene expanded, PVC: polyvinyl chloride, PET: polyethylene terephthalate, ABS: acrylonitrile butadiene styrene, SAN: styrene acrylonitrile, PMMA: poly(methyl methacrylate), PA: polyamide, PC: polycarbonate, PUR: polyurethane)

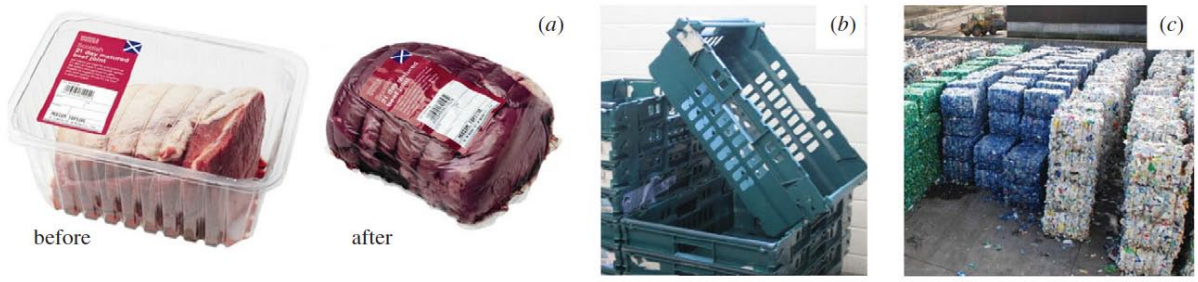

Figure 3: Examples for 3 of the "5Rs": (a) Reduce: A change in packaging design reduces the weight of used polymer by 70%, (b) Reuse: reusable plastic crates utilized e.g. in the retail sector, (c) Recycle: used and sorted plastic bottles can be recycled into new articles like textiles or plastic packaging [17]

To circumvent and minimize the environmental problems related to polymer waste, compliance to the so-called "five Rs" could be a strategies for a more sustainable and less-polluted future. These "five Rs" include **R**eduction (of polymer usage), **R**euse, **R**ecycle, energy **R**ecovery and molecular **R**edesign [1, 17, 18]. Some examples for polymer reduction, reuse and recycling are given in Figure 3. The plastics recycling rate in Europe (EU27 plus

Norway and Switzerland) is relatively high, reaching 26% in 2012. Additionally 36% of plastic waste was incinerated for energy recovery. It has been observed that European countries with statutory landfill ban achieve significantly higher recycling and energy recovery rates. [8] Nevertheless, in the greatest parts of the world most of the plastic waste still ends up in landfills.

The "5th R" - molecular redesign of polymers - is a green chemistry approach that aims to design polymers in a way that the use and generation of hazardous substances is reduced or even prevented throughout their whole lifecycle. This includes also that no toxic or harmful substances are released after the breakdown of the polymer. [19]

A further strategy, with high potential for certain purposes like short-term applications in packaging, agriculture (e.g. mulch films), organic waste or carrier bags, and medical applications, is to use biodegradable polymers [20].

1.2 Structural biodegradable polymers

Several different ways exist to categorize polymers. One possibility is to distinguish polymers regarding their thermal behavior into linear or lightly branched thermoplastics (which melt and solidify again when heated and cooled) and thermosets. The latter do not melt but decompose irreversibly as soon as they reach a certain temperature and are typically highly cross-linked [3]. Carothers suggested to classify polymers on the basis of the chemical reaction applied during the polymerization reaction [21]. In this classification the two main polymer groups would be addition and condensation polymers. Addition polymers are synthesized by addition of unsaturated monomers e.g. in the case of vinyl chloride (Reaction 1).

Reaction 1: Addition polymerization [22]:

$$n\ CH_2{=}CHCl \rightarrow [\text{-}CH_2\text{-}CHCl\text{-}]_n$$

In contrast to that, condensation polymers are derived by condensation reactions of functional groups and theses reactions are accompanied by a loss of water or other small molecules [3, 22]. Examples for condensation polymers are e.g. polyesters (Reaction 2)

Reaction 2: Condensation polymerization [22]

$$n\ HO\text{-}R\text{-}OH + n\ HOOC\text{-}R^1\text{-}COOH \rightarrow HO[\text{-}R\text{-}COO\text{-}R^1\text{-}COO\text{-}]_nH + (n\text{-}1)H_2O$$

Other polymer classifications are based on the origin (natural and synthetic polymers), on the presence of aromatic building blocks (aliphatic and aromatic polymers), on the chemical bonds in the polymer (polyesters, polyamides, polyurethanes, etc...) or the degradability (degradable, non degradable). A further way to classify polymers is to distinguish between functional and structural polymers. As the name suggests, functional polymers do not fulfill a structural purpose but they exhibit e.g. certain optical, electrical, magnetic, electrochromic, antibacterial, or other functional material features and possess distinct adsorption and reactivity behaviors. Very often, the applications of functional polymers are hidden or not as obvious [23]. However, the here presented study focuses on water insoluble structural polymers that are widely used as plastics in all types of everyday applications were a defined structure is needed (e.g. components for construction, instruments, foils or fibers) [23].

In the recent years, biodegradable polymers came into the focus due to changed legislation concerning packaging and usage of plastic carrier bags in several European countries [24]. For that reason, biodegradable polymers are nowadays used for packaging including food packaging purposes and carrier bags, since their environmental impact after usage (disposal) is not as problematic and they do not accumulate in nature. Beside the utilization of biodegradable polymers in packaging in order to reduce waste, they can also be attractive materials for applications in medicine (e.g. vascular grafts, artificial skin, drug delivery systems, scaffolds, bone fixation, etc.) or agriculture (e.g. mulch films or planting containers) [20].

Biodegradability of polymers is not a material property that was invented by human kind. Quite the contrary, nature provides a broad spectrum of biopolymers – and all of them are biodegradable. An overview about naturally occurring polymers including structural ones is given in Table 2.

Table 2: Summary of the most important natural polymers. Adapted from Teegarden [25] and Zhang [26].

Polymer type	Example
polysaccharides	
structural	(hemi)cellulose (wood, cotton, flax, hemp)
reserve	amyloses, amylopectins (starch, glycogen, dextrans)
gel-forming	gums, mucopolysaccharides
proteins	egg white, gelatin, enzymes, muscle, collagen, elastin, silk, wool
polynucleotides	DNA, RNA
polyesters	polyhydroxyalkanoates (poly(3-hydroxybutyrate), cork, cutin
lignins	binder for cellulose fibers, cell walls

Beside those naturally occurring biodegradable polymers, in the recent years synthetic biodegradable polymers were developed and entered the markets. Examples are aliphatic polyesters like poly(glycolic acid), poly(lactic acid), poly(ε-caprolactone), poly(p-dioxanone), poly(ortho esters), poly(butylene succinat) or polycarbonate. Further synthetic materials include biodegradable polyurethanes, polyanhydrides or poly(amino acids). Moreover, copolyesters with varying aliphatic building blocks of different sizes, such as poly(butylene succinate-co-butylene adipate) have been developed. [26, 27]

1.2.1 PBAT – a compostable aliphatic-aromatic copolyester

Generally, aliphatic polymers are much easier biodegraded than aliphatic-aromatic ones. Nevertheless, aliphatic polymers show poor material properties like low melting temperatures [28, 29]. On the contrary, aromatic polyesters like polyethylene terephthalate (PET) exhibit good material properties but are hardly biodegradable and were expected to be more or less inert to biological attack [30]. For that reason, the material properties of aliphatic polymers were improved by combining aliphatic an aromatic monomers in copolyesters [31-33]. The polyester poly(butylene adipate-co-butylene terephthalate short (PBAT) is a synthetic copolymer that contains adipic acid and terephthalic acid buildig blocks in a ratio of approximately 50:50 [34]. PBAT shows interesting material properties and the production is possible from the commodity chemicals terephthalic acid, adipic acid and1,4-butanediol with conventional condensation techniques [32]. Several studies have proven the biodegradability of PBAT under aerobic conditions (composting) [35-37]. During the course of this thesis it was possible to show that also enzymes from the strictly anaerobic organisms *Clostridium botulinum* [38], *Clostridium hathewayi* [39] and *Pelosinus fermentans* [40] hydrolyze this polyester. Figure 4 shows the chemical structure of PBAT.

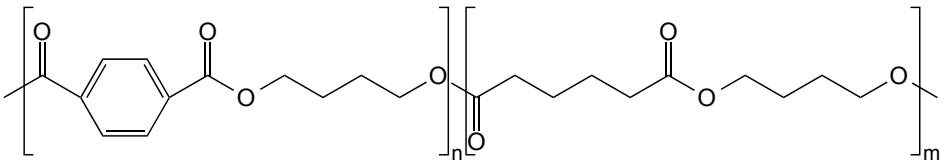

Figure 4: Chemical structure of poly(butylene adipate-co-butylene terephthalate) short PBAT.

The worldwide PBAT production capacity was estimated to be 75,000 tons in the year 2013 [41]. Commercially, PBAT polymers are named Easter Bio® from Eastman Chemical (USA), ecoflex® produced by BASF (Germany) or Origo-Bi® from Novamont (Italy) [27]. PBAT is currently also used for example as a component of polymer blends with e.g. poly(lactic acid) [42] or starch [43].

In this thesis, beside PBAT also the aliphatic polyester poly(butylene adipate), short PBA, was utilized for enzymatic hydrolysis experiments (Figure 5).

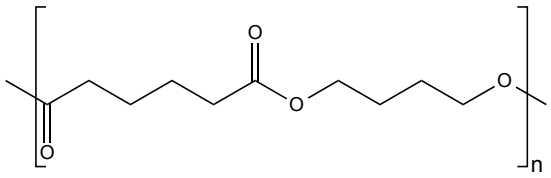

Figure 5: Chemical structure of poly(butylene adipate), short PBA.

1.3 Biodegradation of polymers

Plastics or polymers are considered to be biodegradable if they can undergo decomposition into carbon dioxide, water, methane, biomass or inorganic compounds. This breakdown of polymer chains is catalyzed by the enzymatic action of microorganisms. [44] However, in order to define the biodegradability of a material more precisely it is necessary to specify the environmental conditions and disposal pathways (e.g. sewage treatment, composting, anaerobic sludge treatment, or denitrification) as well as the timeframe during which the degradation takes place [45]. To determine whether a polymer is biodegradable, several standardized testing methods have been established by standardization organizations like the International Standards Organization (ISO), the American Society for Testing and Material (ASTM) or the European Committee for Standardization (CEN). A variety of standard test methods for aerobic and anaerobic degradation in defined environments are available that help to examine the biodegradability of a polymer in an objective way.

Very often deterioration, the loss of physical integrity or the breakdown into smaller polymer particles are mistaken for biodegradation. Fragmentation of a polymer or deterioration can lead to smaller polymer particles. However, this does not mean that the polymer is removed from the environment – quite the contrary it distributes the fragments even wider into the environment [46]. Certain physical-chemical factors like light (photo degradation), heat (thermal degradation) and moisture as well as chemical hydrolysis can lead to deterioration of plastics [46-48].

During deterioration and degradation processes the polymer backbone is (partly) cleaved resulting in distinct changes of the material properties (e.g. discoloration, changes of mechanical, optical or electrical characteristics, crazing, cracking, erosion, phase separation, delamination, change of molecular weight, etc.) [47, 49].

From a biochemical point of view, biodegradation can be distinguished between aerobic and anaerobic biodegradation. In the simplified example given below, $C_{polymer}$ represents a polymer or polymer fragment that consists of carbon, hydrogen and oxygen only. Other elements that might be incorporated into a real polymer would appear in an oxidized or reduced form depending on the availability or absence of oxygen during biodegradation. [45]

Aerobic Biodegradation:

$$C_{polymer} + O_2 \rightarrow CO_2 + H_2O + C_{residue} + C_{biomass}$$

Anaerobic biodegradation:

$$C_{polymer} \rightarrow CO_2 + CH_4 + H_2O + C_{residue} + C_{biomass}$$

When no residual organic material ($C_{residue}$) remains, we speak of complete biodegradation and mineralization is reached if the substrate (here $C_{polymer}$) is completely converted into salts, and inorganic compounds like CO_2, ammonia and H_2O [50]. In nature, aerobic degradation processes are the predominant once while anaerobic degradation occurs in sediments, landfills or biogas plants [51].

The biodegradation of a polymer is a multi step reaction and usually requires numerous microbial communities to be successful [52]. Typically, at least one organism is able to cleave the polymer into smaller oligomers or monomeric subunits, others use these monomers and generate simpler “waste products” and finally these simpler molecules are metabolized by further organisms [47]. Microorganisms that are present in aerobic habitats like in upper soil layers and compost as well as organisms in anaerobic environments like biogas plants or deeper soil layers are not able to take up the large polymers directly, but they need to cleave the polymer into smaller water-soluble intermediates [53]. The initial depolymerization in a biodegradation process is usually catalyzed by extracellular enzymes that are able to adsorb to the polymer surface and cleave distinct chemical bonds (e.g. ester bonds, amide bonds, etc.). Enzymes are not able to penetrate deeper into the polymer structure and for that reason the surface of a polymer is eroded layer by layer. During this enzyme catalyzed erosion process monomers and water-soluble intermediates are formed that are small enough to be transported into the cell. As a consequence, the molecules are introduced into the metabolic pathway and finally new biomass as well as metabolic end products like water, carbon dioxide or methane (during anaerobic processes) are formed. [28, 30] A sketch of the polymer biodegradation process can be found in Figure 6.

Biodegradation can be facilitated by abiotic processes [51] and physical forces. Examples are the molecular weight decreased and mechanical destruction of a polymer by photo degradation, freezing/thawing, heating/cooling or wetting/drying [54, 55]. Due to this fragmentation of the polymer, the surface accessible for hydrolytic enzymes is enlarged and biodegradation is accelerated.

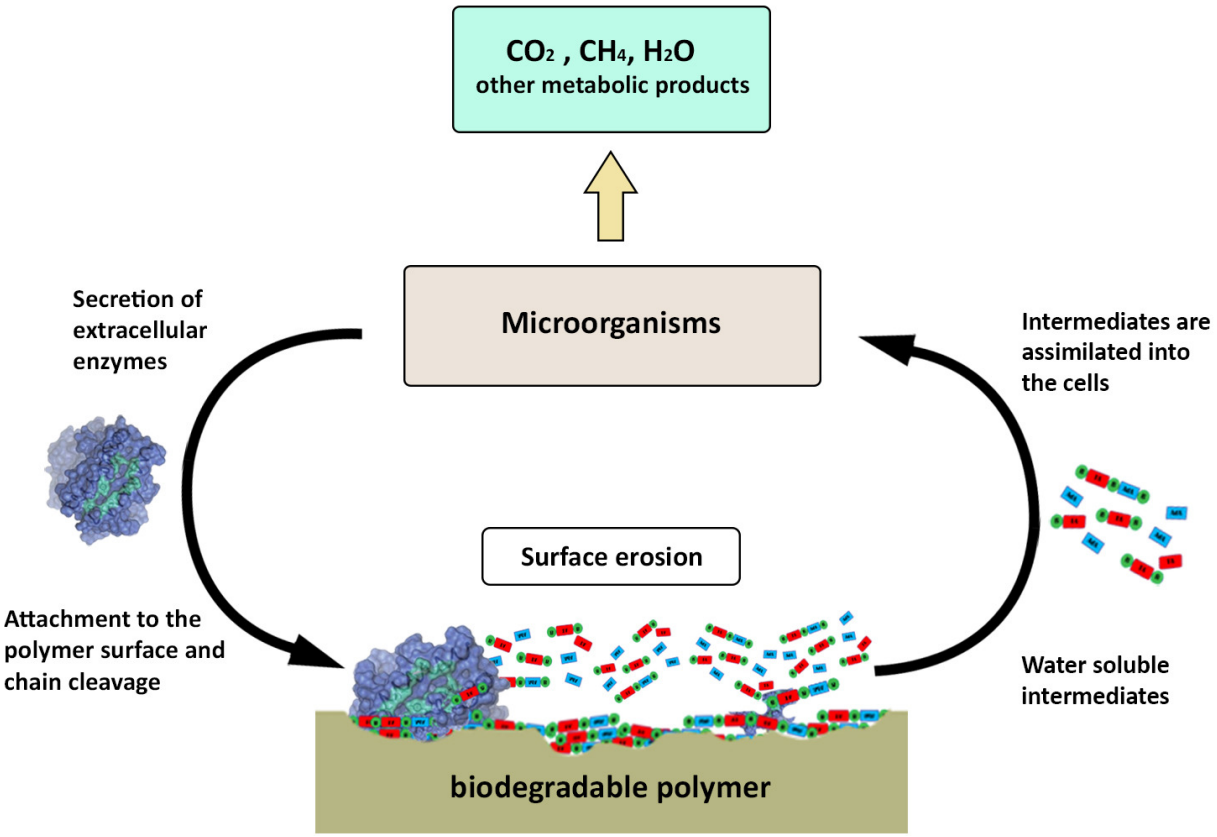

Figure 6: Biodegradation of a biodegradable polymer. Microorganisms secret hydrolytic enzymes that can adsorb to the surface of the polymer. These enzymes catalyze surface erosion of the polymer and water-soluble intermediates are generated. The released oligomeric or monomeric intermediates are small enough to migrate through the cell membrane and are metabolized intracellularly. Metabolic by product like carbon dioxide, methane and water are released. [30, 56]

Several environmental factors like pH, soil or sludge structure, temperature, redox potential, moisture, presence of inhibitors, presence or absence of oxygen and nutrients have an influence on the biodegradability of a polymer. Additionally, the adaptation, activity, abundance and diversity of present microorganisms affect the biodegradation. From a chemical point of view the hydrophobicity, molecular weights, melting temperatures as well as the crystallinities of the polymers play an important role when it comes to biodegradation. [46]

1.4 Anaerobic biodegradation – the biogas process

In the last years, anaerobic degradation processes came into the focus of policy makers as an alternative to conventional composting of organic waste, due to the following reasons: The global greenhouse emission needs to be reduced [57], fossil-fuel reserves decline and additionally the treatment of organic municipal and household waste in biogas plants opens the possibility to recover energy and reduces the overall quantities of waste [58]. Very often, the production of biogas is also a first step towards energy autarchy. Frequently, anaerobic digestion is performed in combination with post-composting to degrade residual organic waste [59]. Biogas is a flexible carrier for renewable energy and can be used e.g. as vehicle fuel as well as for heat and power generation [60].

The production of methane during anaerobic fermentation is a complex process that involves four main phases called hydrolysis, fermentation or acidogenesis, acetogenesis/dehydrogenation and methanogenesis [61].

Hydrolysis of complex organic polymers including proteins, lipids and polysaccharides is the first step during the anaerobic degradation process. Extracellular hydrolytic enzymes convert these high molecular weight compounds into soluble molecules that are small enough to enter the bacterial cells. Since hydrolysis is quite slow and energy consuming, it is the limiting factor during biogas production. [62, 63]

In a second step called *fermentation or acidogenesis*, facultative anaerobic and anaerobic bacteria degrade the monomers further through various fermentative pathways. A number of products including organic acids, alcohols, hydrogen, carbon dioxide, organic-nitrogen and organic-sulfur compounds are created. Here, acetate represents the most important product, since it can be metabolized directly by methanogenic bacteria. [64]

Thereafter, acetate is formed during *acetogenesis*. Acetogenic bacteria transform low molecular weight fatty acids into acetate, carbon dioxide and hydrogen. The removal of hydrogen gas is a crucial factor during this reaction step, since the accumulation of hydrogen might inhibit the metabolism of acetogenic bacteria. [60, 63, 65]

Methanogenesis: Finally, strictly anaerobic methanogenic bacteria produce methane through conversion of acetate (65%) or hydrogenophilic methanogenic bacteria reduce carbon dioxide with the help of hydrogen (35%) [64, 66]. Figure 7 gives an overview about the process steps involved in biogas formation.

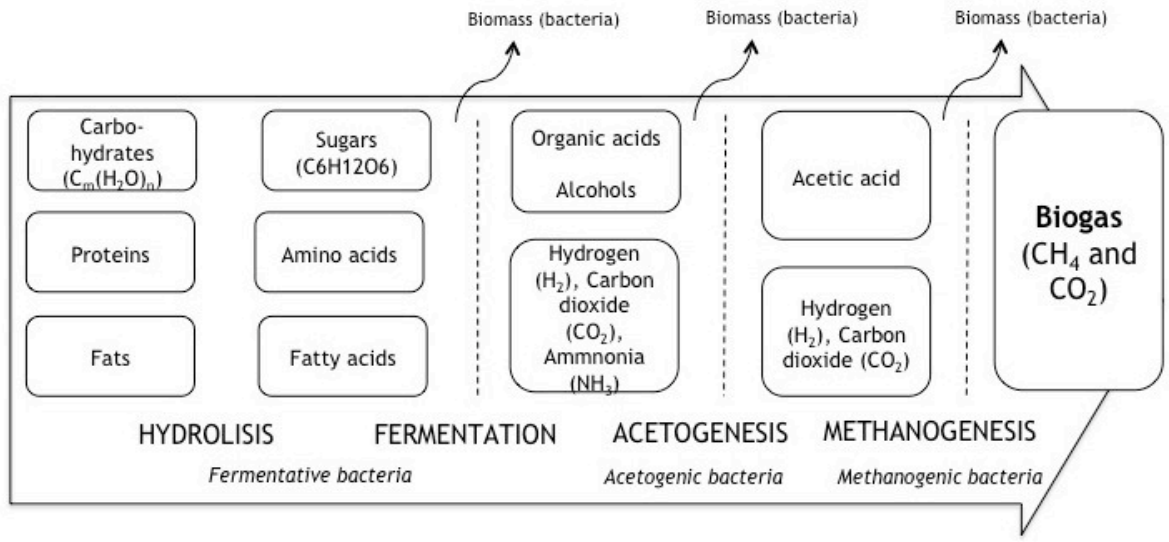

Figure 7: The four phases of biogas production [67].

1.4.1 Microorganisms from anaerobic habitats

The four degradation steps described above are accomplished by diverse microbial consortia that are partly in a syntrophic interaction [61]. Table 3 lists some of the bacteria and archaea involved in the different steps of a biogas process. *Clostridia*, belonging to the phylum of *Firmicutes*, are omnipresent in anaerobic consortia [60, 68] and predominantly involved in the hydrolysis and fermentation steps (Table 3). Since *Clostridia* were also identified in biogas sludge that was known to degrade Ta [69] and they were reported to hydrolyze the polyesters poly(β-hydroxybutyrate) (PHB) and poly(β-caprolactone [70] they represented an interesting source for enzymes during this thesis.

Table 3: Microorganisms involved in the production of methanol. (Adapted from [64, 71].)

Process step	Bacterial group	Conversion	Microorganism
Hydrolysis	Hydrolytic bacteria	Proteins→soluble peptides and amino acids	*Clostridium, Proteus vulgaris, Peptococcus, Bacteroides, Bacillus, Vibrio,*
		Carbohydrates → soluble sugars	*Clostridium, Acetovibrio celluliticus, Staphylococcus, Bacteroides,*
		Lipids → higher fatty acids, alcohols and glycerol	*Clostridium, Micrococcus, Staphylococcus,*
Fermentation	Acidogenic bacteria	Amino acids → fatty acids, acetate and NH_3	*Lactobacillus, Escherichia, Staphylococcus, Bacillus, Pseudomonas, Desulfovibrio, Selenomonas, Sarcina, Veillonella, Streptococcus, Desulfobacter, Desolforomonas,*
		Sugars → intermediate fermentation products	*Clostridium, Eubacterium limosum, Streptococcus,*
Acetogenesis	Acetogenic bacteria	Higher fatty acids or alcohols → hydrogen and acetate	*Clostridium, Syntrophomonas wolfei,*
		Volatile fatty acids and alcohols → hydrogen and acetate	*Syntrophomonas wolfei, Syntrophobacter wolinii,*
Methanogenesis	Carbon dioxide reducing methanogens	Hydrogen and carbon dioxide → methane	*Methanobacterium, Methanobrevibacter, Methanoplanus, Methanospirillum,*
	Aceticlastic methanogens	Acetate → methane and carbon dioxide	*Methanosaeta, Methanosarcina,*

1.5 Enzymatic polyester hydrolysis

Enzymes that hydrolyze natural polyesters are known to either act endo-wise (hydrolyzing within the polymer chain) or exo-wise (hydrolyzing terminal building blocks) on the polymer. This general mode of hydrolysis was probably most extensively studied on endo- and exo-glucanases that play an important role during the degradation of lignocellulose [72]. Endo-/exo-wise means in other words that the enzyme either hydrolyzes randomly more in the middle of the polymer chain (endo-wise) or sequentially cuts off (monomeric) subunits from the chain ends (exo-wise). For an efficient total hydrolysis both types of enzymes (exo and endo) are needed while for initial disintegration of materials endo-wise hydrolysis is sufficient.

Looking at synthetic polymers, several factors influence the biodegradability. First, the appropriate flexibility of the polymer chain if of major importance for an effective enzymatic hydrolysis. Moreover, the active site of the enzyme must be reachable for the polymer. [20, 28, 46]

Usually, synthetic polymers are easier degraded by the action of microorganisms and the activity of enzymes, if the carbon chain in the polymer backbone is interrupted by C-C double bonds, oxygen or nitrogen atoms. Beside the influence of the chemical structure, the enzymatic hydrolysis is dependent on various parameters like polymer crystallinity [73], melting point [74] or tacticity [75]. Enzymes hydrolyze preferably the amorphous or less ordered regions of a polymer [73]. Generally it can be said, that the polymer biodegradation is faster and more effective, the softer (lower T_m value) and the smaller the molecular weight as well as the more hydrophilic the polymer is. Concerning chemical bonds present in the polymer the general rule of thumb for degradability is: esters > ethers > amides > urethanes. In this thesis, the focus is on polyesters. [76]

1.6 Polyester hydrolyzing enzymes

So far, enzymes with hydrolytic activity on polyesters are primarily found within the enzyme family of hydrolases. Examples for members of this enzyme family that have been reported to hydrolyze (synthetic) polymers including esterases (EC 3.1.1.1), cutinases (3.1.1.74), lipases (EC 3.1.1.3), proteases (EC 3.4.X.X.) and PHA depolymerases (EC 3.1.1.75.) are summarized in Table 4.

Table 4: Hydrolases with activity on different polyesters. PBA: poly(butylene adipate), PBAT: poly(butylene adipate-co-butylene terephthalate), PBS: poly(butylene succinate), PBSA: poly(butylene succinate-co-butylene adipate), PBST: poly(butylene succinate-co-butylene terephthalate), PBSTIL: poly(butylene succinate/terephthalate/isophthalate-co-lactate), PCL: poly(ε-caprolactone), PES: poly(ethylene succinate), PET: poly(ethylene terephthalate), PHA: poly(hydroxylalkanoate), PHB: poly(hydroxybutyrate), PHBV: poly(hydroxybutyrate-co-hydroxyvalerate), PHO: poly(hydroxyoctanoate), PHV: poly(hydroxyvalerat), PLA: poly(lactic acid), PTT: poly(trimethylene terephthalate). Adapted and extended from Shah et al. [48]

Enzyme	Microorganism	Activity on Polyester	Reference
Esterases	*Thermobifida alba* Est119	PET	Hu et al. [77]
	Roseateles depolymerans strain TB-87	PES, PCL, PBS, PBSA, PBST, PBAT, PBSTIL	Shah et al. [78, 79]
	Leptothrix sp. strain TB-71	PES, PCL, PLA, PBSA, PBST, PBAT, PBSTIL	Nakajima-Kambe et al. [80, 81]
	Clostridium botulinum ATCC 3502	PBAT	Perz et al. [38]
	Clostridium hathewayi DSM-13479	PBAT	Perz et al. [39]
	Thermobifida halotolerans	PET, PLA	Ribitsch et al. [82]
Cutinases	*Pseudozyma antarctica* JCM10317	PCL, PLA, PBS, PBSA	Shinozaki et al. [83]
	Thermobifida cellulosilytica DSM44535	PET, PBAT, PBA	Herrero Acero et al. [84, 85] Perz et al. [34, 86]
	Thermobifida alba	PET	Ribitsch et al. [87]
	Thermobifida fusca	PTT	Eberl et al. [88]
	Aspergillus oryzae RIB40	PBS	Maeda et al. [89]
	Cryptococcus sp. strain S2	PCL, PLA	Masaki et al. [90] Kawai et al. [91]
	Saccharomonospora viridis	PBAT, PET	Kawai et al. [92] Miyakawa et al. [93]
	Humicola insolens	PBAT, PET	Perz et al. [34]
Lipases	*Paenibacillus amylolyticus*	PLA	Akutsu-Shigeno et al. [94]
	Thermomyces lanuginosus	PTT	Eberl et al. [88]
	Pelosinus fermentans DSM-17108	PBAT	Biundo et al. [40]
Protease	*Cryptococcus sp.* strain S2	PLA	Kawai et al. [91]
PHA depolymerases	*Pseudomonas lemoignei*	PHV	Schöber et al. [95]
	Bacillus thuringiensis	PHB/PHBV	Tseng et al. [96]
	Streptomyces sp. strain AF-111	PHBV	Akbar et al. [97]
	Pseudomonas fluorescens	PHO, PHA	Schirmer et al. [98] Ihssen et al. [99]

The focus of this thesis lays on cutinases and esterases. More detailed information about these enzymes is presented below.

1.6.1 Esterases and Lipases

Esterases (3.1.1.X.) catalyze the formation and hydrolysis of carboxyl ester bonds and belong to the enzyme group of carboxylesterases, also referred to as carboxylester hydrolases. Originally, they were distinguished between lipolytic lipases (EC 3.1.1.3, triacylglycerol hydrolases), that catalyze the conversion of water insoluble long chain triacylglycerols and (carboxyl)esterases (EC 3.1.1.1) that cleave water soluble esters. In the meantime, this classification based on the substrate specificities turned out to be ambiguous since there exists a broad range of overlapping substrate preferences. [100, 101]

Both enzymes possess the typical α/β-hydrolase fold in their three dimensional structure [102]. Figure 8 presents a schematic illustration of an α/β-hydrolase fold. The catalytic triad consists typically of Ser-Asp-His, although Glu replaces Asp in some lipases. Moreover, a consensus sequence (Gly-x-Ser-x-Gly) is usually found around the active site serine. A further motif that has been reported consists of Gly-x-x-Leu. [103, 104]

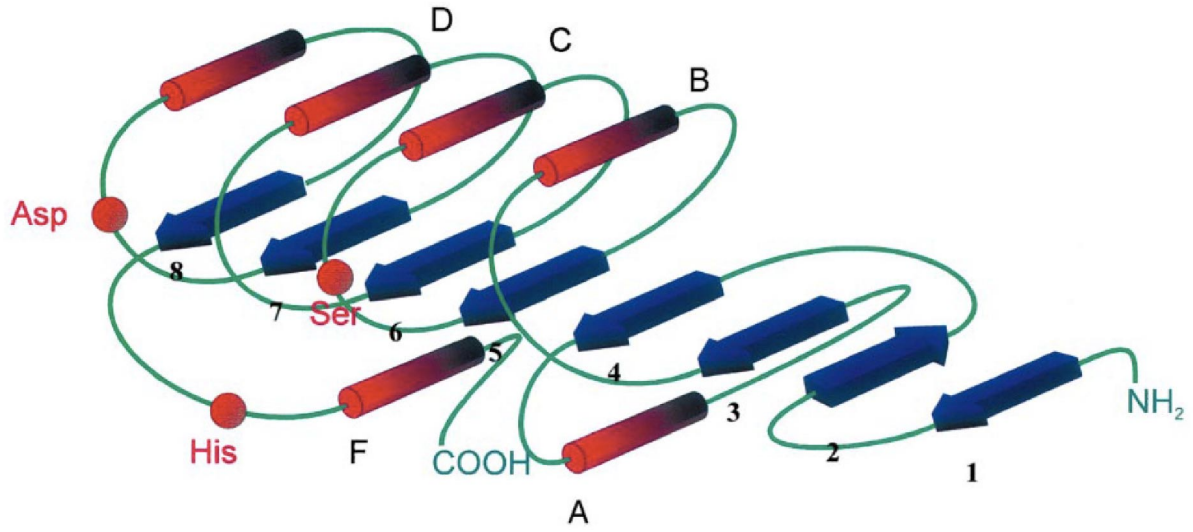

Figure 8: Schematic illustration of the characteristic α/β-hydrolase fold. Red columns present α-helices (A-F) and blue arrows show β-sheets (1-8). The position of the catalytic triad amino acids (Ser, His, Asp) is indicated by red dots. [104]

Chahiniana and co-workers suggested to distinguish lipases and esterases by their kinetic behavior on long chain esters (e.g. olive oil or vinyl laurate) and short chain esters like p-nitrophenyl butyrate, vinyl acetate or vinyl propionate. The short chain length esters that are partially soluble in water are hydrolyzed by lipases and esterases, while long chain length esters are only cleaved by lipases. Moreover, they suggested that the kinetic properties of the two enzymes showed a noticeable difference for short chain length substrates. The hydrolysis rate of lipases reached its maximum after ester saturation was exceeded - leading

already to formation of emulsions. In contrast to that, esterases revealed their maximum activity at lower ester concentrations under the critical micelle concentration. [101]

Besides these findings, esterases can be discriminate from lipases due to so called “interfacial activation”, which was only reported for the latter. Esterases act on Michaelis-Menten kinetic, on the contrary, lipases require a minimum substrate concentration until activity is perceived. This behavior is due to the fact that a hydrophobic domain called “lid” covers the active site of lipases. As soon as a minimum substrate concentration, a hydrophobic organic solvent or triglyceride phase is present, the lipase (i.e. lid) undergoes a conformation change and the active site gets accessible. [104]

1.6.2 Cutinases

Cutinases (EC 3.1.1.74.) are serine hydrolases that can be numbered among the α/β-hydrolase superfamily. In contrast to lipases, cutinases do not possess a catalytic lid that covers the active side and oil-water interfacial effects do not activate their activity. For that reason, the active side is wide enough to interact with high molecular weight polyesters including synthetic ones. The active site itself exhibits the typical catalytic triad of serine-histidine-aspartate. In nature cutinases are secreted by bacteria or fungi and catalyze the hydrolysis of cutin, which consists basically of hydroxylated C18- and C16 fatty acids that are linked with ester bonds (see Figure 9). Cutin is a waxy like polyester that covers the surface of plants, e.g. apples or tomatoes. [105] Together with esterases, a huge variety of cutinases was already proven to catalyze synthetic polyesters (see Table 4, Chapter 1.6), thus they are interesting biocatalysts for industrial applications.

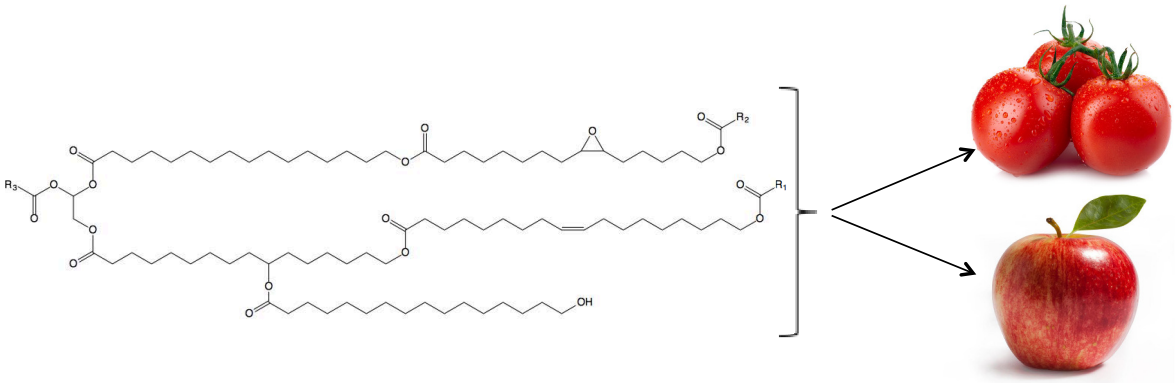

Figure 9: Cutin, the major compound of the protective layer (=cuticle) of plants that coats e.g. tomatoes or apples.

1.7 Potential applications for polyester active enzymes in industrial processes

Generally, the aim of using enzyme during industrial applications is to obtain more sustainable processes, that can be performed at lower temperatures, moderate pHs, without the addition of toxic or harmful solvents and chemicals. Ideally these enzymatic processes are cheaper, faster, save energy and water and lead to equal or even improved product quality when compared to conventional processes. In fact, enzymes could enable reactions that are not possible with conventional methods.

So far, enzymes are used e.g. as food and feed additives, for production of drugs and fine chemicals, in personal care products, soaps and cleaners, or agricultural chemicals. Lipases are reported to be used in the pulp and paper, food, baking, fat, oil and leather industry. Moreover, beside other enzymes, lipases are frequently added to e.g. washing powders and detergents in order to remove grease and protein residues from fabrics. [106, 107] Potential industrial applications for lipases include the synthesis of flavor compounds, biopolymers, enantiopure pharmaceuticals, agrochemicals and biodiesel [108].

Generally, esterases have been reported to be useful biocatalysts for enantioselective applications in organic chemistry, and could outperform conventional chemical synthesis in terms of enantioselectivity. This is of relevance for fine chemicals including the pharmaceutical industry. However, esterases still need to get more efficient for these industrial applications. [100]

Cutinase are able to catalyze esterifications, transesterifications and hydrolysis reactions. For that reason they have a broad field of potential applications in e.g. environmental, textile, food, chemical or detergent industries. [109] Cutinases have already shown potential for the removal of coatings [110], in the functionalization of polyesters [111] and the recycling of polymers [30]. In environmental applications, cutinases could help to biodegrade polymers, pesticides and other waste [112-114].

Cutinases could enable environmental friendlier production steps in the textile industry. One example is the removal of the cuticle layer of the cotton fiber during the production step called cotton sourcing. This process step is necessary to improve the wettability of the fiber, which is essential for proper dyeing and finishing. [115, 116] Similarly, lipases can assist in textile industry to remove size lubricants in order to receive fabrics with improved absorbency, which is important to obtain sufficient levelness after dyeing [117].

Synthetic fibers like PET are frequently used as textile fibers. Like cotton fibers, also synthetic fabrics need to undergo process steps similar to the sourcing of cotton to improve the wettability of the final product. Since cutinases are able to hydrolyze ester bonds on the

surface of the textile, they can help to increase the hydrophilicity of the PET textile. The advantage compared to traditional methods is, that only the surface of the fabric is affected but the fabric strength stays intact. [118-120]

Enzymes including polyesters active ones are already used in a multitude of industrial processes and products. Due to the discovery of novel enzymes and developments in biotechnology, biocatalysts will enter even more production steps and products if not even products and processes we would not think of today.

1.8 References

[1] R.C. Thompson, S.H. Swan, C.J. Moore, F.S. vom Saal, Our plastic age, Philos Trans R Soc Lond B Biol Sci 364(1526) (2009) 1973-6.

[2] F.H. Aamer Ali Shah, Abdul Hameed, Safia Ahmed, Biological degradation of plastics: A comprehensive review, Biotechnology Advances 26 (2008) 246-265.

[3] J.W. Nicholson, The Chemistry of Polymers, 4th edition ed., RSC Publishing, Cambridge, UK, 2012.

[4] H.-G. Elias, Plastics, General Survey, Ullmann's Encyclopedia of Industrial Chemistry, Wiley-VCH Verlag GmbH & Co. KGaA2000.

[5] A.L. Andrady, M.A. Neal, Applications and societal benefits of plastics, Philosophical Transactions of the Royal Society B: Biological Sciences 364(1526) (2009) 1977-1984.

[6] C.Y. Barlow, D.C. Morgan, Polymer film packaging for food: An environmental assessment, Resources, Conservation and Recycling 78 (2013) 74-80.

[7] N.G. McCrum, C.P. Buckley, C.B. Bucknall, Principles of polymer engineering, 2nd edition ed., Oxford University Press Inc., New York, 1997.

[8] Plastics Europe, Plastics - the Facts 2014/2015. 2015 (http://www.plasticseurope.org/ accessed 29.09.2015.).

[9] D.K.A. Barnes, F. Galgani, R.C. Thompson, M. Barlaz, Accumulation and fragmentation of plastic debris in global environments, Philosophical Transactions of the Royal Society of London B: Biological Sciences 364(1526) (2009) 1985-1998.

[10] A. Lechner, H. Keckeis, F. Lumesberger-Loisl, B. Zens, R. Krusch, M. Tritthart, M. Glas, E. Schludermann, The Danube so colourful: A potpourri of plastic litter outnumbers fish larvae in Europe's second largest river, Environ Pollut 188(100) (2014) 177-81.

[11] M. Cole, P. Lindeque, C. Halsband, T.S. Galloway, Microplastics as contaminants in the marine environment: A review, Marine Pollution Bulletin 62(12) (2011) 2588-2597.

[12] P.G. Ryan, C.J. Moore, J.A. van Franeker, C.L. Moloney, Monitoring the abundance of plastic debris in the marine environment, Philos Trans R Soc Lond B Biol Sci 364(1526) (2009) 1999-2012.

[13] R.C. Thompson, Y. Olsen, R.P. Mitchell, A. Davis, S.J. Rowland, A.W.G. John, D. McGonigle, A.E. Russell, Lost at Sea: Where Is All the Plastic?, Science 304(5672) (2004) 838-838.

[14] M. Wagner, J. Oehlmann, Endocrine disruptors in bottled mineral water: Estrogenic activity in the E-Screen, The Journal of Steroid Biochemistry and Molecular Biology 127(1–2) (2011) 128-135.

[15] H.M. Koch, A.M. Calafat, Human body burdens of chemicals used in plastic manufacture, Philosophical Transactions of the Royal Society B: Biological Sciences 364(1526) (2009) 2063-2078.

[16] Plastics Europe, Plastics - the Facts 2015. 2015 (http://www.plasticseurope.org/ accessed 17.05.2016.).

[17] R.C. Thompson, C.J. Moore, F.S. vom Saal, S.H. Swan, Plastics, the environment and human health: current consensus and future trends, Philosophical Transactions of the Royal Society of London B: Biological Sciences 364(1526) (2009) 2153-2166.

[18] J. Hopewell, R. Dvorak, E. Kosior, Plastics recycling: challenges and opportunities, Philosophical Transactions of the Royal Society of London B: Biological Sciences 364(1526) (2009) 2115-2126.

[19] P.T. Anastas, P.H. Bickart, M.M. Kirchhoff, Designing Safer Polymers, John Wiley and Sons, Wiley - Intersciences, New York, 2000.

[20] R. Chandra, R. Rustgi, Biodegradable polymers, Progress in Polymer Science 23(7) (1998) 1273-1335.

[21] W.H. Carothers, Studies on polymerization and rinf formation. I. An introduction to the general theory of condensation polymers, Journal of the American Chemical Society 51(8) (1929) 2548-2559.

[22] P.J. Flory, Principles of Polymer Chemistry, Cornell University Press, Ithaca, New York, 1953.

[23] E. Winkler, H. Pielartzik, A. Schneller, Funktionspolymere-ein interdisziplinäres Forschungsgebiet, Die Angewandte Makromolekulare Chemie 244(1) (1997) 161-181.

[24] H. Kaeb, F. Aeschelmann, L. Dammer, M. Carus, Market study on consumption of biodegradable and compostable plastic products in Europe, Nova-Institut GmbH, Huerth, Germany, 2016.

[25] D.M. Teegarden, Polymer chemistry: Introduction to an inidspensable science, NSTA press, National Science Teachers Association, Arlington, Virginia, 2004.

[26] Z. Zhang, O. Ortiz, R. Goyal, J. Kohn, S. Ebnesajjad, Biodegradable Polymers, Handbook of Polymer Applications in Medicine and Medical Devices, William Andrew Publishing, Oxford, 2014, pp. 303-335.

[27] I. Vroman, L. Tighzert, Biodegradable polymers, Materials 2(2) (2009) 307-344.

[28] E. Marten, R.-J. Mueller, W.-D. Deckwer, Studies on the enzymatic hydrolysis of polyesters I. Low molecular mass model esters and aliphatic polyesters, Polymer Degradation and Stability 80(3) (2003) 485-501.

[29] U. Witt, R.-J. Müller, J. Augusta, H. Widdecke, W.-D. Deckwer, Synthesis, properties and biodegradability of polyesters based on 1,3-propanediol, Macromolecular Chemistry and Physics 195(2) (1994) 793-802.

[30] R.-J. Mueller, Biological degradation of synthetic polyesters—Enzymes as potential catalysts for polyester recycling, Process Biochemistry 41(10) (2006) 2124-2128.

[31] U. Witt, R.-J. Müller, W.-D. Deckwer, Biodegradation behavior and material properties of aliphatic/aromatic polyesters of commercial importance, Journal of environmental polymer degradation 5(2) (1997) 81-89.

[32] U. Witt, R.-J. Müller, W.-D. Deckwer, New biodegradable polyester-copolymers from commodity chemicals with favorable use properties, Journal of environmental polymer degradation 3(4) (1995) 215-223.

[33] U. Witt, R.J. Müller, W.D. Deckwer, Biodegradation of Polyester Copolymers Containing Aromatic Compounds, Journal of Macromolecular Science, Part A 32(4) (1995) 851-856.

[34] V. Perz, K. Bleymaier, C. Sinkel, U. Kueper, M. Bonnekessel, D. Ribitsch, G.M. Guebitz, Substrate specificities of cutinases on aliphatic–aromatic polyesters and on their model substrates, New Biotechnology 33(2) (2016) 295-304.

[35] U. Witt, T. Einig, M. Yamamoto, I. Kleeberg, W.D. Deckwer, R.J. Müller, Biodegradation of aliphatic–aromatic copolyesters: evaluation of the final biodegradability and ecotoxicological impact of degradation intermediates, Chemosphere 44(2) (2001) 289-299.

[36] U. Witt, M. Yamamoto, U. Seeliger, R.-J. Müller, V. Warzelhan, Biodegradable Polymeric Materials—Not the Origin but the Chemical Structure Determines Biodegradability, Angewandte Chemie International Edition 38(10) (1999) 1438-1442.

[37] T. Kijchavengkul, R. Auras, M. Rubino, S. Selke, M. Ngouajio, R.T. Fernandez, Biodegradation and hydrolysis rate of aliphatic aromatic polyester, Polymer Degradation and Stability 95(12) (2010) 2641-2647.

[38] V. Perz, A. Baumschlager, K. Bleymaier, S. Zitzenbacher, A. Hromic, G. Steinkellner, A. Pairitsch, A. Lyskowski, K. Gruber, C. Sinkel, U. Kuper, D. Ribitsch, G.M. Guebitz, Hydrolysis of synthetic polyesters by Clostridium botulinum esterases, Biotechnol Bioeng 113(5) (2016) 1024-34.

[39] V. Perz, A. Hromic, A. Baumschlager, G. Steinkellner, T. Pavkov-Keller, K. Gruber, K. Bleymaier, S. Zitzenbacher, A. Zankel, C. Mayrhofer, C. Sinkel, U. Kueper, K. Schlegel, D. Ribitsch, G.M. Guebitz, An Esterase from Anaerobic Clostridium hathewayi Can Hydrolyze Aliphatic–Aromatic Polyesters, Environmental Science & Technology 50(6) (2016) 2899-2907.

[40] A. Biundo, A. Hromic, T. Pavkov-Keller, K. Gruber, F. Quartinello, K. Haernvall, V. Perz, M.S. Arrell, M. Zinn, D. Ribitsch, G.M. Guebitz, Characterization of a poly(butylene adipate-co-terephthalate)-hydrolyzing lipase from Pelosinus fermentans, Applied Microbiology and Biotechnology 100(4) (2016) 1753-1764.

[41] F. Aeschelmann, M. Carus, W. Baltus, H. Blum, R. Busch, D. Carrez, C. Issbruecker, H. Kaeb, K.-B. Lange, J. Philip, J. Ravenstijn, H. von Pogrell, Bio-based Building Blocks and Polymers in the World – Capacities, Production and Applications: Status Quo and Trends toward 2020, nova-Institut GmbH, Huerth, Germany, 2015, p. 474.

[42] Y.-X. Weng, Y.-J. Jin, Q.-Y. Meng, L. Wang, M. Zhang, Y.-Z. Wang, Biodegradation behavior of poly(butylene adipate-co-terephthalate) (PBAT), poly(lactic acid) (PLA), and their blend under soil conditions, Polymer Testing 32(5) (2013) 918-926.

[43] T.P. de Camargo Andrade-Molina, M.A. Shirai, M. Victória Eiras Grossmann, F. Yamashita, Active biodegradable packaging for fresh pasta, LWT - Food Science and Technology 54(1) (2013) 25-29.

[44] J.H. Song, R.J. Murphy, R. Narayan, G.B.H. Davies, Biodegradable and compostable alternatives to conventional plastics, Philosophical Transactions of the Royal Society of London B: Biological Sciences 364(1526) (2009) 2127-2139.

[45] C. Bastioli, Handbook of biodegradable polymers, Rapra Technology, Shawbury, Shrewsbury, Shropshire, 2005.

[46] A.C. Palmisano, C.A.C. Pettigrew, Biodegradability of Plastics, BioScience 42(9) (1992) 680-685.

[47] A.A. Shah, F. Hasan, A. Hameed, S. Ahmed, Biological degradation of plastics: A comprehensive review, Biotechnology Advances 26(3) (2008) 246-265.

[48] A.A. Shah, S. Kato, N. Shintani, N.R. Kamini, T. Nakajima-Kambe, Microbial degradation of aliphatic and aliphatic-aromatic co-polyesters, Appl Microbiol Biotechnol 98(8) (2014) 3437-47.

[49] J. Pospíšil, S. Nešpůrek, Highlights in chemistry and physics of polymer stabilization, Macromolecular Symposia 115(1) (1997) 143-163.

[50] A.L. Andrady, Assessment of Environmental Biodegradation of Synthetic Polymers, Journal of Macromolecular Science, Part C 34(1) (1994) 25-76.

[51] J.-D. Gu, Microbiological deterioration and degradation of synthetic polymeric materials: recent research advances, International Biodeterioration & Biodegradation 52(2) (2003) 69-91.

[52] C.-L. Chen, H. Macarie, I. Ramirez, A. Olmos, S.L. Ong, O. Monroy, W.-T. Liu, Microbial community structure in a thermophilic anaerobic hybrid reactor degrading terephthalate, Microbiology 150(10) (2004) 3429-3440.

[53] G. Swift, Non-medical biodegradable polymers: environmentally degradable polymers, in: K.J. Domb AJ, Wisman DM (Ed.), Handbook of Biodegradable Polymers, Harwood Academic, Amsterdam, 1997, pp. 473-511.

[54] D. Kockott, Techniques and Mechanisms of Polymer Degradation and StabilizationNatural and artificial weathering of polymers, Polymer Degradation and Stability 25(2) (1989) 181-208.

[55] M. Kamal, B. Huang, Natural and artificial weathering of polymers, in: A.M.M.A. Hamid SH (Ed.), Handbook of Polymer Degradation, Marcel Dekker Inc., New York, 1992, pp. 127-68.

[56] K. Bleymaier, Polyester degrading enzymes from anaerobic sources, Graz University of Technology, Graz, 2015, p. 86.

[57] IPCC, Special report on emission scenarios, in: N. Nakicenovic, R. Swart (Eds.) Cambridge University Press, Geneva, Switzerland, 2000.

[58] S. Zafar, Waste as a renewable energy source. (http://www.alternative-energy-news.info/waste-renewable-energy-source/ accessed 19.05.2016.).

[59] N.-B. Chang, A. Pires, Sustainable Solid Waste Management: A Systems Engineering Approach, John Wiley & Sons Inc., Hoboken, New Jersey, 2015.

[60] P. Weiland, Biogas production: current state and perspectives, Applied Microbiology and Biotechnology 85(4) (2010) 849-860.

[61] I. Angelidaki, L. Ellegaard, B.K. Ahring, A mathematical model for dynamic simulation of anaerobic digestion of complex substrates: Focusing on ammonia inhibition, Biotechnology and Bioengineering 42(2) (1993) 159-166.

[62] P.L. McCarty, F.E. Mosey, Modelling of Anaerobic Digestion Processes (A Discussion of Concepts), Water Science and Technology 24(8) (1991) 17-33.

[63] S.G. Pavlostathis, E. Giraldo‐Gomez, Kinetics of anaerobic treatment: A critical review, Critical Reviews in Environmental Control 21(5-6) (1991) 411-490.

[64] S.E. Nayono, Anaerobic digestion of organic solid waste for energy production, KIT Scientific Publishing, Karlsruhe, 2009.

[65] M.H. Gerardi, The Microbiology of Anaerobic Digesters, John Wiley & Sons, Hoboken, New Jersey, 2003.

[66] O.R. Kotsyurbenko, K.-J. Chin, M.V. Glagolev, S. Stubner, M.V. Simankova, A.N. Nozhevnikova, R. Conrad, Acetoclastic and hydrogenotrophic methane production and methanogenic populations in an acidic West-Siberian peat bog, Environmental Microbiology 6(11) (2004) 1159-1173.

[67] D. Spuhler, Anaerobic Digestion (General). 2010 (http://www.sswm.info/content/anaerobic-digestion-general accessed 19.05.2016.).

[68] L. Krause, N.N. Diaz, R.A. Edwards, K.-H. Gartemann, H. Krömeke, H. Neuweger, A. Pühler, K.J. Runte, A. Schlüter, J. Stoye, R. Szczepanowski, A. Tauch, A. Goesmann, Taxonomic composition and gene content of a methane-producing microbial community isolated from a biogas reactor, Journal of Biotechnology 136(1–2) (2008) 91-101.

[69] A. Lykidis, C.L. Chen, S.G. Tringe, A.C. McHardy, A. Copeland, N.C. Kyrpides, P. Hugenholtz, H. Macarie, A. Olmos, O. Monroy, W.T. Liu, Multiple syntrophic interactions in a terephthalate-degrading methanogenic consortium, ISME J 5(1) (2011) 122-30.

[70] D.M. Abou-Zeid, R.J. Muller, W.D. Deckwer, Degradation of natural and synthetic polyesters under anaerobic conditions, J Biotechnol 86(2) (2001) 113-26.

[71] S. Stronach, T. Rudd, J. Lester, Anaerobic Digestion Processes in Industrial Wastewater Treatment, Springer, Berlin, 1986.

[72] R. Kumar, S. Singh, O. Singh, Bioconversion of lignocellulosic biomass: biochemical and molecular perspectives, Journal of Industrial Microbiology & Biotechnology 35(5) (2008) 377-391.

[73] M. Mochizuki, M. Hirano, Y. Kanmuri, K. Kudo, Y. Tokiwa, Hydrolysis of polycaprolactone fibers by lipase: Effects of draw ratio on enzymatic degradation, Journal of Applied Polymer Science 55(2) (1995) 289-296.

[74] Y. Tokiwa, T. Ando, T. Suzuki, K. Takeda, Biodegradation of Synthetic Polymers Containing Ester Bonds, Agricultural and Synthetic Polymers, American Chemical Society1990, pp. 136-148.

[75] P.J. Hocking, M.R. Timmins, T.M. Scherer, R.C. Fuller, R.W. Lenz, R.H. Marchessault, Enzymatic Degradability of Poly(β-Hydroxybutyrate) as a Function of Tacticity, Journal of Macromolecular Science, Part A 32(4) (1995) 889-894.

[76] K.S. Mohan, T. Srivastava, Microbial deterioration and degradation of polymeric materials, Journal of Biochemical Technology 2(4) (2010) 210-215.

[77] X. Hu, U. Thumarat, X. Zhang, M. Tang, F. Kawai, Diversity of polyester-degrading bacteria in compost and molecular analysis of a thermoactive esterase from Thermobifida alba AHK119, Applied Microbiology and Biotechnology 87(2) (2010) 771-779.

[78] A.A. Shah, T. Eguchi, D. Mayumi, S. Kato, N. Shintani, N.R. Kamini, T. Nakajima-Kambe, Purification and properties of novel aliphatic-aromatic co-polyesters degrading enzymes from newly isolated Roseateles depolymerans strain TB-87, Polymer Degradation and Stability 98(2) (2013) 609-618.

[79] A.A. Shah, T. Eguchi, D. Mayumi, S. Kato, N. Shintani, N.R. Kamini, T. Nakajima-Kambe, Degradation of aliphatic and aliphatic–aromatic co-polyesters by depolymerases from Roseateles depolymerans strain TB-87 and analysis of degradation products by LC-MS, Polymer Degradation and Stability 98(12) (2013) 2722-2729.

[80] T. Nakajima-Kambe, F. Ichihashi, R. Matsuzoe, S. Kato, N. Shintani, Degradation of aliphatic–aromatic copolyesters by bacteria that can degrade aliphatic polyesters, Polymer Degradation and Stability 94(11) (2009) 1901-1905.

[81] T. Nakajima-Kambe, K. Toyoshima, C. Saito, H. Takaguchi, Y. Akutsu-Shigeno, M. Sato, K. Miyama, N. Nomura, H. Uchiyama, Rapid monomerization of poly(butylene succinate)-co-(butylene adipate) by Leptothrix sp, Journal of Bioscience and Bioengineering 108(6) (2009) 513-516.

[82] D. Ribitsch, E. Herrero Acero, K. Greimel, A. Dellacher, S. Zitzenbacher, A. Marold, R.D. Rodriguez, G. Steinkellner, K. Gruber, H. Schwab, G.M. Guebitz, A New Esterase from Thermobifida halotolerans Hydrolyses Polyethylene Terephthalate (PET) and Polylactic Acid (PLA), Polymers 4(1) (2012) 617-629.

[83] Y. Shinozaki, T. Morita, X.H. Cao, S. Yoshida, M. Koitabashi, T. Watanabe, K. Suzuki, Y. Sameshima-Yamashita, T. Nakajima-Kambe, T. Fujii, H.K. Kitamoto, Biodegradable plastic-degrading enzyme from Pseudozyma antarctica: cloning, sequencing, and characterization, Appl Microbiol Biotechnol 97(7) (2013) 2951-9.

[84] E. Herrero Acero, D. Ribitsch, A. Dellacher, S. Zitzenbacher, A. Marold, G. Steinkellner, K. Gruber, H. Schwab, G.M. Guebitz, Surface engineering of a cutinase from Thermobifida cellulosilytica for improved polyester hydrolysis, Biotechnol. Bioeng. in press (2013).

[85] E. Herrero Acero, D. Ribitsch, G. Steinkellner, K. Gruber, K. Greimel, I. Eiteljoerg, E. Trotscha, R. Wei, W. Zimmermann, M. Zinn, A. Cavaco-Paulo, G. Freddi, H. Schwab, G. Guebitz, Enzymatic Surface Hydrolysis of PET: Effect of Structural Diversity on Kinetic Properties of Cutinases from Thremobifida, Macromolecules 44(12) (2011) 4640-4640.

[86] V. Perz, M.T. Zumstein, M. Sander, S. Zitzenbacher, D. Ribitsch, G.M. Guebitz, Biomimetic Approach to Enhance Enzymatic Hydrolysis of the Synthetic Polyester Poly(1,4-butylene adipate): Fusing Binding Modules to Esterases, Biomacromolecules (2015).

[87] D. Ribitsch, E. Herrero Acero, K. Greimel, I. Eiteljoerg, E. Trotscha, G. Freddi, H. Schwab, G.M. Guebitz, Characterization of a new cutinase from Thermobifida alba regarding PET-surface hydrolysis, Biocatalysis and Biotransformation 30(1) (2012) 2-9.

[88] A. Eberl, S. Heumann, R. Kotek, F. Kaufmann, S. Mitsche, A. Cavaco-Paulo, G.M. GÃ¼bitz, Enzymatic hydrolysis of PTT polymers and oligomers, Journal of Biotechnology 135(1) (2008) 45-51.

[89] H. Maeda, Y. Yamagata, K. Abe, F. Hasegawa, M. Machida, R. Ishioka, K. Gomi, T. Nakajima, Purification and characterization of a biodegradable plastic-degrading enzyme from Aspergillus oryzae, Applied Microbiology and Biotechnology 67(6) (2005) 778-788.

[90] K. Masaki, N.R. Kamini, H. Ikeda, H. Iefuji, Cutinase-Like Enzyme from the Yeast Cryptococcus sp. Strain S-2 Hydrolyzes Polylactic Acid and Other Biodegradable Plastics, Applied and Environmental Microbiology 71(11) (2005) 7548-7550.

[91] F. Kawai, K. Nakadai, E. Nishioka, H. Nakajima, H. Ohara, K. Masaki, H. Iefuji, Different enantioselectivity of two types of poly(lactic acid) depolymerases toward poly(l-lactic acid) and poly(d-lactic acid), Polymer Degradation and Stability 96(7) (2011) 1342-1348.

[92] F. Kawai, M. Oda, T. Tamashiro, T. Waku, N. Tanaka, M. Yamamoto, H. Mizushima, T. Miyakawa, M. Tanokura, A novel Ca2+-activated, thermostabilized polyesterase capable of hydrolyzing polyethylene terephthalate from Saccharomonospora viridis AHK190, Applied Microbiology and Biotechnology 98(24) (2014) 10053-10064.

[93] T. Miyakawa, H. Mizushima, J. Ohtsuka, M. Oda, F. Kawai, M. Tanokura, Structural basis for the Ca-enhanced thermostability and activity of PET-degrading cutinase-like enzyme from Saccharomonospora viridis AHK190, Appl Microbiol Biotechnol (2014).

[94] Y. Akutsu-Shigeno, T. Teeraphatpornchai, K. Teamtisong, N. Nomura, H. Uchiyama, T. Nakahara, T. Nakajima-Kambe, Cloning and sequencing of a poly(DL-lactic acid) depolymerase gene from Paenibacillus amylolyticus strain TB-13 and its functional expression in Escherichia coli, Appl Environ Microbiol 69(5) (2003) 2498-504.

[95] U. Schöber, C. Thiel, D. Jendrossek, Poly(3-Hydroxyvalerate) Depolymerase ofPseudomonas lemoignei, Applied and Environmental Microbiology 66(4) (2000) 1385-1392.

[96] C.-L. Tseng, H.-J. Chen, G.-C. Shaw, Identification and Characterization of the Bacillus thuringiensis phaZ Gene, Encoding New Intracellular Poly-3-Hydroxybutyrate Depolymerase, Journal of Bacteriology 188(21) (2006) 7592-7599.

[97] S. Akbar, F. Hasan, A. Nadhman, S. Khan, A.A. Shah, Production and Purification of Poly(3-hydroxybutyrate-co-3-hydroxyvalerate) Degrading Enzyme from Streptomyces sp. AF-111, Journal of Polymers and the Environment 21(4) (2013) 1109-1116.

[98] A. Schirmer, D. Jendrossek, H.G. Schlegel, Degradation of poly(3-hydroxyoctanoic acid) [P(3HO)] by bacteria: purification and properties of a P(3HO) depolymerase from Pseudomonas fluorescens GK13, Appl Environ Microbiol 59(4) (1993) 1220-7.

[99] J. Ihssen, D. Magnani, L. Thöny-Meyer, Q. Ren, Use of Extracellular Medium Chain Length Polyhydroxyalkanoate Depolymerase for Targeted Binding of Proteins to Artificial Poly[(3-hydroxyoctanoate)-co-(3-hydroxyhexanoate)] Granules, Biomacromolecules 10(7) (2009) 1854-1864.

[100] D. Romano, F. Bonomi, M.C. de Mattos, T. de Sousa Fonseca, M.d.C.F. de Oliveira, F. Molinari, Esterases as stereoselective biocatalysts, Biotechnology Advances 33(5) (2015) 547-565.

[101] H. Chahiniana, L. Sarda, Distinction Between Esterases and Lipases: Comparative Biochemical Properties of Sequence-Related Carboxylesterases, Protein & Peptide Letters 16(10) (2009) 1149-1161.

[102] D.L. Ollis, E. Cheah, M. Cygler, B. Dijkstra, F. Frolow, S.M. Franken, M. Harel, S.J. Remington, I. Silman, J. Schrag, The α/β hydrolase fold, Protein engineering 5(3) (1992) 197-211.

[103] Y. Wei, J.L. Schottel, U. Derewenda, L. Swenson, S. Patkar, Z.S. Derewenda, A novel variant of the catalytic triad in the Streptomyces scabies esterase, Nat Struct Biol 2(3) (1995) 218-23.

[104] U.T. Bornscheuer, Microbial carboxyl esterases: classification, properties and application in biocatalysis, FEMS microbiology reviews 26(1) (2002) 73-81.

[105] S. Chen, L. Su, J. Chen, J. Wu, Cutinase: characteristics, preparation, and application, Biotechnol Adv 31(8) (2013) 1754-67.

[106] A. Schmid, F. Hollmann, J.B. Park, B. Bühler, The use of enzymes in the chemical industry in Europe, Current Opinion in Biotechnology 13(4) (2002) 359-366.

[107] O. Kirk, T.V. Borchert, C.C. Fuglsang, Industrial enzyme applications, Current Opinion in Biotechnology 13(4) (2002) 345-351.

[108] K.E. Jaeger, T. Eggert, Lipases for biotechnology, Curr Opin Biotechnol 13(4) (2002) 390-7.

[109] C.M.L. Carvalho, M.R. Aires-Barros, J.M.S. Cabral, Cutinase structure, function and biocatalytic applications, Electronic Journal of Biotechnology 1(3)(15) (1998) 160-173.

[110] K. Greimel, A. Marold, C. Sohar, R. Feola, A. Temel, T. Schoenbacher, E. Herrero Acero, G.M. Guebitz, Enzymatic hydrolysis of polyester based coatings, Reactive and Functional Polymers 73(10) (2013) 1335-1339.

[111] G.M. Guebitz, A. Cavaco-Paulo, Enzymes go big: surface hydrolysis and functionalisation of synthetic polymers, Trends in biotechnology 26(1) (2008) 32-38.

[112] I. Kleeberg, C. Hetz, R.M. Kroppenstedt, R.-J. Müller, W.-D. Deckwer, Biodegradation of Aliphatic-Aromatic Copolyesters by Thermomonospora fusca and Other Thermophilic Compost Isolates, Applied and Environmental Microbiology 64(5) (1998) 1731-1735.

[113] H. Bhardwaj, R. Gupta, A. Tiwari, Communities of Microbial Enzymes Associated with Biodegradation of Plastics, Journal of Polymers and the Environment 21(2) (2013) 575-579.

[114] K. Dutta, S. Sen, V.D. Veeranki, Production, characterization and applications of microbial cutinases, Process Biochemistry 44(2) (2009) 127-134.

[115] P.B. Agrawal, V.A. Nierstrasz, G.H. Bouwhuis, M.M.C.G. Warmoeskerken, Cutinase and pectinase in cotton bioscouring: an innovative and fast bioscouring process, Biocatalysis and Biotransformation 26(5) (2008) 412-421.

[116] Y. Zhang, S. Chen, M. Xu, A. Cavaco-Paulo, J. Wu, J. Chen, Characterization of Thermobifida fusca Cutinase-Carbohydrate-Binding Module Fusion Proteins and Their Potential Application in Bioscouring, Applied and Environmental Microbiology 76 (2010) 6870-6876.

[117] F. Hasan, A.A. Shah, A. Hameed, Industrial applications of microbial lipases, Enzyme and Microbial Technology 39(2) (2006) 235-251.

[118] Å.M. Ronkvist, W. Xie, W. Lu, R.A. Gross, Cutinase-Catalyzed Hydrolysis of Poly(ethylene terephthalate), Macromolecules 42(14) (2009) 5128-5138.

[119] M. Alisch-Mark, A. Herrmann, W. Zimmermann, Increase of the hydrophilicity of polyethylene terephthalate fibres by hydrolases from Thermomonospora fusca and Fusarium solani f. sp. pisi, Biotechnology Letters 28(10) (2006) 681-685.

[120] T. Brueckner, A. Eberl, S. Heumann, M. Rabe, G.M. Guebitz, Enzymatic and Chemical Hydrolysis of Poly(ethylene terephthalate) Fabrics, Journal of Polymer Science Part A: Polymer Chemistry 46 (2008) 6435-6443.

2

2 Aim

This thesis was embedded in a project between the Austrian centre of industrial biotechnology (acib) and an industrial partner. The main research interest was to get a better understanding of the biodegradation mechanism of the synthetic aliphatic-aromatic polyester poly(butylene adipate-co-butylene terephthalate) (PBAT) under anaerobic conditions. For that reason enzymes involved in the hydrolysis processes during the biodegradation should be investigated. Enzymes are responsible for the initial step in microbial mineralization of polyesters, catalyzing the break down, i.e. hydrolysis, of the polymer chain. While several studies have already proven the biodegradability of PBAT under aerobic conditions (including composting), hardly any information was so far available about the anaerobic biodegradation of this polymer. Moreover, there was a lack of knowledge about the enzymes from aerobic and anaerobic organisms involved in these biodegradation processes. Hence, the identification of novel enzymes from anaerobic organisms with hydrolytic activities on PBAT and the examination of PBAT biodegradation in anaerobic environments were additional major goals.

To accomplish these tasks several strategies should be developed in parallel. A variety of oligomeric model substrates as well as PBAT variants of different compositions were synthesized to assess the biodegradability of the different compounds by means of enzymatic hydrolysis experiments.

First, cutinases that have been reported in the past to show activity on polyesters like polyethylene terephthalate (PET) should be tested for their ability to hydrolyze PBAT as well as oligomeric and polymeric PBAT model substrates to serve as a sequence model for in-vitro identification of anaerobic polyesterases. In anaerobic batch tests the hydrolysis rates of PBAT in anaerobic environments should be investigated. An *in-silico* screening should be the starting point for the identification of novel polyester hydrolyzing esterases, which in a next step should be heterologously expressed in *E. coli* and characterized in detail. Finally, the general strategy to mimic nature and improve the activity of a cutinase towards polymers by fusion to a polymer binding module should be studied.

3

3 Publications

The five papers published throughout this PdD thesis can be found in the Appendix page 39 ff.

3.1 Substrate specificities of cutinases on aliphatic-aromatic polyesters and on their model substrates

(See Appendix page 40 ff)

3.2 Data on synthesis of oligomeric and polymeric poly(butylene adipate-co-butylene terephthalate) model substrates for the investigation of enzymatic hydrolysis

(See Appendix page 50 ff)

3.3 An esterase from anaerobic *Clostridium hathewayi* can hydrolyze aliphatic-aromatic polyesters

(See Appendix page 58 ff)

3.4 Hydrolysis of synthetic polyesters by *Clostridium botulinum* esterases

(See Appendix page 79 ff)

3.5 Biomimetic approach to enhance enzymatic hydrolysis of the synthetic polyester poly(1,4-butylene adipate): Fusing binding modules to esterases

(See Appendix page 94 ff)

4

4 General Conclusion

This thesis was part of a project that was a cooperation between ACIB GmbH and an industrial partner. The aim was to investigate the biodegradation of the aliphatic-aromatic copolyester (poly(butylene adipate-co-butylene terephthalate)) (short PBAT, commercial product called ecoflex) under anaerobic conditions. The main research focus was the mechanistic investigation of the enzymatic hydrolysis process as well as the identification of novel polyesterases from anaerobic organisms.

In a first step, two well-known cutinases from aerobic soil and compost inhabitants were investigated to get a first impression of the PBAT hydrolysis. Cutinase 1 from the bacterial strain *Thermobifida cellulosilytica* (Thc_Cut1) and the fungal cutinase from *Humicola insolens* (HiC) have already been investigated in the past and were proven to hydrolyze the aromatic polyester polyethylene terephthalate (PET). Because of that, it stood to reason that these enzymes would also show activity on the aliphatic-aromatic polyester PBAT. Previously, it was demonstrated that cutinases or cutinase like enzymes hydrolyze synthetic polyesters but until now no model substrates with systematic variation of the content of the aromatic constituent terephthalic acid and the chain length of the acids and alcohols were used for enzymatic hydrolysis tests. Beside the commercial polyester PBAT, that contains adipic acid (Ada) and terephthalic acid (Ta) in a ratio of approximately 50:50, six polymeric model substrates with modified Ada:Ta ratios were tested with regard to their enzymatic degradability. These polymeric model substrates exhibited Ta:Ada ratios between 0 mol% Ta and 50 mol% Ta. Moreover, the enzymatic hydrolysis of eight systematically designed oligomeric model substrates with variations of the chain length of the terminal alcohol and acid as well as with varying content of the aromatic component Ta was investigated.

A suitable RP-HPLC method was developed. HPLC based quantification of the main hydrolysis products indicated that HiC and Thc_Cut1 indeed hydrolyze the tested esters. It was remarkable that Thc_Cut1 had a higher affinity to aromatic ester bonds than HiC

resulting in up to three times higher concentration of the aromatic hydrolysis product Ta. Yet, the total amount of released compounds was two times higher after incubation with HiC, meaning that this enzyme exhibited a higher overall hydrolytic activity.

The melting temperatures (T_m) of the tested polyesters were measured through Thermogravimetry and Differential Scanning Calorimetry (TG-DSC). Taking into account these T_m values, it was seen that a lower difference between T_m and the incubation temperature during enzymatic hydrolysis had a positive effect on the hydrolysis rates. At higher incubation temperatures, the polymer chain is more susceptible to the enzymatic hydrolysis - most likely due to higher flexibility of the polymer chain.

Quantification of the released molecules after incubation of oligomeric model substrates with the two cutinases revealed that longer terminal chain length alcohols but shorter chain length acids were hydrolyzed more efficiently.

In a second approach, the biodegradation of PBAT in biogas batches was tested. During these anaerobic batch experiments, imaging methods (CLSM, SEM) and quantification of hydrolysis products clearly demonstrated anaerobic hydrolysis of PBAT and PBAT model substrates in biogas sludge. Accumulation of Ta was observed in the biogas batches within the first two weeks of incubation with the polyester and oligomeric model substrate. After that, Ta concentrations decreased. Presumably, the present microorganisms metabolize Ta after a certain adaptation time. This is in agreement with previous studies that also reported a lag phases until Ta was metabolized. Nevertheless, the measured hydrolysis rates were too low for an effective PBAT hydrolysis in industrial biogas plants.

For that reason, novel polyester hydrolyzing enzymes and their anaerobic microbial producers should be identified and tested. An extensive literature study revealed that potential enzymes of interest are expected within the group of *Clostridium*, because different species had been described to be involved in polymer degradation (e.g. cellulose, poly(β-hydroxybutyrate) or poly(ε-caprolactone)) and *Clostridia* are omnipresent in anaerobic digestion processes. Several extracellular serine hydrolases like lipases, esterases, carboxylesterases and cutinases were already known to hydrolyze synthetic polyesters. Based on these findings, an *in-silico* screening was performed and a number of potentially interesting enzymes could be identified. The genes of interest were codon optimized for expression in *E. coli* BL21-Gold(DE3). Finally, two new esterases from *Clostridium botulinum* ATCC 3502 (Cbotu_EstA and Cbotu_EstB) as well as one esterase from *Clostridium hathewayi* (Chath_Est1) were successfully expressed in good protein yields.

The purified esterase Chath_Est1 was characterized in detail. Only few esterases from anaerobic organisms are known so far. Analysis of the X-ray crystal structure revealed

that Chath_Est1 belongs to the family of α/β-hydrolases, consisting of a central β-sheet surrounded by α-helices. Chath_Est1 showed hydrolytic activity on PBAT and oligomeric model substrates. Even though these results already gave a first hint that microorganisms in anaerobic habitats can degrade man-made PBAT, the decision was to further explore the PBAT degradation ability of risk 1 strain *Clostridium hathewayi*. To do so, *Clostridium hathewayi* cell cultures were incubated with PBAT and indeed hydrolysis products of PBAT were found, implying that this strain shows activity on the man-made polyester. Although previously the enzymatic hydrolysis of PBAT was described, this is the first report about an enzyme from an anaerobic microorganism hydrolyzing this polymer.

Hydrolysis experiments with both purified *Clostridium botulinum* esterases exhibited that the polyesterase activity of Cbotu_EstA on PBAT was six times higher than that of Cbotu_EstB. Moreover, k_{cat} values of Cbotu_EstA on soluble esterase substrates *para*-nitrophenyl acetate and *para*-nitrophenyl butyrate were significantly higher. The typical serine hydrolase active site residues of Ser, Asp and His were found in both enzymes with some differences near the active site aspartate.

Comparing the Cbotu_EstA crystal structure and Cbotu_EstB model, it was seen that the entrance to the Cbotu_EstB active site appears more narrowed. Additionally, Cbotu_EstB is missing the N-terminal extension that forms an arm around the cap domains in the case of Cbotu_EstB. It is very likely that conformation changes are needed to enable the polymeric substrates to access the active site. Consequently, the absence of this N-terminus may be the reason for the lower polyester activity of Cbotu_EstB and its lower stability. The presence of a central β-sheet surrounded by α-helices indicates that Cbotu_EstA belongs to the family of α/β-hydrolases. Beyond that, it is the first polyesterase containing a Zn^{2+} binding site. Since this Zn^{2+} binding site is at a substantial distance to the active site, it is not likely that it has direct influence on the catalytic activity. Perhaps the metal coordination has an effect on the thermostability of the enzyme as also suggested for a similar lipase from *Geobacillus*.

Finally, the effect of a polymer binding module (PBM) of a polyhydroxyalkanoate depolymerase from *Alcaligenes faecalis* fused to the polyester active cutinase Thc_Cut1 was studied. The idea was based on previous studies from our group that indicated enhanced hydrolysis of PET by Thc_Cut1 fused to different binding domains. PBM was attached to the cutinase via two different linker sequences of varying length. The longer linker length decreased the solubility of the enzyme, while no significant increase of polyester activity was observed. For that reason, the cutinase Thc_Cut1_PBM with shorter (natural) linker length was used for further experiments. Inactive mutants of Thc_Cut1 and Thc_Cut1_PBM were

created through site-directed mutagenesis of serine 131 to alanine. Polyester poly(1,4-butylene adipate) (PBA) was used as model substrate in all experiments. The enzymatically catalyzed PBA hydrolysis was followed over time by means of Quartz Crystal Microbalance with dissipation monitoring (QCM-D) analysis and HPLC quantification of the released hydrolysis product adipic acid. With the help of the inactive cutinase mutants it was shown that the adsorption of the cutinase to the PBA film was increased when fused to PBM. QCM-D experiments revealed that inactive cutinases linked with the binding module led to a higher initial mass increase than cutinases without the PBM. Moreover, the active fusion protein Thc_Cut1_PBM hydrolyzed PBA thin films twice as fast (within 40 min) as the native Thc_Cut1. Similar results were obtained during HPLC quantification of release adipic acid and suggested that the activity of an enzyme hydrolyzing polyester can actually be improved by fusion to the naturally occurring binding module.

To sum up, it can be stated that the presented studies reveal essential information, showing that there is a fine line between reasonable material properties and appropriate biodegradability. The novel *Clostridium* esterases are the first described enzymes from anaerobic sources with activity on synthetic polyesters and give a clear hint how PBAT could be degraded in anaerobic environments. The investigation of enzymatic hydrolysis mechanisms helps to understand biodegradation processes and provides important information for industrial applications of these enzymes including polyester modification and recycling. Additionally, information about polyester hydrolyzing microorganisms might lead to novel applications like addition of cell or spore suspensions to biogas plants in order to accelerate polyester biodegradation. Finally, mimicking nature was proven to be one prosperous approach to further increase the activity of enzymes towards defined polymeric substrates by fusion to polymer binding modules.

5

5 Appendix

5.1 List of Publications

5.1.1 Papers

1) **Perz, V**; Bleymaier, K; Sinkel, C; Kueper, U; Bonnekessel, M; Ribitsch, D; Guebitz, GM.: Substrate specificities of cutinases on aliphatic-aromatic polyesters and on their model substrates, NEW BIOTECHNOLOGY. 2016; 33(2): 295-304. (DOI:10.1016/j.nbt.2015.11.004)

2) **Perz, V**; Bleymaier, K; Sinkel, C; Kueper, U; Bonnekessel, M; Ribitsch, D; Guebitz, GM.: Data on synthesis of oligomeric and polymeric poly(butylene adipate-co-butylene terephthalate) model substrates for the investigation of enzymatic hydrolysis, DATA IN BRIEF. 2016; 7: 291-298. (DOI: 10.1016/j.dib.2016.02.029)

3) **Perz, V**; Baumschlager, A; Bleymaier, K; Zitzenbacher, S; Hromic, A; Steinkellner, G; Pairitsch, A; Łyskowski, A; Gruber, K; Sinkel, C; Kueper, U; Ribitsch, D; Guebitz, GM.: Hydrolysis of synthetic polyesters by *Clostridium botulinum* esterases, BIOTECHNOLOGY AND BIOENGINEERING. 2016; 113(5): 1024-1034. (DOI: 10.1002/bit.25874)

4) **Perz, V**; Hromic, A; Baumschlager, A; Steinkellner, G; Pavkov-Keller, T; Gruber, K; Bleymaier, K; Zitzenbacher, S; Zankel, A; Mayrhofer, C; Sinkel, C; Kueper, U; Schlegel, K; Ribitsch, D; Guebitz, GM.: An esterase from anaerobic *Clostridium hathewayi* can hydrolyze aliphatic-aromatic polyesters, ENVIRONMENTAL SCIENCE AND TECHNOLOGY. 2016; 50(6): 2899-2907. (DOI: 10.1021/acs.est.5b04346)

5) **Perz, V**; Zumstein, MT; Sander, M; Zitzenbacher, S; Ribitsch, D; Guebitz, GM.: Biomimetic approach to enhance enzymatic hydrolysis of the synthetic polyester poly(1,4-butylene adipate) – Fusing binding modules to esterases, BIOMACROMOLECULES. 2015; 16(12): 2889-3896. (DOI: 10.1021/acs.biomac.5b01219)

6) Biundo, A; Hromic, A; Pavkov-Keller, T; Gruber, K; Quartinello, F; Haernvall, K; **Perz, V**; Arrell, MS; Zinn, M; Ribitsch, D; Guebitz, GH.: Characterization of a poly(butylene adipate-co-terephthalate)-hydrolyzing lipase from Pelosinus fermentans, APPLIED MICROBIOLOGY AND BIOTECHNOLOGY, 2016; 100(4): 1753-1764. (DOI: 10.1007/s00253-015-7031-1)

7) Greimel, KJ; **Perz, V**; Koren, K; Feola, R; Temel, A; Sohar, C; Acero, EH; Klimant, I; Guebitz, GM.: Banning toxic heavy-metal catalysts from paints: enzymatic cross-linking of alkyd resins, GREEN CHEMISTRY. 2013; 15(2): 381-388. (DOI: 10.1039/C2GC36666E)

8) Hou, S; Hoyle, DM; Haernvall, K; **Perz, V**; Guebitz, GM; Khosravi, E; Blackwell, CJ.: Hydrolytic degradation of ROMP thermosetting materials catalysed by bio-derived acids and enzyme: from network to linear materials, GREEN CHEMISTRY. 2016, submitted.

9) Müller, CA[‡]; **Perz, V**[‡]; Provasnek, C; Quartinello, F; Gübitz, GM; Berg, G.: Hydrolysis of synthetic polyesters by esterases from *Sphagnum* moss-associated bacteria, in preparation.
[‡] shared first co-authors

5.1.2 Oral presentations as presenting author

FEMS 2015 – Maastricht – The Netherlands
Perz, V; Herrero Acero, E; Zitzenbacher, S; Sinkel, C; Kueper, U; Bonnekessel, M; Ribitsch, D; Guebitz, GM; Polymer Biotechnology: Biomimetic concepts, 6th Congress of European Microbiologists, JUNE 7-11, 2015, Maastricht, The Netherlands

Acib Science Days 2015 – Bad Radkersburg – Austria
Perz, V; Haernvall, K; Ribitsch, D; Guebitz, GM; Biodegradable polymers – The enzyme perspective, Acib Science Days 2015, MAY 4-5, 2015, Bad Radkersburg, Austria

Bimate – Slovenj Gradec - Slovenia

Perz, V; Haernvall, K; Sinkel, C; Kueper, U; Bonnekessel, M; Ribitsch, D; Guebitz, GM; Cutinases for aliphatic-aromatic polyester biodegradation, Biopolymer materials and engineering, APR 15-17, 2015, Slovenj Gradec, Slovenia

Biogas Science 2014 – Vienna - Austria

Perz, V; Bleymaier, K; Baumschlager, A; Łyskowski, A; Hromic, A; Gruber, K; Zankel, A; Sinkel, C; Kueper, U; Bonnekessel, M; Ribitsch, D; Guebitz, GM; New enzymes for the degradation of polyesters under anaerobic conditions, Biogas Science 2014, OCT 26-30, 2014, Vienna, Austria

ECB2015 – Edinburgh - Scotland

Perz, V; Baumschlager, A; Bleymaier, K; Lyskowski, A; Hromic, A; Gruber, K; Sinkel, C; Kuper, U; Bonnekessel, M; Ribitsch, D; Guebitz, G; Esterases from Clostridium are involved in anaerobic degradation of synthetic polyester, European Congress on Biotechnology – ECB16, JULY 13-16, 2014, Edinburgh, Scotland

Acib 5 year evaluation – Graz – Austria

Perz, V; Herrero Acero, E; Guebitz, G; Enzymatic hydrolysis of aliphatic-aromatic polyesters in anaerobic environments, Acib 5 year evaluation, MAY 6-7, 2014, Graz, Austria

IPTB - Braga – Portugal

Perz, V; Ribitsch, D; Sinkel, C; Kueper, U; Bonnekessel, M; Guebitz, GM;. Mechanistic insights into enzymatic hydrolysis of biodegradable polyesters, 8th International Conference on Polymer and Fiber Biotechnology, MAY 25-27, 2014, Braga, Portugal

5.1.3 Poster presentations (most relevant)

Biotrans 2015 – Vienna – Austria (Best poster award!)

Perz, V; Baumschlager, A; Bleymaier, K; Hromic, A; Lyskowski, A; Gruber, K; Sinkel, C; Kueper, U; Ribitsch, D; Guebitz, G M; Identification of two novel anaerobic esterases from *Clostridium*, Biotrans 2015, JULY, Vienna, Austria

FEMS 2015 – Maastricht – The Netherlands

Perz, V; Baumschlager, A; Bleymaier, K; Łyskowski, A; Hromic, A; Gruber, K; Zankel, A; Sinkel, C; Kueper, U; Bonnekessel, M; Ribitsch, D; Guebitz, GM; Novel polyesterases involved in anaerobic degradation of synthetic polymers by Clostridium spp., 6th Congress of European Microbiologists, JUNE 7-11, 2015, Maastricht, The Netherlands

ÖGMBT Annual Meeting 2014 – Vienna – Austria

Perz, V; Ribitsch, D; Herrero Acero, E; Zitzenbacher, S; Kubicek CP; Druzhinina, IS; Sinkel, C; Küper, U; Bonnekessel, M; Gübitz, GM; Biomimetic concepts for enzymatic modification of synthetic polymers, 6th ÖGMBT Annual Meeting, SEPT 15-18, 2014, Vienna, Austria

MoDeSt – Portoroz – Slovenia

Perz, V; Ribitsch, D; Härnvall, K; Ihssen, J; Sinkel, C; Küper, U; Bonnekessel, M; Gübitz, GM; New aspects of enzyme based degradation of synthetic polyesters, MoDeSt 2014, AUG 31-SEPT 4, 2014, Portoroz, Slovenia

Applications for Enzyme Technologies 2013 – San Francisco – USA

Perz, V; Ribitsch, D; Sinkel, C; Küper, U; Bonnekessel, M; Gübitz, G M; Enzymatic degradation of polyester materials, Applications for Enzyme Technologies, JUNE 17-18, 2013, San Francisco, USA

5.1.4 Patents

Sinkel, C; Kueper, U; Weingarten, M; Kuenkel, A; Guebitz, G; Ribitsch, D; **Perz, V**; Degradation of polyesters under anaerobic conditions, European Patent Application No: EP 2 876 157 A1

Feola, R; Schonbacher, T; Temel, A; Urbano, E; Ferk, O; Gubitz, G; Herrero Acero, E; Greimel, K; **Perz, V**; Suljanovic, A; Process for curing surface-coating compositions, United States Patent Application No: 2014/0356540 A1

Feola, R; Schönbacher, T; Temel, A; Urbano, E; Ferk, O; Gübitz, G; Herrero Acero, E; Greimel, K; **Perz, V**; Verfahren zur Härtung von Oberflächenbeschichtungsmitteln, Internationale Veröffentlichungsnummer: WO 2012/085016 A1

5.2 Publications that are part of this Ph.D. thesis

On the following pages, the five papers published during the course of this thesis are attached.

New Biotechnology • Volume 33, Number 2 • March 2016 RESEARCH PAPER

Research Paper

Substrate specificities of cutinases on aliphatic–aromatic polyesters and on their model substrates

Veronika Perz[1], Klaus Bleymaier[2], Carsten Sinkel[3], Ulf Kueper[3], Melanie Bonnekessel[3], Doris Ribitsch[1,4] and Georg M. Guebitz[1,4]

[1] acib – Austrian Centre of Industrial Biotechnology, Konrad Lorenz Strasse 20, 3430 Tulln, Austria
[2] acib – Austrian Centre of Industrial Biotechnology, Petersgasse 14, 8010 Graz, Austria
[3] BASF SE, Carl-Bosch-Strasse 38, 67056 Ludwigshafen, Germany
[4] Institute of Environmental Biotechnology, University of Natural Resources and Life Sciences, Konrad Lorenz Strasse 20, 3430 Tulln an der Donau, Austria

The enzymatic hydrolysis of the biodegradable polyester ecoflex and of a variety of oligomeric and polymeric ecoflex model substrates was investigated. For this purpose, substrate specificities of two enzymes of typical compost inhabitants, namely a fungal cutinase from *Humicola insolens* (HiC) and a bacterial cutinase from *Thermobifida cellulosilytica* (Thc_Cut1) were compared. Model substrates were systematically designed with variations of the chain length of the alcohol and the acid as well as with varying content of the aromatic constituent terephthalic acid (Ta).

HPLC/MS identification and quantification of the hydrolysis products terephthalic acid (Ta), benzoic acid (Ba), adipic acid (Ada), mono(4-hydroxybutyl) terephthalate (BTa), mono-(2-hydroxyethyl) terephthalate (ETa), mono-(6-hydroxyhexyl) terephthalate (HTa) and bis(4-hydroxybutyl) terephthalate (BTaB) indicated that these enzymes indeed hydrolyze the tested esters. Shorter terminal chain length acids but longer chain length alcohols in oligomeric model substrates were generally hydrolyzed more efficiently. Thc_Cut1 hydrolyzed aromatic ester bonds more efficiently than HiC resulting in up to 3-fold higher concentrations of the monomeric hydrolysis product Ta. Nevertheless, HiC exhibited a higher overall hydrolytic activity on the tested polyesters, resulting in 2-fold higher concentration of released molecules. Thermogravimetry and differential scanning calorimetry (TG-DSC) of the polymeric model substrates revealed a general trend that a lower difference between melting temperature (T_m) and the temperature at which the enzymatic degradation takes place resulted in higher susceptibility to enzymatic hydrolysis.

Introduction

The legislative and environmental pressure to reduce polymer and packaging waste is increasing. Consequently, there is a strong demand to design and improve polyesters that are not only biodegradable but also meet the requirements of expected material properties. Aliphatic polyesters show, generally spoken, better biodegradability than aliphatic–aromatic copolyesters but sometimes lack the required thermal and mechanical properties [1]. Aromatic polyesters like polyethyleneterephthalate (PET) exhibit very good material properties but were believed to be inert to biological attack [2]. The polymer ecoflex is a polyester that shows promising material features [3] and various studies have already proven its biodegradability under composting conditions [4–6]. Nevertheless, considerably less is known about mechanistic aspects of the enzymatic hydrolysis involved in biodegradation by fungi and bacteria typically present in compost. Consequently, the

Corresponding author: Ribitsch, D. (doris.ribitsch@acib.at)

http://dx.doi.org/10.1016/j.nbt.2015.11.004

substrate specificities of a fungal cutinase (HiC) and a bacterial cutinase (Thc_Cut1) from the compost inhabitants *Humicula insolens* [7] and *Thermobifida cellulosilytica* [8] were compared in this study.

In the late 70s, enzymatic hydrolysis of polyester by a lipase was reported for the first time [9]. Since then, different studies were conducted in order to identify enzymes hydrolyzing polyesters. Marten *et al*. investigated the parameters that are important for lipases to hydrolyze polyesters [10,11]. A kinetic model for the layer-by-layer degradation of aliphatic and aromatic polyester nanoparticles by lipases from *Candida cylindracea* and *Pseudomonas* sp. was described by Herzog *et al*. [12]. *Thermobifida fusca* was identified to be one potent microorganism that is responsible for biodegradation of aliphatic–aromatic copolyesters during composting [13]. A big breakthrough was the identification of polyester active enzymes from *Thermobifida* sp. A hydrolase from *Thermobifida fusca* was proven to be active on aliphatic–aromatic copolyesters [14] and cutinases from *Thermobifida cellulosilytica* [15], *Thermobifida alba* [16] and *Fusarium solani pisi* [17] showed activity on aromatic polyesters like PET leading to surface hydrolysis of the polyester [17]. Recently, also a cutinase-like enzyme from *Saccharomonospora viridis* [18,19] was reported to hydrolyze different polyesters including foils made out of PET and ecoflex. The fungal cutinase from *Humicula insolens* was already demonstrated to have a potential for hydrolysis of polyester [16] or deacetylation of poly(vinyl acetate) [20]. Moreover, HiC was also proven to be able to hydrolyze the polyester backbone of alkyd resins [21]. Other enzymes that were reported to be active on polyesters are, for example, a cutinase-like enzyme from *Pseudozyma antarctica* that degrades polybutylene succinate-*co*-adipate and polybutylene succinate [22]. Some mechanistic studies on the hydrolysis of PET exist about a nitrobenzylesterase from *Bacillus subtilis* [23] and cutinases from *Thermobifida cellulosilytica* [15], but so far, there is a lack of information about enzymatic hydrolysis of aliphatic–aromatic copolyesters. Nevertheless, cutinases are known as attractive biocatalysts for industrial applications including esterification, trans-esterification and hydrolysis [24] in, for example, textile industry and polymer chemistry.

Compost is an interesting source of cutinases that do not only hydrolyze the naturally occurring polyester cutin but are potentially active on synthetic polyesters. In this work, the substrate specificities of two different cutinases from a fungal and a bacterial compost inhabitant were studied in detail, employing systematically designed oligomeric and polymeric ecoflex model substrates. Detailed knowledge about substrate specificities of the enzymes will allow adaptation of the polymer structure towards efficient biodegradation and will also make an enzymatic recycling of polyester building blocks feasible.

Materials and methods

Expression and purification of the enzymes

Thc_Cut1 was expressed in *Escherichia coli* BL21-Gold(DE3) as previously reported [15]. To harvest the cells, 100 ml of the culture were centrifuged (7000 × *g*, 4°C, 20 min) (Sorvall RC-5B Refrigerated Superspeed Centrifuge, Du Pont Instruments, USA). The pellet was resuspended in 10 ml buffer (50 mM NaH_2PO_4, 300 mM NaCl, 10 mM imidazol, pH 8.0) sonicated under ice cooling with two 3-min pulses (duty cycle 80%, output 7–8) on a BRANSON Ultrasonics cell disruptor (USA). Cell fragments were removed through centrifugation (7000 × *g*, 4°C, 30 min). The enzyme was purified by means of affinity chromatography as previously described [15]. The second cutinase HiC was received from Novozymes, purified through ultrafiltration (30 kDa and 10 kDa molecular weight cut off Vivaspin, Sartorius AG, Germany) and purity was confirmed by gel electrophoresis (supplementary material Figure A1).

Protein quantification, activity and temperature stability

Protein concentrations of all tested enzymes were determined with the help of the Bradford-based Bio-Rad Protein Assay (Bio-Rad Laboratories GmbH, Munich, Germany) and bovine serum albumin as standard. The protein assay was performed according to the manufacturers' instructions.

Esterase activity of Thc_Cut1 and HiC was analyzed based on UV/Vis spectroscopy, using the soluble substrate *p*-nitrophenyl butyrate (*p*NPB). 200 μl of 100 mM potassium phosphate buffer pH 7.0 containing the substrate were placed in a 96 well plate. The reaction was started by adding 20 μl of enzyme solution and the increase of the absorbance at 405 nm was recorded for 5 min on a plate reader (Tecan infinite M200, Tecan Austria GmbH). The experiments were conducted at 25°C. A blank reaction containing 20 μl of buffer instead of enzyme solution was measured simultaneously. The hydrolysis of *p*NPB to *p*-nitrophenol leads to an absorbance increase at 405 nm indicating an esterase activity. The molar extinction coefficient for *p*-nitrophenolate 405 nm, 25°C in 100 mM potassium phosphate buffer pH 7.0 was measured to be 11.581 mM^{-1} cm^{-1}.

The activity of all tested enzymes was calculated in Units (U). One U is defined as the amount of enzyme that is needed to catalyze the conversion of 1 μmol of substrate per minute under the given conditions.

Temperature stability was determined by incubating the enzymes in 100 mM potassium phosphate buffer pH 7.0 at 50°C and 100 rpm. The initial specific enzyme activity was measured (time point 0) using *p*NPB as substrate and defined to be 100%. The remaining enzyme activities were then determined after 24 h, 48 h and 72 h.

Synthesis of oligomeric ecoflex model substrates

Synthesis of mono(4-hydroxybutyl) terephthalate (BTa) was accomplished in accordance with Padias *et al*. [25] with modifications. Detailed information is provided in Ref. [26].

The synthesis of BTaB and BTaBTaB was conducted as described by Hässlin *et al*. [27] with one exception: 10 eq instead of 3.3 eq of 1,4-butanediol were used. An alternative synthesis was described by Atfani *et al*. [28].

Syntheses of the BTaB derivates HaBTaBHa, DaBTabDa, TdaBTaBTda, HTaH and BaBTaBBa are described in detail by Perz *et al*. [26].

BaETaEBa was synthesized as previously described [29]. An overview of the chemical structures of all oligomeric model substrates is provided in Fig. 1.

Synthesis of ecoflex and polymeric ecoflex model substrates

The aliphatic–aromatic copolyester ecoflex (poly(butylene adipate-co-butylene terephthalate, short PBAT) contains adipic acid, 1,4-butanediol and terephthalic acid. The adipic acid:terephthalic

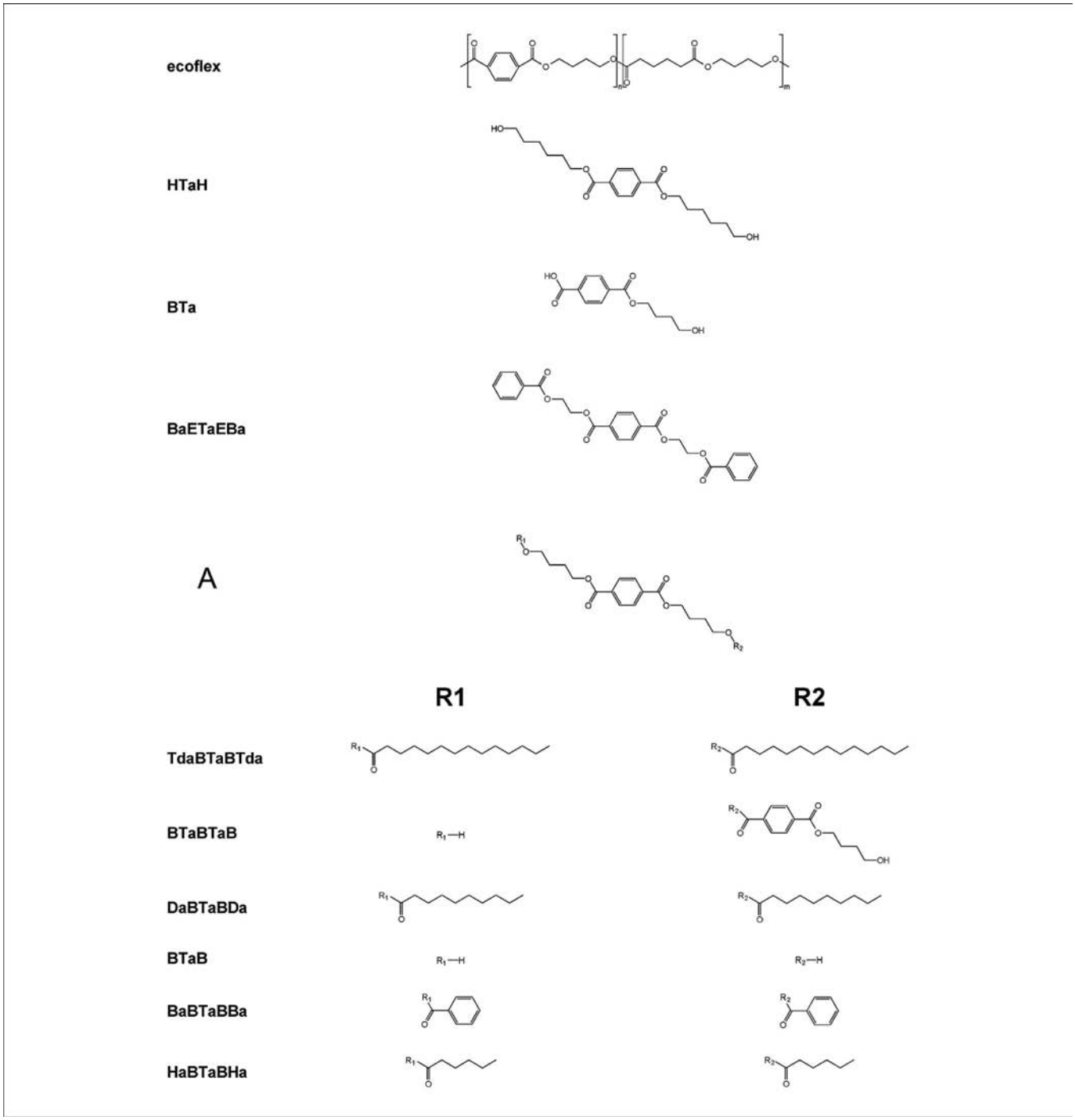

FIGURE 1

Chemical structures of ecoflex, the tested oligomeric ecoflex model substrates HTaH and BTa as well as bis(benzoyloxyethyl) terephthalate (BaETaEBa). The latter was tested as a PET model substrate in a previous study [15]. Basic structure of further model substrates **(A)**. ecoflex (poly(butylene adipate-co-butylene terephthalate)) is an aliphatic–aromatic copolyester that contains adipic acid, 1,4-butanediol and terephthalic acid. The adipic acid:terephthalic acid ratio is approximately 50:50. *Abbreviations*: B: 1,4-butanediol, Ba: benzoic acid, Da: decanoic acid, E: ethylene glycol, H: 1,6-hexanediol, Ha: hexanoic acid, Ta: terephthalic acid, Tda: tetradecanoic acid.

acid ratio is approximately 50:50. Several polymeric ecoflex model substrates with modified Ada:Ta ratios were tested with regard to their degradability. The tested Ada:Ta ratios lay between 0 mol% BTa also called polybutylene adipate (PBTa) to 50 mol% BTa (Ada50_Ta50). Ada:Ta ratios of the tested polymeric model substrates and their determined molecular masses are listed in Table 1.

Detailed information on the syntheses of polybutyleneadipate and poly(butylene adipate-co-butylene terephthalate)s is included in Ref. [26]. Ada:Ta ratios were determined using ^{1}H NMR spectroscopy.

All polymers were milled under dry ice cooling using the Ultra Centrifugal Mill ZM 200 (Retsch, Germany) with a 500 μm

TABLE 1

Characterization of thermal properties of ecoflex, polymeric and oligomeric ecoflex model substrates and molecular weight of polymeric substrates.

Sample	Ada:Ta ratio	T_m [°C]	Molecular weight*	
			M_w [g/mol]	M_w/M_n
Polybutylene adipate	Ada100_Ta0	58.8	52,000	3.1
Poly(butylene adipate-co-butylene terephthalate)	Ada90_Ta10	52.8	45,800	2.9
Poly(butylene adipate-co-butylene terephthalate)	Ada80_Ta20	47.8	32,400	2.9
Poly(butylene adipate-co-butylene terephthalate)	Ada70_Ta30	70.0	26,700	2.8
Poly(butylene adipate-co-butylene terephthalate)	Ada60_Ta40	101.4	29,200	2.8
Poly(butylene adipate-co-butylene terephthalate)	Ada50_Ta50	132.2	31,900	2.7
ecoflex	approx. Ada50_Ta50	125.3	65,000	3.4
TdaBTaBTaTda		69.6		
BTaBTaB		130.9		
DaBTaBDa		61.1		
BTaB		74.3		
BaBTaBBa		111.2		
HTaH		81.5		
HaBTaBHa		<25°C		
BTa		136.6		

*Weight average (M_w), number-average (M_n).

grinding insert. Prior to milling, polymers were embrittled through the addition of liquid nitrogen. Milled polymers were dried at 30°C under nitrogen flow and finally sieved to obtain homogeneous polymer fractions with particle sizes between 100 and 300 μm.

^{1}H NMR spectra and HPLC analysis of synthesis products

The identity and purity of the final products as well as the intermediate products were verified by means of ^{1}H NMR (Varian Inova 400 and DPX 400, $CDCl_3$, $C_2D_2Cl_4$, d-DMSO, tetramethylsilane as internal standard). The HPLC analysis was carried out on an Agilent Series 1100 HPLC system using a Symmetry C_{18}, 5 μm, 4.6 mm × 250 mm column (Waters Corporation, Milford, USA). The gradient was started at 90% A (0.1 v% H_3PO_4 in water), 10% B (0.1 v% H_3PO_4 in acetonitrile) at 10 min, followed by 50% A and 50% B at 20 min, 5% A and 95% B at 30 min, 5% A and 95% B at 32 min, 90% A and 10% B. This concentration was held until minute 40 to equilibrate the system. The flow rate was set to 1 ml min^{-1} and the temperature to 20°C. The eluted products were detected by the UV detector at 220 nm.

Simultaneous thermoanalysis: TG-DSC (thermogravimetry and differential scanning calorimetry)

The melting and decomposition behavior of milled ecoflex as well as of all tested oligomeric and polymeric ecoflex model substrates was analyzed on a STA 449 Jupiter (Erich Netzsch GmbH & Co., Holding KG, Selb, Germany). About 6 mg of sample were weighted into an aluminum pan and sealed under nitrogen. Reference (empty aluminum pan) and samples were heated at a rate of 10°C/min. The polymeric ecoflex model substrates and ecoflex were heated from −20°C to 550°C whereas the oligomeric samples were heated from 20°C to 550°C.

Hydrolysis of ecoflex, polymeric and oligomeric ecoflex model substrates with HiC and Thc_Cut1

Ten milligrams of milled ecoflex and the polymeric ecoflex model substrates with particle sizes between 100 and 300 μm with varying adipic acid (Ada) and terephthalic acid (Ta) ratios were incubated at 50°C and 100 rpm in 2 ml 100 mM potassium phosphate buffer pH 7.0 at a HiC and Thc_Cut1 concentration of 0.6 μM respectively. In the case of oligomeric model substrates the final substrate concentration in the reaction was 6.84 mM. Samples were withdrawn after 24 h, 48 h and 72 h and prepared for HPLC analysis.

Two milliliters of 100 mM potassium phosphate buffer pH 7.0 containing 1 mM BTa were incubated with HiC and Thc_Cut1 for 24 h, 48 h and 72 h at 50°C and 100 rpm. The enzymes were used at a concentration of 0.6 μM. Blank reactions were performed simultaneously containing substrate and buffer only. Sample preparation and analysis were performed as described above.

Blank reactions were performed simultaneously for all substrates and reaction conditions with the difference that no enzyme was added.

The enzyme was removed by methanol precipitation prior to HPLC analysis. This was done by adding 500 μl of ice-cooled methanol to 500 μl of the samples and blanks. After incubation on ice for 15 min samples were centrifuged (Hermle Z300K, MIDSCI, Missouri) for 15 min at 0°C and 14,000 × *g*. The supernatant (800 μl) was acidified with concentrated formic acid to reach a pH of 3. After an incubation of 1 h at 4°C, samples were centrifuged again (15 min, 0°C, 14,000 × *g*) and analyzed by means of HPLC/MS.

HPLC/MS analysis of hydrolysis products

HPLC analysis was carried out using a system consisting of a Dionex UltiMate 3000 Pump (Dionex Cooperation, Sunnyvale, USA), a Dionex ASI-100 automated sample injector, a Dionex

UltiMate 3000 column compartment and a Dionex UVD 340 U photodiode array detector. RP-HPLC separation of the analytes Ada, Ba, Ta, BTa, ETa and BTaB was carried out using a XTerra® RP_{18}, 3.5 μm, 3.0 mm × 150 mm column with precolumn (Waters Corporation, Milford, USA). The samples were eluted from the column using a nonlinear gradient. Concentration of C (0.1% HPLC grade formic acid in HPLC grade water) was always kept at 20%. The gradient was started at 72% A (HPLC grade water), 8% B (acetonitrile) at 4.5 min, followed by 60% A and 20% B at 5 min, 50% A and 30% B at 13 min, 30% A and 50% B at 17 min and 10% A and 70% B at 17.5 min. This concentration was held until 18 min and then brought back to 72% A and 8% B at 19 min. The flow rate was set to 0.5 ml min^{-1} and the column and sample compartment was tempered at 25°C. The injection volume of the prepared samples was 5 μl. The eluted products were detected using UV VIS Spectroscopy at 241 nm, 210 nm and 228 nm.

MS analysis was performed with an Agilent Ion Trap SL (Palo Alto, CA, USA) equipped with an electrospray ionisation coupled to the Dionex HPLC-UVD-system as described above. Initial separation of coupling products was done using the method described above. The hydrolysis products were measured in positive and negative ion mode and the electrospray voltage was set to +3500 V. Dry gas flow was set to 10 l min^{-1} with a temperature of 350°C, nebulizer set to 50 psi. Maximum accumulation time was fixed to 300 ms and the loading of the trap was controlled by the instrument with an ICC of 30,000.

Results and discussion

Enzyme stability

The temperature stability of Thc_Cut1 and HiC was investigated at 50°C in 100 mM potassium phosphate buffer. Both cutinases showed comparable temperature stabilities during 72 h of incubation. No significant activity losses were noticed during the first 24 h of incubation and after 72 h, about 65% of remaining activity was observed.

Possible hydrolysis pathways

The building blocks of ecoflex comprise a dialcohol (1,4-butanediol), terephthalic acid and adipic acid at a ratio of approximately 100:50:50. Ecoflex hydrolysis with cutinases has previously been demonstrated [14,18]. Here, for a detailed study of the substrate specificities of two different cutinases in this general ecoflex architecture, the chain length of the dialcohol was varied in the model substrates. 1,6-Hexanediol (H), 1,4-butanediol (B) and ethyleneglycol (E) were used. Similarly, the chain length of the acid was varied by integrating hexanoic acid (Ha), benzoic acid (Ba), decanoic acid (Da) and tetradecanoic acid (Tda). Out of these oligomers, bis(benzoyloxyethyl) terephthalate) (BaETaEBa) has previously been used to study substrate specificities of enzymes hydrolyzing PET [15,30,31]. The model substrates of different chain length and composition used in this study are listed in Table 1 and Fig. 1.

In Fig. 2, the detected hydrolysis products are exemplarily shown for the model substrate BaBTaBBa. Depending on the substrate specificities, the enzymes preferably hydrolyze the internal ester bonds between terephthalic acid and 1,4-butanediol or the terminal ester bonds between benzoic acid and 1,4 butanediol. Consequently, the ratio of released molecules is varying and shows a typical fingerprint for each enzyme.

Hydrolysis of oligomeric model substrates with HiC

A comparison of the enzymatic hydrolysis of oligomers was performed at 50°C. At this temperature, the enzymes exhibited high activities and stability for more than 3 days in preliminary experiments (data not shown). Hydrolysis of oligomers with terminal alcohols (HTaH and BTaB) indicated that both enzymes have preferences for Ta esterified with longer alcohols (Fig. 3). In contrast, the results of enzymatic hydrolysis of oligomers with acids of different chain length suggested that model substrates with shorter chain length acid end groups are faster hydrolyzed (HaBTaBHa > DaBTaBDa > TdaBTaBTda).

Fast hydrolysis of BaBTaBBa and BaETaEBa with different internal alcohols indicates no negative influence of two additional aromatic rings in the form of terminal benzoic acid residues while here, the ester bond to the larger alcohol was preferably hydrolyzed. Furthermore, HiC was found to preferably cleave B-Ada ester bonds resulting in a higher Ada concentration in ecoflex. B-Ta ester bonds are hydrolyzed as well, but more than 4 times less efficiently.

In addition to the monomer sequence, the melting point T_m has an important influence on the model substrate degradability. Marten *et al.* [10] stated that longer aromatic sequences reduce the biodegradability rate, since these crystalline regions lead to higher melting points and the difference between melting point T_m and degradation temperature is a crucial factor. In this study, the T_m of BTaBTaB and BTaB were measured to be 130.9°C and 74.3°C (Table 1), which was in agreement with previous values [27]. BTaB and HTaH are the only oligomeric model substrates that were soluble in water to a certain degree. Hence, the lower T_m of BTaB in combination with its solubility in aqueous phases could explain the higher hydrolysis efficiency in the case of BTaB if compared to BTaBTaB.

Interestingly, the hydrolysis rate of the model substrate BTaBTaB, which is a possible fragment of ecoflex, was lower than the one of ecoflex (after 72 h of incubation, the BTaBTaB sample exhibited only roughly half of the BTa and Ta concentration of the ecoflex sample). The T_m values for ecoflex and BTaBTaB lay around 130°C (Table 1). Hence, T_m values do not provide a satisfactory answer in this case. The approximate ratio of monomers of ecoflex is butanediol, adipic acid, terephthalic acid 100:50:50. One explanation for the higher hydrolysis rate in ecoflex is that this BTaBTaB sequence is statistically not the predominant monomer sequence. The monomer distribution of statistical copolyesters can be calculated as described by Vollmert [32]. For a copolyester of butanediol, adipic acid, terephthalic acid (100:50:50), 50% single (BTaB), 25% double (BTaBTaB) and 12% triple (BTaBTaBTaB) BTa building blocks would be expected. An additional important point is the difference in the crystallinity of BTaBTaB and ecoflex. The oligomer BTaBTaB is highly crystalline (100%), while ecoflex shows a much lower crystallinity of about 10%. Consequently, the respective sequences should be hydrolyzed much faster in ecoflex as indeed reflected by a higher overall hydrolysis of ecoflex (Fig. 3).

Several studies were conducted in the past to elucidate substrate specificities for enzymes hydrolyzing polyethylene terephthalate (PET), while this was not investigated for ecoflex in such detail. PET hydrolysis was studied with a lipase from *Thermomyces lanuginosus*, a cutinase-like polyesterase from *Saccharomonospora viridis* [18,19] cutinases from *Thermobifida fusca*, *Fusarium solani* [33], *Thermobifida*

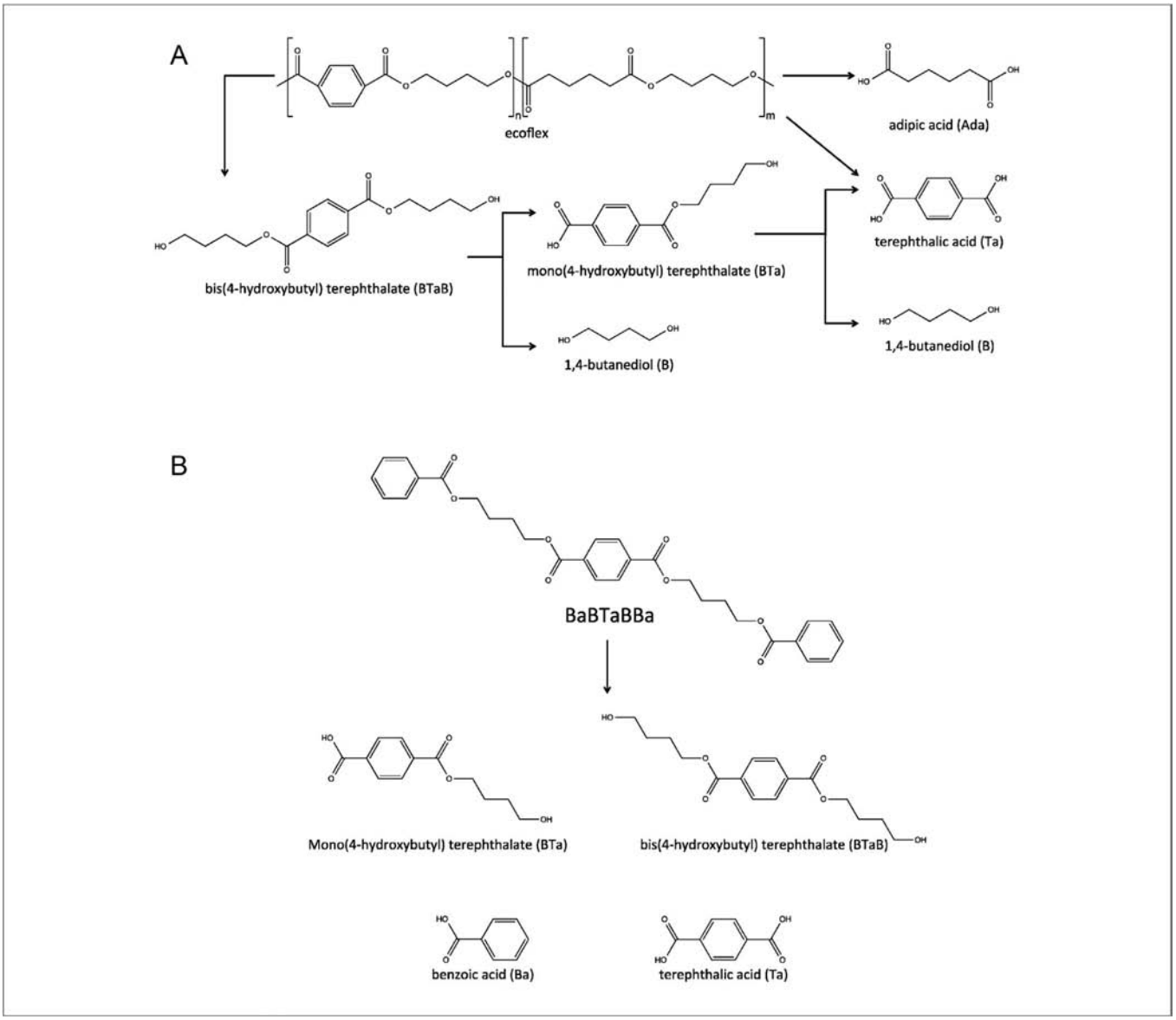

FIGURE 2

(a) Enzymatic hydrolysis of ecoflex. Hydrolysis products detected using HPLC UV/Vis: bis(4-hydroxybutyl) terephthalate (BTaB), mono(4-hydroyxbutyl) terephthalate (BTa), terephthalic acid (Ta) and adipic acid (Ada) in the case of ecoflex. **(b)** Detected and quantified BaBTaBBa hydrolysis products included Ba, Ta, BTa and BTaB.

alba [16,34], a *p*-nitrobenzylesterase from *Bacillus subtilis* [23], an esterase from *Thermobifida halotolerans* [35] and mutants of *Thermobifida cellulosilytica* cutinase 2 [30]. The cutinases from the different *Thermobifida* species show a very high amino acid sequence homology to Thc_Cut1 and are all active on PET. Thus, it is very likely that they would also hydrolyze ecoflex.

Hydrolysis of oligomeric model substrates with Thc_Cut1

The ability of Thc_Cut1 to hydrolyze ecoflex and the oligomeric model substrates was investigated and totally released products after 72 h are shown in Fig. 4. Interestingly, the concentration of the individual products was considerably different after hydrolysis of the oligomeric model substrate by Thc_Cut 1 and HiC. Thc_Cut1 hydrolysis led to much lower BTa concentrations when compared to HiC (see also BTa hydrolysis).

Analysis of Ta concentrations after HiC and Thc_Cut1 hydrolysis conveyed that the Ta concentration is up to 10 times higher in the case of Thc_Cut1 hydrolysis. In contrast, Ba concentration was found to be significantly lower after hydrolysis with Thc_Cut1 when compared to HiC hydrolysis. The Ta/Ba ratio after hydrolysis of BaBTaBBa with Thc_Cut1 was higher than the one after HiC hydrolysis. Taking into account the structure of this oligomer, the lower Ta/Ba ratio indicates that HiC is less specific to the ester bond between Ta and B in the liberated oligomer BTa when compared to Thc_Cut1. In addition, this experiment suggests that Thc_Cut1 has a high specificity to aromatic ester bonds as also indicated by the hydrolysis of the polymeric model substrates.

Hydrolyses of the model substrates BTaB and HTaH led to higher concentrations of Ta in the case of HTaH. Again, incubation with

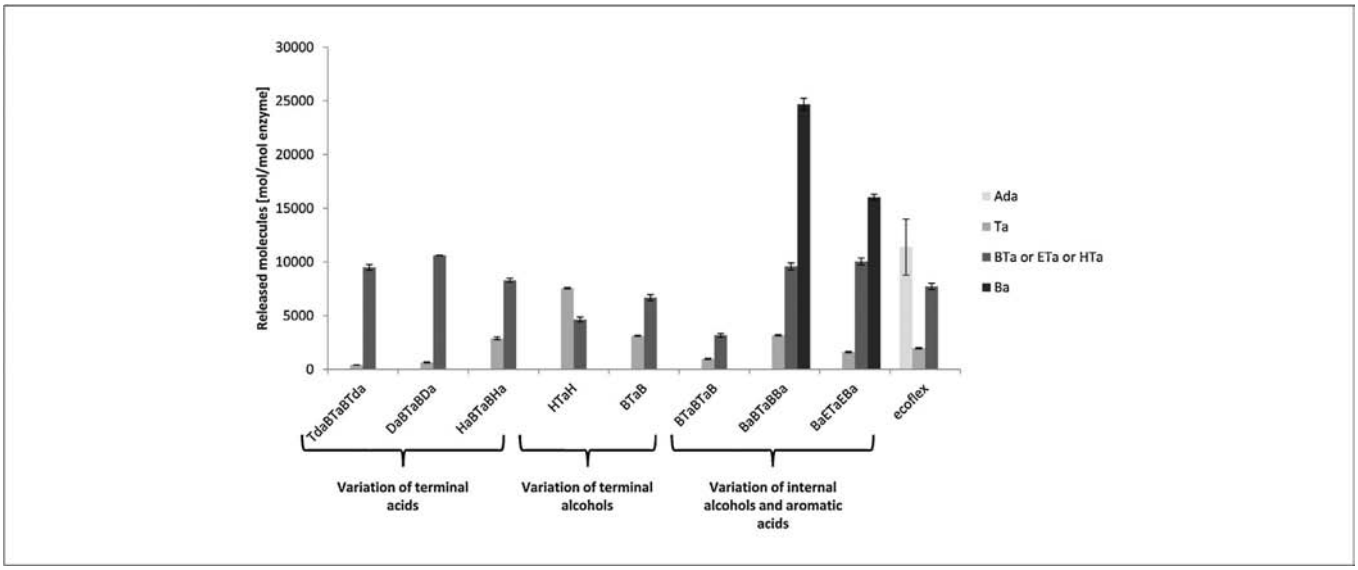

FIGURE 3

Hydrolysis of ecoflex and of oligomeric ecoflex model substrates by a cutinase from *Humicola insolens* (HiC) for 72 h. The reaction was performed under the conditions described in 'Materials and Methods'. ETa and HTa were detected instead of BTa in the cases of BaETaEBa and HTaH respectively. Each bar represents the average of three independent samples; error bars indicate the standard deviation.

Thc_Cut1 led to higher Ta concentrations indicating a more efficient hydrolysis to monomeric subunits than with HiC. However, the total amount of released molecules including Ta and BTa is higher after hydrolysis with HiC.

The amount of Ada and Ta that was set free after incubation of ecoflex with Thc_Cut1 was in the same order of magnitude. Ta concentration after ecoflex hydrolysis with Thc_Cut1 was higher than after incubation with HiC. In summary, Thc_Cut1 can hydrolyze Ta-B and Ada-B ester bonds in equal measure whereas HiC preferably hydrolyzes Ada-B ester bonds.

Hydrolysis of polymeric model substrates with Thc_Cut1 and HiC

During hydrolysis with HiC, the maximum Ada concentration was already reached after 1 or 2 days (data not shown) whereas Ta was released over 3 days. This correlates with the afore-stated results of ecoflex hydrolysis with HiC, where we could see that HiC hydrolyzes B-Ada ester bonds more easily than B-Ta ester bonds.

Both enzymes showed a high activity on ecoflex as well as on the tested polymeric ecoflex model substrates (Fig. 5). The quantified hydrolysis product concentrations of model substrate Ada80_Ta20 seem to be much lower than expected. The reason for this is most

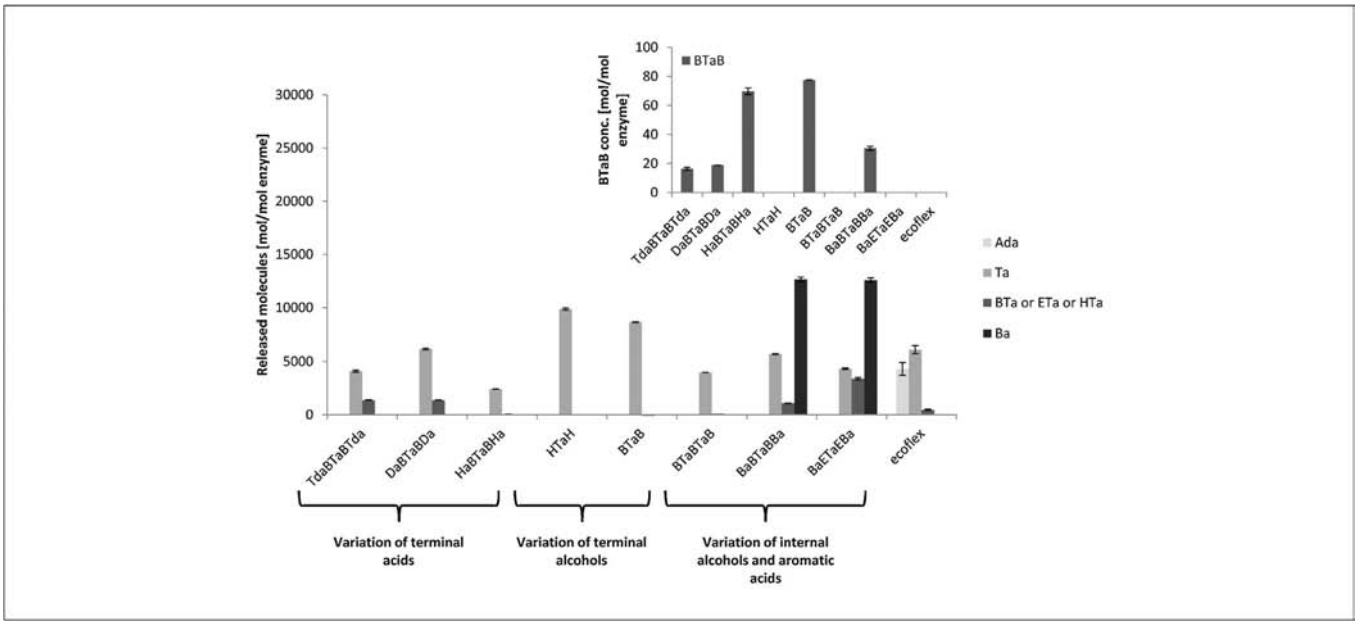

FIGURE 4

Hydrolysis of ecoflex and of oligomeric ecoflex model substrates by a cutinase from *Thermobifida cellulosilytica* (Thc_Cut1) for 72 h. The reaction was performed under the conditions described in 'Materials and Methods'. ETa and HTa were detected instead of BTa in the cases of BaETaEBa and HTaH respectively. Each bar represents the average of three independent samples; error bars indicate the standard deviation.

likely that the melting temperature of the polymers shows a minimum at around 25 mol% BTa. The melting temperature for the Ada80_Ta20 sample was reported to lie at 33°C [36]. Here the T_m of the Ada80_Ta20 sample was measured to be 47.8°C. Since the polymers were incubated at 50°C, this means that the Ada80_Ta20 polymers melted during incubation. This can lead to the effect that some portions of powder particles aggregated and hence the polymer surface was reduced. Consequently, the surface that is available for the cutinase adsorption is lower and further hydrolysis decreases.

Another important point that needs to be considered is the rigidity and crystallinity. The BTa subunit is very rigid whereas the aliphatic BAda subunit is much more flexible. Consequently, PBTa chains show a low mobility that is characterized as a high melting point (T_m), high glass transition temperature (T_g), and high crystallinity. For an enzyme, attacking a polymer chain with low mobility is much more difficult. However, if the ratio of BAda subunits is increased, T_m and T_g are reduced and this leads to a higher mobility of the polymer [36]. Various studies already suggested that the more rigid BTa groups are less susceptible to enzymatic hydrolysis [37,38]. This is also one explanation why BTaBTaB shows a lower hydrolysis rate when compared to oligomers containing more aliphatic groups.

The amounts of the hydrolysis products Ada, Ta and mono-(4-hydroxybutyl) terephthalate (BTa) released by HiC and Thc_Cut1 suggest that these two enzymes act differently on the tested model substrates. For example, incubation of Ada50_Ta50 with HiC resulted in a 5-times higher concentration of Ada than Ta. In contrast, Thc_Cut1 led to Ada and Ta concentrations in the same order of magnitude. For that reason, we can conclude that B-Ada ester bonds are more easily hydrolyzed by HiC than B-Ta ester bonds whereas Thc_Cut1 hydrolyzes both types of ester bonds alike. This is in good correlation with the results from experiments where oligomeric ecoflex model substrate hydrolysis was studied.

It is noticeable that the BTa concentrations in the Thc_Cut1 experiments were very low in contrast to the BTa concentrations after HiC hydrolysis. One possible explanation for this is that HiC is not able to further hydrolyze BTa and the hydrolysis stops at this dimer. In order to prove this theory a supplementary experiment was performed. The total amount of released hydrolysis products was found to be much higher in the case of HiC.

Another important outcome is that the Ta concentration indeed seems to be a crucial factor for the hydrolysis efficiency. Although the total concentration of Ta in the Ada60_Ta40 and Ada70_Ta30 samples is lower than in ecoflex, a higher number of Ta molecules

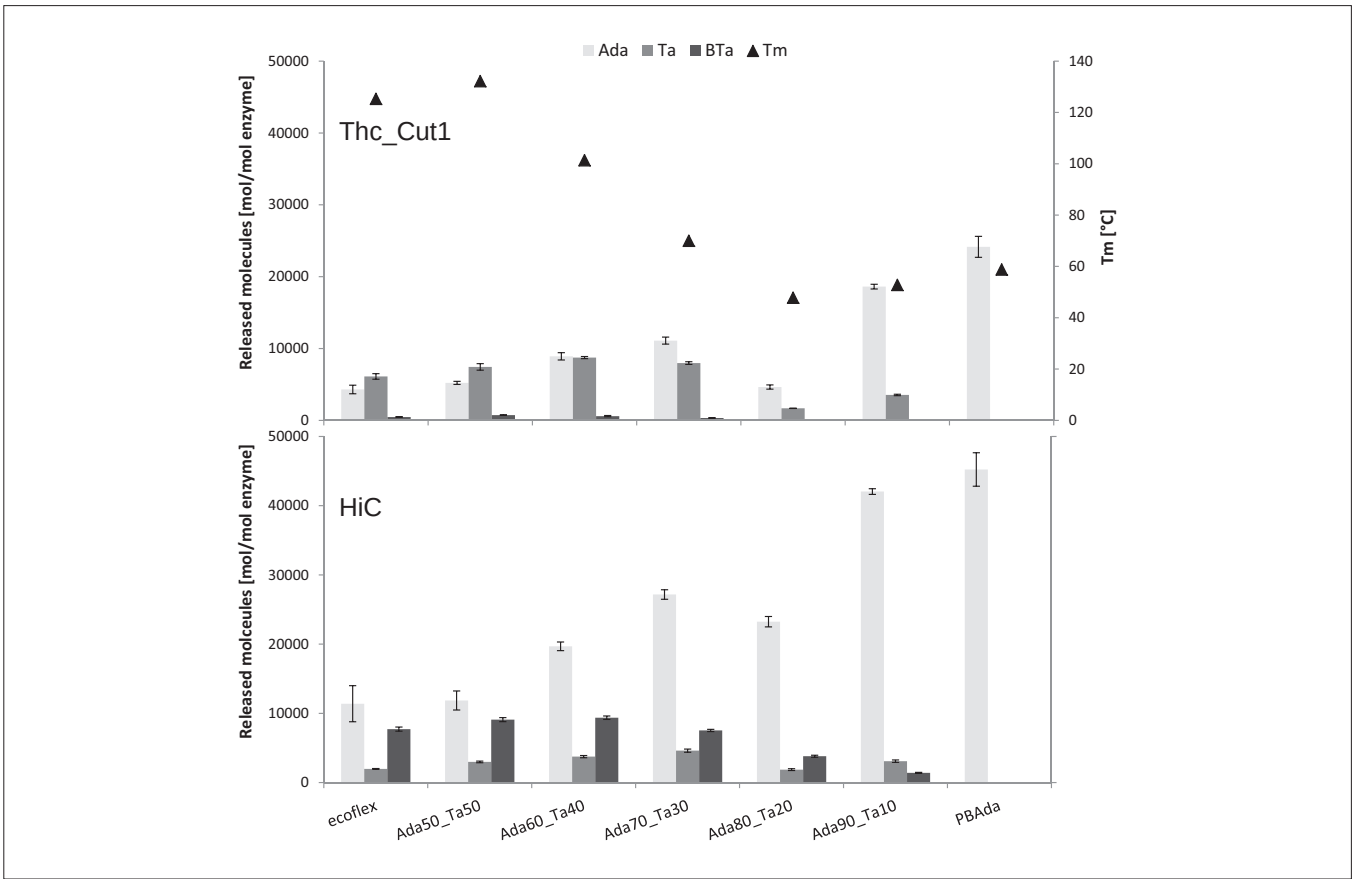

FIGURE 5

Hydrolysis of poly(butylene adipate-co-butylene terephthalate) with different mol% Ada:Ta ratios. Total hydrolysis products after 72 h incubation with Thc_Cut 1 and HiC are shown. The reaction was performed under the conditions described in 'Materials and Methods'. BTaB was only detected in blank reactions. T_m values of polymeric model substrates are displayed as black triangles. Each bar represents the average of three independent samples; error bars indicate the standard deviation.

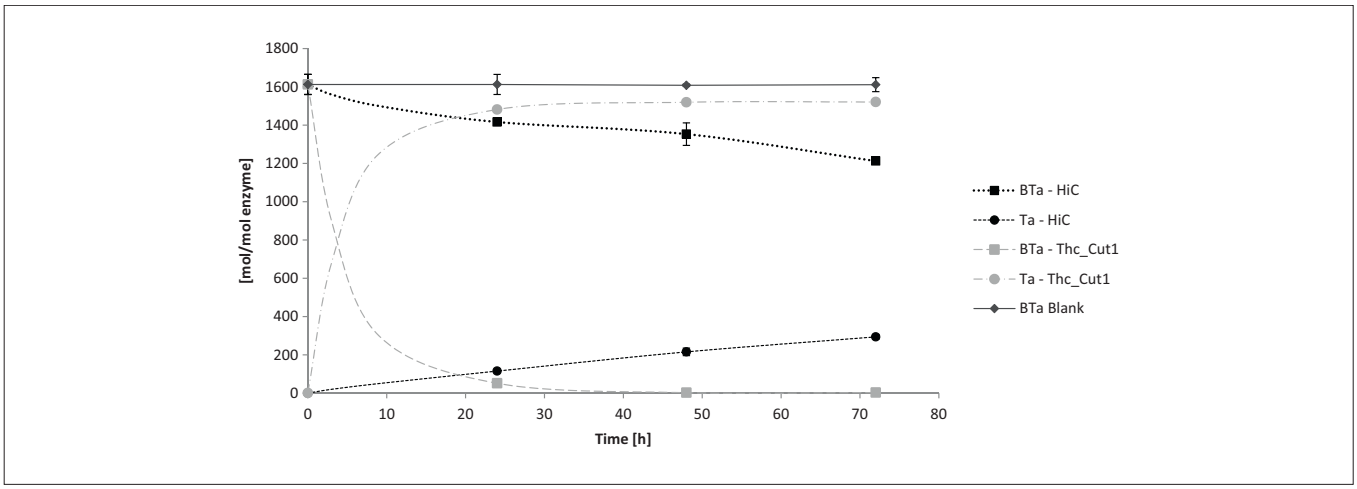

FIGURE 6

Detected molecules after hydrolysis of BTa (mono(4-hydroxybutyl) terephthalate) with HiC and Thc_Cut1 in mol/mol enzyme. The reaction was performed under the conditions described in 'Materials and Methods'. Each data point represents the average of three independent samples; error bars indicate the standard deviation.

was set free after incubation with HiC. The same results were obtained with Thc_Cut1. This proves that there is a fine line between acceptable material properties and sufficient biodegradability in biodegradable plastics.

Hydrolysis of the hydrolysis product BTa

In order to reveal whether the enzymatic hydrolysis stops at a certain point of the reaction, an additional experiment was performed to test the hydrolysis of the degradation product BTa by the given enzymes.

The presented data (Fig. 6) show that Thc_Cut1 hydrolyzes BTa very efficiently. After 24 h almost 100% of the available BTa dimer was converted to Ta and 1,4-butanediol. HiC also hydrolyzes BTa but the process is much slower. The BTa hydrolysis seems to be a bottleneck during enzymatic ecoflex degradation by HiC. Consequently, ecoflex and ecoflex model substrates incubated with HiC show lower Ta concentrations compared to the samples incubated with Thc_Cut1.

These findings correlate with the results obtained in the experiment where oligomeric ecoflex model substrates were hydrolyzed as well as with the results obtained during the experiments with polymeric model substrates.

Conclusion

Both a fungal cutinase from *Humicola insolens* as well as a bacterial cutinase from *Thermobifida cellulosilytica* were able to hydrolyze ecoflex and various ecoflex model substrates. Oligomeric model substrates with longer terminal alcohols but shorter chain length acids were hydrolyzed faster. Furthermore, we observed that generally, a higher content of aromatic building blocks (i.e. Ta) leads to lower hydrolysis rates as demonstrated with model substrates with varying Ta/Ada ratio. In addition, the influence of T_m values of the substrates on the (enzymatic) degradability was confirmed for the two tested cutinases. Interestingly, Thc_Cut1 hydrolyzes aromatic ester bonds more efficiently than HiC, resulting in higher concentrations of the monomeric hydrolysis product Ta. Nevertheless, HiC showed a higher overall hydrolytic activity on the tested polymers and oligomers. These data thus reveal important information both for the design of biodegradable polyesters and for possible enzymatic recycling strategies where obviously combinations of enzymes are the best choice for complete hydrolysis into monomers.

Acknowledgements

This work has been supported by the Federal Ministry of Science, Research and Economy (BMWFW), the Federal Ministry of Traffic, Innovation and Technology (bmvit), the Styrian Business Promotion Agency SFG, the Standortagentur Tirol, the Government of Lower Austria and ZIT – Technology Agency of the City of Vienna through the COMET-Funding Program managed by the Austrian Research Promotion Agency FFG.

Appendix A. Supplementary data

Supplementary data associated with this article can be found, in the online version, at http://dx.doi.org/10.1016/j.nbt.2015.11.004.

References

[1] Witt U, Müller R-J, Augusta J, Widdecke H, Deckwer W-D. Synthesis, properties and biodegradability of polyesters based on 1,3-propanediol. Macromol Chem Phys 1994;195:793–802.
[2] Mueller R-J. Biological degradation of synthetic polyesters – enzymes as potential catalysts for polyester recycling. Process Biochem 2006;41:2124–8.
[3] Witt U, Müller R-J, Deckwer W-D. New biodegradable polyester-copolymers from commodity chemicals with favorable use properties. J Environ Polym Degrad 1995;3:215–23.
[4] Witt U, Yamamoto M, Seeliger U, Müller R-J, Warzelhan V. Biodegradable polymeric materials-not the origin but the chemical structure determines biodegradability. Angew Chem Int Ed 1999;38:1438–42.
[5] Witt U, Einig T, Yamamoto M, Kleeberg I, Deckwer WD, Müller R-J. Biodegradation of aliphatic–aromatic copolyesters: evaluation of the final biodegradability and ecotoxicological impact of degradation intermediates. Chemosphere 2001;44:289–99.
[6] Kijchavengkul T, Auras R, Rubino M, Selke S, Ngouajio M, Fernandez T. Biodegradation and hydrolysis rate of aliphatic aromatic polyester. Polym Degrad Stabil 2010;95:2641–7.
[7] Epstein E. The science of composting. Boca Raton, FL, USA: CRC Press LCC; 1996 : 53–76.
[8] Kukolya J, Nagy I, Laday M, Toth E, Oravecz O, Márialigeti K, et al. *Thermobifida cellulolytica* sp. nov., a novel lignocellulose-decomposing actinomycete. Int J Syst Evol Microbiol 2002;52:1193–9.

[9] Tokiwa Y, Suzuki T. Hydrolysis of polyesters by lipases. Nature 1977;270:76–8.
[10] Marten E, Müller R-J, Deckwer W-D. Studies on the enzymatic hydrolysis of polyesters. II. Aliphatic–aromatic copolyesters. Polym Degrad Stabil 2005;88:371–81.
[11] Marten E, Müller R-J, Deckwer W-D. Studies on the enzymatic hydrolysis of polyesters. I. Low molecular mass model esters and aliphatic polyesters. Polym Degrad Stabil 2003;80:485–501.
[12] Herzog K, Müller RJ, Deckwer WD. Mechanism and kinetics of the enzymatic hydrolysis of polyester nanoparticles by lipases. Polym Degrad Stabil 2006;91:2486–98.
[13] Kleeberg I, Hetz C, Kroppenstedt RM, Müller R-J, Deckwer W-D. Biodegradation of aliphatic–aromatic copolyesters by *Thermomonospora fusca* and other thermophilic compost isolates. Appl Environ Microbiol 1998;64:1731–5.
[14] Kleeberg I, Welzel K, VandenHeuvel J, Mueller RJ, Deckwer WD. Characterization of a new extracellular hydrolase from *Thermobifida fusca* degrading aliphatic–aromatic copolyesters. Biomacromolecules 2005;6:262–70.
[15] Herrero Acero E, Ribitsch D, Steinkellner G, Gruber K, Greimel K, et al. Enzymatic surface hydrolysis of PET: effect of structural diversity on kinetic properties of cutinases from Thermobifida. Macromolecules 2011;44:4632–40.
[16] Ribitsch D, Acero EH, Greimel K, Eiteljoerg I, Trotscha E, Freddi G, et al. Characterization of a new cutinase from *Thermobifida alba* for PET-surface hydrolysis. Biocatal Biotransfor 2012;30:2–9.
[17] Donelli I, Freddi G, Nierstrasz VA, Taddei P. Surface structure and properties of poly-(ethylene terephthalate) hydrolyzed by alkali and cutinase. Polym Degrad Stabil 2010;95:1542–50.
[18] Kawai F, Oda M, Tamashiro T, Waku T, Tanaka N, et al. A novel Ca2+-activated, thermostabilized polyesterase capable of hydrolyzing polyethylene terephthalate from *Saccharomonospora viridis* AHK190. Appl Microbiol Biotechnol 2014;98:10053–64.
[19] Miyakawa T, Mizushima H, Ohtsuka J, Oda M, Kawai F, Tanokura M. Structural basis for the Ca-enhanced thermostability and activity of PET-degrading cutinase-like enzyme from *Saccharomonospora viridis* AHK190. Appl Microbiol Biotechnol 2015;99:4297–307. http://dx.doi.org/10.1007/s00253-014-6272-8.
[20] Ronkvist ÅM, Lu W, Feder D, Gross RA. Cutinase-catalyzed deacetylation of poly(vinyl acetate). Macromolecules 2009;42:6086–97.
[21] Greimel K, Marold A, Sohar C, Feola R, Temel A, Schoenbacher T, et al. Enzymatic hydrolysis of polyester based coatings. React Funct Polym 2013;73:1335–9.
[22] Watanabe T, Shinozaki Y, Yoshida S, Koitabashi M, Sameshima-Yamashita Y, Fujii T, et al. Xylose induces the phyllosphere yeast *Pseudozyma antarctica* to produce a cutinase-like enzyme which efficiently degrades biodegradable plastics. J Biosci Bioeng 2014;117:325–9.
[23] Ribitsch D, Heumann S, Trotscha E, Herrero Acero E, Greimel K, Leber R, et al. Hydrolysis of polyethyleneterephthalate by p-nitrobenzylesterase from *Bacillus subtilis*. Biotechnol Prog 2011;27:951–60.
[24] Fontes Pio T, Alves Macedo G. Chapter 4 cutinases: properties and industrial applications Adv Appl Microbiol, vol. 66. Academic Press; 2009. p. 77–95.
[25] Padias AB, Hall HK. Oligomeric bishydroxybutyl terephthalates from terephthalic acid. J Polym Sci Polym Chem Ed 1981;19:1021–32.
[26] Perz V, Bleymaier K, Sinkel C, Kueper U, Bonnekessel M, Ribitsch D, et al. Oligomeric and polymeric poly(butylene adipate-co-butylene terephthalate) model substrates for the investigation of enzymatic hydrolysis. Data in Brief 2015. submitted.
[27] Hässlin H-W, Dröscher M, Wegner G. Struktur und Eigenschaften segmentierter polyetherester, 3. Synthese definierter Oligomerer des polybutylenterephthalats. Die Makromolekulare Chemie 1980;181:301–23.
[28] Atfani M, Brisse F. Syntheses, characterizations, and structures of a new series of aliphatic–aromatic polyesters. 1. The poly(tetramethylene terephthalate dicarboxylates). Macromolecules 1999;32:7741–52.
[29] Heumann S, Eberl A, Pobeheim H, Liebminger S, Fischer-Colbrie G, Almansa E, et al. New model substrates for enzymes hydrolysing polyethyleneterephthalate and polyamide fibres. J Biochem Biophys Methods 2006;69:89–99.
[30] Herrero Acero E, Ribitsch D, Dellacher A, Zitzenbacher S, Marold A, Steinkellner G, et al. Surface engineering of a cutinase from *Thermobifida cellulosilytica* for improved polyester hydrolysis. Biotechnol Bioeng 2013;110:2581–90.
[31] Ribitsch D, Yebra AO, Zitzenbacher S, Wu J, Nowitsch S, Steinkellner G, et al. Fusion of binding domains to *Thermobifida cellulosilytica* cutinase to tune sorption characteristics and enhancing PET hydrolysis. Biomacromolecules 2013;14:1769–76.
[32] Vollmert B. Grundriss der Makromolekularen Chemie. Karlsruhe: Vollmert-Verlag; 1988.
[33] Eberl A, Heumann S, Brueckner T, Araujo R, Cavaco-Paulo A, Kaufmann F, et al. Enzymatic surface hydrolysis of poly(ethylene terephthalate) and bis(benzoyloxyethyl) terephthalate by lipase and cutinase in the presence of surface active molecules. J Biotechnol 2009;143:207–12.
[34] Kitadokoro K, Thumarat U, Nakamura R, Nishimura K, Karatani H, Suzuki H, et al. Crystal structure of cutinase Est119 from *Thermobifida alba* AHK119 that can degrade modified polyethylene terephthalate at 1.76 A resolution. Polym Degrad Stabil 2012;97:771–5.
[35] Ribitsch D, Herrero Acero E, Greimel K, Dellacher A, Zitzenbacher S, Marold A, et al. A new esterase from *Thermobifida halotolerans* hydrolyses polyethylene terephthalate (PET) and polylactic acid (PLA). Polymers 2012;4:617–29.
[36] Gan Z, Kuwabara K, Yamamoto M, Abe H, Doi Y. Solid-state structures and thermal properties of aliphatic–aromatic poly(butylene adipate-co-butylene terephthalate) copolyesters. Polym Degrad Stabil 2004;83:289–300.
[37] Kasuya K-i, Ishii N, Inoue Y, Yazawa K, Tagaya T, Yatsumoto T, et al. Characterization of a mesophilic aliphatic–aromatic copolyester-degrading fungus. Polym Degrad Stabil 2009;94:1190–6.
[38] Mueller R-J, Kleeberg I, Deckwer W-D. Biodegradation of polyesters containing aromatic constituents. J Biotechnol 2001;86:87–95.

Data in Brief 7 (2016) 291–298

Contents lists available at ScienceDirect

Data in Brief

journal homepage: www.elsevier.com/locate/dib

Data Article

Data on synthesis of oligomeric and polymeric poly(butylene adipate-co-butylene terephthalate) model substrates for the investigation of enzymatic hydrolysis

Veronika Perz [a], Klaus Bleymaier [b], Carsten Sinkel [c], Ulf Kueper [c], Melanie Bonnekessel [c], Doris Ribitsch [a,d,*], Georg M. Guebitz [a,d]

[a] *acib – Austrian Centre of Industrial Biotechnology, Konrad Lorenz Strasse 20, 3430 Tulln, Austria*
[b] *acib – Austrian Centre of Industrial Biotechnology, Petersgasse 14, 8010 Graz, Austria*
[c] *BASF SE, Carl-Bosch-Strasse 38, 67056 Ludwigshafen, Germany*
[d] *Institute of Environmental Biotechnology, University of Natural Resources and Life Sciences, Konrad Lorenz Strasse 20, 3430 Tulln an der Donau, Austria*

ARTICLE INFO

Article history:
Received 27 November 2015
Received in revised form
5 February 2016
Accepted 11 February 2016
Available online 19 February 2016

Keywords:
Oligomer synthesis
Oligomer analysis
Polyester model substrates

ABSTRACT

The aliphatic-aromatic copolyester poly(butylene adipate-co-butylene terephthalate) (PBAT), also known as ecoflex, contains adipic acid, 1,4-butanediol and terephthalic acid and is proven to be compostable [1–3]). We describe here data for the synthesis and analysis of poly(butylene adipate-co-butylene terephthalate variants with different adipic acid:terephatalic acid ratios and 6 oligomeric PBAT model substrates. Data for the synthesis of the following oligomeric model substrates are described: mono(4-hydroxybutyl) terephthalate (**BTa**), bis(4-(hexanoyloxy)butyl) terephthalate (**HaBTaBHa**), bis(4-(decanoyloxy)butyl) terephthalate (**DaBTaBDa**), bis(4-(tetradecanoyloxy)butyl) terephthalate (**TdaBTaBTda**), bis(4-hydroxyhexyl) terephthalate (**HTaH**) and bis(4-(benzoyloxy)butyl) terephthalate (**BaBTaBBa**). Polymeric PBAT variants

DOI of original article: http://dx.doi.org/10.1016/j.nbt.2015.11.004

Abbreviations: Ada, adipic acid; Ba, benzoic acid; BaBTaBBa, bis(4-(benzoyloxy)butyl) terephthalate; BTa, mono(4-hydroxybutyl) terephthalate; BTaB, bis(4-hydroxybutyl) terephthalate; Da, decanoic acid; DaBTaBDa, bis(4-(decanoyloxy)butyl) terephthalate; H, 1,6-hexanediol; Ha, hexanoic acid; HaBTaBHa, bis(4-(hexanoyloxy)butyl) terephthalate; HTaH, bis(4-hydroxyhexyl) terephthalate; PBAT, (poly(butylene adipate-co-butylene terephthalate); Ta, terephthalic acid; Tda, tetradecanoic acid; TdaBTaBTda, bis(4-(tetradecanoyloxy)butyl) terephthalate; THF, tetrahydrofuran.

* Corresponding author at: acib – Austrian Centre of Industrial Biotechnology, Konrad Lorenz Strasse 20, 3430 Tulln, Austria. Tel.: +43 1 47654 4974.
E-mail address: doris.ribitsch@acib.at (D. Ribitsch).

http://dx.doi.org/10.1016/j.dib.2016.02.029

were synthesized with adipic acid:terephatalic acid ratios of 100:0, 90:10, 80:20, 70:30, 60:40 and 50:50. These polymeric and oligomeric substances were used as ecoflex model substrates in enzymatic hydrolysis experiments in the article "Substrate specificities of cutinases on aliphatic-aromatic polyesters and on their model substrates" [4].

Specifications Table

Subject area	Chemistry
More specific subject area	Organic synthesis, synthesis of model substrates for enzymatic hydrolysis experiments and biodegradation tests
Type of data	Synthesis protocols, figure, table, text file
How data was acquired	^{1}H NMR and ^{13}C NMR (Varian Inova 400 and DPX 400, $CDCl_3$, $C_2D_2Cl_4$, d-DMSO, tetramethylsilane as internal standard).HPLC (Agilent Series 1100 HPLC system using a Symmetry C_{18}, 5 μm, 4.6 mm × 250 mm column (Waters Corporation, Milford, USA)).
Data format	Analyzed data
Experimental factors	Starting compounds were either purchased or synthesized using already published synthetic protocols
Experimental features	Model substrates were synthesized and ^{1}H NMR, ^{13}C NMR and HPLC verified their identity and purity.
Data source location	Ludwigshafen, Germany and Tulln an der Donau, Austria
Data accessibility	The data are supplied with this article

Value of the data

- The data indicate the suitability of oligomers as model substrates for bulky polymers.
- The data offer the option to investigate the influence of polymer structures and the mechanism of biodegradation.
- The data allow identification of substrate specificities of enzymes and detailed analysis of cleavage sites during polymer degradation.

Data

Data presented here describe the additional chemical analysis of poly(butylene adipate-co-butylene terephthalate [1–3] variants and oligomeric model substrates. 1H NMR spectra and 13C NMR spectra are provided showing the chemical structure and purity ob synthesized chemicals.

1. Experimental design, materials and methods

1.1. General

The identity and purity of the final products as well as the intermediate products were verified by ^{1}H-NMR and ^{13}C-NMR (Varian Inova 400 and DPX 400) using $CDCl_3$, $C_2D_2Cl_4$, d-DMSO, tetramethylsilane as internal standards. HPLC analysis was carried out on an Agilent Series 1100 HPLC system using a Symmetry

C_{18}, 5 μm, 4.6 mm × 250 mm column (Waters Corporation, Milford, USA). The gradient was started at 90% A (0.1 vol% H_3PO_4 in water), 10% B (0.1 vol% H_3PO_4 in acetonitrile) at 10 min, followed by 50% A and 50% B at 20 min, 5% A and 95% B at 30 min, 5% A and 95% B at 32 min, 90% A and 10% B. This concentration was held until minute 40 to equilibrate the system. The flow rate was set to 1 ml min^{-1} and the temperature to 20 °C. The eluted products were detected by the UV detector at 220 nm. Chemical structures of the produced PBAT model substrates are presented in Fig. 1.

1.2. Synthesis of oligomeric PBAT model substrates

1.2.1. Synthesis of mono(4-hydroxybutyl) terephthalate (BTa)

Step 1 was performed according to Padias and Hall [5].

Step 2: Thionylchloride (980 g, 8.24 mol, 11.4 eq) was added dropwise to a mixture of monomethyl terephthalate (129.1 g, 0.72 mol, 1 eq) and 556 g of toluene. The reaction mixture was then stirred under reflux (80 °C) for 3 h and turned into a yellow solution. The solvent and excess of thionylchloride were removed under reduced pressure to give 122.6 g of methyl terephthaloyl monochloride (86% yield).

Step 3: 1,4-Butanediol (231 g, 2.56 mol, 8.3 eq) and pyridine (124.2 g, 1.57 mol, 5.1 eq) were cooled to 0 °C. A solution of methyl terephthaloyl monochloride (61.3 g, 0.31 mol, 1 eq) and 233 g of methylenchloride was added dropwise over 15 min and it was stirred for further 2 h at room temperature. Then, the reaction mixture was poured into 2 kg of water and brought to pH 1 using 1.5 kg of 1 M HCl. The aqueous phase was extracted using methylene chloride. The solvent was removed under reduced pressure to give 63 g of methyl hydroxybutyl terephthalate (90–95% by ^{1}H NMR, 73–77% yield).

Step 4: Methyl hydroxybutyl terephthalate (22 g, 0.087 mol, 1 eq) was dissolved in 885 ml of tert-butyl methyl ether (MTBE) and chloroform (ratio 1:1 v/v). Dihydropyran (18.3 g, 0.22 mol, 2.5 eq) was added dropwise over 15 min and then 0.8 g of conc. HCl were added to result in a pH of 4. The reaction mixture was stirred for further 18 h at room temperature. The solution was then washed with 314 g of saturated sodium bicarbonate solution and 373 g of water. After drying and removing the solvent under reduced pressure, 38.4 g of crude product were obtained. This crude product was purified by flash chromatography (hexane:ethyl acetate 8:1). 23.8 g of the dihydropyranyl derivative of methyl hydroxybutyl terephthalate was obtained (98.6 HPLC-a%, 80% yield).

Steps 5 and 6: The dihydropyranyl derivative of methyl hydroxybutyl terephthalate (5.08 g, 98.6 HPLC-a%, 16 mmol, 1 eq) and DABCO (2.67 g, 98%, 23 mmol, 1.5 eq) are sealed in a tube and heated to 100 °C for 4 h. At room temperature, the oil was taken up in 100 ml water. To this opaque solution, 25 ml of 10% H_2SO_4 were added. The reaction mixture was heated to 90 °C and then diluted with 75 ml of water to obtain a clear solution. Then, the reaction mixture was allowed to cool to room temperature and was stirred for further 2 h. The obtained precipitate was filtered off, washed two times with 20 ml of water each and finally dried in a nitrogen stream. 2.92 g of monohydroxybutyl terephthalate were obtained. Recrystallization from toluene resulted in 2.42 g of monohydroxybutyl terephthalate (96.6 wt% by ^{1}H NMR, 63% yield; Figs. 2 and 3).

1.2.2. Synthesis of the BTaB derivates HaBTaBHa, DaBTaBDa, TdaBTaBTda, HTaH and BaBTaBBa

For the synthesis of **HaBTaBHa**, 5 g **BTaB** (16 mmol, 1 eq, 91.9 HPLC-a%), 3.15 g triethylamine (32 mmol, 2 eq) and 60 ml toluene were stirred at room temperature while 4.35 g hexanoyl chloride

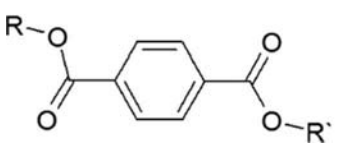

HaBTaBHa	R = R` = 4-(hexanoyloxy)butyl-
DaBTaBDa	R = R` = 4-(decanoyloxy)butyl-
TdaBTaBTda	R = R` = 4-(tetradecanoyloxy)butyl-
HTaH	R = R` = 4-hydroxyhexyl-
BaBTaBBa	R = R` = 4-(benzoyloxy)butyl-

Fig. 1. Overview of chemical structures of oligomeric substrates.

(32 mmol, 2 eq) were added dropwise. (The synthesis of **BTaB** was conducted following Hässlin et al. [6] with modifications that were previously described [4].) After 3 h of stirring at room temperature the solvent was removed under reduced pressure and the crude product was purified by means of flash chromatography (hexane:ethyl acetate 4:1). 5.4 g of **HaBTaBHa** were obtained (92.3 HPLC-a-%, > 95% by ^{1}H NMR, 66% yield). ^{13}C spectrum is shown in Fig. 3. The synthesis of **DaBTaBDa** and **TdaBTaBTda** was performed as described alike with the difference that in the case of **DaBTaBDa**, 6.1 g of decanoyl chloride (32 mmol, 2 eq) were added dropwise and during the synthesis of **TdaBTaBTda**, 7.9 g of myristoyl choride (32 mmol, 2 eq) were added instead of hexanoyl chloride. These syntheses yielded 5.9 g **DaBTaBDa** (98 HPLC-a%, 95% by ^{1}H NMR, 63% yield) and 6.3 g **TdaBTaBTda** (95.9 HPLC-a%, 95% by ^{1}H NMR, 56% yield). ^{13}C spectra are presented in Figs. 4, 5 and 6.

HTaH was synthesized according to Hässlin et al. [6] with some modifications. A yellow suspension of terephthalic acid dichloride (123 g, 0.6 mol, 1 eq), pyridine (71.2 g, 0.9 mol, 1.5 eq), and 200 ml of tetrahydrofuran (THF) was stirred. A colorless solution of 1,6-hexanediol (709.2 g, 6 mol, 10 eq) and 400 ml of THF were added dropwise over 45 min. Meanwhile, the reaction mixture was slowly heated. After addition was complete, the reaction mixture was stirred for further 3 h at reflux temperature (78 °C). Then, at normal pressure, 163 g of THF were distilled off. The residue was brought to room temperature and poured into 2 l ice water. After standing over night, the precipitate was filtered off. The precipitate was taken up with 1.5 l of distilled water and stirred at 50 °C. The mixture was filtered off and the residue was taken up in 1000 ml ethanol at room temperature and filtered off after 2 h stirring. The obtained filtrate was brought to 0 °C. The obtained crystals were filtered off and dried. 54.6 g of **HTaH** were obtained (94 HPLC-a%, 23% yield, byproduct: **HTaHTaH**).

BaBTaBBa was prepared by stirring 140.7 g of 4-chlorobutanol (1.1 mol, 1 eq) and 155 g benzoyl chloride (1.1 mol, 1 eq) at 110 °C for 24 h. A suspension of 91.6 g terephthalic acid (0.55 mol, 0.5 eq) and 161 g DMF (2.2 mol, 2 eq) was added dropwise to the benzoyl protected butyl chloride and subsequently 223.1 g triethylamine was added dropwise (2.2 mol, 2 eq). The reaction mixture was stirred for 24 h at reflux and then extracted using 1350 g toluene. The solid was removed through

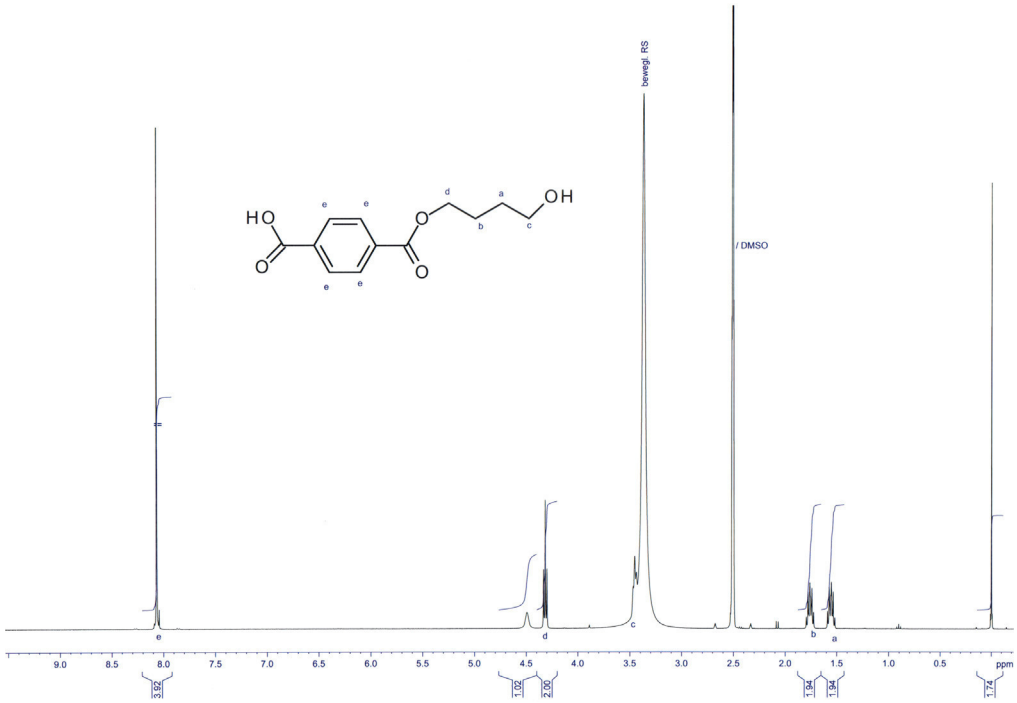

Fig. 2. ^{1}H NMR spectrum of monohydroxybutyl terephthalate (**BTa**).

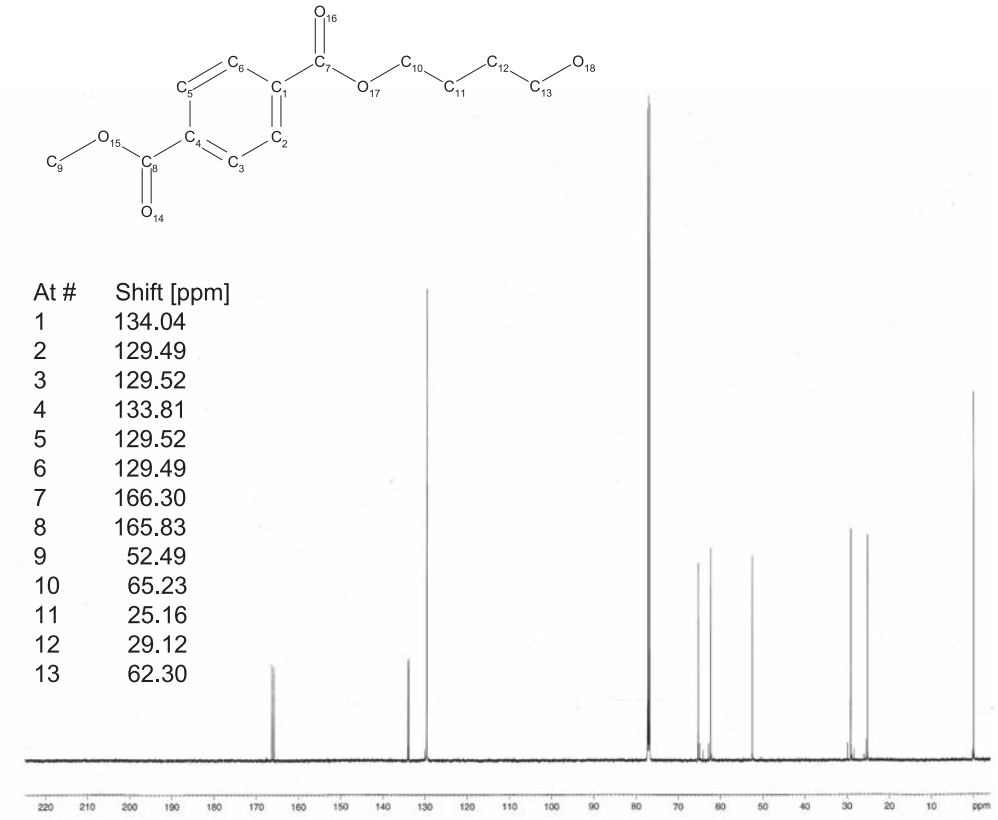

Fig. 3. ^{13}C NMR spectrum of monohydroxybutyl terephthalate (**BTa**) scaffold.

filtration. The organic phase was washed with 450 g of saturated sodium chloride solution and 500 g of distilled water. Finally, anhydrous magnesium sulfate was used for drying the organic phase and the solvent was removed under reduced pressure. Crude **BaBTaBBa** was purified by means of flash chromatography (hexane:ethyl acetate 4:1) and 132 g of product were received (98.3 wt% by quant. ^{1}H-NMR, 46% yield).

1.3. Synthesis of polymeric PBAT model substrates

1.3.1. Synthesis of polybutyleneadipate

For the synthesis of **polybutyleneadipate**, 876.84 g of adipic acid (6 mol, 1 eq), 702.9 g of 1,4-butanediol (7.80 mol, 1.3 eq) and 2.56 g of tetra-n-butyl orthotitanate (7.52 mmol) were stirred at 160 °C with a slight stream of nitrogen applied. Water was distilled from the reaction mixture. The temperature was then slowly increased to 200 °C for 15 min to complete the esterification. To build up molecular weight the temperature was first reduced to 165 °C and high vacuum was applied. Temperature was then increased slowly to a maximum of 230 °C and butanediol distilled from the reaction mixture. After 6 h under high vacuum the highly viscous melt was poured from the reaction vessel and collected on a Teflon film.

1.3.2. Synthesis of poly(butylene adipate-co-butylene terephthalate)s

Exemplarily for **poly(butylene adipate-co-butylene terephthalate)s** with variable Ada:Ta ratios:

For the synthesis of **poly(butylene adipate-co-butylene terephthalate) [90:10]** 99.03 g of dimethyl-terephthalate (0.51 mol, 1 eq), 597.5 g of 1,4-butanediol (6.63 mol, 13 eq) and 1.1 g of tetra-n-butyl ortho-titanate (3.23 mmol) were stirred at 190 °C. A slight stream of nitrogen was applied. Methanol was distilled

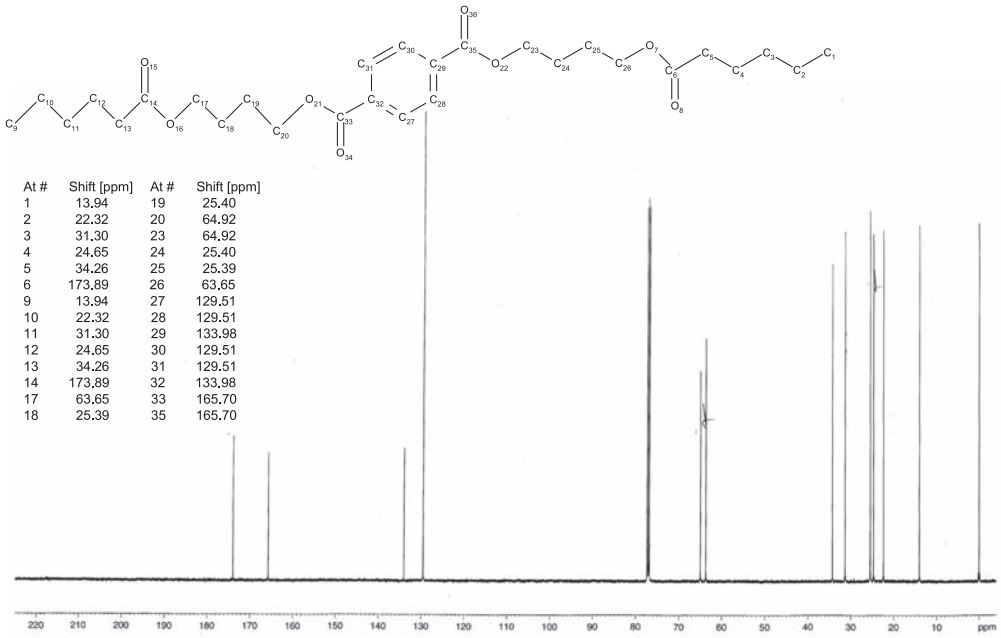

At #	Shift [ppm]	At #	Shift [ppm]
1	13.94	19	25.40
2	22.32	20	64.92
3	31.30	23	64.92
4	24.65	24	25.40
5	34.26	25	25.39
6	173.89	26	63.65
9	13.94	27	129.51
10	22.32	28	129.51
11	31.30	29	133.98
12	24.65	30	129.51
13	34.26	31	129.51
14	173.89	32	133.98
17	63.65	33	165.70
18	25.39	35	165.70

Fig. 4. ^{13}C NMR spectrum of bis(4-(hexanoyloxy)butyl) terephthalate (**HaBTaBHa**).

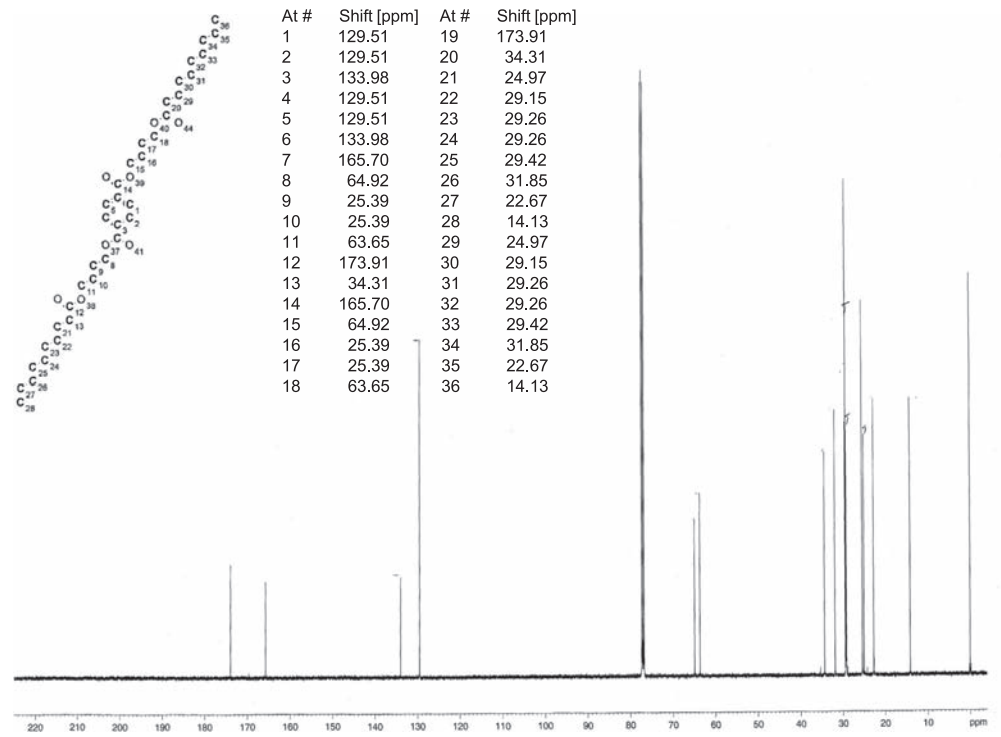

At #	Shift [ppm]	At #	Shift [ppm]
1	129.51	19	173.91
2	129.51	20	34.31
3	133.98	21	24.97
4	129.51	22	29.15
5	129.51	23	29.26
6	133.98	24	29.26
7	165.70	25	29.42
8	64.92	26	31.85
9	25.39	27	22.67
10	25.39	28	14.13
11	63.65	29	24.97
12	173.91	30	29.15
13	34.31	31	29.26
14	165.70	32	29.26
15	64.92	33	29.42
16	25.39	34	31.85
17	25.39	35	22.67
18	63.65	36	14.13

Fig. 5. ^{13}C NMR spectrum of bis(4-(decanoyloxy)butyl) terephthalate (**DaBTaBDa**).

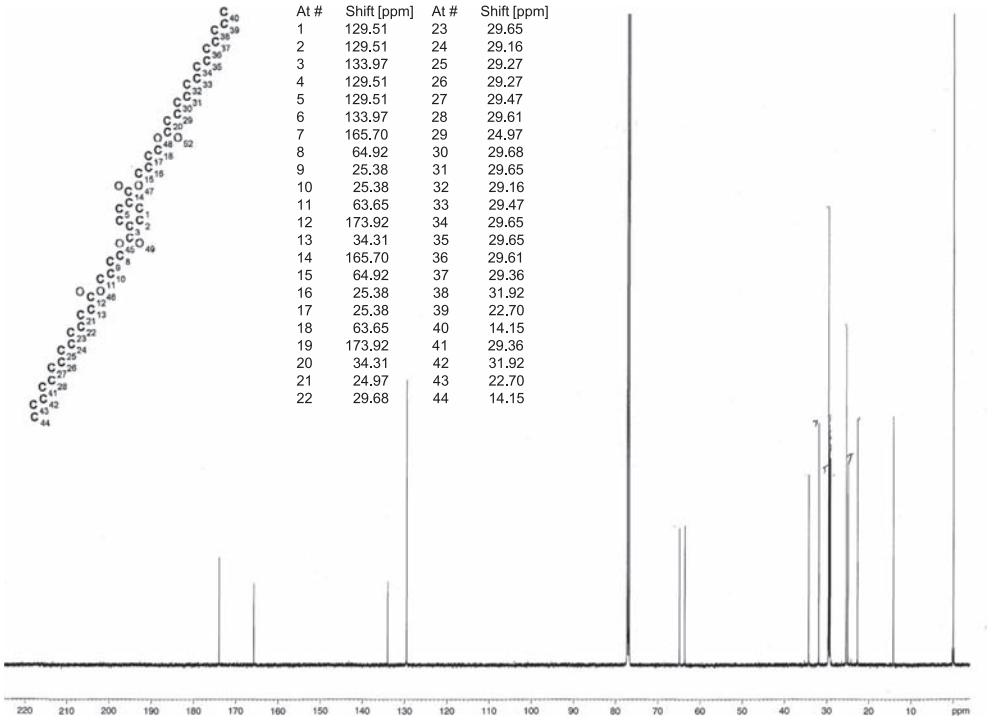

Fig. 6. ^{13}C NMR spectrum of bis(4-(decanoyloxy)butyl) terephthalate (**TdaBTaBTda**).

Table 1
Poly(butylene adipate-co-butylene terephthalate) substrates and their respective adipic acid to terephthalic acid ratios.

Poly(butylene adipate-co-butylene terephthalate) type	Ada:Ta ratio
Ada90_Ta10	89.3:10.7
Ada80_Ta20	78.9:21.1
Ada70_Ta30	68.9:31:1
Ada60_Ta40	58.5:41.5
Ada50_Ta50	48.8:51.2

from the reaction mixture. As soon as methanol distillation was completed, 670.78 g of adipic acid (4.59 mol, 9 eq) were added to the reaction mixture. On addition, the reaction temperature dropped significantly. To remove the water—formed by esterification of adipic acid—from the reaction mixture, the temperature was raised again to 200 °C. After the water distillation was finished, an additional 1.1 g of tetra-n-butyl orthotitanate (3.23 mmol) was added to the melt and high vacuum was applied to distill butanediol from the mixture. The reaction temperature was slowly increased to 220 °C. After 3 h at this temperature, a highly viscous melt was poured from the reaction vessel and collected on a Teflon film. Ada:Ta ratios were determined using ^{1}H NMR spectroscopy (Table 1).

Acknowledgments

This work has been supported by the Federal Ministry of Science, Research and Economy (BMWFW), the Federal Ministry of Traffic, Innovation and Technology (bmvit), the Styrian Business

Promotion Agency SFG, the Standortagentur Tirol, the Government of Lower Austria and ZIT-Technology Agency of the City of Vienna through the COMET-Funding Program managed by the Austrian Research Promotion Agency FFG (Grant number 848951).

Appendix A. Supplementary material

Supplementary data associated with this article can be found in the online version at http://dx.doi.org/10.1016/j.dib.2016.02.029.

References

[1] U. Witt, M. Yamamoto, U. Seeliger, R.-J. Müller, V. Warzelhan, Biodegradable polymeric materials—not the origin but the chemical structure determines biodegradability, Angew. Chem. Int. Ed. 38 (1999) 1438–1442.
[2] U. Witt, T. Einig, M. Yamamoto, I. Kleeberg, W.D. Deckwer, R.J. Müller, Biodegradation of aliphatic–aromatic copolyesters: evaluation of the final biodegradability and ecotoxicological impact of degradation intermediates, Chemosphere 44 (2001) 289–299.
[3] T. Kijchavengkul, R. Auras, M. Rubino, S. Selke, M. Ngouajio, R.T. Fernandez, Biodegradation and hydrolysis rate of aliphatic aromatic polyester, Polym. Degrad. Stab. 95 (2010) 2641–2647.
[4] V. Perz, K. Bleymaier, C. Sinkel, U. Kueper, M. Bonnekessel, D. Ribitsch, G.M. Guebitz, Substrate specificities of cutinases on aliphatic–aromatic polyesters and on their model substrates, New Biotechnol. 33 (2016) 295–304.
[5] A.B. Padias, H.K. Hall, Oligomeric bishydroxybutyl terephthalates from terephthalic acid, J. Polym. Sci.: Polym. Chem. Ed. 19 (1981) 1021–1032.
[6] H.-W. Hässlin, M. Dröscher, G. Wegner, Struktur und Eigenschaften segmentierter polyetherester, 3. Synthese definierter Oligomerer des polybutylenterephthalats, Die Makromol. Chem. 181 (1980) 301–323.

Environmental Science & Technology

Article

pubs.acs.org/est

An Esterase from Anaerobic *Clostridium hathewayi* Can Hydrolyze Aliphatic–Aromatic Polyesters

Veronika Perz,[†] Altijana Hromic,[‡,§] Armin Baumschlager,[‡] Georg Steinkellner,[‡] Tea Pavkov-Keller,[‡] Karl Gruber,[‡,§] Klaus Bleymaier,[‡] Sabine Zitzenbacher,[‡] Armin Zankel,[∥] Claudia Mayrhofer,[∥] Carsten Sinkel,[⊥] Ulf Kueper,[⊥] Katharina Schlegel,[⊥] Doris Ribitsch,*[,†,#] and Georg M. Guebitz[†,#]

[†]Austrian Centre of Industrial Biotechnology ACIB, Konrad Lorenz Strasse 20, 3430 Tulln, Austria

[‡]Austrian Centre of Industrial Biotechnology ACIB, Petersgasse 14, 8010 Graz, Austria

[§]Institute of Molecular Biosciences, University of Graz, Humboldtstrasse 50/III, 8010 Graz, Austria

[∥]Institute of Electron Microscopy and Nanoanalysis, Graz University of Technology, Steyrergasse 17/III, 8010 Graz, Austria

[⊥]BASF SE, Carl-Bosch-Straße 38, 67056 Ludwigshafen, Germany

[#]Institute of Environmental Biotechnology, University of Natural Resources and Life Sciences, Vienna, Konrad Lorenz Strasse 20, 3430 Tulln, Austria

Supporting Information

ABSTRACT: Recently, a variety of biodegradable polymers have been developed as alternatives to recalcitrant materials. Although many studies on polyester biodegradability have focused on aerobic environments, there is much less known on biodegradation of polyesters in natural and artificial anaerobic habitats. Consequently, the potential of anaerobic biogas sludge to hydrolyze the synthetic compostable polyester PBAT (poly(butylene adipate-*co*-butylene terephthalate) was evaluated in this study. On the basis of reverse-phase high-performance liquid chromatography (RP-HPLC) analysis, accumulation of terephthalic acid (Ta) was observed in all anaerobic batches within the first 14 days. Thereafter, a decline of Ta was observed, which occurred presumably due to consumption by the microbial population. The esterase Chath_Est1 from the anaerobic risk 1 strain *Clostridium hathewayi* DSM-13479 was found to hydrolyze PBAT. Detailed characterization of this esterase including elucidation of the crystal structure was performed. The crystal structure indicates that Chath_Est1 belongs to the α/β-hydrolases family. This study gives a clear hint that also micro-organisms in anaerobic habitats can degrade manmade PBAT.

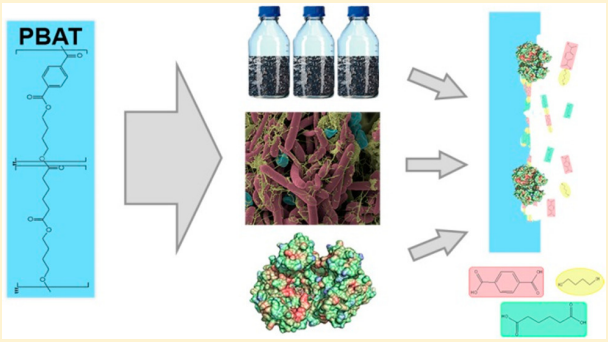

INTRODUCTION

Polymeric materials and polyesters are widely used in everyday life due to interesting material properties such as low density, chemical resistance, simple processability, and low production costs. Synthetic polymers have been designed to resist degradation because long-lasting polymers were urgently needed for a multitude of applications in, for example, automotive industry, electronics, or building and construction. However, for other applications like in agriculture (e.g., mulch films), food packaging, bags for organic waste or carrier bags, the persistence of the polymer is not needed or even a disadvantage. For that reason, biodegradable polyesters have become the focus of research since a few years ago because they combine beneficial material properties with biodegradability in a range of habitats.

The aliphatic–aromatic copolyester PBAT (poly(butyleneadipate-*co*-butyleneterephthalate) is a synthetic polyester used, for example, in food packaging or organic waste bags. When used as packaging materials, PBAT offers special barrier properties (e.g., its high water-vapor permeability) that predestine it for fruit and vegetable packaging, where it helps to prevent growth of molds. PBAT is proven to be compostable,[1,2] which makes it an important raw material for many compostable and biobased plastics. In the microbial mineralization of polyesters, hydrolysis by extracellular enzymes is the first step to produce oligomers and monomers, which can be further metabolized in the microbial cell. Thus, several research groups have studied the enzymatic hydrolysis of PBAT. Generally, aerobic hydrolases such as the cutinase from *Thermobifida cellulosilytica* or *Humicola insolens*,[3] the cutinase-like enzymes from *Saccharomonospora viridis*,[4,5] lipases from *Pseudomonas*

Received: September 7, 2015
Revised: February 10, 2016
Accepted: February 15, 2016
Published: February 15, 2016

DOI: 10.1021/acs.est.5b04346
Environ. Sci. Technol. 2016, 50, 2899–2907

sp.,[6] or a hydrolase from *Thermobifida fusca*[7] are known to hydrolyze PBAT.

In recent years, anaerobic digestion has gained importance in the biological treatment of organic household wastes, often integrated in existing composting plants. The biodegradability of aliphatic−aromatic polyesters under composting conditions was demonstrated by different research groups. In contrast to aerobic composting, there is considerably less information available on the hydrolysis in anaerobic environments. Here, an esterase from *Clostridium hathewayi*[8] (namely, Chath_Est1) was discovered. *C. hathewayi* was lately reclassified to *Hungatella hathewayi*,[9] a representative of the new genus *Hungatella* of the family *Clostridiaceae*. The risk 1 strain was found to hydrolyze PBAT, which shows for the first time that anaerobic micro-organisms are able to degrade synthetic polymer.

EXPERIMENTAL SECTION

Chemicals and Reagents. Milled PBAT, PBAT oligomers (oPBAT), and PHB (polyhydroxybutyrate) as well as oPBAT and PBAT pellets were kindly provided by BASF SE (Germany). The PET model substrate bis(benzoyloxyethyl)-terephthalate (BaETaEBa) was synthesized according to the method described by Heumann et al.[10] Oligomeric PBAT model substrates bis(4-hydroxybutyl) terephthalate (BTaB), mono(4-hydroxybutyl) terephthalate (BTa), and *O,O′*-(butane-1,4-diyl) bis(4-hydroxybutyl) diterephthalate (BTaBTaB) were synthesized as previously described.[11] NMR and high-performance liquid chromatography−mass spectrometry (HPLC−MS) were used to confirm purity.

Methanol and acetonitrile were of HPLC grade and purchased from Roth (Karlsruhe, Germany). All other chemicals were of analytical grade and purchased from Sigma-Aldrich (Germany).

Carrez reagent I and Carrez reagent II were prepared by dissolving 1.06 g of $K_4[Fe(CN)_6]\cdot 3H_2O$ or 2.88 g of $ZnSO_4\cdot 7H_2O$ in 10 mL of ddH_2O, respectively.

Anaerobic Batch Cultures. To study the ability of anaerobic microbial populations to adapt to the synthetic polyester PBAT and the oligomeric PBAT model substrate oPBAT, we prepared anaerobic batch cultures by mixing 170 mL of anaerobic inoculum with 330 mL of mineral salt medium in 1000 mL flasks. Inoculation sludge was originally collected at the biogas plant Strem (Burgenland, Austria) utilizing energy crops, which were fully fermented under mesophilic conditions (37°), sieved to exclude biomass particles >2.0 mm, and pooled before application in cultivation experiments. Before usage in the described experiments, the sludge was kept under mesophilic conditions for several months and fed sporadically with maize silage. The mineral salt medium (EN ISO 11734 L47 "Evaluation of the ultimate anaerobic biodegradability of organic compounds in digested sludge", 1998) had the following composition: 0.27 g of KH_2PO_4, 1.12 g of $Na_2HPO_4\cdot 12H_2O$, 0.53 g of NH_4Cl, 0.075 g of $CaCl_2\cdot 2H_2O$, 0.1 g of $MgCl_2\cdot 6H_2O$, 0.02 g of $FeCl_2\cdot 4H_2O$, 0.001 g of resazurin, 0.1 g of Na_2S, 1000 mL of ddH_2O, and 1 mL of trace element solution. The pH was adjusted to 7.0 using 1 M HCl. Trace element solution[12] contained: 70 mg of $ZnCl_2$, 100 mg of $MnCl_2\cdot 4H_2O$, 200 mg of $CoCl_2\cdot 6H_2O$, 100 mg of $NiCl_2\cdot 6H_2O$, 20 mg of $CuCl_2\cdot 2H_2O$, 50 mg of $NaMoO_4\cdot 2H_2O$, 26 mg of $Na_2SeO_3\cdot 5H_2O$, 1 mL of HCl (25%), and 1000 mL of ddH_2O. The sludge was flushed with oxygen-free nitrogen gas for 20 min l^{-1} to achieve anaerobic cultures. To induce polyesterase expression, we fed-batch-wise added 0.5 g of the microbial polyesters PHB on day 0 and thus subsequently every 30 days to the sample batches oPBAT+ and PBAT+. The PBAT− batch that was not induced with PHB was fed with 0.5 g of maize silage instead. A total of 1 g of milled oPBAT or PBAT (particle size 100−300 μm) was introduced to batch experiments on day 0 to reached a final sample concentration of 0.2% w/v. The control biogas batch was spiked with 6.5 mM of Ta and adipic acid (Ada) on day 0. Anaerobic control batches containing mineral salt medium, 0.02% w/v sodium azide, and the respective substrates were incubated simultaneously at 37 °C. Hydrolysis of PBAT and oPBAT was monitored over a time period of 60 days by means of reverse-phase high-performance liquid chromatography (RP-HPLC) analysis. Samples were taken as triplicates in regular intervals.

RP-HPLC Analysis of Hydrolysis Products in Anaerobic Batch Cultures. Prior to HPLC analysis, a modified Carrez precipitation[13,14] was performed to remove interfering substances from the complex sample matrix. A total of 1 mL was withdrawn from each biogas batch or abiotic control. Samples were centrifuged (Hermle Z300 K, MIDSCI) at 14000*g* for 10 min at 20 °C. A total of 200 μL of each supernatant was then transferred into fresh 1.5 mL reaction tubes and mixed with 780 μL of ddH_2O and 10 μL of Carrez reagent I. The mixture was vortexed and incubated for 1 min at 20 °C. Then, 10 μL of Carrez reagent II was added, and the mixture was vortexed again. Precipitation was conducted at 20 °C for 20 min followed by a centrifugation step (14000*g*, 4 °C, 30 min). A total of 400 μL of the supernatant was mixed with 400 μL of methanol, acidified with formic acid to reach a pH of 3.0, and incubated for 60 min at 4 °C. Samples were centrifuged again (14000*g*, 15 min, 0 °C) and analyzed by means of RP-HPLC with the method that was previously described.[3]

Extraction of Terephthalic Acid from Biogas Sludge. To ensure that a measured decrease of Ta concentration in the batch cultures was not caused by precipitation of Ta, we performed a DMSO extraction 133 days after the start of the experiment. A total of 40 mL of sludge was withdrawn from each batch and centrifuged (4000*g*, 20 min, 20 °C). Pellets were resuspended in 100 mL of DMSO and rotated for 15 min at 30 rpm on a rotation mixer (WiseMix RT-10, Wisd Laboratory Instruments, Czech Republic). The mixture was centrifuged again (4000*g*, 20 min, 20 °C), and the supernatants were Carrez precipitated and prepared for RP-HPLC as described above.

Scanning Electron Microscopy of Biofilm Formation on Polyester Pellets. To investigate biofilm formation on the polyesters, we introduced pellets of PBAT and oPBAT (diameter 0.5 cm) to a separate batch culture using in situ concentrate bags (6.75 × 12 cm; Ankom, Macedon, NY) to facilitate the recovery of the pellets after batch operation. Pellets were removed from the anaerobic batches after 86 days and prepared for scanning electron microscopy. For morphological investigations, scanning electron microscopy (Zeiss ULTRA 55, Carl Zeiss Micro Imaging GmbH, Germany) was performed at primary electron energy of 5 keV. The (poly)ester pellets carrying biological material were imaged with the high-efficiency "in-lens SE detector" using secondary electrons (SE) to get topographic contrast.[15,16] Before application, fresh samples were fixed overnight using glutaraldehyde (3% in 0.1 mol cacodylic acid sodium salt trihydrate, pH 7.2 at 4 °C), stained and double-fixed for at least 3 h at 4 °C with 2% OsO_4

DOI: 10.1021/acs.est.5b04346
Environ. Sci. Technol. 2016, 50, 2899−2907

(in 0.1 mol cacodylic acid sodium salt trihydrate), dehydrated in a graded ethanol series with a final step in propylene oxide, and ultimately dried by critical-point drying (CO_2). For observation, prepared samples were mounted on aluminum stubs using double-sided carbon tape and sputter-coated with Au or Pd.

Investigation of Hydrolytic Activity of *C. hathewayi*. The potential of *C. hathewayi* to hydrolyze PBAT in vivo was analyzed. For this, *C. hathewayi* cultures (strain DSM-13479 obtained from DSMZ) were grown as recommended from DSMZ at 30 °C under anaerobic conditions in 6 × 50 mL of PYX medium (DSMZ medium 104b) supplemented with 0.04 g/L glucose and 10 μM potassium buffer (pH 7.0). The cells were harvested anaerobically in the late exponential growth phase (OD 0.18). The cells were centrifuged (3000*g*, 10 min, 4 °C) and washed with PYX medium for two times to remove all remaining supplements. After the washing procedure, the cells were resuspended in PYX medium to a final OD of 0.6. Each division of 30 mL of the cell suspension was supplemented with 0.04 g/L glucose and 10 μM phosphate buffer, PBAT and oPBAT and 10 μM phosphate buffer, or 10 μM phosphate buffer as a negative control. The sample were incubated for 24 h at 30 °C. Afterward, 25 mL of cell suspension was harvested (3200*g*, 4 °C, 30 min), and supernatant as well as cells were frozen separately. To analyze the hydrolytic activity of enzymes from *C. hathewayi*, we tested the supernatants (after the centrifugation of the cells). To do this, we incubated 10 mg of PBAT with 2 mL of supernatant for 6 days at 100 rpm and 37 °C in a thermomixer (Thermomixer comfort, Eppendorf, Germany). The control (2 mL of PYX medium with 10 mg of PBAT) was treated simultaneously. Additionally, supernatants of all three cultures as well as PYX medium alone were analyzed for hydrolysis products prior to incubation with PBAT. Prior to HPLC quantification, a Carrez precipitation was performed. Hence, 960 μL sample and 20 μL of Carrez reagent I were vortexed and incubated for 1 min at 20 °C. Then, 20 μL of Carrez reagent II were added, and the mixture was vortexed and precipitated at 20 °C for 20 min followed by a centrifugation step (14000*g*, 4 °C, 30 min). The supernatant was acidified with 6 N HCl to reach a pH of 3.0, and the released hydrolysis products Ta, BTa, and BTaB were detected and quantified by means of RP-HPLC.[3]

General Recombinant DNA Techniques. Molecular cloning of the esterase gene was performed by standard methods as described by Sambrook et al.[17] The digestion of DNA with restriction endonucleases *Nde*I and *Hind*III (New England Biolabs), dephosphorylation with alkaline phosphatase (Roche, Germany), and ligation with T4 DNA-ligase (Fermentas, Germany) were performed as described in the manufacturer's protocols. Plasmid DNA was prepared using the Plasmid Mini Kit from Qiagen (Germany). DNA fragments and plasmids were purified by the Qiagen DNA purification kits (Qiagen, Germany), and vector pET26b(+) (Novagen) was used for expression of the esterase carrying a C-terminal 6 × HisTag in *E. coli* BL21-Gold(DE3) (Stratagene).

Cloning of Chath_Est1. The gene coding for the partial *para*-nitrobenzyl esterase from *C. hathewayi* DSM-13479 (accession no. EFC94627.1) was completed according to the sequence alignment with homologous proteins (Figure S1), codon-optimized for expression in *E. coli* and synthesized by GeneArt (Life Technologies). The nucleotide sequence coding for Chath_Est1 fused to the C-terminal 6 × His Tag comprises 1592 base pairs with a GC content of 55%. The plasmid carrying the target gene was digested, purified, and ligated into expression vector pET26b(+) (Novagen, Merck KGaA) over the *Nde*I and *Hind*III restriction sites. The expression vector was then transformed into electrocompetent *E. coli* BL21-Gold(DE3) cells.

The gene was expressed as a fusion protein carrying a C-terminal 6 × HisTag with a molecular weight of 59.2 kDa.

DNA Sequencing, Alignments, and Deposition of Sequence Data. DNA was sequenced as custom service by Agowa, and DNA analysis was performed with Vector NTI Suite 10 (Invitrogen). The Expert Protein Analysis System (ExPASy) proteomics server of the Swiss Institute of Bioinformatics was used to perform a BLAST search, and sequences of related proteins were aligned using the Clustal W program (Swiss EMBnet node server). The complete and codon optimized nucleotide sequence of Chath_Est1 was deposited in the GenBank database under accession no. KT222913.

Expression, Purification, and Protein Concentration of Chath_Est1. The expression at 20 °C and purification of Chath_Est1 was performed in accordance to the previously described expression and purification of Cbotu_EstA and Cbotu_EstB.[18] Protein concentration of the purified enzyme solution was measured using the BIO-Rad Protein Assay (BIO-RAD) and bovine serum albumin as a standard. SDS Page was performed in accordance to Laemmli et al.,[19] and staining of the proteins was done with Coomassie Brilliant Blue R-250.

Esterase Activity and Stability. Esterase activity and kinetic parameters were determined at pH 7.0 and 25 °C as previously described[18] using *para*-nitrophenylacetate (*p*NPA) and *para*-nitrophenylbutyrate (*p*NPB) as substrates (Table 1).

Table 1. Kinetic Parameters of Chath_Est1 on the Soluble Esterase Standard Substrates *p*NPA and *p*NPB

	V_{max} [μmol min^{-1} mg^{-1}]	K_m [mM]	k_{cat} [sec^{-1}]	k_{cat}/K_m [sec^{-1} mM^{-1}]
*p*NPA	2.50 ± 0.20	2.00 ± 0.20	2.47	1.23
*p*NPB	7.00 ± 0.20	2.00 ± 0.20	6.91	3.45

To determine the optimum temperature, we incubated Chath_Est1 in 50 mM potassium phosphate buffer pH 7.0 at 25, 37, and 50 °C and 300 rpm. Activity was measured using *p*NPB as a substrate with the final concentrations of 7.9 mM. The activity determined at time-point zero was defined to be 100%, the decrease in activity was followed for 35 days, and the activity half-life of Chath_Est1 was calculated.

The pH optimum of Chath_Est1 was determined by following the hydrolysis of bis(2-benzoyloxy)ethyl) terephthalate (BaETaEBa) at different pHs. For this purpose, 10 mg of BaETaEBa was incubated for 23 h at 37 °C and 300 rpm with 6 μM Chath_Est1 in 2 mL of buffered solutions with 50 mM citrate phosphate at pH 4.0, pH 5.0, and pH 6.0, potassium phosphate at pH 7.0, pH 8.0, and pH 9.0, and glycine−NaOH at pH 10.0. Samples were withdrawn,[18] and RP-HPLC analysis was performed[3] as previously described.

The hydrolysis of BaETaEBa was additionally followed over time. Samples containing 2 mL of 50 mM potassium phosphate buffer pH 7.0, 10 mg of BaETaEBa, and 6 μM Chath_Est1 were incubated at 37 °C and 300 rpm for 0, 1, 3, 5, 8, 20, and 24 h. Samples were withdrawn and analyzed as described above.

Hydrolysis of the Polyester PBAT and Oligomeric PBAT Model Substrates. The ability of Chath_Est1 to

DOI: 10.1021/acs.est.5b04346
Environ. Sci. Technol. 2016, 50, 2899−2907

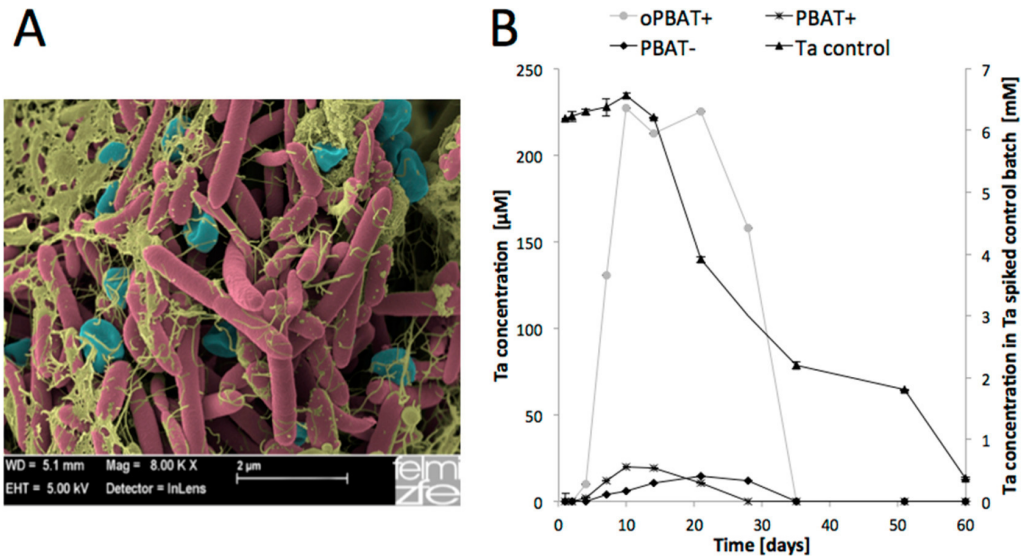

Figure 1. (A) SEM image of oPBAT after incubation in biogas plant sludge inoculated anaerobic batch cultures for 86 days. Additional images can be found in Figure S2. (B) Liberation of terephthalic acid from PBAT and oPBAT incubated in biogas plant sludge inoculated anaerobic batch cultures in the presence (+) and absence (−) of PHB as inductor. As a control, a batch culture was spiked with 6.5 mM Ta. Each data point represents the average of three independent samples; displayed error bars indicate respective minimum and maximum values. An example of an HPLC profile can be found in Figure S3.

hydrolyze PBAT and the model substrates BTaB and BTaBTaB was tested by incubating 0.6 μM Chath_Est1 with 10 mg PBAT or 13.5 mM BTaB and BTaBTaB, respectively. The samples were incubated for 48 and 72 h at 37 °C and 300 rpm on a thermomixer (Thermomixer Comfort, Eppendorf) in a total volume of 1 mL of 50 mM potassium phosphate buffered solution pH 7.0. Reactions were stopped, methanol precipitation was performed, and hydrolysis products Ta, Ada, BTa and BTaB were quantified via RP-HPLC as previously described.[3] Control reactions were performed simultaneously without addition of Chath_Est1.

Crystallization of Chath_Est1. Crystallization experiments were performed by the sitting-drop vapor diffusion method using different commercial crystallization screens (the Index Screen from Hampton Research and the Morpheus Screen from Molecular Dimensions). Sitting drops were prepared by mixing 0.5 μL of the protein solution (at a concentration of 30 mg/mL) with an equal volume of mother liquor, which were pipetted using an ORYX 8 pipetting robot from Douglas Instruments. The trays were incubated at 20 °C. First, crystal clusters were observed after approximately 1 week. Well-diffracting Chath_Est1 crystals were obtained with 1.0 M ammonium sulfate, 0.1 M HEPES, pH 7.0 and 0.5% w/v polyethylene glycol 8000 (Index Screen, condition C11).

Data Collection and Processing. X-ray diffraction data were collected to a maximum resolution of 1.9 Å on beamline P11 (λ = 1.033 Å) at the PETRA III/DESY (Hamburg, Germany). The crystals were monoclinic (space group $P2_1$) with unit-cell parameters a = 62.05 Å, b = 241.83 Å, and c = 83.58 Å, β = 90.0°.

The data were processed using the XDS package.[20] The structure was solved by molecular replacement using the structure of the thermostable carboxylesterase Est55 from *Geobacillus stearothermophilus* (PDB code 2OGS, 36% sequence identity).[21] The initial model was built using the mr-Rosetta module of PHENIX[22] yielding four molecules of Chath_Est1 in the asymmetric unit consistent with the calculated Matthews coefficient.[23] Structure rebuilding and refinement were performed using the programs Coot[24] and PHENIX.[22] Clear electron density was observed for the majority of the amino acids except the first N-terminal residue (Met) and 20 C-terminal residues in all four chains. Residual density was interpreted as phosphate ions in all chains. The final structure was validated using MolProbity.[25] Detailed statistics pertaining to data processing and structure refinement are summarized in Table S1. The atomic coordinates and structure factors have been deposited in the Protein Data Bank under the code 5A2G.

Modeling. To build the model of the covalent tetrahedral intermediate compound, we used a molecular model of methyl acetate in the first step to fit the molecule into the proposed active site of the Chath_Est1 structure. The substrate was prepared and optimized using YASARA.[26] The carboxylic oxygen of the substrate in its anionic form was fit into the proposed oxyanion hole, and the methyl acetate was covalently bond to the active-site serine oxygen (Ser-200), mimicking the covalent tetrahedral intermediate. The protonation and tautomerization states of His residues were chosen according to hydrogen-bonding networks. Asp, Glu, Arg, and Lys residues were treated as charged. The active-site His-416 was modeled to be protonated. This initial complex was subjected to a molecular mechanics optimization using YASARA with the AMBER03 force field[27] applying the standard optimization protocol. This energy-minimized complex was used to build and extend the tetrahedral intermediate to the BTaB substrate and was also subjected to a molecular mechanics optimization. The final polymer complex was built by successively adding new functional groups and polymer subunits, keeping the extensions as close as possible to the surface of the protein by also keeping reasonable bond angles and dihedrals. Between all addition steps, energy minimization of the complex structure was performed and water was deleted, where it clashed with the added functional groups. This model was then used for a final energy minimization step, resulting in the proposed model of the active site complex. Figures were prepared using PyMOL

DOI: 10.1021/acs.est.5b04346
Environ. Sci. Technol. 2016, 50, 2899−2907

(DeLano WL (2002); PyMOL Molecular Graphics System, version 1.5.0.4, Schrödinger LLC), and surface hydrophobicity was generated using VASCo.[28,29]

RESULTS AND DISCUSSION

Hydrolysis Products in Anaerobic Batch Cultures. Biodegradable polyesters such as PBAT are used, for example, in organic waste bags or food packaging. So far, kitchen and organic waste is usually biologically treated in composting plants. Nevertheless, the trend of the recent years is to recover energy from organic waste during anaerobic digestion, often in combination with postcomposting, to degrade residual organic waste.[30] The biodegradability of PBAT was proven and studied under aerobic conditions (composting).[1,2] However, there is considerably less known about the anaerobic biodegradation of PBAT. Consequently, the hydrolysis of PBAT by "anaerobic" enzymes was investigated in this study.

In a first step, the general degradation ability of PBAT in biogas sludge was investigated. SEM analysis of oPBAT and PBAT pellets that were incubated in biogas sludge showed formation of biofilms on the surface consisting both of cocci and rod-shaped bacteria (Figures 1A and S2). RP-HPLC analysis of the control batch that was spiked with 6.5 mM Ada and Ta revealed that Ada is metabolized in the sludge quite efficiently. After 21 days, the concentration of Ada in the spiked control batch was beneath the detection limit of 0.5 mM (data not shown). In the PBAT sample batches (oPBAT+, PBAT+, and PBAT−), no Ada could be detected due to immediate metabolization when released from the polymer. Generally, aliphatic compounds are more easily biodegraded than aromatic ones. Sotto et al. observed relatively fast biodegradation rates for different aliphatic monomers including Ada.[31] Consequently, the analysis of released molecules in the batch tests was focused on Ta.

In all PBAT batches, the Ta concentration raised within the first 14 days of incubation indicating a certain degree of oPBAT and PBAT hydrolysis (Figure 1B). Interestingly, Ta concentration started to decrease significantly after day 21 in all batches, including the Ta spiked control batch. After 35 days, Ta was no longer detectable in the sample batches, and after 60 days, only 6% of initial Ta concentration was detected in the spiked control batch. In abiotic control batches, no hydrolysis products were detected. Ta extraction with DMSO that was performed after 133 days did not regain Ta from any of the biogas batches, including the control batch. This led to the assumption that Ta was indeed metabolized by the action of microorganisms in all biogas batches. Several other research groups have already reported the biodegradation of Ta by different aerobic microorganisms such as species from *Bacillus*,[32] *Pseudomonas*,[33] and *Arthrobacter*.[34] Moreover, anaerobic consortia exhibited Ta biodegradation potential[35,36] and were analyzed to identify the key organisms responsible for Ta biodegradation.[37−39] It might be that the biogas sludge needs a certain time to adapt to Ta and starts to metabolize Ta after 3 weeks, when alternative C-sources are limited. Kleerebezem et al.[36] reported Ta degradation in a first-stage reactor after 300 days and in the second-stage reactor from day 1.

One parameter that influences the hydrolysis of PBAT seems to be the size of the polymer, as the lower-molecular-weight model substrate, oPBAT, was hydrolyzed considerably faster. Melting temperatures (T_m) of PBAT and oPBAT lay around 125 °C; however, the melting range of oPBAT was broader and started at lower temperatures. One PBAT batch (PBAT+) was spiked with the naturally occurring polyester PHB with the aim to induce esterase expression. PBAT+ reached a maximum Ta concentration of about 20.0 μM after 10 days, whereas in the PBAT batch, without inducing PHB (PBAT-), the maximum Ta concentration was detected to be 14.4 μM after 21 days. The maximum Ta concentration in PBAT+ was higher and was reached faster in comparison to PBAT−. This indicates that PHB (i.e., hydrolysis products) may induce the secretion of enzymes that are capable of degrading PBAT.

In Silico Search for Anaerobic Polysterases. On the basis of the above indication for anaerobic degradation of PBAT, the next step was dedicated to identification of anaerobic organisms and enzymes responsible for PBAT hydrolysis. Consequently, an in silico screening for enzymes from anaerobic organisms with activity on synthetic polyesters was performed to identify active microorganisms and their respective polyesterases. *Clostridium* species belonging to the phylum of Firmicutes are described to be omnipresent in biogas sludge,[40,41] including an anaerobic consortium known to biodegrade Ta.[39] Several proteins extracted from a Ta-degrading biofilm were annotated to *Clostridium*.[37] Typically, *Clostridium* species are described to be important for degradation of cellulosic material,[42] but they are also reported to hydrolyze the polyesters poly(β-caprolactone) (PCL) and poly(β-hydroxybutyrate) (PHB).[43] Nevertheless, the so far identified *Clostridium* strains with significant activity on PCL did not hydrolyze poly(butylene terephthalate-*co*-butylene adipate).[44]

An extensive search of the NCBI protein database revealed that the risk 1 strain *C. hathewayi* (also *H. hathewayi*) carries the gene for a putative, partial esterase that has been completed according to the sequences of highly homologous proteins (Figure S1) and named Chath_Est1. On the basis of our own metagenomics-based identification of hydrolytic *Clostridia* and of others who found the closely related *C. saccharolyticum* WM1 in biogas sludge,[45] we have specifically selected the risk 1 strain *C. hathewayi* for further investigation because this strain is attractive for bioaugmentation anaerobic communities to enhance plastics degradation.

Hydrolysis of PBAT by *C. hathewayi* Cultures. To analyze the ability of *C. hathewayi* to hydrolyze PBAT, we preincubated resting cells in PYX medium supplemented with PBAT and oPBAT. One sample supplemented with glucose and one sample without further addition were used as the control. *C. hathewayi* supernatants obtained from these three preincubations were then incubated with PBAT. Degradation products of PBAT were found, even though the amount of monomers differed. The supernatants from the cultures that were preincubated with PBAT and oPBAT to stimulate the expression of polyesterases showed an elevated level of released Ta and BTa in comparison to the cultures that were preincubated in PYX medium or PYX medium supplemented with glucose (Figure 2).

Biochemical Properties of Chath_Est1. Expression of the codon-optimized Chath_Est1 gene carrying the C-terminal 6 × HisTag resulted in production of soluble protein but also in significant amounts of inclusion bodies. The highest protein yields were obtained after 20 h of induction at 20 °C and 160 rpm (Figure S5).

The temperature stability of Chath_Est1 was tested at pH 7.0 at 25, 37, and 50 °C with the soluble substrate *p*NPB. Chath_Est1 exhibited the highest stability at 25 °C with 85%

DOI: 10.1021/acs.est.5b04346
Environ. Sci. Technol. 2016, 50, 2899−2907

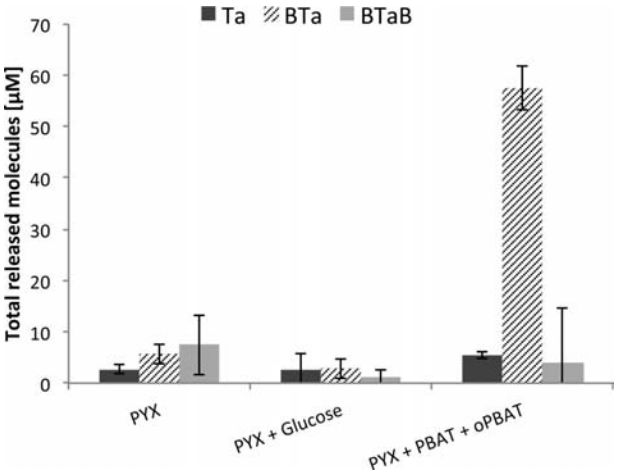

Figure 2. Total released molecules after incubation of *C. hathewayi* cell supernatants with PBAT for 6 days at 37 °C and 100 rpm. Released molecules are shown in μM and were quantified by means of HPLC analysis. Ta: terephthalic acid; BTa: mono(4-hydroxybutyl) terephthalate; BTaB: bis(4-hydroxybutyl) terephthalate. Each bar represents the average of three independent samples; error bars indicate the standard deviation. *C. hathewayi* was preincubated in PYX in the absence or presence of glucose or PBAT and oPBAT and the respective culture supernatants were analyzed. Hydrolysis products were quantified in controls incubated under identical conditions (i.e., culture supernatants without PBAT, PYX medium alone, or PYX with PBAT) and were subtracted. Examples of RP-HPLC profiles can be found in the Figure S4.

activity remaining after 35 days. The activity half-lives at 37 and 50 °C were determined to be 10 days and 20 min, respectively. Chath_Est1 shows significant activity in a pH range of 6.0 to 8.0 (Figure S6). For this reason, the neutral pH 7.0 was chosen for further characterizations of the esterase.

The water-soluble esterase substrates *p*NPA and *p*NPB were utilized to determine the kinetic parameters of Chath_Est1. V_{max} and k_{cat} of Chath_Est1 were more than 2 times higher for *p*NPB compared to *p*NPA, whereas K_m values were in the same range for both standard substrates.

Hydrolysis of PBAT and Model Substrates by Chath_Est1. During the incubation of BaETaEBa with Chath_Est1, the release of the hydrolysis products ETa, Ta, and Ba was quantified by RP-HPLC (Figure 3). ETaE and BaE were not found, leading to the assumption that these esters were fast hydrolyzed to their constituents and, therefore, not accumulated in the reaction mixture. Taking into account the structure of the model substrate, Chath_Est1 seems to release the Ta subunits more efficiently than the Ba subunits. The concentrations of released Ta and Ba are in the same range. However, two Ba subunits but just one Ta would be available in the BaETaEBa molecule. This is in contrast to the recently investigated esterases Cbotu_EstA and Cbotu_EstB from *Clostridium botulinum*, which preferably released Ba.[18]

Chath_Est1 hydrolyzed PBAT as well as the oligomeric model substrates BTaB and BTaBTaB that are possible fragments of the PBAT polymer. After 72 h, the highest concentration of released molecules was observed with the substrate BTaB followed by BTaBTaB and PBAT, which was hydrolyzed slower by 2 orders of magnitude (Figure S7).

Overall Structure of Chath_Est1. The X-ray crystal structure of Chath_Est1 was determined at 1.90 Å resolution

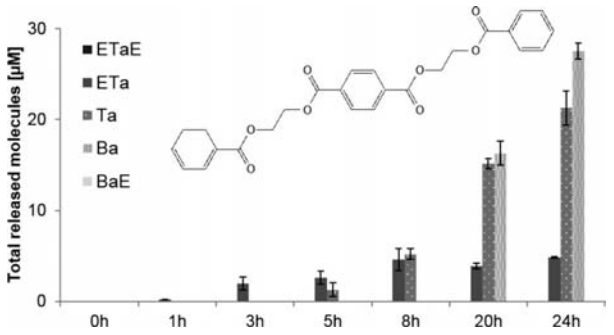

Figure 3. Chemical structure of BaETaEBa and released molecules after hydrolysis with 6 μM Chath_Est1 at 37 °C and 300 rpm in 50 mM potassium phosphate buffer pH 7.0. Released molecules are shown in μM. ETaE: bis(2-hydroxyethyl) terephthalate, ETa: mono(2-hydroxyethyl) terephthalate, Ta: terephthalic acid, BaE: 2-hydroxyethyl benzoate, and Ba: benzoic acid. Quantification was performed with RP-HPLC. Each bar represents the average of three independent samples; error bars indicate the standard deviation.

(Table S1). The crystal belongs to the monoclinic space group $P2_1$) and contains four esterase molecules in the asymmetric unit. According to an analysis of intermolecular interactions in the crystal using the PDBePISA server,[46] Chath_Est1 is most likely present as dimer in solution. The overall structure consists of a central β-sheet surrounded by α-helices, indicating that Chath_Est1 belongs to the family of α/β-hydrolases (Figure S8). The structures of the four crystallographically independent esterase molecules are very similar to pairwise root-mean-square-deviations (rmsd) ranging from 0.208 to 0.220 calculated using the program PyMOL.

On the basis of sequence and structure comparisons, we determined that Chath_Est1 contains a catalytic triad formed by Ser-200, His-416, and Glu-323 (Figure 4). The entrance to

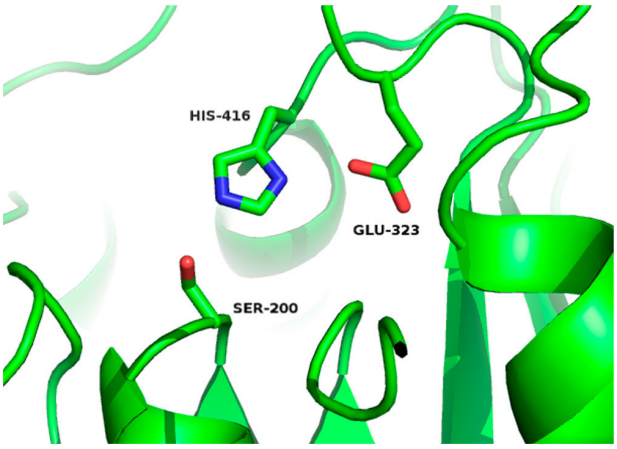

Figure 4. Catalytic triad of Chath_Est1.

the active site is formed by loops and helices. Residues 67−74 and 430−434 form one side of the entrance, whereas residues 329−333 and 274−282 form the rest of the entrance. The active site is located at the base of the open cavity (Figure 5), which was also observed in *p*NB esterase (PDB code: 1C7I)[47] and in the thermostable carboxylesterase Est55 from *Geobacillus stearothermophilus* (PDB code: 2OGS).[21] The presence of Glu instead of Asp in the catalytic triad is similar to the situation in acetylcholine esterase.[48] The sequence identity of Chath_Est1

DOI: 10.1021/acs.est.5b04346
Environ. Sci. Technol. 2016, 50, 2899−2907

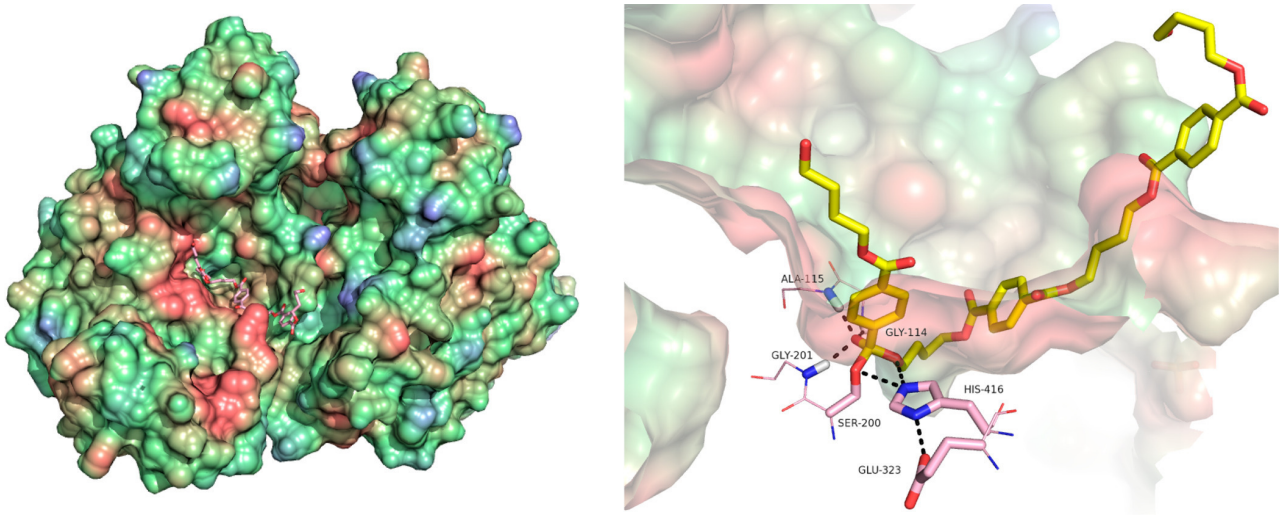

Figure 5. Left: model of the Chath_Est1 dimer structure with the open active site in complex with the poly substrate (shown in stick representation). The surface is colored by hydrophobicity values (blue hydrophilic to red hydrophobic). Right: proposed covalent tetrahedral intermediate of the poly substrate. The oxyanion hole and the active site residues are shown in a stick representation. The covalently bound poly substrate is shown in yellow. The surface is shown transparently and colored by hydrophobicity values (blue hydrophilic to red hydrophobic).

compared to carboxylesterase Est55 is about 36% and about 34% to *p*NB esterase, respectively[47] (Figure S9). The active site residues are in similar positions as in the other two structures.

We modeled a structure mimicking the tetrahedral intermediate formed during the hydrolysis of the substrate (Figure 5 and Figure S10). In that model, the active site can be divided into two regions by a plane defined by the hydroxyl oxygen atom of Ser-200 as well as the central carbon atom and the oxyanion of the tetrahedral substrate intermediate. The active site His-416 is located on one side of this plane and is correctly positioned to protonate the alcoholic leaving group. The oxyanion hole is formed by the helix, at the N-terminal end of which the active site Ser-200 is located, and by the main chain amide groups of Gly-114, Ala-115, and Gly-201.

In conclusion, with the results described here we tried to portray anaerobic biodegradation of PBAT from the crude sludge via an anaerobic organism through to a mechanistic focus on polyesterases that are responsible for the initial enzymatic hydrolysis. We have shown that typical anaerobic sludges are able to hydrolyze PBAT to a certain degree, and the released monomers Ada and Ta are not detectable anymore. Nevertheless, PBAT hydrolysis rates are very low. On the basis of the presented results, it is impossible to say if PBAT is hydrolyzed completely, and the efficient degradation of PBAT in industrial biogas plants with retention times of about 3 weeks is not feasible so far. The application of polyesterase inducing naturally occurring polyesters such as PHB might be an option to stimulate the growth of microorganisms expressing hydrolytic enzymes with activity on PBAT for improved PBAT hydrolysis in anaerobic environments. In addition, we have cloned and heterologously expressed the esterase Chath_Est1 from the anaerobic risk 1 strain *C. hathewayi* that hydrolyzes the synthetic polyester PBAT. The crystal structure of Chath_Est1 was solved and will help to improve the knowledge about polyesterases in general. Closing the circle, our experiments indicate that *C. hathewayi* cells (i.e., their enzymes in the supernatants) are hydrolyzing PBAT.

The present study gives a hint about how and by which kind of microorganisms these manmade plastics could be biodegraded in anaerobic environments. The knowledge about micro-organisms that are hydrolyzing polyesters such as PBAT could also open the door for new applications, such as the addition of cell or spore suspensions to biogas plants to enhance the anaerobic biodegradation of biodegradable polymers that are, for example, used in food packaging or organic waste bags.

■ ASSOCIATED CONTENT

Supporting Information

The Supporting Information is available free of charge on the ACS Publications website at DOI: 10.1021/acs.est.5b04346.

A table showing crystallographic parameters. Figures showing alignment of homologous sequences starting with amino acid 351; SEM images of oPBAT pellets; RP-HPLC profiles; expression profile of Chath_Est1; released molecules after incubation of BaETaEBa with 6 μM Chath_Est1 at different pHs; hydrolysis of PBAT, BTaBTaB, and BTaB; α/β hydrolase fold represented on chain A; alignment of Chath_Est1 (green) with *Geobacillus stearothermophilus* carboxylesterase; and cut through the dimer structure to the active site pocket of Chath_Est1. (PDF)

■ AUTHOR INFORMATION

Corresponding Author

*Phone: +43-1-47654-4974; e-mail: doris.ribitsch@acib.at.

Notes

The authors declare no competing financial interest.

■ ACKNOWLEDGMENTS

This work has been supported by the Federal Ministry of Science, Research, and Economy (BMWFW); the Federal Ministry of Traffic, Innovation, and Technology (bmvit); the Styrian Business Promotion Agency SFG; the Standortagentur Tirol; the Government of Lower Austria; and ZIT, the Technology Agency of the City of Vienna, through the

DOI: 10.1021/acs.est.5b04346
Environ. Sci. Technol. 2016, 50, 2899−2907

COMET-Funding Program managed by the Austrian Research Promotion Agency FFG.

REFERENCES

(1) Witt, U.; Einig, T.; Yamamoto, M.; Kleeberg, I.; Deckwer, W. D.; Müller, R. J. Biodegradation of aliphatic−aromatic copolyesters: evaluation of the final biodegradability and ecotoxicological impact of degradation intermediates. *Chemosphere* **2001**, *44* (2), 289−299.

(2) Kijchavengkul, T.; Auras, R.; Rubino, M.; Selke, S.; Ngouajio, M.; Fernandez, R. T. Biodegradation and hydrolysis rate of aliphatic aromatic polyester. *Polym. Degrad. Stab.* **2010**, *95* (12), 2641−2647.

(3) Perz, V.; Bleymaier, K.; Sinkel, C.; Kueper, U.; Bonnekessel, M.; Ribitsch, D.; Guebitz, G. M. Substrate specificities of cutinases on aliphatic−aromatic polyesters and on their model substrates. *New Biotechnol.* **2016**, *33* (2), 295−304.

(4) Kawai, F.; Oda, M.; Tamashiro, T.; Waku, T.; Tanaka, N.; Yamamoto, M.; Mizushima, H.; Miyakawa, T.; Tanokura, M. A novel Ca2+-activated, thermostabilized polyesterase capable of hydrolyzing polyethylene terephthalate from Saccharomonospora viridis AHK190. *Appl. Microbiol. Biotechnol.* **2014**, *98* (24), 10053−10064.

(5) Kawai, S.; Nakagawa, M.; Ohashi, H. Degradation mechanisms of a nonphenolic -O-4 lignin model dimer by Trametes versicolor laccase in the presence of 1-hydroxybenzotriazole. *Enzyme Microb. Technol.* **2002**, *30*, 482−489.

(6) Marten, E.; Müller, R.-J.; Deckwer, W.-D. Studies on the enzymatic hydrolysis of polyesters. II. Aliphatic−aromatic copolyesters. *Polym. Degrad. Stab.* **2005**, *88* (3), 371−381.

(7) Kleeberg, I.; Welzel, K.; VandenHeuvel, J.; Mueller, R. J.; Deckwer, W. D. Characterization of a New Extracellular Hydrolase from Thermobifida fusca Degrading Aliphatic−Aromatic Copolyesters. *Biomacromolecules* **2005**, *6* (1), 262−270.

(8) Steer, T.; Collins, M. D.; Gibson, G. R.; Hippe, H.; Lawson, P. A. Clostridium hathewayi sp. nov., from Human Faeces. *Syst. Appl. Microbiol.* **2001**, *24* (3), 353−357.

(9) Kaur, S.; Yawar, M.; Kumar, P. A.; Suresh, K. Hungatella effluvii gen. nov., sp. nov., an obligately anaerobic bacterium isolated from an effluent treatment plant, and reclassification of Clostridium hathewayi as Hungatella hathewayi gen. nov., comb. nov. *Int. J. Syst. Evol. Microbiol.* **2014**, *64* (3), 710−718.

(10) Heumann, S.; Eberl, A.; Pobeheim, H.; Liebminger, S.; Fischer-Colbrie, G.; Almansa, E.; Cavaco-Paulo, A.; Gubitz, G. M. New model substrates for enzymes hydrolysing polyethyleneterephthalate and polyamide fibres. *J. Biochem. Biophys. Methods* **2006**, *69* (1−2), 89−99.

(11) Perz, V.; Bleymaier, K.; Sinkel, C.; Kueper, U.; Bonnekessel, M.; Ribitsch, D.; Guebitz, G. M. Data on synthesis of oligomeric and polymeric poly(butylene adipate-co-butylene terephthalate) model substrates for the investigation of enzymatic hydrolysis. *Data in Brief* **2016**, in press.

(12) Schlegel, H. G. *Allgemeine Mikrobiologie*. Georg Thieme Verlag: New York, 1992; Vol. 7, p 634.

(13) Carrez, C. Estimation of lactose in Milk. *Ann. Chim. Anal.* **1908**, *13*, 17−22.

(14) Culhaoglu, T.; Zheng, D.; Mechin, V.; Baumberger, S. Adaptation of the Carrez procedure for the purification of ferulic and p-coumaric acids released from lignocellulosic biomass prior to LC/MS analysis. *J. Chromatogr. B: Anal. Technol. Biomed. Life Sci.* **2011**, *879* (28), 3017−22.

(15) Weiss, S.; Lebuhn, M.; Andrade, D.; Zankel, A.; Cardinale, M.; Birner-Gruenberger, R.; Somitsch, W.; Ueberbacher, B. J.; Guebitz, G. M. Activated zeolite–suitable carriers for microorganisms in anaerobic digestion processes? *Appl. Microbiol. Biotechnol.* **2013**, *97* (7), 3225−38.

(16) Goldstein, J. I.; Newbury, D. E.; Echlin, P.; Joy, D.; Lyman, C. E.; Lifshin, E.; Sawyer, L.; Michael, J. *Scanning Electron Microscopy and X-Ray Microanalysis*. Kluwer Academic/Plenum Publisher: New York, 2003; p 690.

(17) Sambrook, J. E.; Fritsch, E. F.; Maniatis, T. *Molecular Cloning: A Laboratory Manual.*; Cold Spring Harbor: New York, 1989; Vol. 2.

(18) Perz, V.; Baumschlager, A.; Bleymaier, K.; Zitzenbacher, S.; Hromic, A.; Steinkellner, G.; Pairitsch, A.; Łyskowski, A.; Gruber, K.; Sinkel, C.; Küper, U.; Ribitsch, D.; Guebitz, G. M. Hydrolysis of synthetic polyesters by Clostridium botulinum esterases. *Biotechnol. Bioeng.* **2015**, 1.

(19) Laemmli, U. K. Cleavage of structural proteins during the assembly of the head of bacteriophage T4. *Nature* **1970**, *227* (5259), 680−5.

(20) Kabsch, W. XDS. *Acta Crystallogr., Sect. D: Biol. Crystallogr.* **2010**, *66* (2), 125−32.

(21) Liu, P.; Ewis, H. E.; Tai, P. C.; Lu, C. D.; Weber, I. T. Crystal structure of the Geobacillus stearothermophilus carboxylesterase Est55 and its activation of prodrug CPT-11. *J. Mol. Biol.* **2007**, *367*, 212−23.

(22) Adams, P. D.; Afonine, P. V.; Bunkoczi, G.; Chen, V. B.; Davis, I. W.; Echols, N.; Headd, J. J.; Hung, L. W.; Kapral, G. J.; Grosse-Kunstleve, R. W.; McCoy, A. J.; Moriarty, N. W.; Oeffner, R.; Read, R. J.; Richardson, D. C.; Richardson, J. S.; Terwilliger, T. C.; Zwart, P. H. PHENIX: a comprehensive Python-based system for macromolecular structure solution. *Acta Crystallogr., Sect. D: Biol. Crystallogr.* **2010**, *66* (2), 213−221.

(23) Winn, M. D.; Ballard, C. C.; Cowtan, K. D.; Dodson, E. J.; Emsley, P.; Evans, P. R.; Keegan, R. M.; Krissinel, E. B.; Leslie, A. G.; McCoy, A.; McNicholas, S. J.; Murshudov, G. N.; Pannu, N. S.; Potterton, E. A.; Powell, H. R.; Read, R. J.; Vagin, A.; Wilson, K. S. Overview of the CCP4 suite and current developments. *Acta Crystallogr., Sect. D: Biol. Crystallogr.* **2011**, *67* (4), 235−42.

(24) Emsley, P.; Lohkamp, B.; Scott, W. G.; Cowtan, K. Features and development of Coot. *Acta Crystallogr., Sect. D: Biol. Crystallogr.* **2010**, *66* (4), 486−501.

(25) Chen, V. B.; Arendall, W. B., 3rd; Headd, J. J.; Keedy, D. A.; Immormino, R. M.; Kapral, G. J.; Murray, L. W.; Richardson, J. S.; Richardson, D. C. MolProbity: all-atom structure validation for macromolecular crystallography. *Acta Crystallogr., Sect. D: Biol. Crystallogr.* **2010**, *66* (1), 12−21.

(26) Krieger, E.; Koraimann, G.; Vriend, G. Increasing the precision of comparative models with YASARA NOVA - a self-parameterizing force field. *Proteins: Struct., Funct., Genet.* **2002**, *47* (3), 393−402.

(27) Duan, Y.; Wu, C.; Chowdhury, S.; Lee, M. C.; Xiong, G.; Zhang, W.; Yang, R.; Cieplak, P.; Luo, R.; Lee, T.; Caldwell, J.; Wang, J.; Kollman, P. A Point-Charge Force Field for Molecular Mechanics Simulations of Proteins Based on Condensed-Phase Quantum Mechanical Calculations. *J. Comput. Chem.* **2003**, *24* (16), 1999−2012.

(28) Steinkellner, G.; Rader, R.; Thallinger, G.; Kratky, C.; Gruber, K. VASCo: computation and visualization of annotated protein surface contacts. *BMC Bioinf.* **2009**, *10* (1), 32.

(29) Sanner, M. F.; Olson, A. J.; Spehner, J. C. Reduced surface: An efficient way to compute molecular surfaces. *Biopolymers* **1996**, *38* (3), 305−320.

(30) Chang, N.-B.; Pires, A. *Sustainable Solid Waste Management: A Systems Engineering Approach*. John Wiley & Sons Inc.: Hoboken, NJ, 2015; p 936.

(31) Siotto, M.; Sezenna, E.; Saponaro, S.; Innocenti, F. D.; Tosin, M.; Bonomo, L.; Mezzanotte, V. Kinetics of monomer biodegradation in soil. *J. Environ. Manage.* **2012**, *93* (1), 31−37.

(32) Karegoudar, T. B.; Pujar, B. G. Degradation of terephthalic acid by a Bacillus species. *FEMS Microbiol. Lett.* **1985**, *30* (1−2), 217−220.

(33) Wang, Z.-J.; Teng, L.-h.; Zhang, J.; Huang, X.-L.; Zhang, J.-F. Study on optimal biodegradation of terephthalic acid by an isolated Pseudomonas sp. *African Journal of Biotechnology* **2011**, *10* (16), 3143−3148.

(34) Zhang, Y.-M.; Sun, Y.-Q.; Wang, Z.-J.; Zhang, J. Degradation of terephthalic acid by a newly isolated strain of Arthrobacter sp.0574. *S. Afr. J. Sci.* **2013**, *109* (7), 1−4.

(35) Kleerebezem, R.; Hulsoff Pol, L. W.; Lettinga, G. Anaerobic biodegradability of phthalic acid isomers and related compounds. *Biodegradation* **1999**, *10* (1), 63−73.

(36) Kleerebezem, R.; Beckers, J.; Hulshoff Pol, L. W.; Lettinga, G. High rate treatment of terephthalic acid production wastewater in a

DOI: 10.1021/acs.est.5b04346
Environ. Sci. Technol. 2016, 50, 2899−2907

two-stage anaerobic bioreactor. *Biotechnol. Bioeng.* **2005**, *91* (2), 169−79.
(37) Wu, J. H.; Wu, F. Y.; Chuang, H. P.; Chen, W. Y.; Huang, H. J.; Chen, S. H.; Liu, W. T. Community and proteomic analysis of methanogenic consortia degrading terephthalate. *Appl. Environ. Microbiol.* **2013**, *79* (1), 105−12.
(38) Wu, J. H.; Liu, W. T.; Tseng, I. C.; Cheng, S. S. Characterization of microbial consortia in a terephthalate-degrading anaerobic granular sludge system. *Microbiology* **2001**, *147* (2), 373−382.
(39) Lykidis, A.; Chen, C. L.; Tringe, S. G.; McHardy, A. C.; Copeland, A.; Kyrpides, N. C.; Hugenholtz, P.; Macarie, H.; Olmos, A.; Monroy, O.; Liu, W. T. Multiple syntrophic interactions in a terephthalate-degrading methanogenic consortium. *ISME J.* **2011**, *5* (1), 122−30.
(40) Krause, L.; Diaz, N. N.; Edwards, R. A.; Gartemann, K.-H.; Krömeke, H.; Neuweger, H.; Pühler, A.; Runte, K. J.; Schlüter, A.; Stoye, J.; Szczepanowski, R.; Tauch, A.; Goesmann, A. Taxonomic composition and gene content of a methane-producing microbial community isolated from a biogas reactor. *J. Biotechnol.* **2008**, *136* (1−2), 91−101.
(41) Weiland, P. Biogas production: current state and perspectives. *Appl. Microbiol. Biotechnol.* **2010**, *85* (4), 849−860.
(42) Schluter, A.; Bekel, T.; Diaz, N. N.; Dondrup, M.; Eichenlaub, R.; Gartemann, K. H.; Krahn, I.; Krause, L.; Kromeke, H.; Kruse, O.; Mussgnug, J. H.; Neuweger, H.; Niehaus, K.; Puhler, A.; Runte, K. J.; Szczepanowski, R.; Tauch, A.; Tilker, A.; Viehover, P.; Goesmann, A. The metagenome of a biogas-producing microbial community of a production-scale biogas plant fermenter analysed by the 454-pyrosequencing technology. *J. Biotechnol.* **2008**, *136* (1−2), 77−90.
(43) Abou-Zeid, D. M.; Muller, R. J.; Deckwer, W. D. Degradation of natural and synthetic polyesters under anaerobic conditions. *J. Biotechnol.* **2001**, *86* (2), 113−126.
(44) Abou-Zeid, D. M.; Muller, R. J.; Deckwer, W. D. Biodegradation of aliphatic homopolyesters and aliphatic-aromatic copolyesters by anaerobic microorganisms. *Biomacromolecules* **2004**, *5* (5), 1687−97.
(45) Murray, W. D.; Khan, A. W.; van den Berg, L. Clostridium saccharolyticum sp. nov., a Saccharolytic Species from Sewage Sludge. *Int. J. Syst. Bacteriol.* **1982**, *32* (1), 132−135.
(46) Krissinel, E.; Henrick, K. Inference of macromolecular assemblies from crystalline state. *J. Mol. Biol.* **2007**, *372* (3), 774−97.
(47) Spiller, B.; Gershenson, A.; Arnold, F. H.; Stevens, R. C. A structural view of evolutionary divergence. *Proc. Natl. Acad. Sci. U. S. A.* **1999**, *96* (22), 12305−12310.
(48) Sussman, J. L.; Harel, M.; Frolow, F.; Oefner, C.; Goldman, A.; Toker, L.; Silman, I. Atomic structure of acetylcholinesterase from Torpedo californica: a prototypic acetylcholine-binding protein. *Science* **1991**, *253* (5022), 872−9.

DOI: 10.1021/acs.est.5b04346
Environ. Sci. Technol. 2016, 50, 2899−2907

Supporting Information

An esterase from anaerobic *Clostridium hathewayi* can hydrolyze aliphatic-aromatic polyesters

Veronika Perz [a], Altijana Hromic [b,c], Armin Baumschlager [b], Georg Steinkellner [b], Tea Pavkov-Keller [b], Karl Gruber [b,c], Klaus Bleymaier [b], Sabine Zitzenbacher [b], Armin Zankel [d], Claudia Mayrhofer [d], Carsten Sinkel [e], Ulf Kueper [e], Katharina Schlegel [e], Doris Ribitsch [a,f,*], Georg M. Guebitz [a,f]

[a] *Austrian Centre of Industrial Biotechnology ACIB, Konrad Lorenz Strasse 20, 3430 Tulln, Austria*

[b] *Austrian Centre of Industrial Biotechnology ACIB, Petersgasse 14, 8010, Graz, Austria*

[c] *Institute of Molecular Biosciences, University of Graz, Humboldtstrasse 50/III, 8010 Graz, Austria*

[d] *Institute of Electron Microscopy and Nanoanalysis, Graz University of Technology, Steyrergasse 17/III, 8010 Graz, Austria*

[e] *BASF SE, Carl-Bosch-Straße 38, 67056 Ludwigshafen, Germany*

[f] *Institute of Environmental Biotechnology, University of Natural Resources and Life Sciences, Vienna, Konrad Lorenz Strasse 20, 3430 Tulln, Austria*

*Corresponding author: Doris Ribitsch, doris.ribitsch@acib.at, phone: ++43 1 47654 4974

Content

Table S1. Crystallographic parameters of Chath_Est1 from *Clostridium hathewayi*

X-ray source	PETRA III, DESY Hamburg
wavelength (Å)	1.033
Temperature	100 K
Space group	$P2_1$
Cell dimensions	
a, *b*, *c* (Å)	62.05, 241.83, 83.58
β (°)	90.0
Resolution (Å)	
high resolution shell	60-1.90 (2.00-1.90)
Total no. reflections	471113
Unique no. reflections	163181
Multiplicity	2.9 (2.7)
Completeness (%)	84.1 (74.3)
R_{merge} (%)	8.8 (59.2)
<I/σI>	7.8 (2.1)
R_{work} / R_{free}	18.86/23.74
No. atoms	
Protein	17373
Water	1592
Mean B factor	24.9
R.m.s. deviations	
Bond lengths (Å)	0.005
Bond angles (°)	0.914
Ramachandran outliers (%)	0.2
Most favored residues (%)	95.6
PDB	5A2G

```
                ....|....| ....|....| ....|....| ....|....| ....|....|
                      360        370        380        390        400
  EFC94627.1    GHGKELKTVF AEAYPGKSPV DLLTLDTIFR GPTKEFVRSL AAAGGSVYSY
WP_022032810    GHGKELKAVF AEAYPGKSPV DLLTLDTIFR GPTKEFVRSL AAAGGSVYSY
WP_025529448    GRGKELKAVF AEAYPGKNPA DLLTLDTIFR GPTREFVRAL AAAGGSVYSY
WP_002603106    GRGKELKAVF AEAYPGKNPA DLLTLDTIFR GPTREFVRAL AAAGGSVYSY

                ....|....| ....|....| ....|....| ....|....| ....|....|
                      410        420        430        440        450
  EFC94627.1    LFALEFPYQN QKTA------ ---------- ---------- ----------
WP_022032810    LFALEFPYQN QKTAWHCSDI PFIFHNTELV PVANIPEVSD RLEEQMFGAV
WP_025529448    LFALEFPYQN QKTAWHCSDI PFVFHNTELV PVANIPGVSD RLEEQIFGAV
WP_002603106    LFALEFPYQN QKTAWHCSDI PFVFHNTELV PAANIPEVSD RLQEQIFGAV

                ....|....| ....|....| ....|....| ....|....| ....|....|
                      460        470        480        490        500
  EFC94627.1    ---------- ---------- ---------- ---------- ----------
WP_022032810    MAFARSGKPE YGGLPQWPAS RENDEATMIF DRVCEVRHNH DNRLLKLHAE
WP_025529448    MAFARTGKPE YEGLPQWPAS REDDEATMIF DRVCEVRHNH DDRLLKLHAE
WP_002603106    MAFARTGKPE YEGLPQWPAS REDDEATMIF DRVCEVRHNH DDRLLKLHAE

                ....|....| ....|....|
                      510        520
  EFC94627.1    ---------- ----------
WP_022032810    LSPKFDLAAV MAEMGDEIQH
WP_025529448    ASPKFDLAAM MAKMGDEIQH
WP_002603106    ASPKFDLAAM MTKMGDEIQH
```

Figure S1. Alignment of homologous sequences starting with amino acid 351. EFC94627.1 partial para-nitrobenzyl esterase from *Clostridium hathewayi* DSM-13479; WP_022032810 *para*-nitrobenzyl esterase from *Clostridium hathewayi* CAG:224; WP_025529448 carboxylesterase from *Hungatella hathewayi*; WP_002603106 hypothetical protein from *Hungatella hathewayi*.

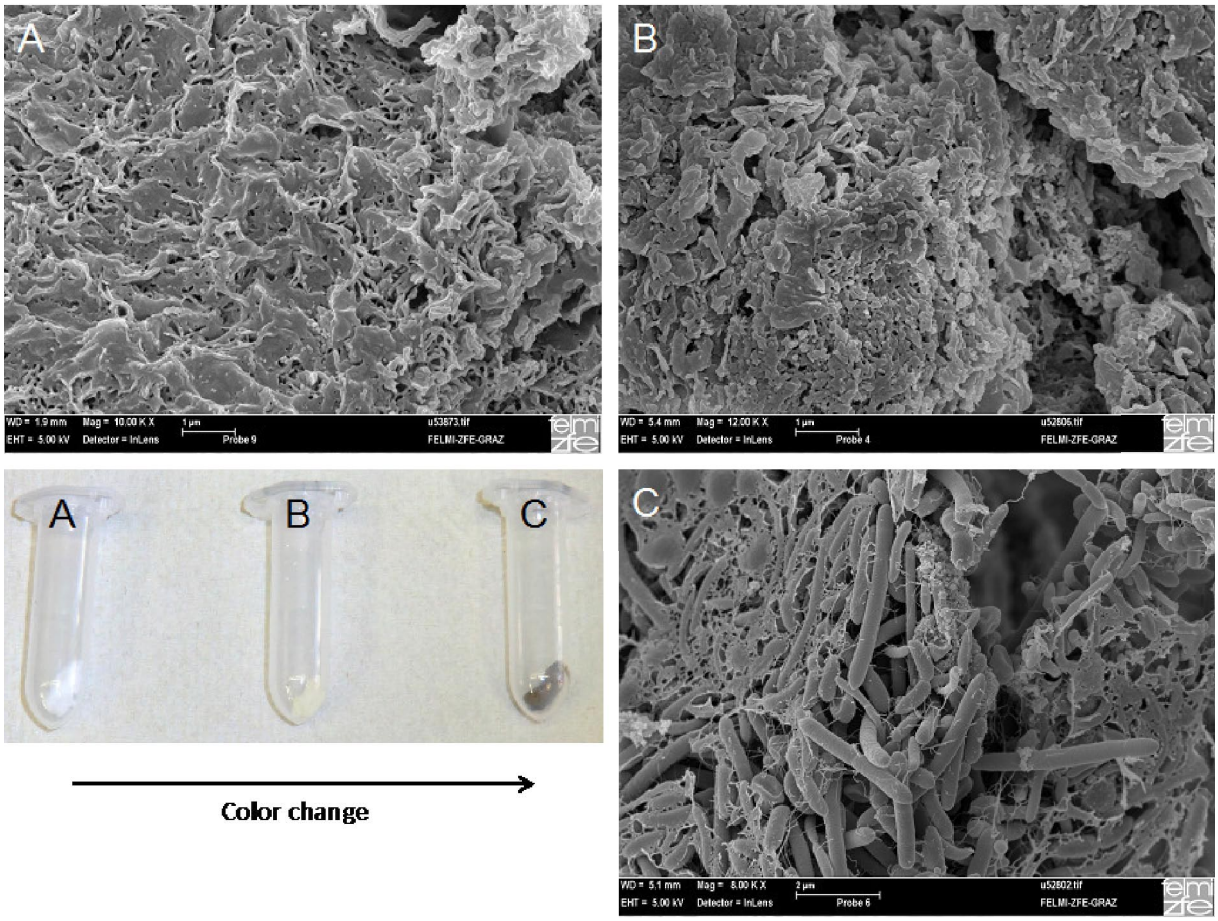

Figure S2. SEM images of oPBAT pellets. A: untreated oPBAT sample. B: oPBAT sample after batch-wise incubation in abiotic medium. C: oPBAT sample with biofilm after batch-wise incubation in biogas sludge. The incubation was performed under the conditions described in the experimental section.

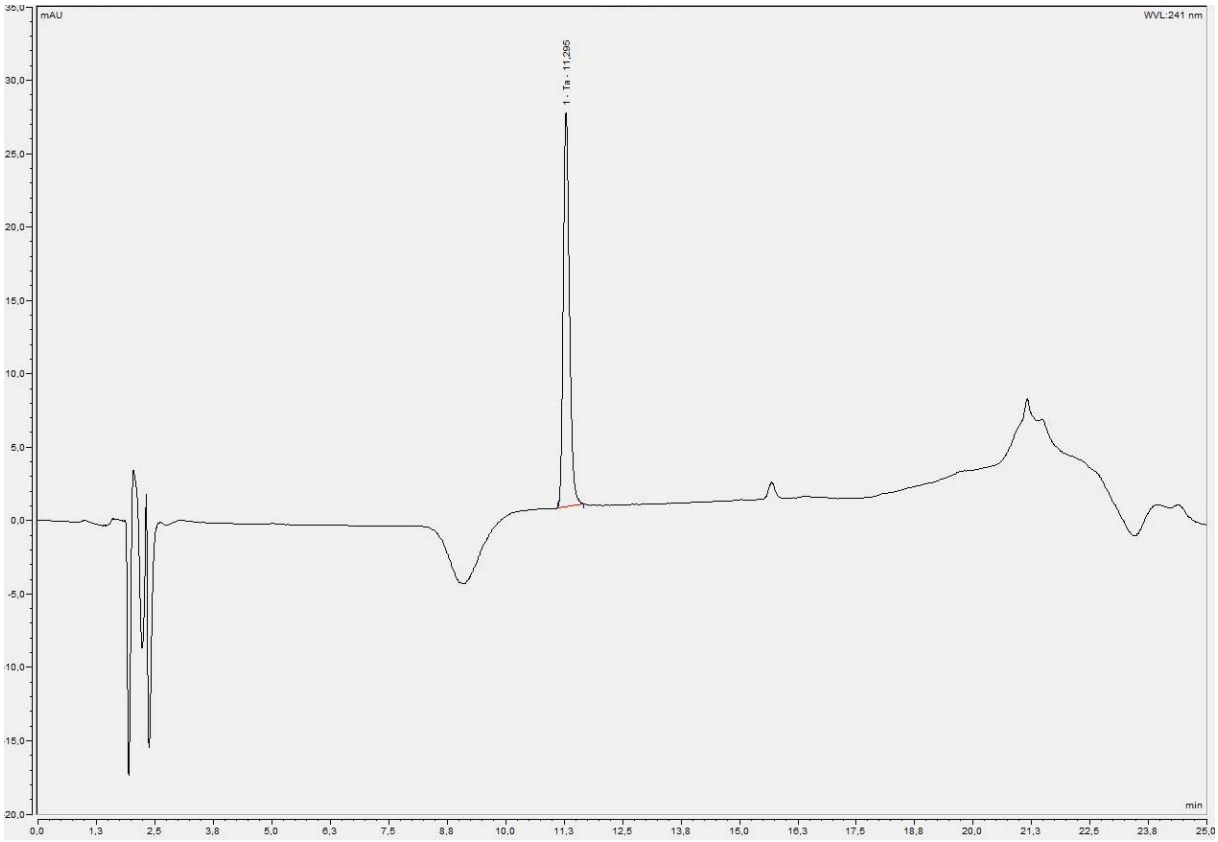

Figure S3. RP-HPLC profile of the oPBAT batch after 28 days of incubation. Liberated Ta: terephthalic acid was quantified.

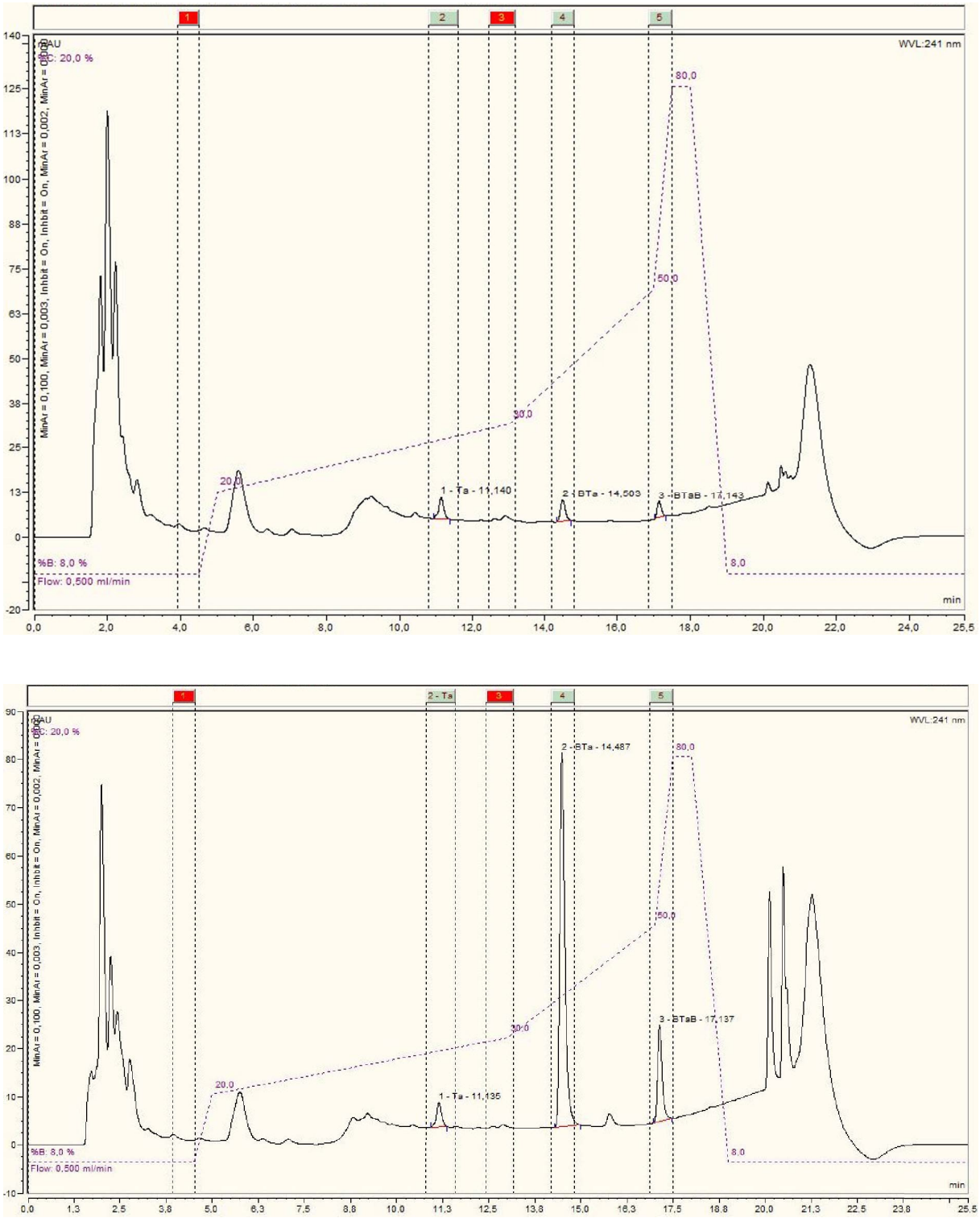

Figure S4. RP-HPLC profiles of *C. hathewayi* cell supernatant samples "PYX + Glucose" (above) and "PYX + PBAT + oPBAT" (below). Liberated hydrolysis products Ta: terephthalic acid; BTa: mono(4-hydroxybutyl) terephthalate and BTaB: bis(4-hydroxybutyl) terephthalate were quantified.

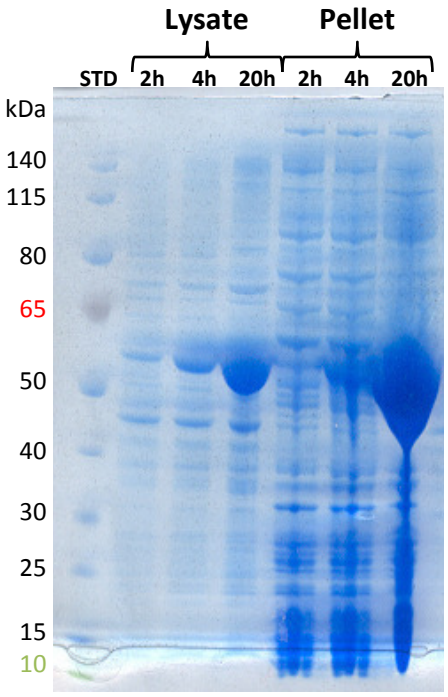

Figure S5. Expression profile of the heterologous gene Chath_Est1 in *E. coli* BL21(DE3) at 20 °C and 160 rpm for 20 h after induction with 0.05 M IPTG. Lysates and pellets were withdrawn and analyzed after 2 , 4 h, and 20 h after induction with IPTG.

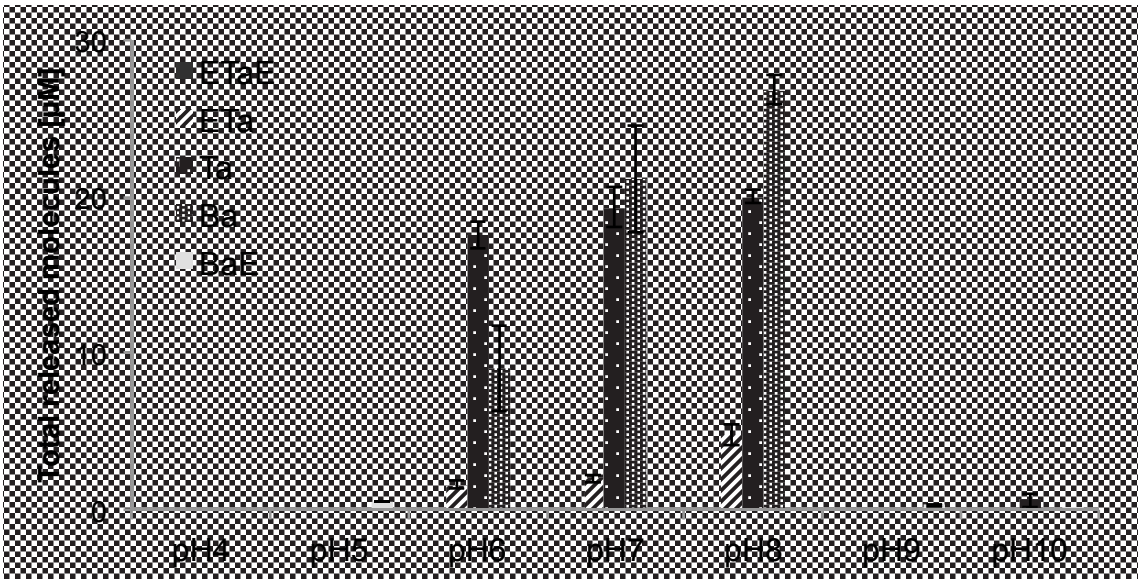

Figure S6. Released molecules after incubation of BaETaEBa with 6 μM Chath_Est1 for 23 h and 37 °C at different pHs. The release molecules are shown in μM, ETaE: bis(2-hydroxyethyl) terephthalate, ETa: mono(2-hydroxyethyl) terephthalate, Ta: terephthalic acid, BaE: 2-hydroxyethyl benzoate and Ba: benzoic acid were quantified by means of HPLC analysis. Each bar represents the average of three independent samples; error bars indicate the standard deviation.

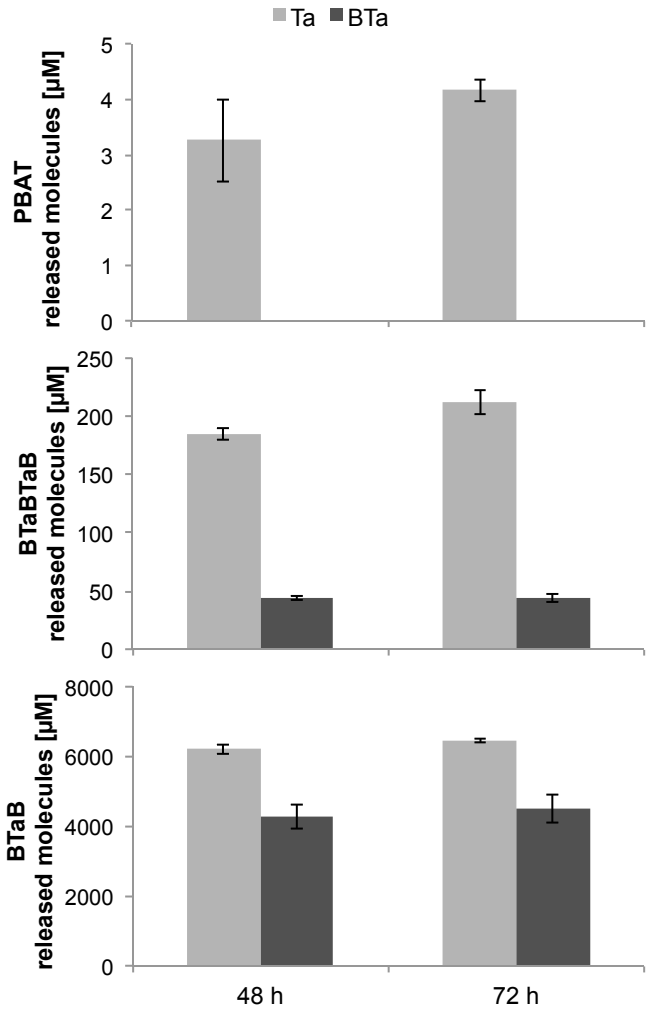

Figure S7. Hydrolysis of PBAT, BTaBTaB and BTaB by 0.6 □M Chath_Est1 at pH 7.0 and 37 °C. Released products (in μM) were quantified by means of RP-HPLC analysis. Ta: terephthalic acid; BTa: mono(4-hydroxybutyl) terephthalate; BTaB: bis(4-hydroxybutyl) terephthalate. Each bar represents the average of three independent samples; error bars indicate the standard deviation.

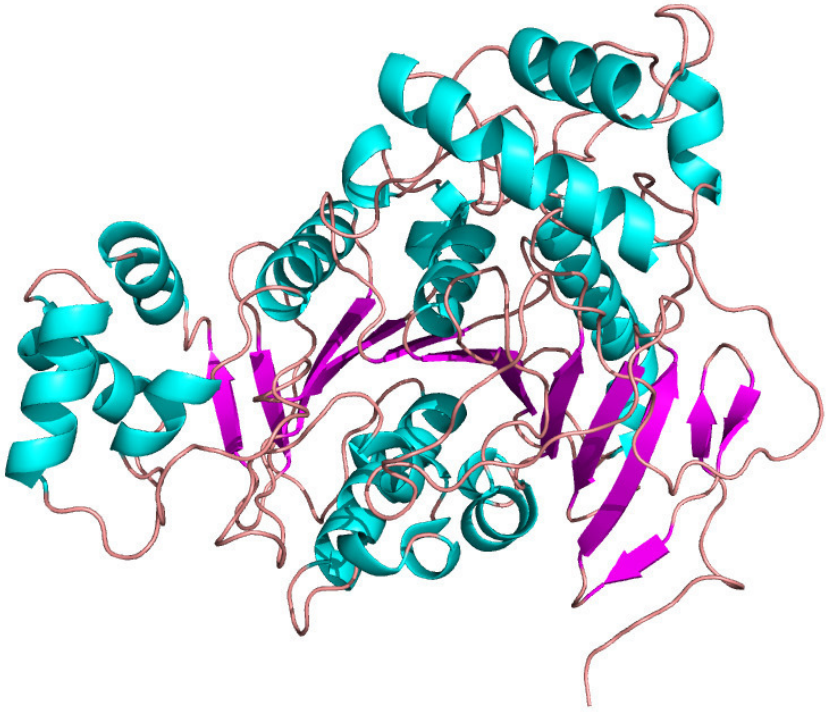

Figure S8. α/β hydrolase fold represented on chain A: alpha helices (cyan), beta sheets (magenta) and loops (salmon).

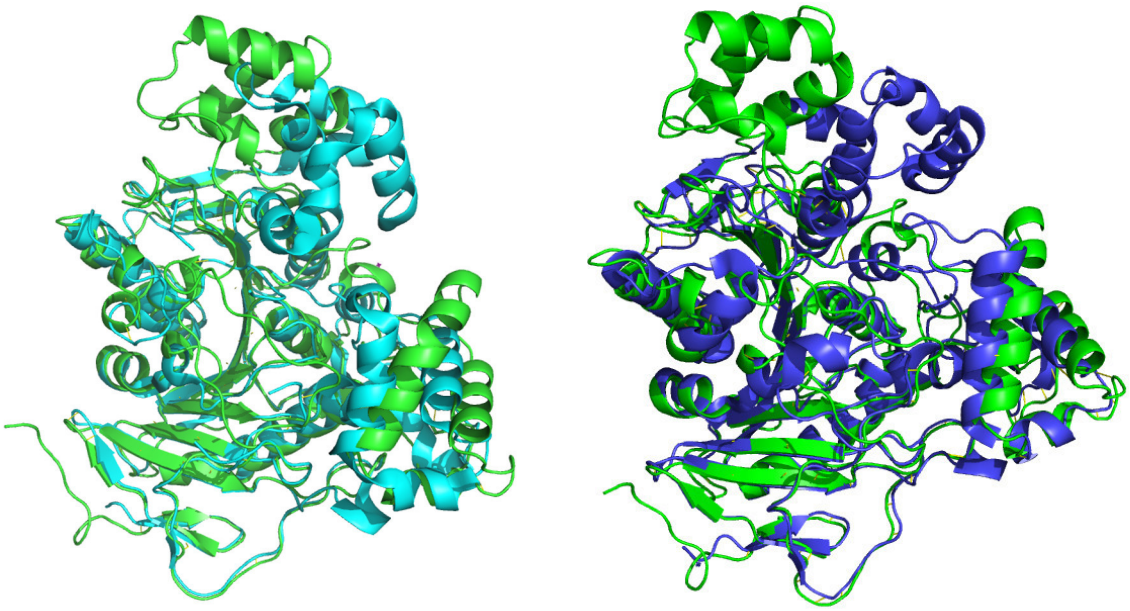

Figure S9. Alignment of Chath_Est1 (green) with *Geobacillus stearothermophilus* carboxylesterase Est55 (cyan, left) and pNB esterase (blue, right)

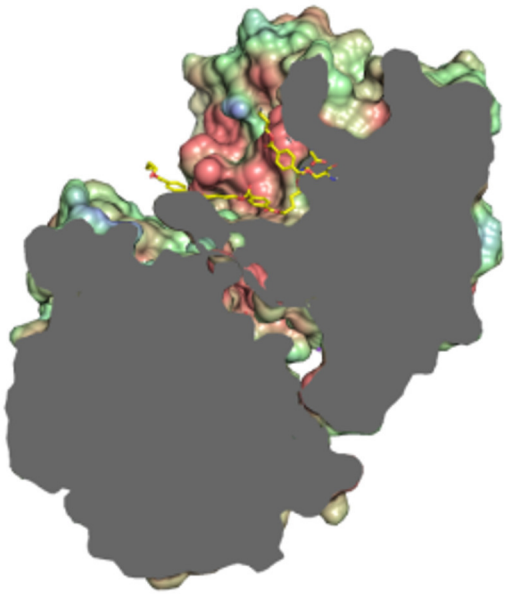

Figure S10. Cut through the dimer structure to the active site pocket of Chath_Est1.

ARTICLE

BIOTECHNOLOGY and BIOENGINEERING

Hydrolysis of Synthetic Polyesters by *Clostridium botulinum* Esterases

Veronika Perz,[1] Armin Baumschlager,[2] Klaus Bleymaier,[2] Sabine Zitzenbacher,[2] Altijana Hromic,[2,3] Georg Steinkellner,[2] Andris Pairitsch,[3] Andrzej Łyskowski,[2] Karl Gruber,[2,3] Carsten Sinkel,[4] Ulf Küper,[4] Doris Ribitsch,[1,5] Georg M. Guebitz[1,5]

[1]acib—Austrian Centre of Industrial Biotechnology, Konrad Lorenz Strasse 20, Tulln 3430, Austria

[2]acib—Austrian Centre of Industrial Biotechnology, Graz, Austria

[3]Institute of Molecular Biosciences, University of Graz, Graz, Austria

[4]BASF SE, Ludwigshafen, Germany

[5]Institute of Environmental Biotechnology, University of Natural Resources and Life Sciences, Vienna, Konrad Lorenz Strasse 20, Tulln 3430, Austria;
telephone: +43-1-47654-4974; fax: +43-1-2272-66280-503; e-mail: doris.ribitsch@acib.at

ABSTRACT: Two novel esterases from the anaerobe *Clostridium botulinum* ATCC 3502 (Cbotu_EstA and Cbotu_EstB) were expressed in *Escherichia coli* BL21-Gold(DE3) and were found to hydrolyze the polyester poly(butylene adipate-co-butylene terephthalate) (PBAT). The active site residues (triad Ser, Asp, His) are present in both enzymes at the same location only with some amino acid variations near the active site at the surrounding of aspartate. Yet, Cbotu_EstA showed higher k_{cat} values on *para*-nitrophenyl butyrate and *para*-nitrophenyl acetate and was considerably more active (sixfold) on PBAT. The entrance to the active site of the modeled Cbotu_EstB appears more narrowed compared to the crystal structure of Cbotu_EstA and the N-terminus is shorter which could explain its lower activity on PBAT. The Cbotu_EstA crystal structure consists of two regions that may act as movable cap domains and a zinc metal binding site.

Biotechnol. Bioeng. 2016;113: 1024–1034.

KEYWORDS: polyesterase; esterase; polymer hydrolysis; anaerobic digestion; zinc dependent enzyme; (poly(butylene adipate-co-butylene terephthalate) (PBAT)

Current address of Andrzej Łyskowski is Faculty of Chemistry—Department of Biochemistry and Biotechnology, Rzeszów University of Technology, al. Powstańców Warszawy 6, Rzeszów 35-959, Poland.
Correspondence to: D. Ribitsch

Contract grant sponsor: Federal Ministry of Science, Research and Economy (BMWFW)
Contract grant sponsor: Federal Ministry of Traffic
Contract grant sponsor: Innovation and Technology (bmvit)
Received 16 September 2015; Revision received 20 October 2015; Accepted 26 October 2015
Accepted manuscript online 2 November 2015;
Article first published online 20 November 2015 in Wiley Online Library (http://onlinelibrary.wiley.com/doi/10.1002/bit.25874/abstract).
DOI 10.1002/bit.25874

Introduction

Conventional polyesters that are frequently used as one-way material in for example food packaging, fast food dishes, plastic bags, or foils as well as in fiber materials are strongly debated due to their accumulation in nature and their high environmental impact in all kinds of ecosystems worldwide including rivers (Lechner et al., 2014), soils and oceans (Cole et al., 2011). For this reason biodegradable and compostable polymers came into focus of governments, costumers and industries.

In the recent years different polymers of natural origin including polyhydroxyalkanoates (PHAs), starch, cellulose as well as man-made synthetic polymers like poly(ε-caprolactone), polylactic acid (PLA), cellulose acetate, poly(butylene succinate) (PBS) or poly(butylene adipate-co-butylene terephthalate) (PBAT) were investigated concerning their material properties, biodegradability and possible fields of application (Shah et al., 2014).

The synthetic aliphatic-aromatic copolyester PBAT was proven to be biodegradable and also exhibits interesting material properties (Witt et al., 1995, 2001). PBAT is produced on an industrial scale and used as a component of polymer blends for example in combination with starch (de Camargo Andrade-Molina et al., 2013) or PLA (Weng et al., 2013). Data published by the German nova-Institut (Aeschelmann et al., 2015) suggested a world-wide PBAT production capacity of 75,000 tons for the year 2013. Typical commercial products containing PBAT include mulch films, organic waste bags or packaging material.

The biological decomposability of PBAT under composting conditions was demonstrated by different research groups (Kijchavengkul et al., 2010; Witt et al., 1999, 2001). Moreover, hydrolysis of PBAT by cutinases from the aerobic *Humicola insolens* and *Thermobifida cellulosilytica* was recently mechanistically investigated (Perz et al., 2015). PBAT foils used for organic waste and carrier bags (Soroudi and Jakubowicz, 2013) or food packaging

(de Camargo Andrade-Molina et al., 2013) might often end up in biogas plants. However, there is considerably less information on the hydrolysis of PBAT in anaerobic environments.

Beside the conventional aerobic biodegradation test, only anaerobic sludges, sediments and isolated strains have been tested for their ability to biodegrade polyesters (Budwill et al., 1992; Reischwitz et al., 1997; Yagi et al., 2014) including PBAT (Abou-Zeid et al., 2001, 2004). In the dark anaerobic environments with neutral pH, enzymatic hydrolysis is expected to be the predominant mechanisms for biodegradation of PBAT. However, the enzymes of these anaerobic organisms that are actually hydrolyzing the polymers were neglected so far.

In this study, for the very first time two anaerobic polyesterases were identified, heterologously expressed in *E. coli*, characterized and their PBAT hydrolysis mechanisms were investigated in detail.

Materials and Methods

Chemicals and Reagents

Amorphous solvent casted polyethylene terephthalate (PET) films (film thickness 0.25 mm) were purchased from Goodfellow (U.K.). The PET model substrate bis-(benzoyloxyethyl) terephthalate (BaETaEBa) was synthesized as previously described by Heumann et al. (2006).

Oligomeric PBAT model substrates bis(4-hydroxybutyl) terephthalate (BTaB), *O,O′*-(butane-1,4-diyl) bis(4-hydroxybutyl) diterephthalate (BTaBTaB), bis(4-(benzoyloxy) butyl) terephthalate (BaBTaBBa), bis(4-(decanoyloxy) butyl) terephthalate (DaBTaBDa), bis(4-(tetradecanoyloxy) butyl) terephthalate (TdaBTaBTda) and polymeric model substrates with variations in the adipic acid (Ada): terephthalic acid (Ta) ratios (Ada100_Ta0, Ada90_Ta10, Ada80_Ta20, Ada70_Ta30, Ada60_Ta40, Ada50_Ta50) were synthesized and purified according to the methods that were previously described (Perz et al., 2015). Purity was confirmed by means of ^{1}H NMR and HPLC/MS. Particle sizes were determined to be within the range of 100–300 μm.

PBAT (poly(butylene adipate-co-butylene terephthalate) was kindly provided by BASF SE.

All used polymers were of pure nature in order to exclude any influences by additives.

All other chemicals were of analytical grad and purchased from Sigma (Germany).

General Recombinant DNA Techniques

Molecular cloning of the genes was performed by standard methods (Sambrook et al., 1989). Digestion of DNA with the restriction endonucleases *Nde*I and *Hind*III (New England Biolabs), dephosphorylation with alkaline phosphatase (Roche, Germany) and ligation with T4 DNA-ligase (Fermentas, Germany) were performed in accordance to the manufacturers' instructions. Plasmid DNA was isolated with Plasmid Mini Kit from Qiagen (Germany) and plasmids and DNA fragments were purified with Promega DNA purification kits (Promega, Germany). Vector pET26b(+) (Novagen) was chosen for expression of the constructed fusion proteins carrying a C-terminal 6xHisTag in *E. coli* BL21-Gold(DE3) (Stratagene, La Jolla, CA).

Cloning, Expression, and Purification of Hydrolases in *E. coli*

Two genes coding for putative secreted lipases from *Clostridium botulinum* str. ATCC 3502 were codon optimized for expression in *E. coli* and synthesized without signal peptide by GeneArt® (Life Technologies, Grand Island, NY). The plasmids carrying the synthetic genes were digested with *Nde*I and *Hin*dIII, purified, ligated into pET26b(+) (Novagen, Merck KGaA, Germany) and transformed in *E. coli* BL21-Gold(DE3). Freshly transformed *E. coli* BL21-Gold(DE3) cells were used to inoculate 20 mL LB-medium supplemented with 40 μg/mL kanamycin and cultivation was carried out overnight at 37°C and 150 rpm. Then, the overnight culture was used to inoculate a 500 mL shake flask containing 200 mL of the same medium to an $OD_{600} = 0.1$. The culture was incubated at 37°C and 150 rpm until an $OD_{600} = 0.8$ was reached. After cooling down to 20°C the expression was induced by addition of IPTG to a final concentration of 0.05 mM. Following incubation for 20 h at 20°C and 160 rpm, the cells were harvested by centrifugation (25 min, 10°C, 3,200*g*). Cell pellets from 100 mL cell culture were resuspended in 30 mL Ni-NTA Lysis Buffer (50 mM NaH_2PO_4, 300 mM NaCl, 10 mM imidazole, pH 8.0). The resuspended cells were sonicated with 3 times 30 s pulses under ice cooling (Vibra Cell, Sonics Materials, Meryin/Satigny, Switzerland). Lysates were then centrifuged (30 min, 10°C, 3,200*g*) and purified according to the manufacturer's protocol (IBA GmbH, Goettingen, Germany). Finally, the buffer was exchanged for 100 mM Tris HCl pH 7.0 with PD-10 columns (GE Healthcare, Vienna, Austria) and these purified enzyme solutions were used for further investigation, hydrolysis experiments as well as for crystallization.

DNA Sequencing, Alignments, and Deposition of Sequence Data

DNA was sequenced as custom service by Agowa (Germany). DNA analysis was performed with Vector NTI Suite 10 (Invitrogen, Vienna, Austria). BLAST search was performed using the ExPASy (Expert Protein Analysis System) proteomics server of the Swiss Institute of Bioinformatics, and sequences of related proteins were aligned using the Clustal W program (Swiss EMBnet node server). The codon optimized nucleotide sequences of Cbotu_EstA and Cbotu_EstB have been deposited in the GenBank database under accession numbers KP859619 and KP859620.

Protein Analysis

Protein concentrations were determined using the BIO-RAD Protein Assay (BIO-RAD) and bovine serum albumin as protein standard according to the manufacture's instructions. SDS–PAGE was carried out corresponding to Laemmli (1970) and proteins were stained with Coomassie Brillant Blue R-250.

Standard Assay for Esterase Activity

Esterase activity was measured using *para*-nitrophenyl acetate (*p*NPA) and *para*-nitrophenyl butyrate (*p*NPB) as substrates (Ribitsch et al., 2011). The substrates were used in final concentrations of 7.9 mM *p*NPB or 6.7 mM *p*NPA. Activity

was measured in 50 mM Tris–HCl pH 7.0 and 25°C by following the increase of absorbance of *para*-nitrophenol ($\varepsilon_{405nm} = 11.86\ L\ mmol^{-1}cm^{-1}$) at 405 nm in a Tecan plate reader.

Kinetic parameters were determined in 50 mM Tris–HCl pH 7.0 at 25°C with substrate concentrations in the range of 50 μM to 10 mM. Kinetic parameters were calculated with SigmaPlot 11.0/Software—Enzyme Kinetics 1.3 (Systat Software GmbH, Erkrath, Germany) utilizing the Michaelis—Menten model.

Circular Dichroism Spectroscopy

CD spectra were recorded on a Jasco PS-150J spectropolarimeter using a 0.02 cm water-jacketed cylindrical cell, thermostatically controlled by an external computer-controlled water bath Julabo F25. Thermal denaturation data were recorded in the temperature range 25–95°C with following parameters: heating rate 1°C/min, response 1s, resolution 0.2°C. The protein concentration was 0.75 mg/mL in 100 mM Tris–HCl buffer, pH 8.0. The melting temperature was estimated as the point of inflection of the temperature dependent mean residue ellipticity at 208 nm.

Temperature Optimum and Stability

The optimal temperature of the purified enzymes was determined on a double beam U2900 spectrophotometer (Hitachi High-Technologies Corporation, Japan) in combination with a Pharmacia LKB MultiTempII waterbath (Pharmacia, Sweden). The final reaction mixture contained 7.9 mM *p*NPB in 50 mM potassium phosphate buffer pH 7.0 and was incubated at different temperatures in the range of 20–75°C. The activity was measured by following the increase of absorbance of *para*-nitrophenol ($\varepsilon_{405nm} = 11.86\ mMol^{-1}cm^{-1}$) at 405 nm.

Temperature stability was determined by incubating the enzymes in 50 mM potassium phosphate buffer pH 7.0 at 25, 37, 50°C and 300 rpm. The initial specific enzyme activity was measured (time point 0) using *p*NPB as substrate and defined to be 100%. The remaining enzyme activities were then determined for 35 days and activity half-lives of Cbotu_EstA and Cbotu_EstB were calculated.

Determination of pH Optimum

To determine the pH optimum of Cbotu_EstA 10 mg of bis-(2-benzoyloxy) ethyl) terephthalate (BaETaEBa) were incubated in buffered enzyme solutions at different pHs for 1 h at 50°C. The pH optimum of Cbotu_EstB was measured after 23 h incubation at 25°C and 37°C due to the lower activity and different temperature stability pattern of this enzyme. The following buffer solutions were used, each in a concentration of 50 mM: citrate phosphate at pH 4.0, 5.0 and 6.0, potassium phosphate at pH 7.0, 8.0 and 9.0 and glycine-NaOH at pH 10.0. The final enzyme concentration in the samples was 6 μM.

Samples were withdrawn by diluting 500 μL of the samples with 500 μL ice cooled methanol and enzyme precipitation was performed on ice for 15 min. Thereafter, samples were centrifuged at 0°C and 12,500*g* for 15 min. 600 μL of the supernatants were transferred to HPLC vials and acidified with conc. HCl to reach a final pH of 4.0. Blank reactions were performed simultaneously containing substrate and buffer only. Analysis and quantification of the released hydrolysis products benzoic acid (Ba), terephthalic acid (Ta), mono(2-hydroxyethyl) terephthalate (ETa) and hydroxyethyl-benzoate (ETaE) was performed by means of RP-HPLC as previously described (Herrero Acero et al., 2011).

Hydrolysis of PET Films

PET films were cut into pieces of 0.5 × 1 cm, washed as previously described (Herrero Acero et al., 2011) and incubated in 2 mL 50 mM citrate phosphate pH 6.0 or 50 mM potassium phosphate pH 7.0 and pH 8.0 containing 6 μM Cbotu_EstA at 50°C and 100 rpm in 2 mL eppendorf tubes. Samples were taken after 11 days, prepared for RP-HPLC analysis as described above and RP-HPLC was performed (Herrero Acero et al., 2011). Blank reactions were performed simultaneously containing PET foil and buffer only.

Hydrolysis of PBAT and Oligomeric PBAT Model Substrates

Generally, 1 mL of 0.6 μM enzyme solution was incubated with 10 mg PBAT or polymeric PBAT model substrates, respectively. Polymeric model substrates differed in the adipic acid (Ada) to terephthalic acid (Ta) ratios namely Ada100_Ta0, Ada90_Ta10, Ada80_Ta20, Ada70_Ta30, Ada60_Ta40, Ada50_Ta50 (Table I). Oligomeric model substrates BTaB, BTaBTaB, BaBTaBBa, DaBTaBDa, and TdaBTaBTda were incubated with a concentration of 6.84 mM, respectively.

Incubations of PBAT as well as of model substrates that are possible PBAT hydrolysis products (BTaB, BTaBTaB) with Cbotu_EstA were performed for 24, 48 and 72 h at 300 rpm, 37°C and 50°C in 50 mM citrate phosphate pH 6.0 or 50 mM potassium phosphate pH 7.0 and pH 8.0, respectively. Furthermore, model substrates BTaB, BTaBTaB, BaBTaBBa, DaBTaBDa, and TdaBTaBTda as well as polymeric model substrates were incubated with Cbotu_EstA for 24, 48, and 72 h at 100 rpm and 50°C in 100 mM potassium phosphate buffer pH 7.0.

The activity of Cbotu_EstB was tested on PBAT, BTaB, and BTaBTaB at 37°C, 300 rpm and pH 7.0 and samples were taken after 24, 48, and 72 h. To verify that buffer capacities were sufficient throughout the whole experiments, the pH values were checked after the incubation. The reactions were stopped, samples were prepared for HPLC analysis, and the hydrolysis products Ta, Ba, Ada, mono(4-hydroxybutyl) terephthalate (BTa) and BTaB were quantified by means of RP-HPLC as previously described (Perz et al., 2015).

Crystallization

A novel multicomponent buffer system (Newman, 2004) was applied for additional purification using a Superdex 200 HiLoad 16/60 column from GE Healthcare. For this purpose a multicomponent buffer containing 0.12 M succinic acid, 0.5 M sodium dihydrogen phosphate monohydrate and 0.4 M glycine, pH 8.0 was applied. After purification, the protein fractions were pooled, concentrated using Amicon® Ultra Centrifugal filters (30,000 NMWL) from Merck Millipore Ltd and used for setting up crystallization trials. Crystallization experiments were performed by

Table I. PBAT model substrates with variations in adipic acid (Ada) and terephthalic acid (Ta) ratios, their respective viscosity numbers, molecular weights, melting temperatures, (T_m) and glass transition temperatures (T_g).

			Molecular weight[a]			
PBAT type	Ada:Ta ratio	Viscosity number [mL/g]	M_w [g/mol]	M_w/M_n	T_m [°C]	T_g [°C]
Ada100_Ta0	100: 0		52,000	3.1	58.8	−59
Ada90_Ta10	89.3: 10.7	107.3	45,800	2.9	52.8	−52
Ada80_Ta20	78.9: 21.1	105.7	32,400	2.9	47.8	−48
Ada70_Ta30	68.9: 31:1	100.6	26,700	2.8	70.0	−50
Ada60_Ta40	58.5: 41.5	94.0	29,200	2.8	101.4	−45
Ada50_Ta50	48.8: 51.2	94.3	31,900	2.7	132.2	–

Analysis of T_m was performed as previously described (Perz et al., 2015). T_g values were determined using the Differential Scanning Calorimeter Q2000 (TA Instruments). Analyses were conducted from −80°C to 200°C at a linear heating rate of 20°C/min.

[a]weight average (M_w), number-average (M_n).

the sitting-drop vapor diffusion method using commercial crystallization screens (the Index Screen from Hampton Research and the Morpheus Screen from Molecular Dimensions). Sitting drops were prepared by mixing 0.5 μL of the protein solution (at a concentration of 20 mg/mL) with an equal volume of mother liquor, which were pipetted using ORYX 6 pipetting robot from Douglas Instruments. The trays were incubated at 20°C. First crystal clusters were observed after approximately two weeks. Well diffracting Cbotu_EstA crystals were obtained with 0.1 M Tris, pH 8.5 and 2 M ammonium sulfate (condition number six from the Index Screen).

Crystal Structure Determination

X-ray diffraction data were collected to a maximum resolution of 1.2 Å on beamline BM30A at the ESRF in Grenoble, France. The crystal was monoclinic (space group $P2_1$) with unit-cell parameters $a = 51.24$, $b = 64.71$, $c = 69.79$ Å and $\beta = 106.93°$. The data were processed using the programs XDS (Kabsch, 2010) and Scala (Evans, 2006). The structure was solved by molecular replacement using the structure of the L1 lipase from *Geobacillus stearothermophilus* (PDB code: 1KU0, 46% sequence identity to Cbotu_EstA) (Jeong et al., 2002) yielding one molecule in the asymmetric unit. This is consistent with the calculated Matthews coefficient. The structure was refined using the programs PHENIX (Adams et al., 2010) and COOT (Emsley et al., 2010). Clear electron density was observed for the whole protein chain except for the 27 N-terminal residues. In the later cycles of the refinement water molecules were added. Large residual electron density in the vicinity of the amino acids Asp130, His150, His156, and Asp302 was interpreted as a zinc ion. Additional residual density features were modeled by two potassium ions. Anisotropic atomic displacement parameters were refined for all protein atoms as well as for the zinc and potassium ions. Hydrogen atoms were added to the protein structure and refined as "riding" on the respective heavy atom. Detailed statistics regarding data processing and structure refinement are summarized in Supplementary Table S1. Atomic coordinates and structure factors have been deposited in the Protein Data Bank under the accession code 5AH1.

Modeling

The model of Cbotu_EstB was built using YASARA Structure (v. 13.9.8) applying the homology modeling protocol (Krieger et al., 2002). In addition to the best five templates (PDB codes 4FDM, 3AUK, 4FKB, 2DSN, and 1JI3) identified by a PSI-BAST search using five iterations and an E-value cutoff of 0.001, the crystal structure of Cbotu_EstA was used as a template. The overall sequence identity between Cbotu_EstB and Cbotu_EstA is about 40%, the other templates were lipases with sequence identities of only about 35%. Therefore, we chose the model obtained using the Cbotu_EstA structure as template for analysis. In all models, amino acids around the Zn-binding region were distorted most likely due to the model building procedure. These conformations were corrected and the geometry was optimized using the YAMBER2 force field.

Results and Discussion

Identification of *Clostridium botulinum* Hydrolases

From the different species described to be involved in anaerobic digestion processes as well as in polymer degradation, *Clostridium* species showed the most promising candidates as a source for new polymer degrading enzymes. *Clostridia* belong to the phylum of *Firmicutes* and different studies showed that *Clostridia* are omnipresent in anaerobic digestion communities (Krober et al., 2009; Pobeheim et al., 2010; Weiland, 2010) were they seem to play an important role for example during the hydrolysis of cellulosic plant material (Schluter et al., 2008). In addition, different *Clostridium* species were proven to degrade polymers such as poly(β-hydroxybutyrate) (PHB) and poly(ε-caprolactone) (PCL) (Abou-Zeid et al., 2001).

Enzymes that exhibit the ability to hydrolyze PBAT were assumed to be found within the family of extracellular serine hydrolases since members of this enzyme class like lipases (EC 3.1.1.3), carboxylesterases (EC 3.1.1.1) and cutinases (3.1.1.74) have been reported to hydrolyze (synthetic) polymers. Lipases (Marten et al., 2005) and cutinases (Herrero Acero et al., 2011; Perz et al., 2015; Ribitsch et al., 2012) have already been described to hydrolyze synthetic polymers like PET or PBAT.

For identification of potential polyesterases from *Clostridium sp.*, the NCBI genome database was searched for available genomic sequences. Genomic sequences of two *Clostridium species* known from literature to be active on polyester have been found, *Clostridium acetobutylicum* and *Clostridium botulinum*. These genomic sequences were *in-silico* screened for secreted hydrolases.

The screening resulted solely in identification of two hydrolases from *Clostridium botulinum* ATCC 3502 named Esterase A (Cbotu_EstA, *ATCC 3502*, GenBank accession number CAL82416.1) and Esterase B (Cbotu_EstB, *ATCC 3502*, GenBank accession number CAL83600.1). Both enzymes were also referred to as putative secreted lipases sharing 40% sequence identity and were chosen for further investigations.

Cloning, Heterologous Expression and Purification of Esterases From *Clostridium botulinum*

The identified and codon optimized genes carrying an C-terminal 6xHisTag for rapid purification were cloned over the *Nde*I and *Hind*III restriction sites without the natural signal peptide (aa 1–29 in CbotuEstA and aa 1–30 in Cbotu_EstB) into pET26b(+).

The expression was performed in *E. coli* BL21-Gold(DE3) at 20°C and samples were taken 2, 4, and 20 h after induction with 0.05 M IPTG to analyze the expression behavior. Cells were harvested 20 h after induction and the expression behavior was analyzed by means of SDS–PAGE.

SDS–PAGE analysis (Supplementary Fig. S1) revealed that induction at 160 rpm and 20°C for 20 h resulted in highly overexpressed recombinant protein bands in the soluble fraction around 50 kDa which corresponded well to the calculated mass of Cbotu_EstA (51.7 kDa) and Cbotu_EstB (45.5 kDa). Both esterases from *C. botulinum* were intracellularly expressed in their soluble active form and as inclusion bodies. Cbotu_EstA and Cbotu_EstB were purified via HisTag affinity chromatography. Typically, 130 mg purified Cbotu_EstA and 80 mg purified Cbotu_EstB were obtained from 300 mL cell culture.

Determination of Kinetic Parameters with *p*NPA and *p*NPB

In a first step the kinetic parameters of Cbotu_EstA and Cbotu_EstB were determined on the water-soluble standard substrates *p*NPB and *p*NPA. The V_{max} as well as the k_{cat} values of Cbotu_EstA on *p*NPA were 2–3 orders of magnitude higher compared to Cbotu_EstB, the K_m values were in the same range. In the case of Cbotu_EstB, V_{max}, K_m, and k_{cat} on *p*NPB and on *p*NPA were comparable while Cbotu_EstA showed lower activity on *p*NPB but yet one order of magnitude higher than Cbotu_EstB. (Table II).

Temperature Optimum and Stability

Cbotu_EstA showed a temperature optimum at 60°C and esterase activity was observed in the range of 20–70°C. The temperature optimum of Cbotu_EstB was determined to be 40°C and the activity range of this enzyme was between 20°C and 60°C (Supplementary Fig. S2).

The stability of Cbotu_EstA and Cbotu_EstB was investigated at 25°C, 37°C and 50°C and significant differences were observed between the temperature stabilities of these two esterases. Cbotu_EstA showed higher stabilities than Cbotu_EstB at all tested temperatures. Cbotu_EstA exhibited an activity half-life of 6 h at 50°C and after 3 days 25% remaining activity were observed. At 37°C the activity half-life was estimated to be 17 days and after incubation at 25°C for 35 days the specific activity lay still around 60%. Nevertheless the absolute activity was highest at 50°C and for that reason this temperature was chosen for detailed hydrolysis experiments.

Cbotu_EstB showed after 5 min incubation at 50°C only 11% of the initial specific activity and no activity could be detected after 20 min. The half-life of Cbotu_EstB was measured to be 2.5 days at 37°C and 10 days at 25°C.

Thermal denaturation experiments using CD-spectroscopy yielded a similar picture. While the melting point of Cbotu_EstA was determined as approximately 60°C, the melting temperature for Cbotu_EstB was 45°C indicating a significantly lower thermal stability of the latter.

Substrate Specificities on BaETaEBa

When incubated with BaETaEBa at different pHs, distinct hydrolysis pathways were observed for the two esterases (Supplementary Fig. S3). Cbotu_EstA showed activity in the range of pH 4.0–10.0 with a maximum at pH 7.0 and pH 8.0 based on the total amount of released molecules. Interestingly, the highest concentration of released ETa was measured at pH 6.0 whereas the highest concentration of Ba was found after incubation at pH 8.0. This means that Cbotu_EstA released different ratios of the hydrolysis products depending on the pH. Apparently, a change in the selectivity of Cbotu_EstA takes place depending on the pH. In general, a higher amount of released Ta and ETa indicates preferential cleavage of the internal ester bond between Ta and E in a first step (Fig. 1, right side), while higher concentrations of Ba suggest a favored hydrolysis of the terminal ester bond between Ba and E (Fig. 1, left side). This is one feasible explanation for the existence of two pH optima at pH 6.0 (highest concentration of released Ta and ETa) and pH 8.0 (highest concentration of released Ba.)

In contrast to that, Cbotu_EstB showed significant activity in the range of pH 5.0 to pH 8.0 with an activity maximum at pH 7.0 with Ba, ETa, and Ta as main hydrolysis products. Again at pH 5.0 and pH 6.0 a shift of the ratios of release molecules was perceived but towards higher concentration of Ta indicating an increased hydrolysis of Ta-E ester bonds (Fig. 1, right side) at lower pH values. Figure 1 describes the theoretical hydrolysis of BaBTaBBa in the case of distinct substrate specificities.

Table II. Kinetic parameters of Cbotu_EstA and Cbotu_EstB on the soluble esterase substrates *p*NPA and *p*NPB.

	V_{max} [μmol min^{-1} mg^{-1}]		K_m [mM]		k_{cat} [sec^{-1}]		k_{cat}/K_m [sec^{-1} mM^{-1}]	
	*p*NPA	*p*NPB	*p*NPA	*p*NPB	*p*NPA	*p*NPB	*p*NPA	*p*NPB
Cbotu_EstA	1150.00 ± 66.00	83.40 ± 2.70	1.70 ± 0.30	1.95 ± 0.23	990.92	71.86	582.89	36.85
Cbotu_EstB	6.00 ± 0.04	7.70 ± 0.3	0.85 ± 0.01	1.30 ± 0.60	4.55	5.84	5.35	4.49

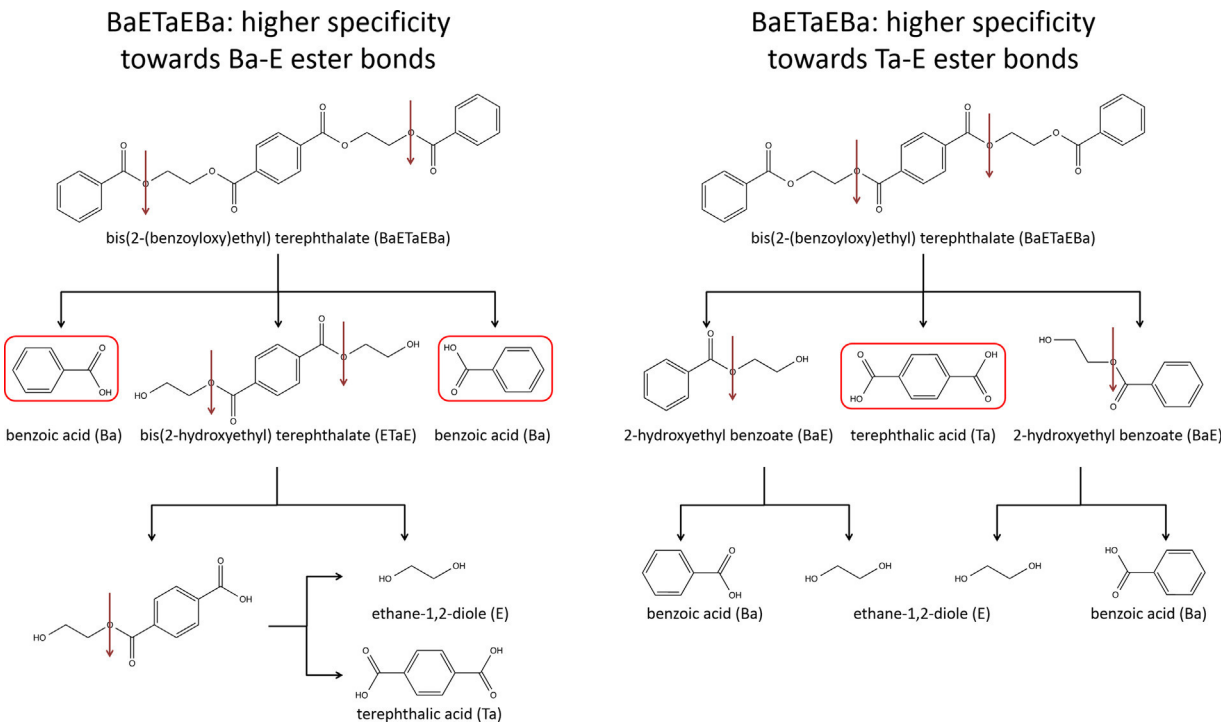

Figure 1. Determination of substrate specificities. Main monomeric release products for higher Ba-E or Ta-E ester bond substrate specificity are marked in red, respectively.

Hydrolysis of PET

When incubated with PET foils at pH 6.0, pH 7.0 and pH 8.0 and 50°C, Cbotu_EstA released only marginal concentrations of the hydrolysis products Ta, ETa, and ETaE when compared to the blank while Cbotu_EstB did not show any activity (data not shown).

Hydrolysis of PBAT and Oligomeric PBAT Building Blocks

The hydrolytic activities of Cbotu_EstA and Cbotu_EstB on PBAT and oligomeric PBAT building block BTaB (partly soluble) and BTaBTaB (insoluble) were tested. All substrates were used in excess.

Cbotu_EstB showed only marginal activity on PBAT but was able to hydrolyze the smaller oligomeric model substrates BTaB and BTaBTaB (Fig. 2). BTaB and BTaBTaB are possible PBAT building blocks and the ability of Cbotu_EstB to hydrolyze these lower molecular weight substrates indicates that the size of the PBAT polymer might be the obstacle for an efficient PBAT degradation. In Figure 3 possible enzymatic degradation pattern of PBAT are described.

Cbotu_EstA was active on the low molecular weight model substrates BTaB and BTaBTaB, which are PBAT building blocks, as well on the polymer itself. Different ratios of the released hydrolysis products Ta, BTa, and BTaB were observed depending on the pH. Interestingly, during PBAT hydrolysis the predominantly released molecule at pH 6.0 was BTaB. In contrast, at pH 8.0 hardly any BTaB but predominantly Ta and BTa were detected. When incubated with BTaB and BTaBTaB, Cbotu_EstA also released higher concentrations of Ta at pH 8.0 when compared to pH 6.0 (Fig. 4).

Hydrolysis of Oligomeric and Polymeric PBAT Model Substrates

In order to gain a more detailed mechanistic insight into the hydrolysis behavior of Cbotu_EstA, the enzyme was incubated with a variety of oligomeric and polymeric PBAT model substrates. Beside oligomer BTaB, all other substrates were insoluble in the reaction mixture and all substrates were used in excess. Cbotu_EstA had a higher activity on the model substrate DaBTaBDa with the shorter terminal C10 acids than on TdaBTaBTda containing terminal C14 acids (Fig. 5). An additional aromatic Ta subunit in the substrate BTaBTaB led to a strong decrease in activity when compared to substrate BTaB. The hydrolysis product BTaB was further degraded to BTa and the release BTa dimer was present in very high concentrations in all samples. It was observed that Cbotu_EstA is able to further hydrolyze BTa into Ta and butane-1, 4-diole (B) but the hydrolysis of this B-Ta ester bond seems to be a bottleneck of total hydrolysis by Cbotu_EstA. Hydrolysis of model substrate BaBTaBBa led to a Ta/Ba ratio that lies far on the side of Ba. This means that Cbotu_EstA liberates the terminal Ba groups much more efficiently than the internal Ta group. Taking into account the structure of this model substrate, the low Ta/Ba ratio indicates that Cbotu_EstA is less specific to the ester bond between Ta and B in the liberated oligomer BTa. The low specificity of Cbotu_EstA on the BTa fragment is evident from the high BTa

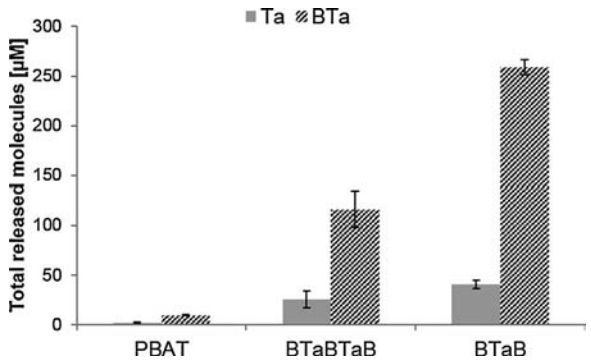

Figure 2. Hydrolysis of PBAT, BTaBTaB, and BTaB with 0.6 μM Cbotu_EstB at pH 7.0. Total released molecules after 72 h of incubation at 37°C. Ta, terephthalic acid; BTa, mono(4-hydroxybutyl) terephthalate. Each bar represents the average of three independent samples; error bars indicate the standard deviation.

concentrations that accumulated in all hydrolysis experiments (Figs. 2, 4, 5 and 6).

Polymeric PBAT model polymers with variations of Ta:Ada ratios were investigated for their degradability by Cbotu_EstA. Hydrolysis of Ada70_Ta30 by Cbotu_EstA yielded in an Ada to Ta ration of 31:1 while equal specificities to both ester bonds should lead to a ration of 7:3 (Fig. 6). Hence, it can be stated that Cbotu_EstA hydrolyzed the Ada-B ester bonds in the polymer to a much higher extend than the Ta-B ester bonds.

Generally, a higher Ada content in the polymer leads to higher hydrolysis activity. Although the Ta content was decreasing from 50% in Ada50_Ta50 to 10% in the Ada90_Ta10 polymer, a clear increase of released BTa and BTaB molecules was observed. In case of the polymers PBAT, Ada50_Ta50 as well as Ada60_Ta40, Cbotu_EstA showed a considerably lower activity. When comparing the melting temperature (T_m) of the tested polymer variants it was detected that the polymer with the lowest difference between reaction temperature and T_m (here Ada90_Ta10) led to the highest enzyme activity. Data for Ada80_Ta20 need to be interpreted differently, since the T_m of Ada80_Ta20 lies beneath the reaction temperature of 50°C. Due to the possible melting of the Ada80_Ta20 polymer, the surface that is accessible for the enzyme is reduced, leading to slightly lower concentration of hydrolysis products. Similar results were recently obtained during hydrolysis of these polymers with a cutinase from *Humicola insolens* and cutinase 1 from *Thermobifida cellulosilytica* (Perz et al., 2015).

Crystal Structure of Cbotu_EstA

The structure of Cbotu_EstA was determined using x-ray crystallography to a resolution of 1.2 Å. The crystallographic parameters are listed in Supplementary Table S1. The crystal was monoclinic (space group $P2_1$) and contained one esterase molecule in the asymmetric unit. The overall structure consists of a central β-sheet surrounded by α-helices indicating that Cbotu_EstA belongs to the family of α/β-hydrolases (Fig. 7). According to an analysis of intermolecular interactions in the crystal using the PDBePISA server (Krissinel and Henrick, 2007) the esterase is most likely present as a monomer in solution.

A BLAST search (Altschul et al., 1997) against the Protein Data Bank (PDB) yielded the lipase L1 from *Geobacillus stearothermophilus* (PDB code: 1KU0) as the most similar hit (46% sequence identity). This structure was also used as the search template for molecular replacement. Based on a structural alignment with this lipase (root-mean-square-deviation of 0.6 Å for 261 superimposed Cα-atoms), the catalytic triad in Cbotu_EstA consists of Ser182, His426 and Asp384 with the serine located at the tip of the "nucleophile elbow." As expected for an α/β-hydrolase, the sequence of Cbotu_EstA contains the conserved Gly-X-Ser-X-Gly motif, which includes the catalytic serine residue. The region

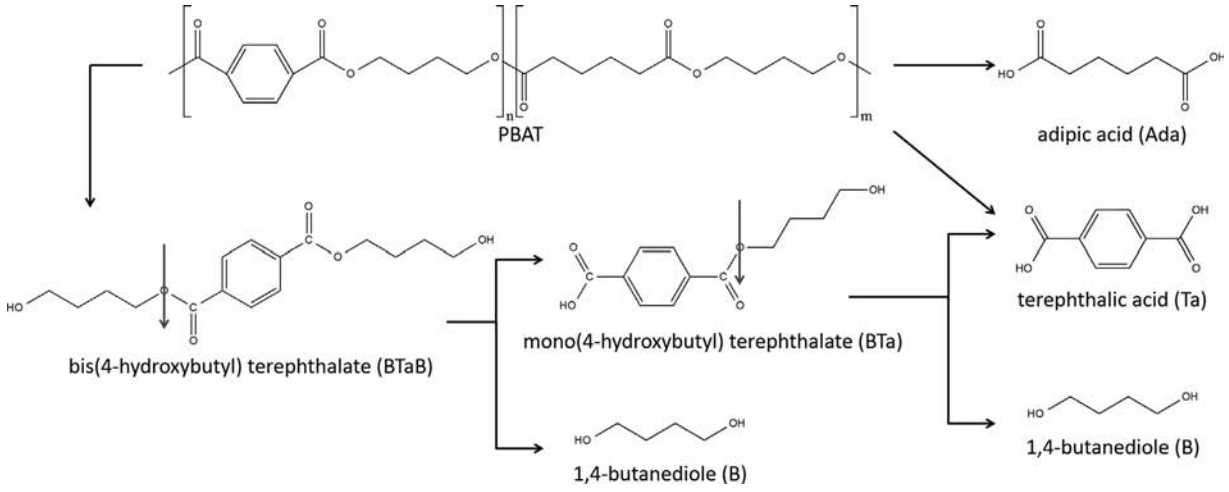

Figure 3. Possible PBAT hydrolysis products that were detected by means of RP-HPLC and UV–VIS detection include BTaB, bis(4-hydroxybutyl) terephthalate; BTa, mono(4-hydroxybutyl) terephthalate; Ta, terephthalic acid and Ada, adipic acid.

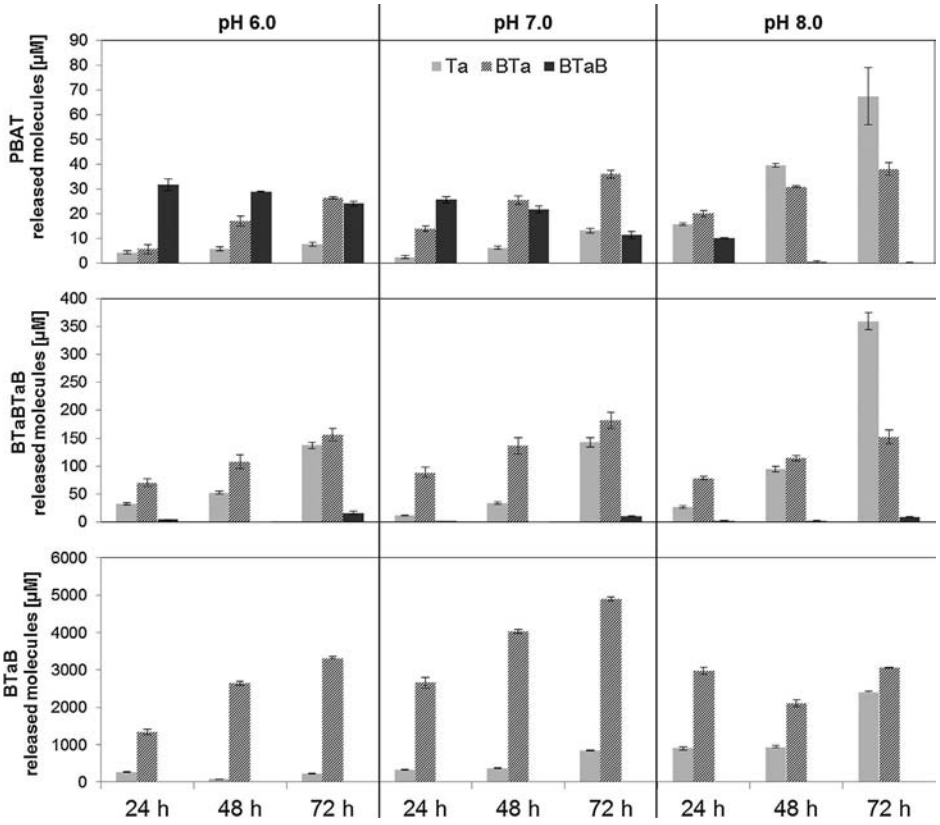

Figure 4. Hydrolysis of PBAT, BTaBTaB, and BTaB with 0.6 µM Cbotu_EstA at pH 6.0, pH 7.0 and pH 8.0 at 50°C and 300 rpm. Ta, therephthalic acid; BTa, mono(4-hydroxybutyl) terephthalate; BTaB, bis(4-hydroxybutyl) terephthalate. Each bar represents the average of three independent samples; error bars indicate the standard deviation.

around the catalytic serine is occupied by mostly non-polar residues indicating the hydrophobicity of the substrate binding site.

In addition to the α/β-hydrolase core, a cap domain is present consisting of residues 236–303 and residues 334–378 (Fig. 7). These residues cover the active site and the catalytic triad. The N-terminal residues 28–63 form an "arm" that is wrapped around this cap (Fig. 7). A similar cap or lid has been described for the *Geobacillus* lipase (Jeong et al., 2002). This cap prevents access to the active site

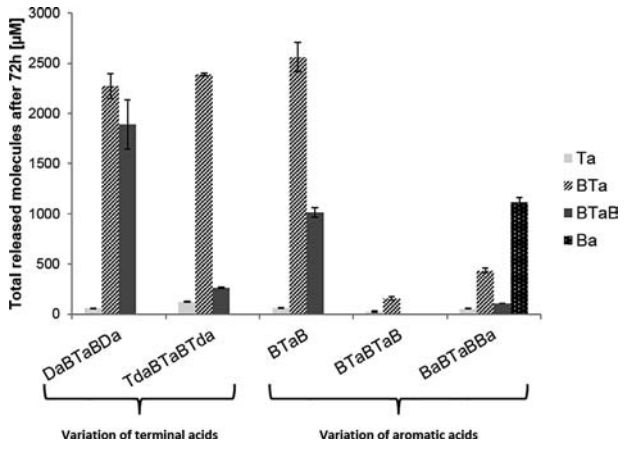

Figure 5. Analysis of the Cbotu_EstA hydrolysis pattern of different oligomeric PBAT model substrates. Total released molecules are shown after 72 h. Each bar represents the average of three independent samples; error bars indicate the standard deviation.

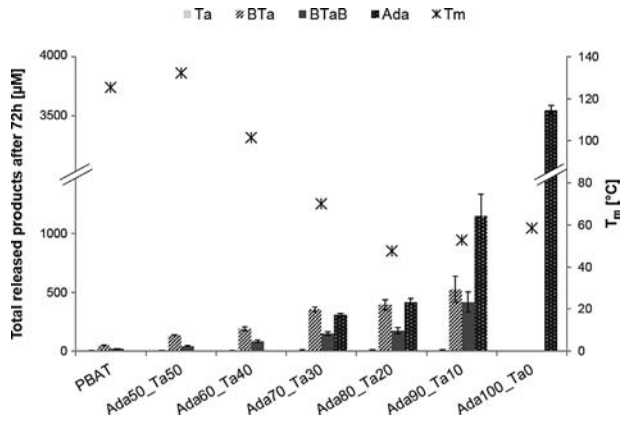

Figure 6. Hydrolysis of PBAT and polymeric PBAT model substrates containing different mol% ratios of adipic acid and terephthalic acid. Total released molecules after 72 h of incubation with Cbotu_EstA. T_m values of all substrates are displayed as black stars on the secondary axis. Each bar represents the average of three independent samples; error bars indicate the standard deviation.

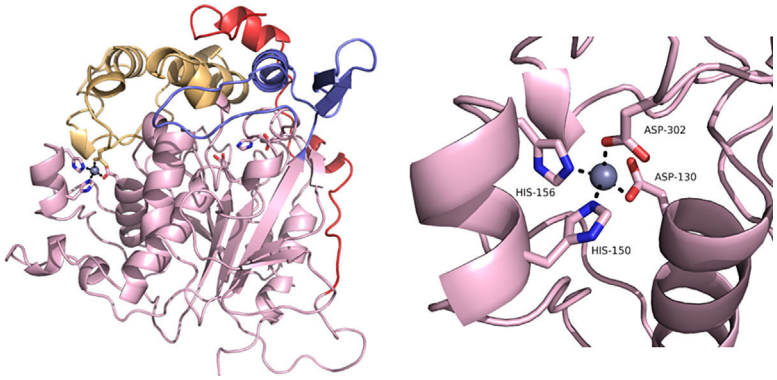

Figure 7. Left: Overall structure of Cbotu_EstA. The α/β-hydrolase core is shown in pink. The two components of the cap domain are shown in dark yellow (residues 236–303) and blue (residues 334–378). The N-terminal arm is shown in red. The figure was prepared using the program PyMOL (http://www.pymol.org). Right: Zn-binding site in the structure of Cbotu_EstA. The zinc ion is shown as a gray sphere and the coordinating residues as sticks. Black dashed lines represent the metal ligand coordination. The figure was prepared using the program PyMOL (http://www.pymol.org).

indicating that Cbotu_EstA adopts a closed conformation in the present crystal structure. In this conformation the access of larger substrates is prevented. Thus, hydrolysis of polymeric substrates very likely requires large conformational changes in this part of the molecule (i.e., opening of the lid/cap).

We also identified a metal binding site in the structure of Cbotu_EstA, in which we placed a zinc ion. This ion is tetragonally coordinated by the side chains of Asp130, His150, His156, and Asp302 (Fig. 7). The metal ligand distances are in range of 1.9–2.1 Å, consistent with zinc as the central ion. This zinc binding site is located close to the surface of the enzyme at a distance of 19.3 Å from the catalytic serine residue. A very similar site was observed at the equivalent position in the structure of the *Geobacillus* lipase (Jeong et al., 2002). In that case, metal coordination was discussed as one important factor for the thermostability of the protein and was also ascribed an important role in the regulation of the lid opening (Jeong et al., 2002). Consistent with the latter hypothesis one of the coordinating residues in Cbotu_EstA (Asp302) is part of the cap domain described above. As in the *Geobacillus* lipase additional interactions exist between residues in the vicinity of the metal binding site and the cap domain. A direct involvement of the zinc binding site in catalysis appears to be less likely because of the significant distance of the metal ion from the active site.

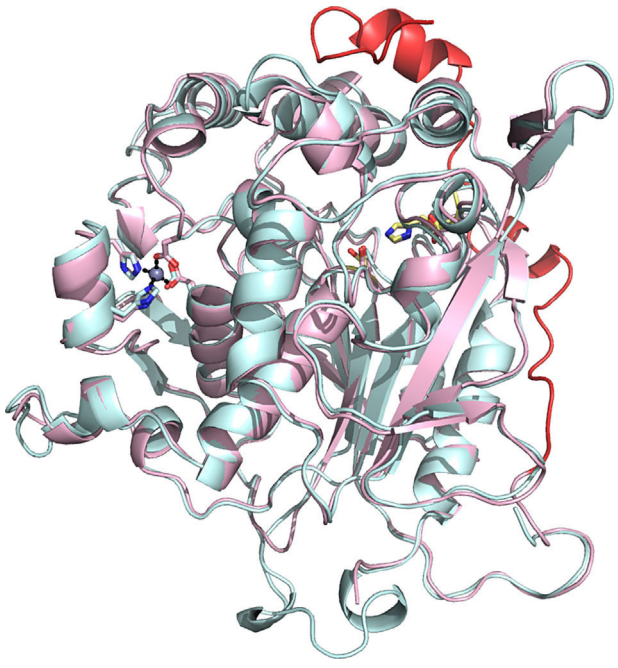

Figure 8. Comparison of Cbotu_EstA and Cbotu_EstB. The modeled structure of Cbotu_EstB is shown in cyan, the crystal structure of Cbotu_EstA in pink. The N-terminal arm in Cbotu_EstA (residues 28–63) is shown in red. Active site and zinc coordinating residues are shown as sticks. The zinc ion is represented by a gray sphere. The figure was prepared using the program PyMOL (http://www.pymol.org).

Comparison of Cbotu_EstA and Cbotu_EstB

To compare Cbotu_EstB and Cbotu_EstA we created a model of Cbotu_EstB. The model shows that the active site of Cbotu_EstB is very similar and contains the triad Ser124, His370 and Asp328. There are some differences in the immediate surrounding of the active site aspartate: Ser228, Thr333 and Gln392 in Cbotu_EstA and Ala171, Cys278 and Ala336 in Cbotu_EstB. These residues, however, are quite remote from the substrate binding site and the active serine. Therefore, these differences are very likely not responsible for the difference in activity between the two enzymes. The zinc-binding site is completely conserved in Cbotu_EstB and it is located in the same position remote from the active site. The corresponding residues are Asp66, His86, His92 and Asp247.

As described above, an N-terminal extension of Cbotu_EstA (residues 28–63) forms an arm that wraps around the cap domains. This part is completely missing in the sequence of Cbotu_EstB (Fig. 8). Because conformational changes in the cap domains are very likely necessary to allow the access of polymeric substrates, the absence of this N-terminal arm may well be the reason for the observed differences in substrate acceptance between the two

esterases. In addition, it may also influence the stability of the enzymes. Apart from the longer N-terminus in Cbotu_EstA no spatial clustering of aligned residue differences were observed between the two enzymes.

Conclusion

In this study we identified for the first time enzymes from anaerobic organisms, which hydrolyze the synthetic polyester PBAT. Since *Clostridium* species are very abundant in anaerobic digestion processes this gives a hint how this polyester could be degraded in anaerobic environments.

Two novel esterases (Cbotu_EstA and Cbotu_EstB) from *Clostidium botulinum* were characterized in detail. Cbotu_EstA is the first polyesterase known to contain a Zn^{2+} binding site. The crystal structure of Cbotu_EstA indicates that hydrolysis of polymeric substrates most likely requires a movement of the cap domain. When compared to Cbotu_EstB, both differences outside and close to the active site may explain significantly different hydrolysis activities on oligomeric/polymeric substrates. Obtained mechanistic data on enzyme substrate specificities will provide important information regarding the future design of biodegradable polymers under anaerobic conditions.

This work has been supported by the Federal Ministry of Science, Research and Economy (BMWFW), the Federal Ministry of Traffic, Innovation and Technology (bmvit), the Styrian Business Promotion Agency SFG, the Standortagentur Tirol, the Government of Lower Austria and Business Agency Vienna through the COMET-Funding Program managed by the Austrian Research Promotion Agency FFG. We highly appreciate the support of the beamline staff at the ESRF in Grenoble, France during diffraction data collection.

References

Abou-Zeid DM, Muller RJ, Deckwer WD. 2001. Degradation of natural and synthetic polyesters under anaerobic conditions. J Biotechnol 86(2):113–126.

Abou-Zeid DM, Muller RJ, Deckwer WD. 2004. Biodegradation of aliphatic homopolyesters and aliphatic-aromatic copolyesters by anaerobic microorganisms. Biomacromolecules 5(5):1687–1697.

Adams PD, Afonine PV, Bunkoczi G, Chen VB, Davis IW, Echols N, Headd JJ, Hung L-W, Kapral GJ, Grosse-Kunstleve RW, McCoy AJ, Moriarty NW, Oeffner R, Read RJ, Richardson DC, Richardson JS, Terwilliger TC, Zwart PH. 2010. PHENIX: A comprehensive Python-based system for macromolecular structure solution. Acta Crystallogr Sect D 66(2):213–221.

Aeschelmann F, Carus M, Baltus W, Blum H, Busch R, Carrez D, Issbruecker C, Kaeb H, Lange K-B, Philip J, Ravenstijn J, von Pogrell H. 2015. Bio-based building blocks and polymers in the world—capacities, production and applications: Status quo and trends toward 2020. Huerth, Germany: nova-Institut GmbH. p 474.

Altschul SF, Madden TL, Schaffer AA, Zhang J, Zhang Z, Miller W, Lipman DJ. 1997. Gapped BLAST and PSI-BLAST: A new generation of protein database search programs. Nucleic Acids Res 25(17):3389–3402.

Budwill K, Fedorak PM, Page WJ. 1992. Methanogenic degradation of poly (3-hydroxyalkanoates). Appl Environ Microbiol 58(4):1398–1401.

Cole M, Lindeque P, Halsband C, Galloway TS. 2011. Microplastics as contaminants in the marine environment: A review. Mar Pollut Bulletin 62(12):2588–2597.

de Camargo Andrade-Molina TP, Shirai MA, Victória Eiras Grossmann M, Yamashita F. 2013. Active biodegradable packaging for fresh pasta. LWT—Food Sci Technol 54(1):25–29.

Emsley P, Lohkamp B, Scott WG, Cowtan K. 2010. Features and development of Coot. Acta Crystallogr Sect D 66(4):486–501.

Evans P. 2006. Scaling and assessment of data quality. Acta Crystallogr Sect D 62(1):72–82.

Herrero Acero E, Ribitsch D, Steinkellner G, Gruber K, Greimel K, Eiteljoerg I, Trotscha E, Wei R, Zimmermann W, Zinn M, Cavaco-Paulo A, Freddi G, Schwab H, Guebitz G. 2011. Enzymatic surface hydrolysis of PET: Effect of structural diversity on kinetic properties of cutinases from thremobifida. Macromolecules 44(12):4640.

Heumann S, Eberl A, Pobeheim H, Liebminger S, Fischer-Colbrie G, Almansa E, Cavaco-Paulo A, Gübitz GM. 2006. New model substrates for enzymes hydrolysing polyethyleneterephthalate and polyamide fibres. J Biochem Biophys Methods 69(1–2):89–99.

Jeong ST, Kim HK, Kim SJ, Chi SW, Pan JG, Oh TK, Ryu SE. 2002. Novel zinc-binding center and a temperature switch in the Bacillus stearothermophilus L1 lipase. J Biol Chem 277(19):17041–17047.

Kabsch W. 2010. XDS. Acta Crystallogr Sect D 66(2):125–132.

Kijchavengkul T, Auras R, Rubino M, Selke S, Ngouajio M, Fernandez RT. 2010. Biodegradation and hydrolysis rate of aliphatic aromatic polyester. Polym Degrad Stab 95(12):2641–2647.

Krieger E, Koraimann G, Vriend G. 2002. Increasing the precision of comparative models with YASARA NOVA—a self-parameterizing force field. Proteins 47(3):393–402.

Krissinel E, Henrick K. 2007. Inference of macromolecular assemblies from crystalline state. J Mol Biol 372(3):774–797.

Krober M, Bekel T, Diaz NN, Goesmann A, Jaenicke S, Krause L, Miller D, Runte KJ, Viehover P, Puhler A, Schluter A. 2009. Phylogenetic characterization of a biogas plant microbial community integrating clone library 16S-rDNA sequences and metagenome sequence data obtained by 454-pyrosequencing. J Biotechnol 142(1):38–49.

Laemmli UK. 1970. Cleavage of structural proteins during the assembly of the head of bacteriophage T4. Nature 227(5259):T4–T5.

Lechner A, Keckeis H, Lumesberger-Loisl F, Zens B, Krusch R, Tritthart M, Glas M, Schludermann E. 2014. The Danube so colourful: A potpourri of plastic litter outnumbers fish larvae in Europe's second largest river. Environ Pollut 188(0):177–181.

Marten E, Müller R-J, Deckwer W-D. 2005. Studies on the enzymatic hydrolysis of polyesters. II. Aliphatic-aromatic copolyesters. Poly Degrad Stab 88(3):371–381.

Newman J. 2004. Novel buffer systems for macromolecular crystallization. Acta Crystallogr D Biol Crystallogr 60(Pt 3):610–612.

Perz V, Bleymaier K, Sinkel C, Kueper U, Bonnekessel M, Ribitsch D, Guebitz GM. 2015. Substrate specificities of cutinases on aliphatic-aromatic polyesters and on their model substrates. New Biotechnol, in press.

Pobeheim H, Munk B, Müller H, Berg G, Guebitz GM. 2010. Characterization of an anaerobic population digesting a model substrate for maize in the presence of trace metals. Chemosphere 80(8):829–836.

Reischwitz A, Stoppok E, Buchholz K. 1997. Anaerobic degradation of poly-3-hydroxybutyrate and poly-3-hydroxybutyrate-co-3-hydroxyvalerate. Biodegradation 8(5):313–319.

Ribitsch D, Heumann S, Trotscha E, Herrero Acero E, Greimel K, Leber R, Birner-Gruenberger R, Deller S, Eiteljoerg I, Remler P, Weber T, Siegert P, Maurer KH, Donelli I, Freddi G, Schwab H, Guebitz GM. 2011. Hydrolysis of polyethyleneterephthalate by para-nitrobenzylesterase from Bacillus subtilis. Biotechnol Prog 27(4):951–960.

Ribitsch D, Herrero Acero E, Greimel K, Eiteljoerg I, Trotscha E, Freddi G, Schwab H, Guebitz GM. 2012. Characterization of a new cutinase from Thermobifida alba regarding PET-surface hydrolysis. Biocatal Biotransform 30(1):2–9.

Sambrook JE, Fritsch EF, Maniatis T. 1989. Molecular cloning: A laboratory manual. Cold Spring Harbor, New York: Cold Spring Harbor Press.

Schluter A, Bekel T, Diaz NN, Dondrup M, Eichenlaub R, Gartemann KH, Krahn I, Krause L, Kromeke H, Kruse O, Mussgnug JH, Neuweger H, Niehaus K, Puhler A, Runte KJ, Szczepanowski R, Tauch A, Tilker A, Viehover P, Goesmann A. 2008. The metagenome of a biogas-producing microbial community of a production-scale biogas plant fermenter analysed by the 454-pyrosequencing technology. J Biotechnol 136(1–2):77–90.

Shah AA, Kato S, Shintani N, Kamini NR, Nakajima-Kambe T. 2014. Microbial degradation of aliphatic and aliphatic-aromatic co-polyesters. Appl Microbiol Biotechnol 98(8):3437–3447.

Soroudi A, Jakubowicz I. 2013. Recycling of bioplastics, their blends and biocomposites: A review. Eur Polym J 49(10):2839–2858.

Weiland P. 2010. Biogas production: Current state and perspectives. Appl Microbiol Biotechnol 85(4):849–860.
Weng Y-X, Jin Y-J, Meng Q-Y, Wang L, Zhang M, Wang Y-Z. 2013. Biodegradation behavior of poly(butylene adipate-co-terephthalate) (PBAT), poly(lactic acid) (PLA), and their blend under soil conditions. Polym Test 32(5):918–926.
Witt U, Müller R-J, Deckwer W-D. 1995. New biodegradable polyester-copolymers from commodity chemicals with favorable use properties. J Environ Polym Degrad 3(4):215–223.
Witt U, Yamamoto M, Seeliger U, Müller R-J, Warzelhan V. 1999. Biodegradable polymeric materials—not the origin but the chemical structure determines biodegradability. Angew Chem Int Ed 38(10):1438–1442.
Witt U, Einig T, Yamamoto M, Kleeberg I, Deckwer WD, Müller RJ. 2001. Biodegradation of aliphatic-aromatic copolyesters: Evaluation of the final biodegradability and ecotoxicological impact of degradation intermediates. Chemosphere 44(2):289–299.
Yagi H, Ninomiya F, Funabashi M, Kunioka M. 2014. Mesophilic anaerobic biodegradation test and analysis of eubacteria and archaea involved in anaerobic biodegradation of four specified biodegradable polyesters. Polym Degrad Stab 110(0):278–283.

Supporting Information

Additional supporting information may be found in the online version of this article at the publisher's web-site.

Supplementary Material

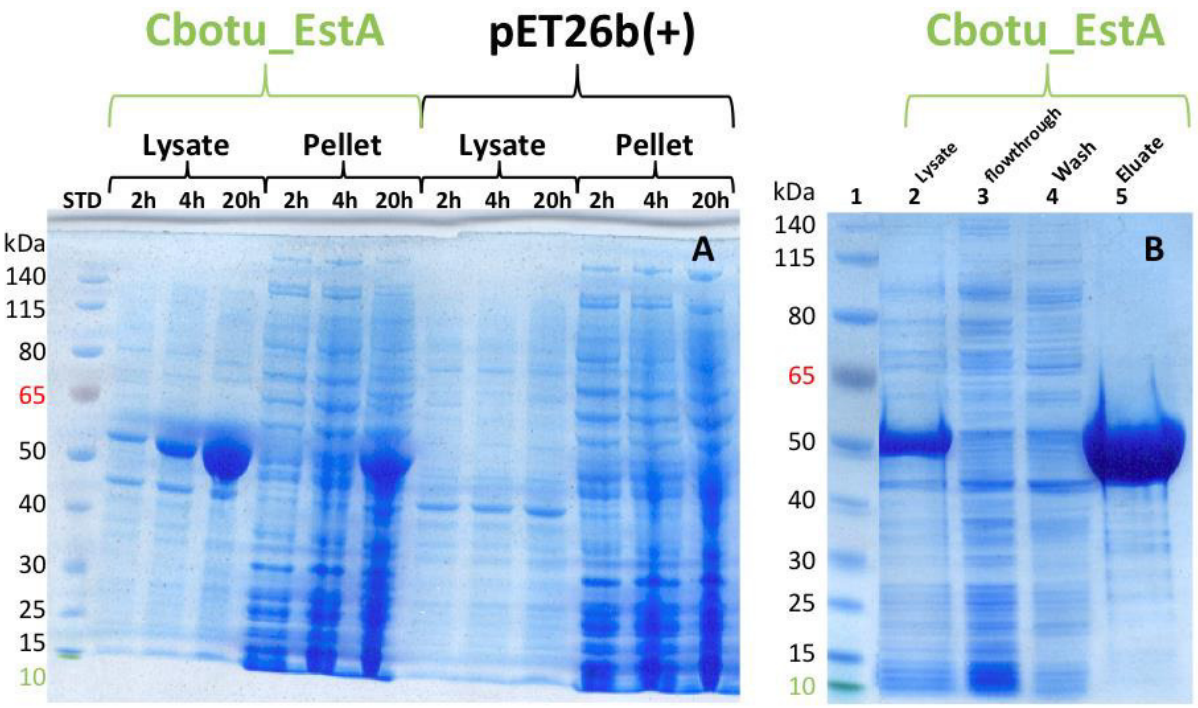

Figure S1. (A) Example of a typical expression profile of the heterologous gene Cbotu_EstA in *E. coli* BL21(DE3) at 20 °C and 150 rpm for 20 h after induction with 0.05 M IPTG. Shown are the lysates from samples that were withdrawn 2 , 4 h, and 20 h after induction with IPTG, as well as the pellets. As a control, *E. coli* BL21(DE3) containing the empty expression vector pET26b(+) was used. Sizes of the expression product Cbotu_EstA: 51.7 kDa. (B) SDS-PAGE analysis of Cbotu_EstA after HisTag purification. Samples were taken after 20 h of induction at 20 °C, centrifuged, disrupted and purified. Lane 1, standard (STD); lane 2, soluble cell lysate; lane 3, flowthrough; lane 4, eluate from washing step; lane 5, purified Cbotu_EstA. SDS-Gel used: NuPAGE® Tris-Acetate Mini Gels; STD, PageRuler® Prestained Protein Ladder.

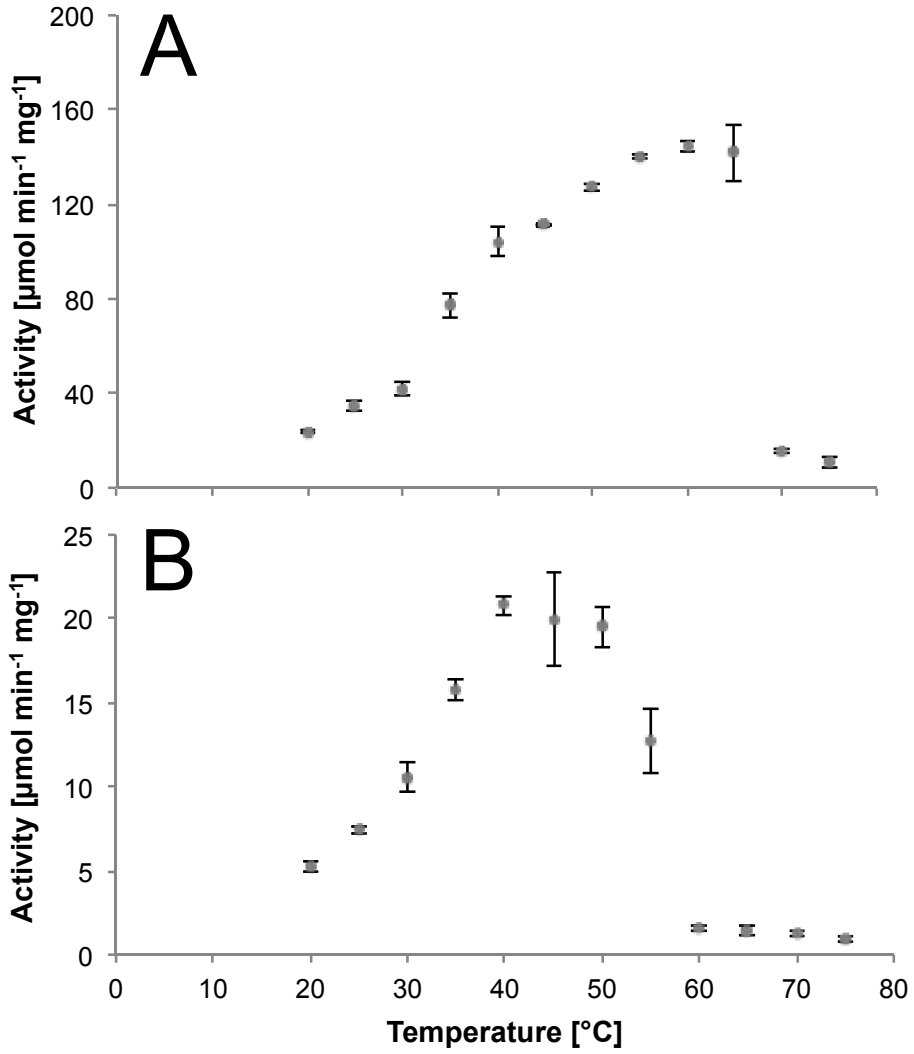

Figure S2. Effect oft the temperature on the specific activity of (A) Cbotu_EstA and (B) Cbotu_EstB in the presence of 7.9 mM *p*NPB in 50 mM potassium phosphate buffer pH 7.0. Each data point represents the average of three independent samples; error bars indicate the standard deviation.

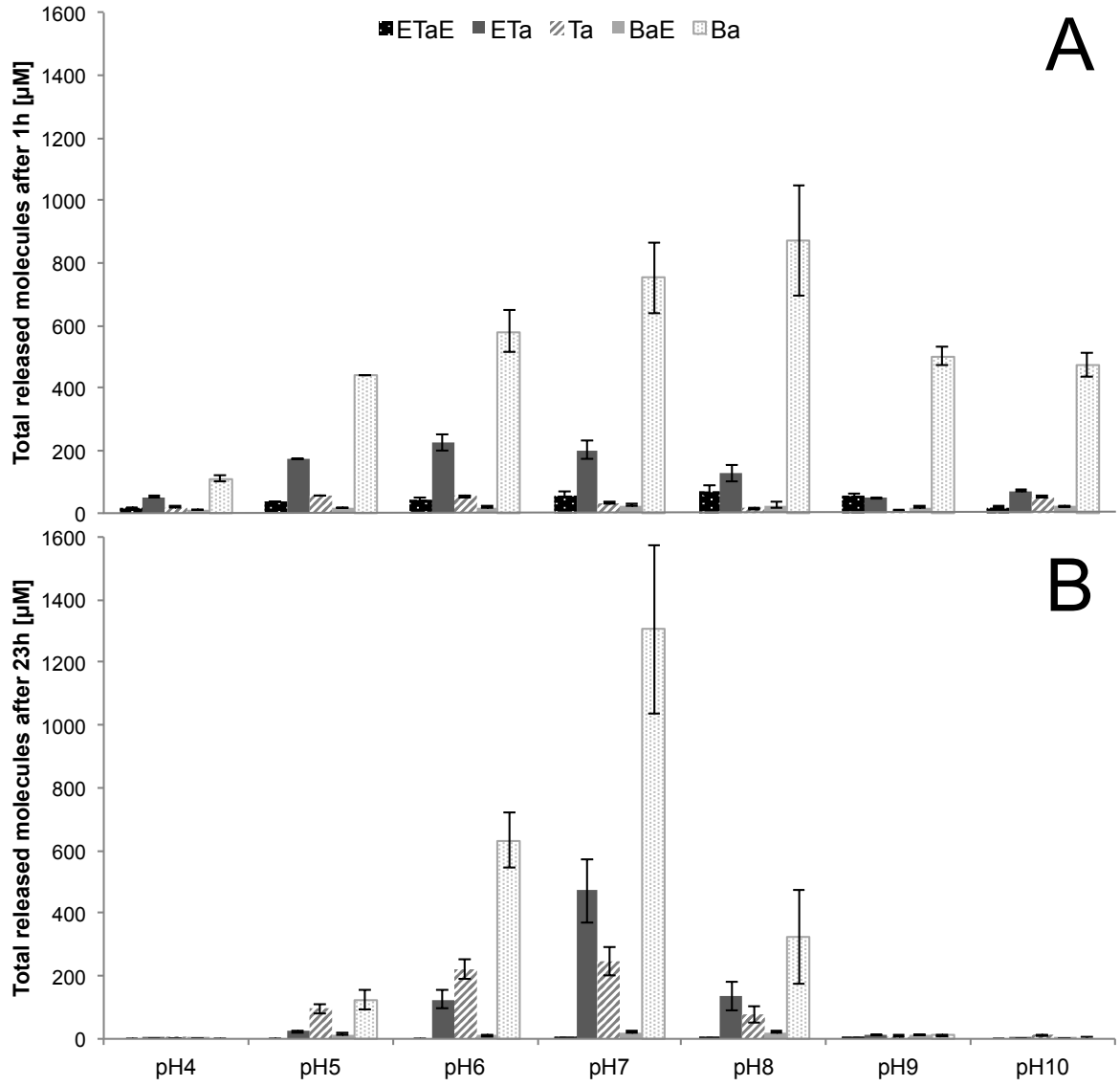

Figure S3. Determination of pH optima of the two *C. botulinum* esterases after incubation with the substrate BaETaEBa at different pHs. (**A**) Cbotu_EstA was incubated for 1 h at 50 °C. (**B**) Cbotu_EstB was incubated for 23 h at 37 °C. The release molecules ETaE: bis(2-hydroxyethyl) terephthalate, ETa: mono(2-hydroxyethyl) terephthalate, Ta: terephthalic acid, BaE: 2-hydroxyethyl benzoate and Ba: benzoic acid were quantified by means of HPLC analysis. Each bar represents the average of three independent samples; error bars indicate the standard deviation.

Table S1. Data collection and refinement statistic

X-ray source	ESRF-BM30A
Wavelength (Å)	0.9777
Temperature	100 K
Space group	$P2_1$
Cell dimensions	
a, *b*, *c* (Å)	51.24, 64.71, 69.79
α, β, γ (°)	90.0, 106.93, 90.0
Resolution (Å)	49.02-1.20 (1.26-1.20)
Unique reflections	121016
Multiplicity	4.9 (3.8)
Completeness (%)	88.6 (50.5)
R_{merge}	0.060 (0.410)
R_{meas}	0.066 (0.475)
R_{pim}	0.016 (0.234)
<I/sI>	13.0 (2.8)
R_{work} / R_{free}	0.1293/0.1493
No. of non-H atoms	
Protein	4005
Ions	3
Water	604
Average B-factors (Å^2)	
Protein	13.6
Ions	10.5
Water	25.5
R.m.s. deviations	
Bond lengths (Å)	0.008
Bond angles (°)	1.2
Ramachandran plot (% favored/allowed/outliers)	96.9/3.1/0.0

Article

pubs.acs.org/Biomac

Biomimetic Approach to Enhance Enzymatic Hydrolysis of the Synthetic Polyester Poly(1,4-butylene adipate): Fusing Binding Modules to Esterases

Veronika Perz,[†] Michael Thomas Zumstein,[‡] Michael Sander,[‡] Sabine Zitzenbacher,[§] Doris Ribitsch,*[,†,∥] and Georg M. Guebitz[†,∥]

[†]Austrian Centre of Industrial Biotechnology, ACIB, Konrad Lorenz Strasse 20, 3430 Tulln, Austria

[‡]Department of Environmental Systems Science, Institute of Biogeochemistry and Pollutant Dynamics, Swiss Federal Institute of Technology Zurich (ETHZ), Universitätstrasse 16, 8092 Zurich, Switzerland

[§]Austrian Centre of Industrial Biotechnology, ACIB, Petersgasse 14/V, 8010 Graz, Austria

[∥]Institute of Environmental Biotechnology, University of Natural Resources and Life Sciences, Vienna, Konrad Lorenz Strasse 20, 3430 Tulln, Austria

Supporting Information

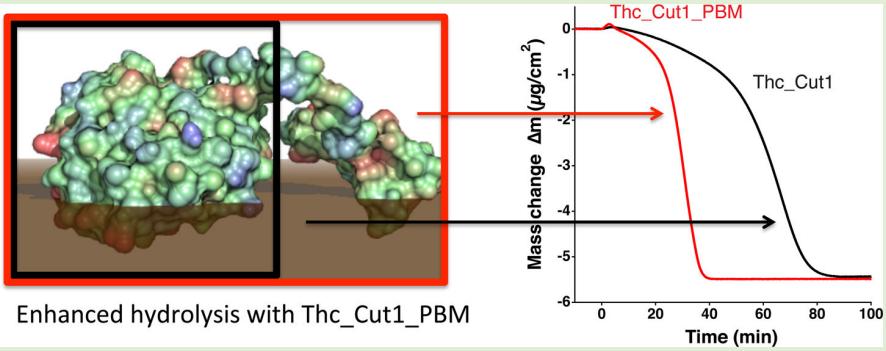

ABSTRACT: Mimicking a concept of nature for the hydrolysis of biopolymers, the *Thermobifida cellulosilytica* cutinase 1 (Thc_Cut1) was fused to a polymer binding module (PBM) to enhance the hydrolysis of the polyester poly(1,4-butylene adipate) (PBA). Namely, the binding module of a polyhydroxyalkanoate depolymerase from *Alcaligenes faecalis* (Thc_Cut1_PBM) was attached to the cutinase via two different linker sequences varying in length. In order to investigate the adsorption behavior, catalytically inactive mutants both of Thc_Cut1 and Thc_Cut1_PBM were successfully constructed by site-directed mutagenesis of serine 131 to alanine. Quartz crystal microbalance with dissipation monitoring (QCM-D) analysis revealed that the initial mass increase during enzyme adsorption was larger for the inactive enzymes linked with the PBM as compared to the enzyme without the PBM. The hydrolysis rates of PBA were significantly enhanced when incubated with the active, engineered Thc_Cut1_PBM as compared to the native Thc_Cut1. Thc_Cut1_PBM completely hydrolyzed PBA thin films on QCM-D sensors within approximately 40 min, whereas twice as much time was required for the complete hydrolysis by the native Thc_Cut1.

INTRODUCTION

The activity of enzymes toward synthetic polymers including aliphatic and aromatic polyesters has been the research focus of several studies in recent years. Not only the degradation of polyesters but also their surface modifications and functionalizations are of considerable interest, e.g., for applications in the textile or fiber industry.[1] For these applications, the hydrophilicity or reactivity of a polyester surface very often needs to be increased. As compared to harsher chemical methods, enzymes have been proven to be an environmentally benign and effective alternative to introduce new reactive groups for functionalization into synthetic polymers.[2−4] The class of hydrolases offers a broad spectrum of polyester active enzymes including cutinases, lipases, esterases, and cutinase-like enzymes from aerobic and anaerobic bacteria and fungi.[5−10] Polyesters that were enzymatically hydrolyzed so far include polyethylene terephthalate (PET), poly(butylene adipate-*co*-butylene terephthalate) (PBAT), polylactic acid (PLA),[11] poly(ε-caprolactone) (PCL),[12] polyhydroxyalkanoates (PHAs),[5,6,13] cutin,[14] poly(butylene succinate-*co*-butylene terephthalate) (PBST),[15] poly(butylene succinate) (PBS),[16] and poly(1,4-butylene adipate) (PBA).[9] A kinetic model was developed to describe the layer-

Received: September 10, 2015
Revised: November 10, 2015
Published: November 13, 2015

DOI: 10.1021/acs.biomac.5b01219
Biomacromolecules 2015, 16, 3889−3896

by-layer degradation of aromatic and aliphatic polyester nanoparticles by lipases from *Pseudomonas* sp. and *Candida cylindracea*.[7] Marten et al. examined the enzymatic polyester hydrolysis by lipases from *Pseudomonas species* and the parameters controlling aliphatic and aliphatic-aromatic polyester degradation.[16,17] Different polyesters, including foils made out of PET and PBAT, were reported to be hydrolyzed by a cutinase-like enzyme from *Saccharomonospora viridis*,[8,18] and the hydrolysis of PET by a nitrobenzylesterase from *Bacillus subtilis*[19] was studied mechanistically.

Cutinases seem to be the most effective enzymes for the hydrolysis of synthetic polyesters.[20] Cutinases from different species like *Humicola insolens*,[9,21] *Thermobifida halotolerans*,[11] *Thermobifida fusca*,[22,23] *Thermobifida alba*,[21] *Thermobifida cellulosilytica*,[24] and *Fusarium solani pisi*[3] have been shown to hydrolyze synthetic polyesters. Ronkvist et al.[25] demonstrated that the activity and stability of the cutinase at high temperatures is a crucial factor during PET hydrolysis when comparing cutinases from *Humicola insolens*, *Pseudomonas mendocina*, and *Fusarium solani*. Cutinases from thermophilic *Thermobifida* species like cutinase 1 from *Thermobifida cellulosilytica* (Thc_Cut1) show excellent thermal stabilities and activities between 50 and 60 °C which makes them promising candidates for polyester hydrolyses also at higher temperatures, at which polymers exhibit higher backbone flexibility and therefore higher accessibility of the ester bonds in the backbone to enzymatic hydrolysis.[16,26]

An alternative strategy to the identification of novel wild-type cutinases[27] or other hydrolytic enzymes with hydrolytic activities on synthetic polyesters[10,28] is to enhance the activity of known enzymes and, thereby, to broaden their application domain in possible industrial processes. Surface engineering[29] and active site mutagenesis[30,31] were performed to increase the hydrophobic character of certain enzyme regions and to enlarge the active site, respectively. These modifications of certain amino acids increased the turnover rates significantly compared to those of the wild-type cutinases. Obviously, adsorption to the polymer and interaction of the enzyme with the polymer surface are crucial steps during polyester hydrolysis. In this respect, surface properties, including the hydrophobicity of the cutinase, are of great importance.[24] The fusion of hydrophobins[32,33] or polymer binding modules (PBMs)[34−36] to the cutinases are two approaches to improve the adsorption of cutinases and, thereby, to enhance the hydrolytic activity toward polyesters.

Polymer binding modules found in nature are responsible for the coordinated adsorption and desorption of enzymes during hydrolysis processes. They are typically linked via a spacer to the catalytic domain of the enzymes, e.g., of cellulases.[37] Binding modules (often also referred to as binding domains) generally have affinities to certain polymers, such as PHAs,[38,39] xylan,[40] or cellulose.[37,41] There are two suggested mechanisms by which these binding modules enhance enzymatic polymer hydrolysis. First, the binding modules increase the concentration of active enzyme on the substrate surface.[40] Second, Din et al. reported that the cellulose binding domain from *Cellulomonas fimi* endoglucanase A is able to partially disrupt the polymer surface of highly crystalline cellulose, thereby facilitating substrate hydrolysis.[42,43] While there is evidence that the first mechanism applies to all carbohydrate binding modules, this does not seem to be the case for the second mechanism.[44] In this context, the specificity of binding modules to different polymers is of interest. Kasuya et al. showed that substrate binding domains of PHA depolymerases adsorbed to the surfaces of different PHAs, while no adsorption was observed to polysaccharide granules of chitin or Avicel.[38] Carrard et al. demonstrated that different cellulose binding domains attached to the same catalytic domain resulted in constructs that exhibited different abilities to hydrolyze crystalline cellulose.[45] These findings suggest that specific binding module−substrate interactions exist and that therefore binding modules need to be selected that match the targeted polymers.

Recently, we have shown that the addition of such polymer binding modules to a cutinase can enhance its hydrolytic activity on PET.[36] However, no such biomimetic approaches have been previously reported to improve enzymatic hydrolysis of synthetic aliphatic polyesters. In this study, we chose poly(1,4-butylene adipate) (PBA) as the model polymer for aliphatic polyesters, including poly(1,4-butylene succinate). We have fused the PBM from a polyhydroxyalkanoate depolymerase from *Alcaligenes faecalis*[36] to Thc_Cut1, tested for potential effects of the length of the linker used to fuse PBM onto Thc_Cut1, and assessed the hydrolytic activity of the native and modified Thc_Cut1 toward PBA by both hydrolysis product analysis and quartz crystal microbalance with dissipation monitoring (QCM-D) measurements that were optimized to derive molecular-level information on the mass changes and dissipation dynamics of PBA films during enzymatic hydrolysis. QCM-D is an *in situ* surface technique that allows one to monitor the adsorbed mass on a piezoelectric quartz crystal sensor with high sensitivity (1 ng/cm^2). It has previously been employed for *in situ* enzymatic hydrolysis studies of natural polymers including cellulose,[46] polyhydroxyalkanoates (PHA),[47] poly(lactic acid) (PLA),[48] and chitin.[49] This study is also the first to report the adsorption of inactive mutants of Thc_Cut1 and Thc_Cut1_PBM onto PBA films using QCM-D. Using the inactive mutants in QCM-D experiments allowed us to provide a detailed analysis of the adsorption/desorption characteristics of the cutinases with and without the binding domain.

MATERIALS AND METHODS

Granular PBA (melting point (T_m), 57.7 °C; glass transition temperature (T_g), −59 °C; number-average molecular weight (M_n), 19800 g/mol; weight-average molecular weight (M_w), 52100 g/mol); melting enthalpy (ΔH_m), 68.5 J/g) was kindly provided by BASF SE. All chemicals were of analytical grade and purchased from Sigma (Germany). Carrez reagent I and Carrez reagent II were prepared by dissolving 1.06 g of $K_4[Fe(CN)_6]\cdot 3H_2O$ or 2.88 g of $ZnSO_4\cdot 7H_2O$ in 10 mL of ddH_2O, respectively.

Cloning and Expression of Fusion Proteins. Constructions of fusion proteins were performed as described recently,[36] using the natural linker length in the engineering of Thc_Cut1_PBM and the linker twice for Thc_Cut1_2x_PBM. Expression was done at 20 °C for 21 h. The proteins were purified by affinity chromatography.[24]

Preparation of Inactive Mutants. Inactive mutants Thc_Cut1_S131A and Thc_Cut1_PBM_S131A were prepared using the QuikChange multi site-directed mutagenesis kit (Stratagene). To this end, plasmids pET26b(+)Thc_Cut1[24] and pET26b(+)Thc_Cut1_PBM[36] and megaprimers carrying the appropriate mutation were used for exchanging the catalytic serine 131 with alanine (see Supporting Information, Table S1). The PCR-products were transformed in *E. coli* BL21-Gold(DE3). Expression and purification was performed as described previously.[24]

Stability of Thc_Cut1 and Thc_Cut1_PBM. The enzyme stability was determined by incubating the purified Thc_Cut1 and Thc_Cut1_PBM at a concentration of 1 $mg_{cutinase}$/mL in 100 mM Tris

DOI: 10.1021/acs.biomac.5b01219
Biomacromolecules 2015, 16, 3889−3896

HCl buffer (pH 7.0) on a temperature-controlled horizontal shaker (20 °C; 150 rpm). The initial specific activity was measured (time point 0) using the soluble standard substrates *para*-nitrophenyl butyrate (*p*NPB) in 50 mM potassium phosphate buffer at pH 7.0 and *para*-nitrophenyl acetate (*p*NPA) in 50 mM Tris HCl buffer at pH 7.0 at substrate concentrations of 10.55 mM and 8.26 mM, respectively. The increase of absorbance of *para*-nitrophenol ($\varepsilon_{405\text{ nm potassium phosphate}}$ = 9.36 L $mol^{-1}cm^{-1}$; $\varepsilon_{405\text{ nm TrisHCl}}$ = 9.03 L $mol^{-1}cm^{-1}$) at 405 nm was followed on a Eon BioTek microplate spectrophotometer (BioTek Instruments, Winooski, USA). The change in esterase activity over time was determined by measuring substrate conversion after 1 h, 2 h, 5 h, 24 h, and 48 h of incubation.

HPLC Quantification of Adipic Acid Released from PBA by Cutinase Variants. Thc_Cut1 and Thc_Cut1_PBM, as well as the inactive mutants Thc_Cut1_S131A and Thc_Cut1_PBM_S131A, were tested for their ability to hydrolyze PBA. Generally, 2 mL of 0.06 μM buffered enzyme solution was incubated with 10 mg of milled PBA (particle size between 100 and 300 μm). Incubations of PBA with the Thc_Cut1 variants were performed for 1 h, 2 h, and 5 h at 150 rpm and 20 °C in 100 mM potassium phosphate buffer at pH 7.0.

Prior to HPLC analysis of the hydrolysis product adipic acid (Ada), a modified Carrez precipitation[50,51] was performed to remove interfering substances from the sample matrix. The reactions were stopped by combining 100 μL of sample with 860 μL of ddH_2O and 20 μL of Carrez reagent I, and the pH was adjusted to 5.0 using 6 N HCl. The mixture was vortexed and incubated for 1 min at 20 °C. Then, 20 μL of Carrez reagent II were added, the mixture was vortexed again, and precipitation was performed for 20 min at 20 °C. The samples were centrifuged (13.000 rpm, 30 min, 20 °C) using Centrifuge 5414D from Eppendorf (Germany). Finally, supernatants were filtered using 45 μm nylon filters and analyzed via HPLC-RI.

HPLC-RI Analysis of Hydrolysis Products. HPLC analysis was carried out on a HPLC system consisting of an HP/Agilent 1100 Series Iso Pump G1310A (Agilent Technologies, Santa Clara, USA), an HP/Agilent 1100 Series ALS G1313A automated sample injector, and an HP/Agilent 1100 Series G1316A thermostatic column compartment. HPLC separation was carried out using a ICSep ION-300, 7 μm, 7.8 mm × 300 mm column with a precolumn (Transgenomic, Inc., Omaha, USA). Samples were eluted from the column using 0.01 N H_2SO_4 as eluent. The flow rate was set to 0.325 mL min^{-1}, and the column compartment was maintained at 45 °C. The injection volume was 40 μL. Detection of Ada was performed using the refractive index detector RID G1382A from HP/Agilent.

Enzyme Adsorption and PBA Hydrolysis Experiments Using QCM-D. The formations of PBA thin films and the subsequent enzymatic PBA hydrolysis experiments were performed in several steps. In brief, PBA was dissolved in chloroform (0.5%(w/w)) and spin coated onto a gold-coated QCM-D sensor (QSX 301, QSense or 201401 Cr/Au, Microvacuum Ltd.) using a spin coater (WS-650MZ-23NPP, Laurell Technologies). The sensor was spun at 4000 rpm for 1 min (acceleration: 1500 rpm/s). After air-drying, spin-coated sensors were incubated in buffered solutions (pH 7.0, 3 mM tris-(hydroxymethyl)-aminomethane and 10 mM KCl) for 14 h at 25 °C. The sensors were subsequently mounted onto four separate flow cells of a QCM-D E4 system (Q-Sense), and an enzyme-free buffer solution (pH 7.0, same buffer as above) was run over the sensors (volumetric flow rate: 20 μL/min) until stable readings for the resonance frequency, Δf_n (Hz), and the corresponding energy dissipation values, ΔD_n, were obtained for the fundamental frequency (n = 1) and several overtones (n = 3 to 11; in odd numbers) of the oscillation. The data from the fifth overtone (n = 5) was used for data analysis. A cutinase-containing solution of the same pH and ionic composition was subsequently delivered over the sensors at the same volumetric flow rate. Changes in Δf_n and ΔD_n values were continuously monitored. When these values had leveled off, the sensors were removed from the flow cells, rinsed with Milli-Q water, and dried in a stream of N_2. Changes in the areal adlayer mass density, Δm (ng/cm^2), during the enzymatic hydrolysis were calculated from the measured Δf_n using the Sauerbrey equation:

$$\Delta m = C \times -\frac{\Delta f_n}{n} \quad (1)$$

where C (17.7 ng·cm^{-2}·Hz^{1-}) is the sensor-specific mass sensitivity constant, and Δf_n (Hz) is the frequency shift of the nth overtone.

To assess the masses of PBA coated on each sensor and the fraction of the coated mass that was removed, the resonance frequency of each sensor was measured in air after drying (i) prior to the PBA coating step, (ii) after the PBA coating step, and (iii) after the enzymatic hydrolysis. In between independent hydrolysis experiments, QCM-D sensors were cleaned as detailed by Armanious et al.[52]

RESULTS AND DISCUSSION

Effect of Linker Length on the Activity of Thc_Cut1_PDB Fusion Enzymes. The effect of binding sequences on enzymatic hydrolysis of PBA was investigated. In a first step, the effect of the linker length between Thc_Cut1 and the PBM from the polyhydroxyalkanoate depolymerase of *Alcaligenes faecalis* was investigated. The functions of linkers in recombinant fusion proteins are to covalently join functional domains (here a PBM) to the enzyme while ensuring an appropriate distance between the enzyme and the added domain to minimize potential interferences and to allow maximum flexibility of the catalytic domain, to restore or improve folding, or to allow for the *in vivo* release of the free protein drug domain to ultimately improve bioactivity.[53] For this reason, Thc_Cut1 was fused in two different ways over the natural linker region of cellobiohydrolase I from *Hypocrea jecorina* (CBH I) to the PBM. First, the natural linker consisting of 24 amino acids was used yielding Thc_Cut1_PBM. Additionally, a longer linker region was prepared using the natural linker of CBH I twice (Thc_Cut1_2x_PBM) in order to attain a higher flexibility of the functional domain on the polymer. Expression in *E. coli* BL21-Gold(DE3) resulted in comparable amounts of soluble protein for Thc_Cut1 and Thc_Cut1_PBM but only very low amounts of Thc_Cut1_2x_PBM (Figure S1). Both fusion proteins were purified from cleared lysates and their activities were tested on an insoluble polymeric substrate as previously described.[36] Independent of the linker length, both constructs showed the same activities on the polymer and significantly higher activities compared to the native Thc_Cut1 (shown in Figure S2). While increasing the linker length strongly decreased the solubility of the engineered protein under the chosen assay conditions (Figure S1), the longer linker length did not seem to largely increase the activity on the polymer. Hence, because it was expressed in higher yields, the fusion protein with the natural linker length (i.e., Thc_Cut1_PBM) was further used in this study.

Stability of Thc_Cut1 and Thc_Cut1_PBM. Under the given experimental conditions (i.e., 20 °C, 150 rpm, and 100 mM Tris HCl buffer at pH 7.0), no significant decreases in the hydrolytic activities of Thc_Cut1 and Thc_Cut1_PBM on the soluble substrates *p*NPA and *p*NPB were detected over the entire tested incubation time (i.e., 48 h).

HPLC Quantification of Adipic Acid Released from PBA by Cutinase Variants. The hydrolytic activities of the different Thc_Cut1 variants (i.e., the active and inactive variants of both the native Thc_Cut1 and the engineered ThC_Cut1_PBM) toward milled PBA were tested by incubating the respective enzymes with PBA for 1, 2, and 5 h (Figure 1) in buffered solutions. In the presence of inactive mutants Thc_Cut1_S131A and Thc_Cut1_PBM_S131A, no Ada was released from PBA. This finding confirms that active

DOI: 10.1021/acs.biomac.5b01219
Biomacromolecules 2015, 16, 3889−3896

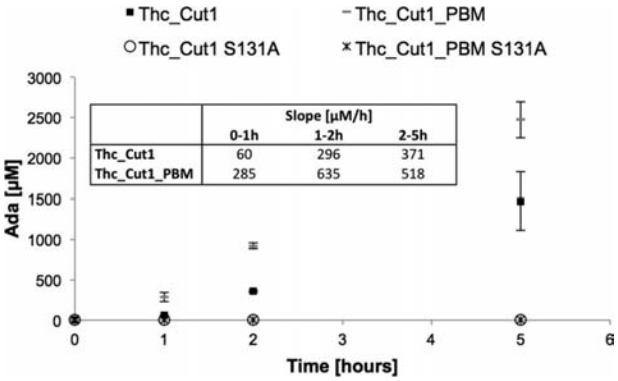

Figure 1. Adipic acid (Ada) released upon hydrolysis of poly(1,4-butylene adipate) (PBA) with 0.06 μM of different catalytically active and inactive (S131A) cutinase (Thc_Cut1) variants with and without the polymer binding modules (PBM). Each data point represents the average of three independent samples; error bars indicate the standard deviation.

site mutagenesis inactivated the enzyme. Incubations with the engineered Thc_Cut1_PBM resulted in significantly larger amounts of released Ada as compared to incubations with the native Thc_Cut1. Interestingly, this enhancement in Ada release was more pronounced in the first phase of the hydrolysis as indicated by the different hydrolysis rates (slopes in inlet of Figure 1): while the extent of PBA hydrolysis by Thc_Cut1_PBM was almost five times higher than that by Thc_Cut1 over the first hour of incubation, the concentration of released Ada after 5 h in systems containing Thc_Cut1_PBM was only 1.7-fold higher than that in systems containing Thc_Cut1. HPLC quantification of released Ada after 5 h revealed that 6.9 ± 1.7% (mean ± standard deviation, n = 3) and 11.7 ± 1,1% (mean ± standard deviation, n = 3) of the Ada present in the tested PBA polymer were hydrolytically liberated by Thc_Cut1 and Thc_Cut1_PBM, respectively.

The release kinetics of Ada from PBA suggests that there was a lag phase of approximately 1 h in the hydrolysis of PBA by Thc_Cut1, whereas no such lag phase was observed for Thc_Cut1_PBM. It is conceivable that the lag phase for Thc_Cut1 reflected delayed adsorption of this variant onto the PBA polymer surface. This explanation is supported by the observation of a similar lag phase during hydrolysis by Thc_Cut1 in the QCM-D measurements (see Figure 2a). Moreover, a detailed analysis of the adsorption characteristics of the inactive mutants Thc_Cut1_S131A and Thc_Cut1_PBM_S131A revealed that the initial increase in adsorbed cutinase mass was higher for the inactive cutinase with a binding domain as compared to the inactive cutinase without a binding domain (Figure 3). These findings strongly suggest that more efficient adsorption of the active cutinase linked to the binding domain to the PBA surfaces facilitates initial PBA hydrolysis.

PBA Thin Film Hydrolysis Investigated by QCM-D. To complement the finding that fusing a PBM to Thc_Cut1 increased the amount of adipic acid released into the solution and hence enhanced the hydrolysis of PBA, we made use of a QCM-D based approach to study enzymatic polyester hydrolysis. Figure 2 shows the results of a representative experiment, in which the hydrolysis dynamics of spin-coated PBA thin films by Thc_Cut1 and Thc_Cut1_PBM were studied at pH 7.0 and 20 °C.

The constant masses measured for times t < 0 min, when enzyme-free pH-buffered solution was delivered to the flow cell, demonstrated that there was little (if any) nonenzymatic hydrolysis of PBA in the absence of active cutinase (Figure 2a). Starting at time t = 0 min, Thc_Cut1 and Thc_Cut1_PBM containing solutions were continuously delivered to the flow cells. Immediately following the switch from enzyme-free to enzyme-containing solutions, subtle mass increases were measured, reflecting the adsorption of cutinase molecules to the PBA film surfaces. Subsequently, the sensed masses decreased. These mass decreases were ascribed to the hydrolytic cleavage of ester bonds in PBA, resulting in the

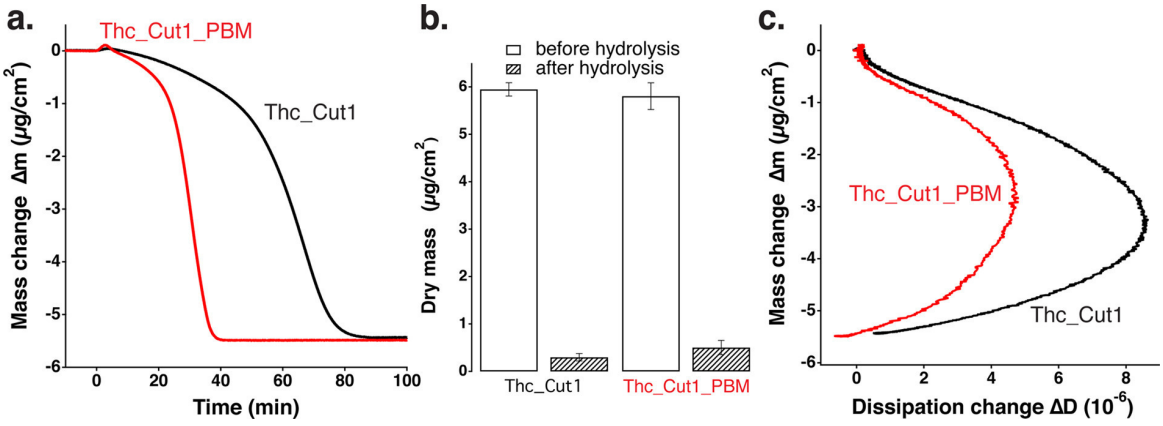

Figure 2. Changes in the masses and viscoelastic properties of poly(1,4-butylene adipate) (PBA) thin films during hydrolysis by cutinase 1 of *Thermobifida cellulosilytica* (Thc_Cut1, black curves) and the same cutinase fused to a polymer binding module (Thc_Cut1_PBM, red curves), as detected using QCM-D. Experiments were conducted at 20 °C and pH 7.0 under constant volumetric flow rates (= 20 μL min^{-1}) of cutinase solutions (equimolar concentrations of 59.4 nM). (a) Changes of the thin film masses over time during film equilibration (t < 0 min) and during the delivery of enzyme-containing solutions to the flow cells (t > 0 min). (b) Masses of the adlayers on the sensors before (open bars) and after (hatched bars) the hydrolysis experiments, determined by QCM-D measurements of the dried sensors in air. Error bars represent standard deviations of triplicate experiments. (c) Changes in the masses of the adlayers during the experiment versus changes in the energy dissipation of the adlayers. The data are from the same experiments that are shown in panel a.

DOI: 10.1021/acs.biomac.5b01219
Biomacromolecules 2015, 16, 3889−3896

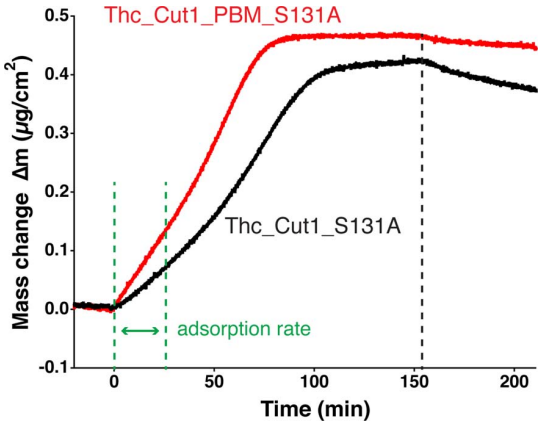

Figure 3. Changes in the adlayer masses over time during the adsorption of an inactive mutant of the cutinase of *Thermobifida cellulosilytica* (Thc_Cut1_S131A, black curves) and the same inactive cutinase fused to a polymer binding module (Thc_Cut1_PBM_S131A, red curves) onto poly(1,4-butylene adipate) (PBA) films, as detected by QCM-D. Experiments were conducted at 20 °C and pH 7.0 under a constant volumetric flow rate (= 20 μL·min^{-1}) and from cutinase solutions of identical nominal concentrations (59.4 nM). Time zero indicates the time point at which enzyme-containing solutions were delivered to the flow cells. The vertical dashed green lines enclose the time frame over which the changes in adsorbed masses versus time were fitted to obtain initial adsorption rates. The vertical dashed black line indicates the time point at which the adlayers were rinsed with enzyme-free buffers of the same pH.

release of soluble oligomeric and/or monomeric hydrolysis products from the film into the solutions. Finally, stable mass readings were obtained after 40 and 85 min for Thc_Cut1_PBM and Thc_Cut1, respectively, indicating that the sensor surfaces were depleted of hydrolyzable PBA.

To investigate the extents of hydrolysis, we used QCM-D to measure the dry masses of the sensors before and after the hydrolysis experiments in air. These measurements showed that 95.0 ± 1.4% (mean ± standard deviation, n = 3) and 87 ± 8% (mean ± standard deviation, n = 3) of the initial PBA film masses were lost from the QCM-D sensors during hydrolyses by Thc_Cut1 and Thc_Cut1_PBM, respectively (Figure 2b). The finding of mass removals slightly smaller than 100% likely resulted from positive mass contributions of Thc_Cut1 and Thc_Cut1_PBM that adsorbed to the gold surface of the QCM-D sensors after the PBA films were hydrolytically removed. The QCM-D experiments therefore demonstrate that PBA thin films were extensively (if not completely) hydrolyzed by both cutinases.

Figure 2c shows that the adlayer energy dissipation values were highest when the two cutinases had removed approximately half of the adlayer masses, demonstrating that the adlayers progressed through soft intermediate states during the hydrolysis. The maximum attained dissipation values were larger during the hydrolysis of PBA by Thc_Cut1 (i.e., 9.0 (±1.4)·10^{-6}), as compared to Thc_Cut1_PBM (5.3 ± (1.0)·10^{-6}).

To assess the kinetics of PBA film hydrolysis by the two enzymes, we compared the times required for the films to reach their most dissipative intermediate states. These times were 65 ± 13 min and 36 ± 6 min for Thc_Cut1 and Thc_Cut1_PBM, respectively, confirming that fusing the PBM to Thc_Cut1 leads to faster PBA hydrolysis as compared to the native variant. The time required for complete film hydrolysis was also shorter when using Thc_Cut1_PBM as compared to Thc_Cut1.

We used the inactive mutants of the native and engineered cutinases (i.e., Thc_Cut1_S131A and Thc_Cut1_PBM_S131A) to selectively study changes in the adsorption characteristics of Thc_Cut1 that resulted from fusing the PBM to the enzyme (i.e., mass and dissipation dynamics resulting from the adsorption of the inactive mutants were not compromised by PBA hydrolysis dynamics). Figure 3 shows the changes in the adlayer masses during the adsorption of the two inactive cutinase variants onto the PBA films. The initial rates by which adsorbed masses increased, obtained from linear fits of the mass increases over time between 0 and 25 min (indicated by vertical green dashed lines), were 3.2 ± 0.7 ng·cm^{-2}·min^{-1} (mean ± standard deviation, n = 5) and 5.0 ± 0.5 ng·cm^{-2}·min^{-1} (mean ± standard deviation, n = 3) for the inactive Thc_Cut1_S131A and the inactive Thc_Cut1_PBM_S131A, respectively. The higher initial rates at which adsorbed masses increased for Thc_Cut1_PBM_S131A supports the fact that the presence of the PBM enhanced the adsorption of the cutinase to PBA film surfaces.

After the initial phase, adsorption rates decreased and the adsorbed masses plateaued, suggesting that the enzymes had occupied all adsorption sites on the PBA surfaces (i.e., attainment of the surface jamming limits). This explanation is supported by a very good agreement between the experimentally measured final adsorbed masses and the predicted final masses for a monolayer of Thc_Cut1, as detailed in the Supporting Information. Upon rinsing these surfaces with enzyme-free solutions for 50 min, 12.1 ± 2.0 mass % (mean ± standard deviation, n = 5) and 3.0 ± 1.2 mass % (mean ± standard deviation, n = 3) of the adsorbed Thc_Cut1_S131A and Thc_Cut1_PBM_S131A, respectively, were removed from the PBA thin films. The adsorption of both enzymes was therefore highly irreversible. However, the smaller decrease in adsorbed mass detected for the cutinase with the PBM supported the fact that it enhanced the affinity of the enzyme to the PBA film.

To investigate the effect of the PBM on the replacement of cutinase from the PBA film surfaces, we adsorbed the inactive cutinase variants with and without PBM onto PBA films (phase I, Figure 4a). After surface saturation by the inactive cutinases, we replaced the initial inactive enzyme solutions with enzyme-free buffer for 50 min to remove all nonadsorbed inactive cutinases. Subsequently, solutions containing the active cutinase variants with and without PBM were delivered to the flow cells (phase II, starting at 210 min).

Figure 4a shows that the PBA films onto which the inactive variant of the enzyme (i.e., Thc_Cut1_S131A) was adsorbed during phase I (black and green traces) were quickly and completely hydrolyzed by both active cutinase variants (i.e., Thc_Cut1 and Thc_Cut1_PBM) during phase II. However, when delivering both active enzymes variants to the films with preadsorbed inactive cutinase containing PBM (i.e., Thc_Cut1_PBM_S131A; blue and red traces), the mass losses that resulted from PBA hydrolysis were delayed. Also, the mass losses slowed down for both active cutinase variants after approximately half of the polyester films were removed from the sensors (Figure 4a and b).

Furthermore, following the adsorption of inactive cutinase variants lacking the PBM in phase I, the hydrolysis of the PBA

DOI: 10.1021/acs.biomac.5b01219
Biomacromolecules 2015, 16, 3889−3896

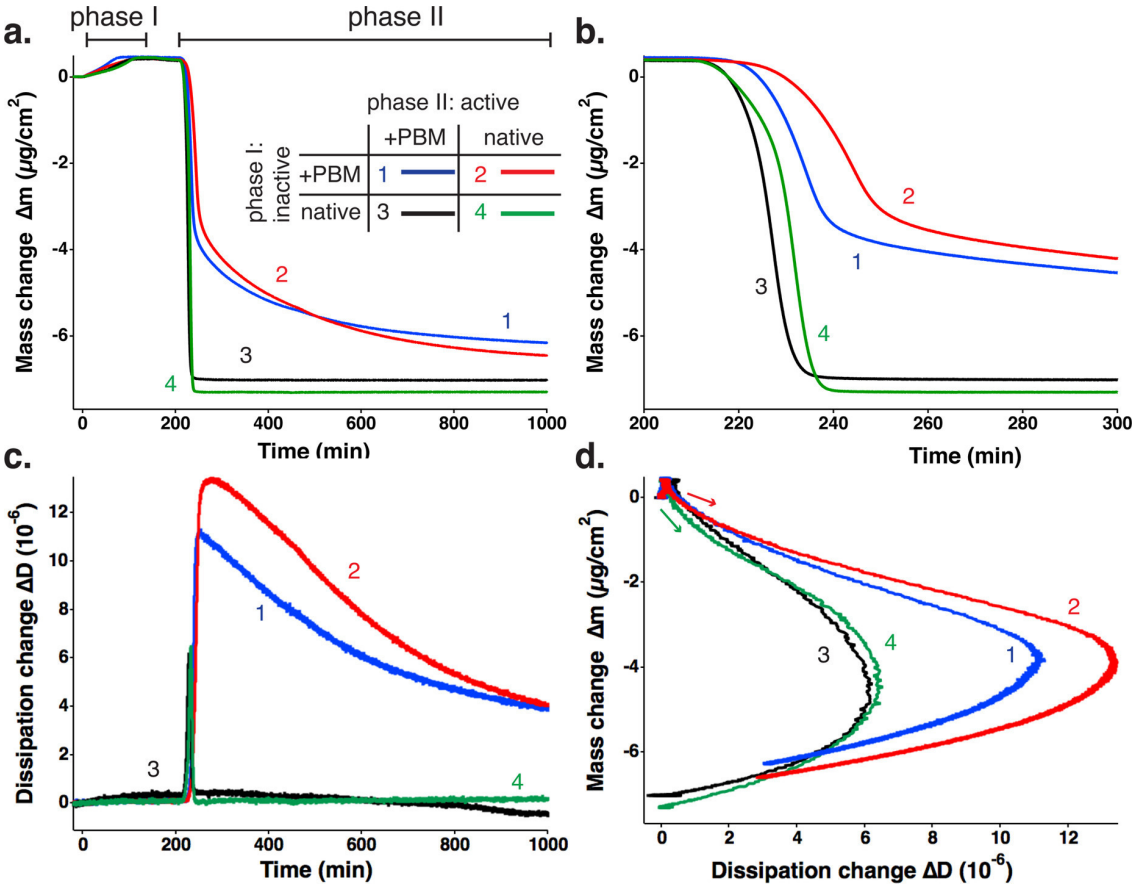

Figure 4. Hydrolysis experiments of poly(1,4-butylene adipate) (PBA) thin films by active variants of the cutinase of *Thermobifida cellulosilytica* (Thc_Cut1 (without polymer binding module (PMB) and Thc_Cut1_PBM (with PMB)) after preadsorbing the inactive variants of the same enzyme (Thc_Cut1_S131A, Thc_Cut1_PBM_S131A) onto the PBA films, as investigated by QCM-D. Panels a–d show different representations of the same hydrolysis experiments performed at 20 °C and pH 7.0. During phase I (0–160 min), solutions containing inactive cutinase variants were delivered to the PBA film surfaces at volumetric flow rates of 20 μL min^{-1}. During phase II (210–1000 min), solutions containing the active cutinase variants were delivered at the same volumetric flow rates. Between phases I and II, enzyme-free solutions were delivered at the same volumetric flow rates to remove nonadsorbed enzymes. The color and number codes shown in panel a specify the different combinations in which inactive/active cutinase variants were delivered. These codes apply to all panels. (a) Mass changes of the thin PBA films over time. (b) Zoomed in view of data shown in panel a. (c) Changes in energy dissipation values of the PBA films over time. (d) Changes in the film masses plotted versus changes in the energy dissipation values of the films. Arrows highlight the initial slopes of Δm versus ΔD.

by both active cutinase variants rapidly progressed through soft film intermediates to final states characterized by low dissipation values and low adsorbed masses (green and black traces in Figure 4c and d). However, when the inactive mutant with PBM was preadsorbed to the PBA films in phase I, the subsequent delivery of both active enzyme variants resulted in more dissipative, soft PBA film intermediates that were subsequently only slowly hydrolyzed. In these cases, hydrolysis was incomplete at the end of the experiments. These findings suggest that the inactive enzyme variant fused to the PBM that was preadsorbed in phase I remained associated with the films throughout phase II, consistent with the enhanced affinity of enzymes containing PBM to PBA.

Figure 4d shows that the hydrolysis of PBA by both active cutinase variants formed more dissipative films on a per mass loss basis when inactive cutinases containing the PBM were preadsorbed to the PBA in phase I, compared to the films obtained after preadsorbing inactive cutinases without PBM (also evidenced from the different slopes of $\Delta m/\Delta D$ indicated by the green and red arrows).

In summary, this experiment showed that preadsorbing inactive, PBM-containing, Thc_Cut1 onto a PBA film significantly altered the kinetics and dynamics of the subsequent Thc_Cut1-mediated hydrolysis of the PBA. Conversely, hydrolysis of the PBA by the active enzyme variants after preadsorption of inactive Thc_Cut1 without PBM were comparable to the hydrolysis measured without the preadsorption phase (comparison of Figures 2a and 4b). These findings suggest that the active enzyme variants delivered in phase II quickly replaced the inactive enzyme variant without PBM. It is possible that the preadsorbed inactive PBM-containing Thc_Cut1 irreversibly block parts of the PBA film surfaces, leading to film hydrolysis dynamics with a more pronounced vertical to horizontal erosion as compared to the system in which inactive cutinases without PBA were preadsorbed.

CONCLUSIONS

We successfully demonstrated that fusing the polymer binding module from polyhydroxyalkanoate depolymerase from *Alcali-*

DOI: 10.1021/acs.biomac.5b01219
Biomacromolecules 2015, 16, 3889–3896

genes faecalis to cutinase 1 from *Thermobifida cellulosilytica* enhanced the rate at which it hydrolyzed the polyester PBA as compared to the native Thc_Cut1. The enhancement was demonstrated by larger amounts of adipic acid monomers released from PBA, as quantified by HPLC analysis, as well as by the mass losses from thin PBA films determined by QCM-D measurements. QCM-D measurements with the inactive cutinase variants support the fact that fusion with PBM increased the affinity of the cutinase to the PBA films. In a larger context, this work highlights that the biomimetic approach of fusing binding modules to enzymes is a powerful approach to improve the efficiency and target orientation of enzymes in industrial applications of both polymer hydrolysis and surface functionalization.

■ ASSOCIATED CONTENT

Supporting Information

The Supporting Information is available free of charge on the ACS Publications website at DOI: 10.1021/acs.biomac.5b01219.

Primer sequences for site-directed mutagenesis, SDS−PAGE analysis, HPLC analysis, and prediction of monolayer adsorbed masses of Thc_Cut1 (PDF)

■ AUTHOR INFORMATION

Corresponding Author

*Phone: +43 1 47654 4974. E-mail: doris.ribitsch@acib.at.

Notes

The authors declare no competing financial interest.

■ ACKNOWLEDGMENTS

This work has been supported by the Federal Ministry of Science, Research and Economy (BMWFW), the Federal Ministry of Traffic, Innovation and Technology (bmvit), the Styrian Business Promotion Agency SFG, the Standortagentur Tirol, the Government of Lower Austria, and ZIT - Technology Agency of the City of Vienna through the COMET-Funding Program managed by the Austrian Research Promotion Agency. FFG., M.Z., and M.S. thank the Joint Research Network on Advanced Materials and Systems (JONAS) program of BASF SE and ETH Zurich for financial support.

■ REFERENCES

(1) Karmakar, S. R. *Chemical Technology in the Pretreatment Processes of Textiles*; Elsevier: Amsterdam, 1999; Vol. *12*.

(2) Brueckner, T.; Eberl, A.; Heumann, S.; Rabe, M.; Guebitz, G. M. Enzymatic and Chemical Hydrolysis of Poly(ethylene terephthalate) Fabrics. *J. Polym. Sci., Part A: Polym. Chem.* **2008**, *46*, 6435−6443. Brueckner, T.; Eberl, A.; Heumann, S.; Rabe, M.; Guebitz, G. M. Enzymatic and Chemical Hydrolysis of Poly(ethylene terephthalate) Fabrics. *Journal of Polymer Science Part A: Polymer Chemistry* **2008**, *46*, 6435−6443.

(3) Donelli, I.; Freddi, G.; Nierstrasz, V. A.; Taddei, P. Surface structure and properties of poly-(ethylene terephthalate) hydrolyzed by alkali and cutinase. *Polym. Degrad. Stab.* **2010**, *95* (9), 1542−1550.

(4) Wei, R.; Oeser, T.; Zimmermann, W. Synthetic polyester-hydrolyzing enzymes from thermophilic actinomycetes. *Adv. Appl. Microbiol.* **2014**, *89*, 267−305.

(5) Ihssen, J.; Magnani, D.; Thoeny-Meyer, L.; Ren, Q. Use of Extracellular Medium Chain Length Polyhydroxyalkanoate Depolymerase for Targeted Binding of Proteins to Artificial Poly[(3-hydroxyoctanoate)-co-(3-hydroxyhexanoate)] Granules. *Biomacromolecules* **2009**, *10* (7), 1854−1864.

(6) Jaeger, K. E.; Steinbüchel, A.; Jendrossek, D. Substrate specificities of bacterial polyhydroxyalkanoate depolymerases and lipases: bacterial lipases hydrolyze poly(omega-hydroxyalkanoates). *Appl. Environ. Microbiol.* **1995**, *61* (8), 3113−3118.

(7) Herzog, K.; Mueller, R. J.; Deckwer, W. D. Mechanism and kinetics of the enzymatic hydrolysis of polyester nanoparticles by lipases. *Polym. Degrad. Stab.* **2006**, *91* (10), 2486−2498.

(8) Kawai, F.; Oda, M.; Tamashiro, T.; Waku, T.; Tanaka, N.; Yamamoto, M.; Mizushima, H.; Miyakawa, T.; Tanokura, M. A novel Ca2+-activated, thermostabilized polyesterase capable of hydrolyzing polyethylene terephthalate from Saccharomonospora viridis AHK190. *Appl. Microbiol. Biotechnol.* **2014**, *98* (24), 10053−10064.

(9) Perz, V.; Bleymaier, K.; Sinkel, C.; Kueper, U.; Bonnekessel, M.; Ribitsch, D.; Guebitz, G. M. Substrate specificities of cutinases on aliphatic-aromatic polyesters and on their model substrates. *New Biotechnol.* **2015**, in press.

(10) Perz, V.; Baumschlager, A.; Bleymaier, K.; Zitzenbacher, S.; Hromic, A.; Steinkellner, G.; Pairitsch, A.; Lyskowski, A.; Gruber, K.; Sinkel, C.; Kueper, U.; Ribitsch, D.; Guebitz, G. M., Hydrolysis of synthetic polyesters by *Clostridium botulinum* esterases. *Biotechnol. Bioeng.* **2015**, in press. DOI: 10.1002/bit.25874.

(11) Ribitsch, D.; Herrero Acero, E.; Greimel, K.; Dellacher, A.; Zitzenbacher, S.; Marold, A.; Diaz Rodriguez, R.; Schwab, H.; Guebitz, G. M. A new esterase from Thermobifida halotolerans hydrolyses PET and PLA. *Polymers* **2012**, *4* (1), 617−629.

(12) Murphy, C. A.; Cameron, J. A.; Huang, S. J.; Vinopal, R. T. Fusarium polycaprolactone depolymerase is cutinase. *Appl. Environ. Microbiol.* **1996**, *62* (2), 456−60.

(13) Schirmer, A.; Jendrossek, D.; Schlegel, H. G. Degradation of poly(3-hydroxyoctanoic acid) [P(3HO)] by bacteria: purification and properties of a P(3HO) depolymerase from Pseudomonas fluorescens GK13. *Appl. Environ. Microbiol.* **1993**, *59* (4), 1220−7.

(14) Korpecka, J.; Heumann, S.; Billig, S.; Zimmermann, W.; Zinn, M.; Ihssen, J.; Cavaco-Paulo, A.; Guebitz, G. M. Hydrolysis of Cutin by PET-Hydrolases. *Macromol. Symp.* **2010**, *296* (1), 342−346.

(15) Honda, N.; Taniguchi, I.; Miyamoto, M.; Kimura, Y. Reaction Mechanism of Enzymatic Degradation of Poly(butylene succinate-co-terephthalate) (PBST) with a Lipase Originated from Pseudomonas cepacia. *Macromol. Biosci.* **2003**, *3* (3−4), 189−197.

(16) Marten, E.; Müller, R.-J.; Deckwer, W.-D. Studies on the enzymatic hydrolysis of polyesters I. Low molecular mass model esters and aliphatic polyesters. *Polym. Degrad. Stab.* **2003**, *80* (3), 485−501.

(17) Marten, E.; Müller, R.-J.; Deckwer, W.-D. Studies on the enzymatic hydrolysis of polyesters. II. Aliphatic−aromatic copolyesters. *Polym. Degrad. Stab.* **2005**, *88* (3), 371−381.

(18) Miyakawa, T.; Mizushima, H.; Ohtsuka, J.; Oda, M.; Kawai, F.; Tanokura, M. Structural basis for the Ca-enhanced thermostability and activity of PET-degrading cutinase-like enzyme from Saccharomonospora viridis AHK190. *Appl. Microbiol. Biotechnol.* **2015**, *99*, 4297.

(19) Ribitsch, D.; Heumann, S.; Trotscha, E.; Herrero Acero, E.; Greimel, K.; Leber, R.; Birner-Gruenberger, R.; Deller, S.; Eiteljoerg, I.; Remler, P.; Weber, T.; Siegert, P.; Maurer, K.-H.; Donelli, I.; Freddi, G.; Schwab, H.; Guebitz, G. M. Hydrolysis of polyethyleneterephthalate by p-nitrobenzylesterase from Bacillus subtilis. *Biotechnol. Prog.* **2011**, *27* (4), 951−960.

(20) Chen, S.; Su, L.; Chen, J.; Wu, J. Cutinase: characteristics, preparation, and application. *Biotechnol. Adv.* **2013**, *31* (8), 1754−67.

(21) Ribitsch, D.; Herrero Acero, E.; Greimel, K.; Eiteljoerg, I.; Trotscha, E.; Freddi, G.; Schwab, H.; Guebitz, G. M. Characterization of a new cutinase from Thermobifida alba for PET-surface hydrolysis. *Biocatal. Biotransform.* **2012**, *30* (1), 2−9.

(22) Kleeberg, I.; Welzel, K.; VandenHeuvel, J.; Mueller, R. J.; Deckwer, W. D. Characterization of a New Extracellular Hydrolase from Thermobifida fusca Degrading Aliphatic−Aromatic Copolyesters. *Biomacromolecules* **2005**, *6* (1), 262−270.

(23) Barth, M.; Oeser, T.; Wei, R.; Then, J.; Schmidt, J.; Zimmermann, W. Effect of hydrolysis products on the enzymatic degradation of polyethylene terephthalate nanoparticles by a polyester

DOI: 10.1021/acs.biomac.5b01219
Biomacromolecules 2015, 16, 3889−3896

hydrolase from Thermobifida fusca. *Biochem. Eng. J.* **2015**, *93* (0), 222−228.
(24) Herrero Acero, E.; Ribitsch, D.; Steinkellner, G.; Gruber, K.; Greimel, K.; Eiteljoerg, I.; Trotscha, E.; Wei, R.; Zimmermann, W.; Zinn, M.; Cavaco-Paulo, A.; Freddi, G.; Schwab, H.; Guebitz, G. Enzymatic Surface Hydrolysis of PET: Effect of Structural Diversity on Kinetic Properties of Cutinases from Thermobifida. *Macromolecules* **2011**, *44* (12), 4632−4640.
(25) Ronkvist, Å. M.; Xie, W.; Lu, W.; Gross, R. A. Cutinase-Catalyzed Hydrolysis of Poly(ethylene terephthalate). *Macromolecules* **2009**, *42* (14), 5128−5138.
(26) Mueller, R.-J. Biological degradation of synthetic polyesters—Enzymes as potential catalysts for polyester recycling. *Process Biochem.* **2006**, *41* (10), 2124−2128.
(27) Nyyssölä, A.; Pihlajaniemi, V.; Järvinen, R.; Mikander, S.; Kontkanen, H.; Kruus, K.; Kallio, H.; Buchert, J. Screening of microbes for novel acidic cutinases and cloning and expression of an acidic cutinase from Aspergillus niger CBS 513.88. *Enzyme Microb. Technol.* **2013**, *52* (4−5), 272−278.
(28) Perz, V.; Hromic, A.; Baumschlager, A.; Steinkellner, G.; Pavkov-Keller, T.; Gruber, K.; Bleymaier, K.; Zitzenbacher, S.; Zankel, A.; Mayrhofer, C.; Sinkel, C.; Kueper, U.; Schlegel, K.; Ribitsch, D.; Guebitz, G. M.An esterase from anaerobic *Clostridium hathewayi* can hydrolyze aliphatic-aromatic polyesters, *Environmental Science and Technology*, submitted for publication.
(29) Herrero Acero, E.; Ribitsch, D.; Dellacher, A.; Zitzenbacher, S.; Marold, A.; Steinkellner, G.; Gruber, K.; Schwab, H.; Guebitz, G. M. Surface engineering of a cutinase from Thermobifida cellulosilytica for improved polyester hydrolysis. *Biotechnol. Bioeng.* **2013**, *110* (10), 2581−90.
(30) Araújo, R.; Silva, C.; O'Neill, A.; Micaelo, N.; Guebitz, G.; Soares, C. M.; Casal, M.; Cavaco-Paulo, A. Tailoring cutinase activity towards polyethylene terephthalate and polyamide 6,6 fibers. *J. Biotechnol.* **2007**, *128* (4), 849−857.
(31) Silva, C.; Da, S.; Silva, N.; Matama, T.; Araujo, R.; Martins, M.; Chen, S.; Chen, J.; Wu, J.; Casal, M.; Cavaco-Paulo, A. Engineered Thermobifida fusca cutinase with increased activity on polyester substrates. *Biotechnol. J.* **2011**, *6* (10), 1230−9.
(32) Ribitsch, D.; Herrero Acero, E.; Przylucka, A.; Zitzenbacher, S.; Marold, A.; Gamerith, C.; Tscheliessnig, R.; Jungbauer, A.; Rennhofer, H.; Lichtenegger, H.; Amenitsch, H.; Bonazza, K.; Kubicek, C. P.; Druzhinina, I. S.; Guebitz, G. M. Enhanced cutinase-catalyzed hydrolysis of polyethylene terephthalate by covalent fusion to hydrophobins. *Appl. Environ. Microbiol.* **2015**, *81* (11), 3586−92.
(33) Espino-Rammer, L.; Ribitsch, D.; Przylucka, A.; Marold, A.; Greimel, K. J.; Herrero Acero, E.; Guebitz, G. M.; Kubicek, C. P.; Druzhinina, I. S. Two novel class II hydrophobins from Trichoderma spp. stimulate enzymatic hydrolysis of poly(ethylene terephthalate) when expressed as fusion proteins. *Appl. Environ. Microbiol.* **2013**, *79* (14), 4230−8.
(34) Zhang, Y.; Chen, S.; Xu, M.; Cavaco-Paulo, A.; Wu, J.; Chen, J. Characterization of Thermobifida fusca Cutinase-Carbohydrate-Binding Module Fusion Proteins and Their Potential Application in Bioscouring. *Appl. Environ. Microbiol.* **2010**, *76* (20), 6870−6876.
(35) Zhang, Y.; Wang, L.; Chen, J.; Wu, J. Enhanced activity toward PET by site-directed mutagenesis of Thermobifida fusca cutinase-CBM fusion protein. *Carbohydr. Polym.* **2013**, *97* (1), 124−9.
(36) Ribitsch, D.; Yebra, A. O.; Zitzenbacher, S.; Wu, J.; Nowitsch, S.; Steinkellner, G.; Greimel, K.; Doliska, A.; Oberdorfer, G.; Gruber, C. C.; Gruber, K.; Schwab, H.; Stana-Kleinschek, K.; Acero, E. H.; Guebitz, G. M. Fusion of Binding Domains to Thermobifida cellulosilytica Cutinase to Tune Sorption Characteristics and Enhancing PET Hydrolysis. *Biomacromolecules* **2013**, *14* (6), 1769−1776.
(37) Boraston, A. B.; Bolam, D. N.; Gilbert, H. J.; Davies, G. J. Carbohydrate-binding modules: fine-tuning polysaccharide recognition. *Biochem. J.* **2004**, *382*, 769−781.
(38) Kasuya, K. i.; Ohura, T.; Masuda, K.; Doi, Y. Substrate and binding specificities of bacterial polyhydroxybutyrate depolymerases. *Int. J. Biol. Macromol.* **1999**, *24* (4), 329−336.
(39) Shinomiya, M.; Iwata, T.; Doi, Y. The adsorption of substrate-binding domain of PHB depolymerases to the surface of poly(3-hydroxybutyric acid). *Int. J. Biol. Macromol.* **1998**, *22* (2), 129−135.
(40) Bolam, D. N.; Ciruela, A.; McQueen-Mason, S.; Simpson, P.; Williamson, M. P.; Rixon, J. E.; Boraston, A.; Hazlewood, G. P.; Gilbert, H. J. Pseudomonas cellulose-binding domains mediate their effects by increasing enzyme substrate proximity. *Biochem. J.* **1998**, *331* (3), 775−781.
(41) Thongekkaew, J.; Ikeda, H.; Masaki, K.; Iefuji, H. Fusion of cellulose binding domain from Trichoderma reesei CBHI to Cryptococcus sp. S-2 cellulase enhances its binding affinity and its cellulolytic activity to insoluble cellulosic substrates. *Enzyme Microb. Technol.* **2013**, *52* (4−5), 241−246.
(42) Din, N.; Damude, H. G.; Gilkes, N. R.; Miller, R. C.; Warren, R. A.; Kilburn, D. G. C1-Cx revisited: intramolecular synergism in a cellulase. *Proc. Natl. Acad. Sci. U. S. A.* **1994**, *91* (24), 11383−11387.
(43) Din, N.; Gilkes, N. R.; Tekant, B.; Miller, R. C.; Warren, R. A. J.; Kilburn, D. G. Non-Hydrolytic Disruption of Cellulose Fibres by the Binding Domain of a Bacterial Cellulase. *Bio/Technology* **1991**, *9* (11), 1096−1099.
(44) Abou Hachem, M.; Nordberg Karlsson, E.; Bartonek-Roxa, E.; Raghothama, S.; Simpson, P. J.; Gilbert, H. J.; Williamson, M. P.; Holst, O. Carbohydrate-binding modules from a thermostable Rhodothermus marinus xylanase: cloning, expression and binding studies. *Biochem. J.* **2000**, *345* (1), 53−60.
(45) Carrard, G.; Koivula, A.; Soderlund, H.; Beguin, P. Cellulose-binding domains promote hydrolysis of different sites on crystalline cellulose. *Proc. Natl. Acad. Sci. U. S. A.* **2000**, *97* (19), 10342−7.
(46) Turon, X.; Rojas, O. J.; Deinhammer, R. S. Enzymatic Kinetics of Cellulose Hydrolysis: A QCM-D Study. *Langmuir* **2008**, *24* (8), 3880−3887.
(47) Yamashita, K.; Aoyagi, Y.; Abe, H.; Doi, Y. Analysis of adsorption function of polyhydroxybutyrate depolymerase from Alcaligenes faecalis T1 by using a quartz crystal microbalance. *Biomacromolecules* **2001**, *2* (1), 25−28.
(48) Yamashita, K.; Kikkawa, Y.; Kurokawa, K.; Doi, Y. Enzymatic degradation of poly(l-lactide)film by proteinase K: quartz crystal microbalance and atomic force microscopy study. *Biomacromolecules* **2005**, *6* (2), 850−857.
(49) Wang, C.; Kittle, J. D.; Qian, C.; Roman, M.; Esker, A. R. Chitinase Activity on Amorphous Chitin Thin Films: A Quartz Crystal Microbalance with Dissipation Monitoring and Atomic Force Microscopy Study. *Biomacromolecules* **2013**, *14* (8), 2622−2628.
(50) Carrez, C. Estimation of lactose in Milk. *Ann. Chim. Anal.* **1908**, *13*, 17−22.
(51) Culhaoglu, T.; Zheng, D.; Mechin, V.; Baumberger, S. Adaptation of the Carrez procedure for the purification of ferulic and p-coumaric acids released from lignocellulosic biomass prior to LC/MS analysis. *J. Chromatogr. B: Anal. Technol. Biomed. Life Sci.* **2011**, *879* (28), 3017−22.
(52) Armanious, A.; Aeppli, M.; Sander, M. Dissolved organic matter adsorption to model surfaces: adlayer formation, properties, and dynamics at the nanoscale. *Environ. Sci. Technol.* **2014**, *48* (16), 9420−9.
(53) Chen, X.; Zaro, J. L.; Shen, W.-C. Fusion protein linkers: property, design and functionality. *Adv. Drug Delivery Rev.* **2013**, *65* (10), 1357−1369.

DOI: 10.1021/acs.biomac.5b01219
Biomacromolecules 2015, 16, 3889−3896

Supporting Information

Table S1: Primer sequences for site-directed mutagenesis

Primer name	**Nucleotide sequences**
Thc_Cut1_Ser131Ala.FW	5'-CGA CTG GCG GTC ATG GGC CAC GCC ATG GGC GGC GGC GGC ACC CTG-3'
Thc_Cut1_Ser131Ala.REV	5'-CAG GGT GCC GCC GCC GCC CAT GGC GTG GCC CAT GAC CGC CAG TCG-3'

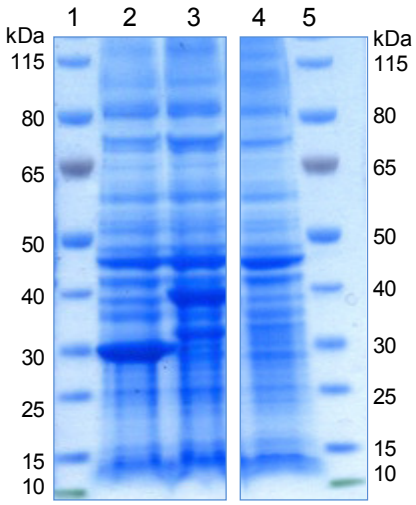

Figure S1: SDS-PAGE analysis (4−12%) of fusion proteins expressed in *E. coli* BL21-Gold(DE3) and purified by 6xHisTag. Lanes 1 and 5: standard Novex Sharp Protein Standard (Invitrogen); lanes 2-4: soluble cell fractions of Thc_Cut1 (29.4 kDa), Thc_Cut_PBM (38.0 kDa) and Thc_Cut1_2xPBM (40.3 kDa).

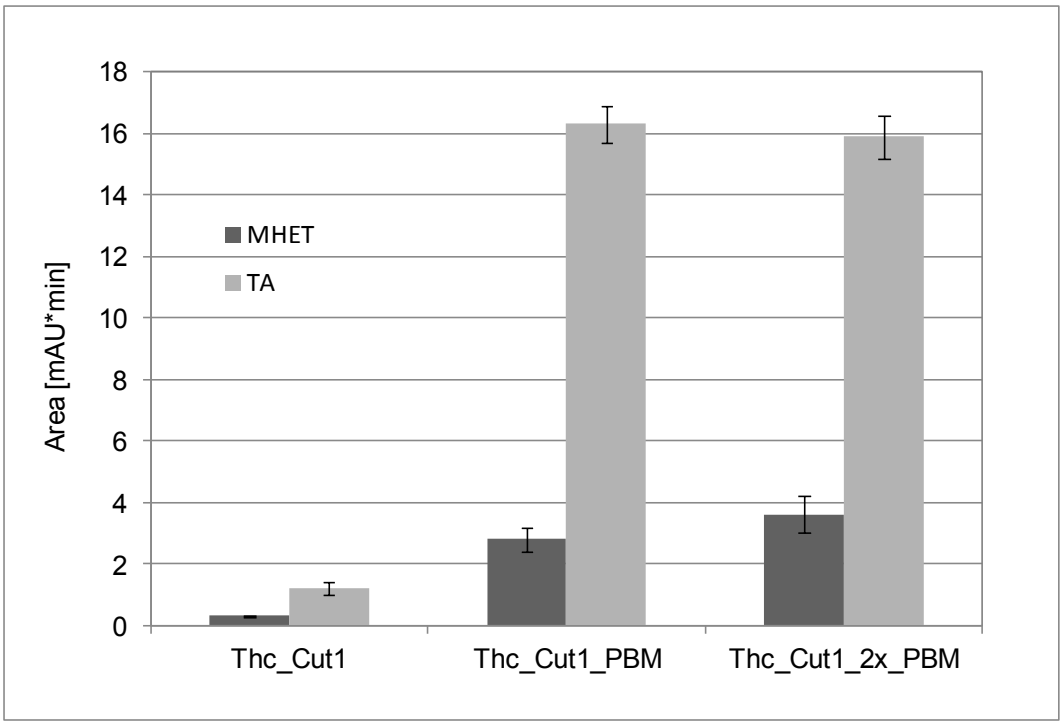

Figure S2: HPLC Analysis of soluble hydrolysis products of PET film. Completely amorphous PET films (purchased from Goodfellow) 1 x 2 cm were incubated with 2 µM Thc_Cut1, Thc_Cut1_PBM and Thc_Cut1_2x_PBM in K_2HPO_4/KH_2PO_4 buffer pH 7.0 at 50 °C for 24 h; TA, terephthalic acid; MHET, mono(2-hydroxyethyl) terephthalate.

Prediction of monolayer adsorbed masses of Thc_Cut1

The X-ray crystallographic structure of Thc_Cut1 has not been resolved. We therefore have to assume a shape for the cutinase to be able to estimate the mass associated with a Thc_Cut1 monolayer at the jamming limit of the surface. For simplicity, we assume that Thc_Cut1 has a spherical shape. The molar mass of Thc_Cut1 is 29442 Da (and that of the inactive mutant 29426 Da). The minimum radius, R_{min} (nm) of a spherical enzyme can be estimated according to: [1]

Equation S1.

$$R_{\min} = 0.066 \cdot M^{1/3}$$

where M (Da) is the molecular weight of the enzyme.

Using equation S1, we estimated a R_{min} of Thc_Cut1 (and the inactive Thc_Cut1) of approximately 2 nm.

The jamming limit for monodisperse spheres on flat surfaces is θ= 0.547 (i.e., 54.7% of the surface area are occupied by the adsorbed spheres) [2, 3]. The maximum thickness of the formed Thc_Cut1 monolayer would be approximately 4 nm, corresponding to the diameter of the 'spherical' cutinases. According to Bingen et al. [4] and Vörös [5], approximately 60% of the monolayer mass detected by QCM-D is due to water that couples to the oscillation of the sensor (note: in contrast to optical techniques that determine the 'dry' adsorbed mass, QCM-D also detects adlayer associated water and hence the total 'wet' mass of the adlayer). Assuming a density of the formed adlayer of approximately $\rho_{adlayer}$= 1.14 g/cm^3 (which is estimated from the densities of water (ρ_{H2O}= 1g/cm^3) and protein ($\rho_{protein}$= 1.35 g/cm^3), we predict a monolayer adsorbed wet mass of $m_{adlayer}$= 1.14 g/cm^3 * 4*10^{-7} cm≈ 450 ng /cm^2.

This predicted value for a monolayer adsorbed mass of the cutinase at the surface jamming limit is in very good agreement with the experimentally measured value for the inactive mutant of $\Delta m = 420 \pm 30$ ng/cm^2 (mean ± standard deviation, n=5). We note that the slightly smaller experimental than predicted final adsorbed masses may reflect that the experiments resulted in surface coverages that had not reached the theoretically possible surface coverages (i.e., $\theta = 0.547$).

Because of the measurement principle of QCM-D (i.e., piezoacustic resonator) and, as a result, the fact that QCM-D also detects adlayer-associated water, we do not expect a significantly larger monolayer adsorbed mass of Thc_Cut1_PBM. While the cutinase fused to the PBM has a higher molecular weight (i.e., 37997.2 Da) than the native Thc_Cut1 (i.e., 29442 Da; see above), we expect that the PBM is very closely associated with the Thc_Cut1 *via* the linker and that the Thc_Cut1_PBM will adsorb to the polyester surface *via* the PBM. As a result, we expect that most (if not all) of the additional protein mass of the PBM will be within the hydration coat of the Thc_Cut1 core structure, and, as a consequence, not significantly increase the adlayer wet mass. Consistently, the final adsorbed mass of Thc_Cut1_PBM of $\Delta m = 457 \pm 18$ ng/cm^2 (mean ± standard deviation, n=3) was only slightly larger than the final adsorbed wet mass of Thc_Cut1 without the PBM.

References

1. Erickson, H. P., Size and shape of protein molecules at the nanometer level determined by sedimentation, gel filtration, and electron microscopy. *Biol Proced Online* **2009,** 11, 32-51.

2. Schaaf, P.; Talbot, J., Surface exclusion effects in adsorption processes. *The Journal of Chemical Physics* **1989,** 91, (7), 4401-4409.

3. Hinrichsen, E. L.; Feder, J.; Jøssang, T., Geometry of random sequential adsorption. *Journal of Statistical Physics* **1986,** 44, (5-6), 793-827.

4. Bingen, P.; Wang, G.; Steinmetz, N. F.; Rodahl, M.; Richter, R. P., Solvation Effects in the Quartz Crystal Microbalance with Dissipation Monitoring Response to Biomolecular Adsorption. A Phenomenological Approach. *Analytical Chemistry* **2008,** 80, (23), 8880-8890.

5. Vörös, J., The Density and Refractive Index of Adsorbing Protein Layers. *Biophysical Journal* **2004,** 87, (1), 553-561.